Title

Connected Vehicles: An Integrated Analysis of Safety, Mobility, and Environmental Sustainability (SME)

Author

Tian, Danyang

Publication Date

2018

Peer reviewed|Thesis/dissertation

UNIVERSITY OF CALIFORNIA
RIVERSIDE

Connected Vehicles: An Integrated Analysis of Safety, Mobility, and Environmental Sustainability (SME)

A Dissertation submitted in partial satisfaction
of the requirements for the degree of

Doctor of Philosophy

in

Electrical Engineering

by

Danyang Tian

December 2018

Dissertation Committee:
Dr. Matthew J. Barth, Chairperson
Dr. Hamed Mohsenian-Rad
Dr. Guoyuan Wu

The Dissertation of Danyang Tian is approved:

Committee Chairperson

University of California, Riverside

ACKNOWLEDGMENT

I would like to express my sincere appreciation to my advisor, Dr. Matthew J. Barth, for his continuous support and effective guidance throughout research and work. Dr. Barth encourages me to maximize my potential to promote my personal development from a student to an independent researcher. Dr. Barth has a sharp sense of the development trend in the overall transportation field and always looks at the big picture for both the short-term and the long-term development. He is always willing to offer help, and his extensive knowledge and creative thinking drove me to proceed when I met challenges in transportation research. I couldn't have completed this dissertation without Dr. Barth's invaluable insights, guidance, and support.

I also want to thank Dr. Hamed Mohsenian-Rad and Dr. Guoyuan Wu for their service in the dissertation committee. Special thanks to Dr. Guoyuan Wu for his countless hours and valuable suggestions in research discussions. His experience in the subject area guides me to finish many of my research projects. Special thanks go to Dr. Kanok Boriboonsomsin for his professional comments and suggestions in many of my research papers and projects. Special thanks also go to Dr. Peng Hao for providing me valuable comments about traffic state prediction modeling on my dissertation. Their help and encouragement drove me to complete many major work in this dissertation. Moreover, the faculties I have took class from were also very wonderful people, such as Professor Hamed Mohsenian-Rad, Professor Yingbo Hua, and Professor Zak M. Kassas, I want to extend my gratitude to all of them for their devoted instruction.

I would like to thank my colleagues Mike Todd, Alex Vu, and Daniel Sandez because I learned a lot from them when I got involved in different CE-CERT activities and I also want to thank my lab-mates Dr. David P. Kari, Dr. Qiu (Apple) Jin, Dr. Ji (Jill) Luo, Nigel Williams, Fei Ye, Chao Wang, Ziran Wang, the visiting scholars Dr. Weixia Li, and Dr. Xiaonian Shan for their help and pleasant collaboration during my doctoral study. I also want to thank Alta Vasquez and Carolyn Ray who helped me with different things for always providing convenience and making CE-CERT a great place to learn and work.

Finally, I would like to acknowledge the Department of Electrical and Computer Engineering (ECE) of UC Riverside, CE-CERT at UC Riverside, Honda R&D Americas, Inc., the California Department of Transportation, the National Center for Sustainable Transportation (NCST), UCCONNECT, the Women's Transportation Seminar Inland Empire Chapter, and Esther F. Hays family for fully or partially supporting my study and research in this dissertation.

The major contents in the dissertation have been published in the Institute of Electrical and Electronics Engineers (IEEE) Intelligent Transportation Systems Magazine, IEEE Transactions on Intelligent Transportation Systems, IEEE Intelligent Transportation Systems Conference, IEEE Intelligent Vehicles Symposium, and Transportation Research Board Annual Meeting, respectively.

DEDICATION

I would like to thank my parents for their unconditional and endless love. They are always by my side whenever I face any decisions. Thanks to my dear husband for his continuous encouragement, understanding, tolerance, and love. Their love was the main driving force in my work and life.

I wouldn't have adjusted to the new environment that quickly without the help of my dear friends Wei (Sarah) Mi, Qianhui (Phoebe) Zhu, and Lanting Cheng. I would like to thank them for their company when I both felt happy and unhappy, they are not only friends but also my instructors who enlightened me in life. It was a pleasure to be friends with all of them. I hope our friendships will last a lifetime.

ABSTRACT OF THE DISSERTATION

Connected Vehicles: An Integrated Analysis of Safety, Mobility, and Environmental Sustainability (SME)

by

Danyang Tian

Doctor of Philosophy, Graduate Program in Electrical Engineering
University of California, Riverside, December 2018
Dr. Matthew J. Barth, Chairperson

Connected Vehicles (CVs) have the potential to serve as a valuable source of traffic data in some transportation research areas from traffic state monitoring to transportation management and control strategies, due to the low cost, wide coverage, and relative high accuracy. CV technology also enables a variety of CV-based applications which present an opportunity to provide vehicles and drivers with situational awareness and improve upon the limited behaviors of conventional vehicles. Increasing efforts in the development and deployment of CV-enabled applications are ongoing to improve traffic safety, mobility, environmental sustainability, efficiency, and driving comfort. CVs have been analyzed separately for safety, mobility, and environmental sustainability (SME), however, very few studies evaluate these three performance measures holistically. There are important co-benefits and tradeoffs among SME when evaluating impacts CVs bring.

In this dissertation research, an integrated holistic analysis framework has been developed to evaluate CV applications from SME impacts both qualitatively and

quantitatively. Furthermore, a unique innovative use of “entropy” has been developed and applied in the transportation field to help evaluate CVs holistically. Under the developed qualitative analysis framework for SME, a series of innovative CV-based applications have been developed, taking the SME tradeoffs and co-benefits into consideration. These developed CV-based applications include Lane Speed Monitoring (LSM), Optimal Lane Selection (OLS) application, and Cooperative Smart Lane Selection (CSLS) application. Specifically, the LSM guides the vehicle driver to the fastest lane by utilizing short-range downstream vehicle information, helping the vehicle driver achieve mobility benefits. The OLS adopts longer-range connectivity and guides the application-equipped vehicle driver to go through a micro-route to reduce the travel time and the potential conflict risk of each individual application-equipped vehicle, obtaining mobility and safety co-benefits. The CSLS application is designed from the cooperative perspective which can be regarded as an evolved version on top of LSM, to increase mobility for the overall traffic system. These CV applications can be dynamically managed under various traffic conditions and users’ needs. As a future work, an ideal goal is to develop applications with all SME co-benefits considered by using strategies such as combining different applications.

TABLE OF CONTENTS

LIST OF TABLES xiv

LIST OF FIGURES xv

1 INTRODUCTION 1

1.1 Motivation 1

1.1.1 Congestion Impacts on Road Transportation Systems 1

1.1.2 Connected Vehicle Environment 3

1.1.3 Connected Vehicle Deployment 5

1.1.4 Performance Measures 7

1.2 Problem Statement 8

1.3 Contribution of the Dissertation 9

1.4 Organization of the Dissertation 12

2 RESEARCH BACKGROUND 1: CONNECTIVITY TECHNOLOGIES 14

2.1 Dedicated Short Range Communication (DSRC) 14

2.1.1 A Brief Introduction of DSRC 14

2.1.2 DSRC Model in Simulation 17

2.2 Cellular based Vehicle-to-Everything (C-V2X) Communication 19

2.2.1 A Brief Introduction of C-V2X 19

2.2.2 C-V2X Model in Simulation 21

2.3 Other Wireless Communication Technologies 23

3 RESEARCH BACKGROUND 2: CONVENTIONAL MOEs AND MICROSCOPIC TRANSPORTATION SIMULATION TOOLS AND MODELS 24

3.1 Measures of Effectiveness (MOEs) for CV-Based Applications Performance Evaluation 24

3.1.1 Safety MOEs 24

3.1.2 Mobility MOEs 25

3.1.3 Environmental MOEs 25

3.2 Microscopic Transportation Simulation Tools and Models 26

4 FRAMEWORK OF PERFORMANCE MEASUREMENT AND MOEs CO-BENEFITS AND TRADEOFFS FOR CONNECTED VEHICLES BASED APPLICATIONS 30

4.1 Performance-Oriented Taxonomy of CV-Based Applications 31

4.2 Category Summary ... 33
4.3 Co-benefit Analysis of Typical V2X-Based CV Applications ... 36
4.3.1 Vehicle-Centric CV-Based Applications ... 37
4.3.1.1 Safety & Mobility Co-Benefits ... 37
4.3.1.2 Safety Benefits ... 37
4.3.1.3 Environmental Impacts & Safety Co-Benefits ... 39
4.3.1.4 Environmental Impacts Benefits ... 41
4.3.1.5 Environmental Impacts & Mobility Co-Benefits ... 41
4.3.1.6 Mobility Benefits ... 42
4.3.2 Infrastructure-Centric CV-Based Applications ... 42
4.3.2.1 Safety & Mobility Co-Benefits ... 42
4.3.2.2 Safety Benefits ... 44
4.3.2.3 Environmental Impacts Benefits ... 47
4.3.2.4 Environmental Impacts & Mobility Co-Benefits ... 48
4.3.3 Traveler-Centric CV-Based Applications ... 49
4.3.3.1 Safety Benefits ... 49
4.3.3.2 Mobility Benefits ... 50
4.4 Summary ... 51
5 AN INNOVATIVE FRAMEWORK TO EVALUATE THE PERFORMANCE OF CONNECTED VEHICLE APPLICATIONS: FROM THE PERSPECTIVE OF SPEED VARIATION-BASED ENTROPY ... 53
5.1 Introduction ... 53
5.2 Representative CV Applications ... 54
5.2.1 High Speed Differential Warning (HSDW) Application ... 54
5.2.2 Eco-Speed Harmonization (ESH) Application ... 54
5.2.3 Eco-Approach and Departure (EAD) Application ... 55
5.3 Framework of Speed Variation-based Entropy (SVE) ... 55
5.3.1 Entropy ... 55
5.3.2 Speed Variation-based Entropy (SVE) ... 56
5.3.3 Curve Fitting of Discrete SVE Distributions ... 59
5.4 Simulation Setup ... 60

5.4.1 Simulation Model ... 60
5.4.2 Simulation Scenarios ... 62
5.5 Simulation Results ... 62
5.5.1 SVE-based MOE Evaluation for CV Applications ... 62
5.5.1.1 CV Applications' Effects on Traffic ... 62
5.5.1.2 Sensitivity Analysis ... 65
5.5.2 Correlations between SVE and Conventional MOEs ... 69
5.5.2.1 Baseline SVE versus Conventional MOEs ... 69
5.5.2.2 SVE versus Conventional MOEs for Three Selected CV Applications.. 70
5.5.2.3 Discussions ... 77
5.6 Summary ... 78
6 DEVELOPMENT AND EVALUATION OF A V2V-BASED LANE SPEED MONITORING APPLICATION ... 80
6.1 System Architecture ... 81
6.2 Lane-Level Traffic Speed Estimation ... 82
6.3 Simulation Setup ... 84
6.3.1 Simulation Tools ... 84
6.3.2 Simulation Network Model ... 85
6.3.3 Simulation Scenarios ... 85
6.3.4 Simulation Runs ... 88
6.4 Simulation Results and Analysis ... 89
6.4.1 Mobility ... 89
6.4.1.1 Sensitivity Analysis on Penetration Rate ... 90
6.4.1.2 Sensitivity Analysis on Traffic Volume ... 91
6.4.2 Safety ... 92
6.4.2.1 Sensitivity Analysis on Penetration Rate ... 92
6.4.2.2 Sensitivity Analysis on Traffic Volume ... 94
6.4.3 Environmental Sustainability ... 95
6.4.3.1 Sensitivity Analysis on Penetration Rate ... 95
6.4.3.2 Sensitivity Analysis on Traffic Volume ... 96
6.5 SME Tradeoff Analysis of the LSM Application ... 97

6.6 Speed-Variation Based Entropy Analysis for LSM 100
6.7 Summary 105
7 CONNECTED VEHICLE-BASED LANE SELECTION ASSISTANCE 106
7.1 Introduction 106
7.2 Problem Formulation 109
7.3 Lane Selection Assistance Application 113
7.3.1 Spatial-Temporal Discretization 113
7.3.2 Lane-Level Traffic State Prediction 114
7.3.3 Optimal Lane Selection Algorithm 118
7.4 Simulation Setup 121
7.4.1 Simulation Network Model 121
7.4.2 Implementation Details 122
7.4.3 Simulation Scenarios 123
7.5 Simulation Analysis 126
7.5.1 An Example of the Individual Vehicle 126
7.5.2 Statistical Analysis of the Application Performance 128
7.5.2.1 Measures of Effectiveness (MOEs) 128
7.5.2.2 Sensitivity Analysis 130
7.5.2.3 Safety Performance Analysis 140
7.6 Summary 140
8 COOPERATIVE SMART LANE SELECTION APPLICATION AND DYNAMIC MANAGEMENT AMONG CV APPLICATIONS 142
8.1 Introduction 142
8.2 System Architecture 145
8.3 Lane Assignment Strategy 148
8.4 Simulation Setup 151
8.4.1 Network 151
8.4.2 General Parameters Settings of VISSIM 153
8.4.3 Scenario 154
8.5 Simulation Results and Analysis 155
8.5.1 CSLS Mobility and Safety Analysis in Hypothetical Network 155

8.5.2 Mobility Comparison between CSLS and LSM in Hypothetical Network 159
8.5.3 CSLS Mobility and Safety Analysis in Real-World Network 161
8.6 Summary 166
9 CONCLUSIONS AND FUTURE WORK 169
9.1 Conclusions 169
9.2 Selected Publications Resulting from This Research 173
9.3 Future Work 174
BIBLIOGRAPHY 176

LIST OF TABLES

Table 2-1. Comparison: Use Cases and Performance 21
Table 4-1. Category Summary of CV-Based Applications in Terms of Different MOEs 35
TABLE 4-2. SYMBOLS FOR MOEs CO-BENEFITS AND TRADEOFFS IN THE LITERATURE REVIEW TABLES 36
TABLE 4-3. VEHICLE-CENTRIC CV-BASED APPLICATIONS 40
TABLE 4-4. INFRASTRUCTURE-CENTRIC CV-BASED APPLICATIONS................................. 45
TABLE 4-5. TRAVELER-BASED CV-BASED APPLICATIONS 51
TABLE 5-1. CONVENTIONAL MOEs OF PENETRATION RATE SENSITIVITY ANALYSIS........ 67
TABLE 5-2. CONVENTIONAL MOEs OF TRAFFIC VOLUME SENSITIVITY ANALYSIS 69
TABLE 5-3. CORRELATION COEFFICIENTS BETWEEN SVE AND CONVENTIONAL MOEs (25,000 VEHICLES/RUN)... 72
Table 5-4 Correlation coefficients between SVE and conventional MOEs (Heavy Traffic, 20% Penetration Rate) 78
TABLE 6-1. NUMERICAL RESULTS OF THE LSM CASE STUDY 98
TABLE 6-2 CONVENTIONAL MOEs OF TRAFFIC VOLUME SENSITIVITY ANALYSIS 102
TABLE 7-1. LANE SELECTION ASSISTANCE ALGORITHM 120
TABLE 7-2. THE RECOMMENDED NUMBER AND THE ACTUAL LANE CHANGING NUMBER OF APPLICATION-EQUIPPED VEHICLES (1200 APPLICATION-EQUIPPED VEHICLE SAMPLES, 1-MIN INFO UPDATE CYCLE, 100% PENETRATION RATE OF COMMUNICATION-CAPABLE VEHICLES, 32,000 VEHICLES PER RUN) 133
TABLE 7-3. THE AVERAGE VALUES FOR MAPE, MAE, AND RMSE IN THE HEAVY TRAFFIC SCENARIOS (100% PENETRATION RATE OF COMMUNICATION-CAPABLE VEHICLES, 32000 VEHICLES/RUN)... 134
TABLE 7-4. THE AVERAGE VALUES OF MAPE, MAE, AND RMSE OF THE ST-MODEL AND THE BASIC ESTIMATION MODEL UNDER MODERATE TRAFFIC (100% PENETRATION RATE OF COMMUNICATION-CAPABLE VEHICLES, 25,000 VEHICLES PER RUN) 136
TABLE 7-5. THE MEAN ACTUAL LANE CHANGE NUMBER AND POTENTIAL CONFLICT FREQUENCY FOR THE PROPOSED APPLICATION (100% PENETRATION RATE OF COMMUNICATION-CAPABLE VEHICLES, 25,000 VEHICLES PER RUN) AND THE CORRESPONDING BASELINE.. 140

LIST OF FIGURES

Figure 1-1. Year-to-Year Congestion Trends in the United States (2015 to 2016) 1
Figure 1-2. Road Traffic Deaths by Type of Road User 2
Figure 1-3. Connectivity Functionalities of the Connected Vehicle.................................. 3
Figure 1-4. Worldwide CV Applications/Projects... 5
Figure 1-5. Co-Benefit and Tradeoff Analysis Framework from Safety, Mobility, and Environmental Impacts for CV-Based Applications 9
Figure 1-6. Organization of the Dissertation 13
Figure 2-1. DSRC Sync Time Intervals 15
Figure 2-2. Layered Architecture for DSRC 15
Figure 2-3. SAE J2735 DSRC Basic Safety Message Part I 16
Figure 2-4. Combined (Both Long-Range and Short-Range Communication) Development Scenario for Private Vehicles 19
Figure 2-5. C-V2X Layers and Architecture 20
Figure 2-6. V2X Communications via the Network 20
Figure 2-7. Demand to Delay in Control and User Planes for 4G/5G Networks 22
Figure 3-1. Overview of the Performance Measurement Framework (We focused MOEs in Red in This Dissertation) 26
Figure 3-2. Interaction among Different Modeling Tools, and the Corresponding MOEs Outputs 29
Figure 4-1. Taxonomy of CV-Based Applications 34
Figure 5-1. Possible HSDW Scenarios 54
Figure 5-2. Three-Step Procedure for SVE Calculation 57
Figure 5-3. Time-Speed Diagram for Two Individual Trips 58
Figure 5-4. Road Network of the California SR-91E in Real-World and PARAMICS ... 61
Figure 5-5. Time SVE Distributions of Three Different CV Applications (25,000 Vehicles/Run, 20% Penetration Rate)... 65
Figure 5-6. SVE Distributions of Different Penetration Rates in ESH and EAD Scenarios (25,000 Vehicles/Run) 67
Figure 5-7. SVE Distributions of Different Traffic Volumes in EAD Scenario (Baseline Cases and 20% Penetration Rate) 68
Figure 5-8. Baseline SVE Correlations with Three Conventional MOEs (0% Penetration Rate, 25,000 Veh/Run) 70
Figure 5-9. SVE versus Three Conventional MOEs across Different Penetration Rate Levels for Three Different CV Applications (Moderate Traffic) 74
Figure 5-10. SVE versus Three Conventional MOEs across Two Different Congestion Levels for Three Different CV Applications (20% Penetration Rate of Application-Equipped Vehicles)... 77
Figure 6-1. System Architecture for Lane Speed Monitoring 82
Figure 6-2. Example of Speed Monitoring for Average-Speed-Based Algorithm 84

Figure 6-3. Road Network of California SR-91E in Real-World and Paramics............... 87
Figure 6-4. Survey Results Corresponding to Parameters Selection in Algorithm 87
Figure 6-5. Survey Results Corresponding to Driver Behavior in Algorithm.................. 88
Figure 6-6. Detailed Flowchart of the Developed Lane Speed Monitoring Application.. 89
Figure 6-7. Average Speed Improvement Comparison at LOS D 90
Figure 6-8. Average Speed Improvement Comparison at 20% Penetration Rate............. 91
Figure 6-9. Average Speed Improvement Comparison at 20% Penetration Rate............. 92
Figure 6-10. Relative Conflict Frequency under Different Penetration Rates at LOS D . 93
Figure 6-11. Relative Conflict Frequency for Overall at 20 % Penetration Rate and Baseline Case 94
Figure 6-12. Average Energy Difference vs Penetration Rates at LOS D........................ 95
Figure 6-13. Average Energy Difference vs LOS at 20% Penetration Rate..................... 96
Figure 6-14. Average Energy Difference vs LOS at 20% Penetration Rate..................... 97
Figure 6-15. Radar Plots of Three Normalized MOEs for LSM 99
Figure 6-16. SVE Distributions of Different Traffic Volumes in LSM scenario (Baseline Cases and 20% Penetration Rate) 101
Figure 6-17. SVE versus Three Conventional MOEs across Different Penetration Rate Levels for LSM (moderate traffic).. 103
Figure 6-18. SVE versus Three Conventional MOEs across Two Different Congestion Levels for LSM (20% Penetration Rate of Application-Equipped Vehicles)................. 104
Figure 7-1. An Example of the Problem Description 110
Figure 7-2. Information Flow of the Lane Selection Assistance Application 112
Figure 7-3. Sketch Map of Spatial Discretization on Freeways 114
Figure 7-4. An Illustrative Example of the Optimal Lane-Level Path in a Discretized Roadway Network 120
Figure 7-5. Road Network of the California SR-91E in Real-World and PARAMICS . 122
Figure 7-6. An Example of the Application-Equipped Vehicle (Left) and the Corresponding Baseline (Right). (a) Trajectory. (b) Velocity. (c) Lane Index 128
Figure 7-7. Measures of Effectiveness for Different Congestion Levels. (a) Mean Absolute Percentage Error (b) Relative Travel Time Difference 132
Figure 7-8. Relative Travel Time Difference with and without the Lane Change Lock 134
Figure 7-9. Measures of Effectiveness for Different Penetration Rates of Communication-Capable Vehicles. (a) Mean Absolute Percentage Error. (b) Relative Travel Time Difference 137
Figure 7-10. Measures of Effectiveness Analysis for Different Information Update Cycle (a) Mean Absolute Percentage Error (b) Relative Travel Time Difference.................... 139
Figure 8-1. Schematic Diagrams for the CSLS Application.. 146
Figure 8-2. Flowchart of CSLS Application Algorithm 147
Figure 8-3.Traffic Networks under Study.. 152
Figure 8-4. Influence of CSLS Application on Mobility and Safety 158
Figure 8-5. Influence of LSM Application on Mobility 160

Figure 8-6. Influence of CSLS Application on Mobility and Safety (Real-World Network) 165
Figure 8-7. Parameters Tuning Strategy 167

1 INTRODUCTION

1.1 Motivation

1.1.1 Congestion Impacts on Road Transportation Systems

Ever-growing travel demand contributes to significant congestion on both highways and major urban corridors during peak hours [1]. The U.S. Federal Highway Administration's Urban Congestion Report estimated that the average duration of daily congestion in 2016 was more than four hours in more than fifty American metropolitan areas and the hours of congestion keep increasing (see Figure 1-1).

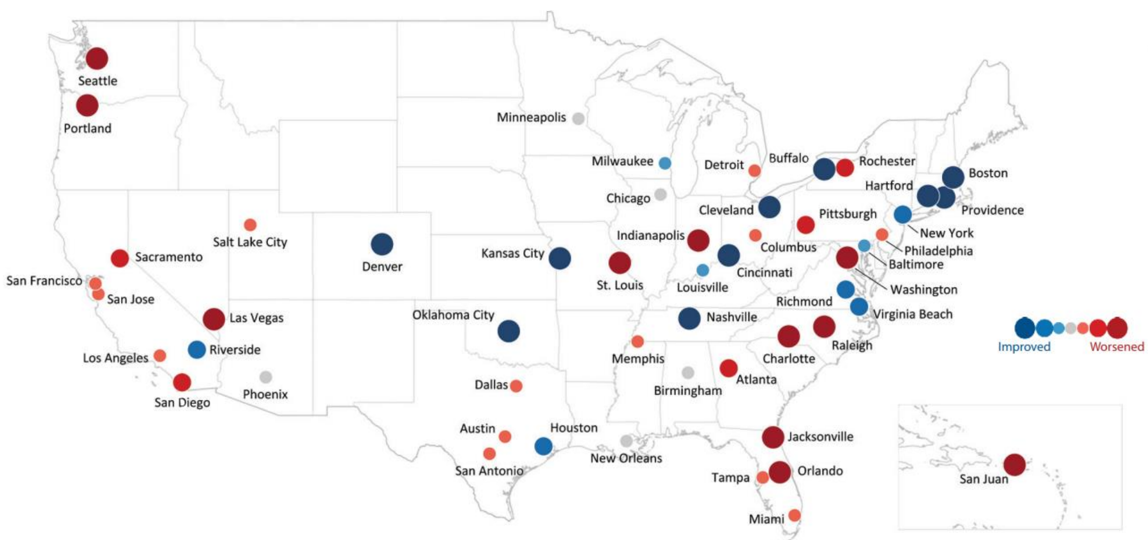

Figure 1-1. Year-to-Year Congestion Trends in the United States (2015 to 2016) (from [2])

Traffic congestion especially occurs in metropolitan cities, and causes negative chain effects in other aspects of the society. Increased delay in travel time [1], accidents (see Figure 1-2), air pollution, and noise pollution are some of the major problems that are faced by people living in these areas. According to the National Highway Traffic Safety Administration's (NHTSA) report [3], over 30,000 people perish in crashes on U.S.

highways in 2016. The global status report on road safety 2015 indicates that worldwide the total number of road traffic deaths has plateaued at 1.25 million per year [4]. Regarding the environmental aspect impacts, according to the U.S. Environmental Protection Agency's (EPA) annual report [5], the transportation sector is one of the largest contributors to nationwide greenhouse gas (GHG) emissions, which increased by 4.2% in 2015, the third successive year of increases in transport emissions [6].

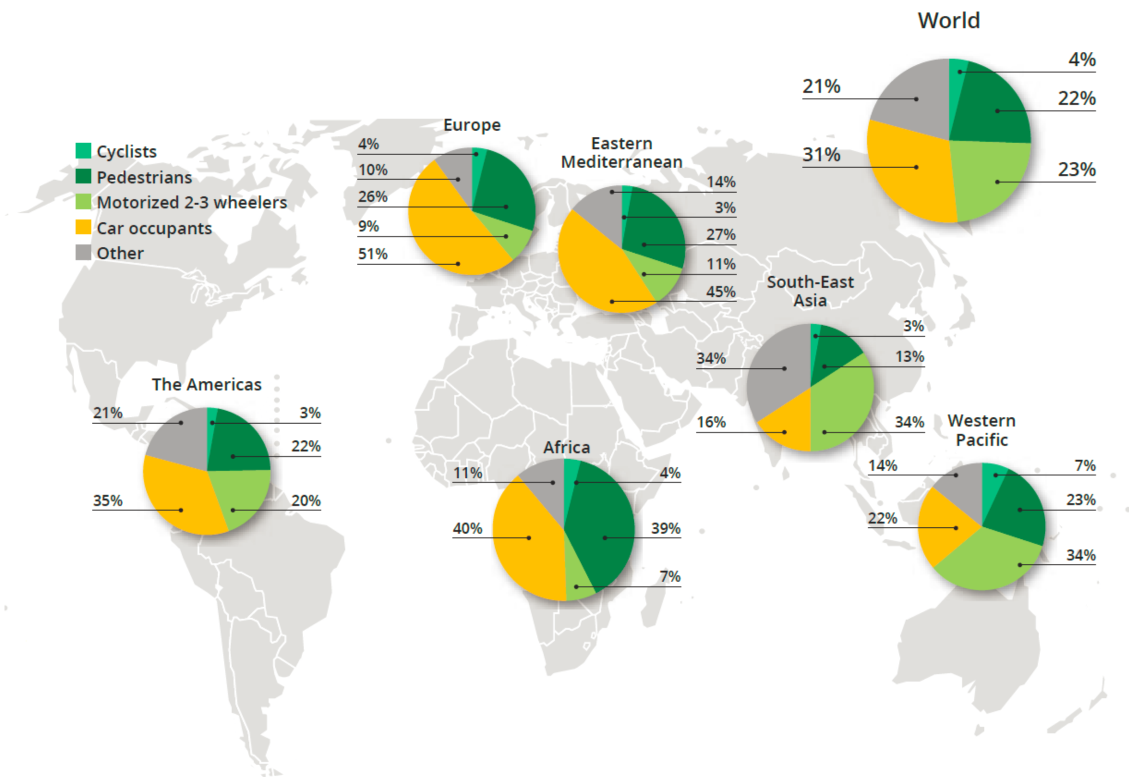

Figure 1-2. Road Traffic Deaths by Type of Road User (from [4])

Many long standing, traditional measures have been employed to provide traffic management in roadways, in order to alleviate congestion and improve transportation service capability. Data collection is undoubtedly the most important link in the whole process chain, based on which traffic monitoring is obtained and able to be applied for further traffic management strategies. For decades, the most commonly used methods for traffic data collection usually include fixed sensors and infrastructure, for example, the inductive loop detectors (ILD)) [7]. However, the ever growing nature of traffic makes it difficult to purely use such traditional approaches to estimate (even predict) the traffic status in real time thereby to make better management decisions [8].

1.1.2 Connected Vehicle Environment

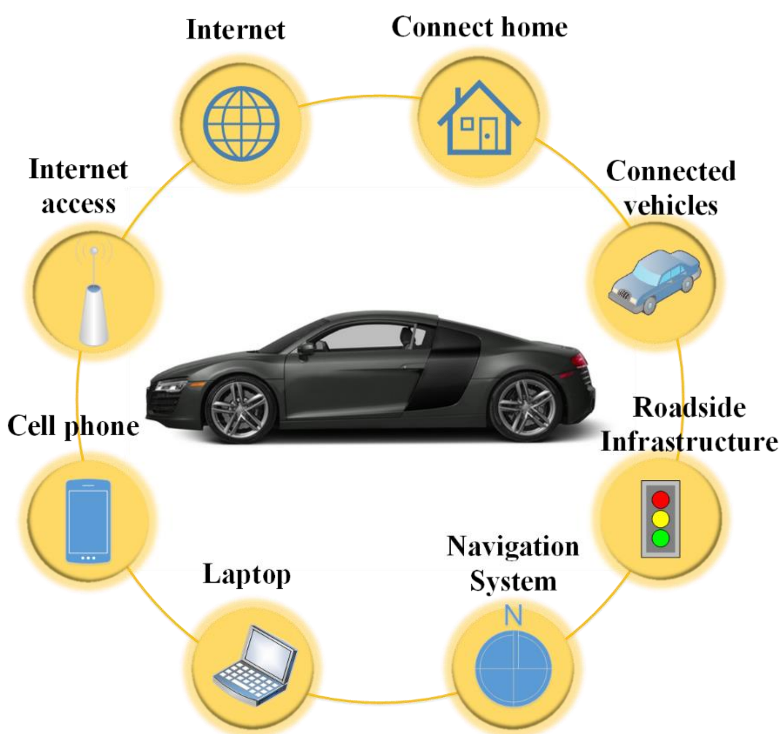

Figure 1-3. Connectivity Functionalities of the Connected Vehicle

Exploiting the innovative connectivity characteristics of vehicles as a source of traffic data has drawn some attention, primarily due to the low cost, wide coverage and high accuracy of the extracted data. Connected Vehicles (CVs) are also known as Cooperative Intelligent Transport Systems (C-ITS), which refer to vehicles with increasing levels of connectivity and allow them to communicate with their surrounding environment, such as other connected vehicles and the roadside infrastructure. Connectivity among vehicles can provide information to the driver about traffic, weather conditions, and even assist with routing options, enabling a wide range of connectivity services, as shown in Figure 1-3.

According to the work in [9], CV uptake is estimated to reach up to 25% of total annual global vehicles sales (under a case where there is rapid technology development and moderate global CV uptake). Although it is not necessary for vehicles with some levels of automation to be connected, it is very likely that vehicles with autonomous capabilities will increasingly rely on connectivity since they will also need the ability to receive and transmit data to achieve full autonomy [9].

A variety of methods for Vehicle-to-Everything (V2X) data exchange has been studied [10]-[12], mainly including two major types of communications: Wireless Access in the Vehicular Environment (WAVE) based Dedicated Short-Range Communications (DSRC) and cellular based communications. DSRC devices are capable of providing high availability and low latency channels for critical safety applications [13] through the IEEE 802.11p standard [14] which was specifically designed for automobile communication, and they require on-board units for every communication-capable terminal [15]. In contrast, cellular-based devices (e.g., smartphones) can be integrated with different connectivity services and applications by built-in sensors. In addition to smartphones, there are cellular-based Vehicle-to-Everything (C-V2X) communications (developed in [16]-[17]) which reuses upper layers defined by automotive industry and C-ITS established service and app layers, which makes it well compatible with existing V2X technologies [16]. For the C-

V2X network communications, vehicles can send messages to server via unicast. C-V2X can use LTE Broadcast to broadcast messages from a V2X server to vehicles and beyond. It has wide coverage networks communications and can be used by more latency tolerant cases. More details on connectivity technologies background is introduced in Chapter 2.

1.1.3 Connected Vehicle Deployment

With the help of vehicular connectivity, traditional passenger vehicles have become increasingly intelligent, which opens the door for the evolution of CV-based applications. In combination with vehicle-equipped sensors (for example, GPS, radar, camera, and Lidar, etc.), connected vehicle-enabled applications would significantly improve vehicle safety, traffic efficiency and driving comfort [15], [18].

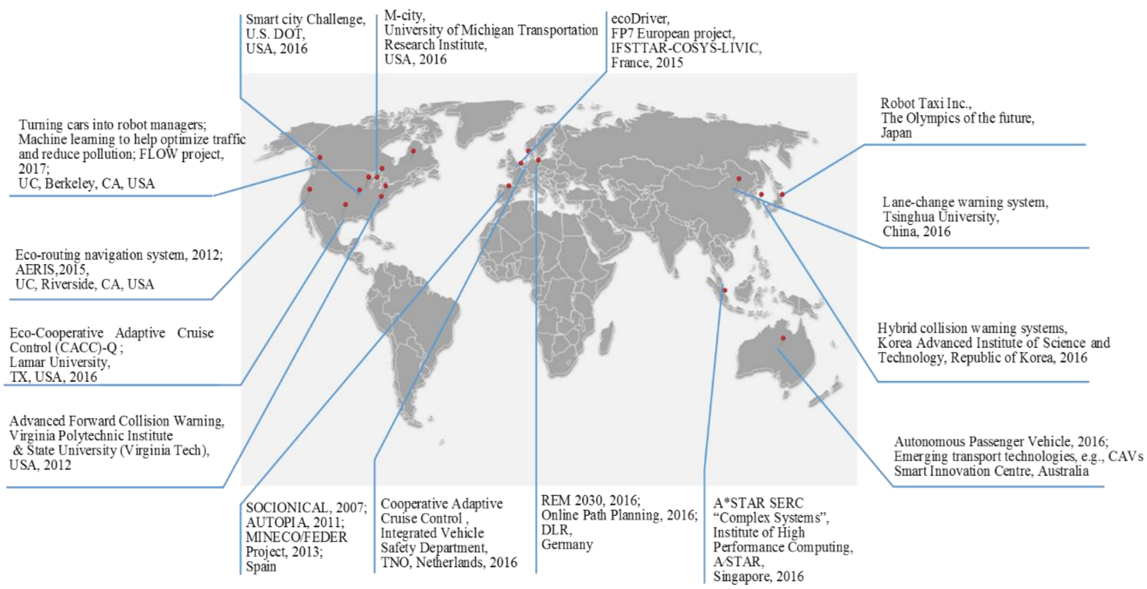

Figure 1-4. Worldwide CV Applications/Projects

CV-based applications have emerged rapidly as a key component of Intelligent Transportation Systems (ITS) and a major pillar of the Smart City Challenge in the U.S. [19]. A great quantity of relevant applications have been developed by automobile manufacturers, such as Volvo Cars' autonomous driving mode research, Toyota Motor Corporation's investment in Artificial Intelligence (AI) to reduce car accidents and showcase Vehicle-to-Everything (V2X) systems, BMW's Enlighten application showing traffic signal status ahead [20], and Honda's early deployment and effectiveness evaluation of V2X applications [21]. Also, the U.S. Department of Transportation (USDOT), with support from both public and private sectors, has developed the Connected Vehicle Reference Implementation Architecture (CVRIA) [22], which lays the foundation for many CV application development and implementation. In Europe, the European Commission has invested in CV research through programs such as seventh Framework Program and Horizon 2020 [23]. At the same time, there have been significant research activities in the area of CV technology in Asia as well. For example, Japan is setting up Robot Taxi Inc. to operate driverless cars and an online service to transport passengers to stadiums of the 2020 Summer Olympics [24].

Moreover, a number of effort has been made by different agencies to advance and promote CV research. For instance, the CVRIA summarized a large number of applications developed under the Safety Pilot program [25], the Dynamic Mobility Application (DMA) program [26], the Applications for the Environment: Real-time Information Synthesis (AERIS) program [27], and the Road Weather Connected Vehicle Applications program [28] funded by the U.S. Department of Transportation (USDOT). Also, the European Union (EU) and other countries funded several projects on the development of CV applications [29], [30].

1.1.4 Performance Measures

To evaluate the performance of various CV applications, a variety of conventional Measures of Effectiveness (MOEs) have been proposed over the years, in order to inform practitioners, researchers, and city and government planners of potential impacts of implementing specific CV programs. Safety, mobility, and environmental sustainability are the three cornerstones to evaluate the performance of the CV applications. In the literature, a variety of performance indices (PIs) were used to gauge the relevant impacts. For example, with regard to the safety MOE, Jiang et al. used time-to-collision (TTC) as the surrogate measure of collision severity to address vehicle-to-pedestrian (V2P) conflict, with the goal of providing databases for future CV development [31]. Fan et al. evaluated traffic conflicts using the Surrogate Safety Assessment Model (SSAM) [32]-[33], in which the TTC can be predicted according to relative speed and longitudinal offset between two adjacent vehicles. As for mobility MOEs, Ernst et al. proposed the estimated travel time distribution as a measure of effectiveness to conduct a comparative study on vehicle identification methods [34]. Also, the corridor efficiency, i.e., the ratio of vehicle miles traveled (VMT) to vehicle hours traveled (VHT), was used in traffic models to measure highway congestion [35]. In addition to average speed, many other parameters, such as Positive Kinetic Energy (PKE), Total Absolute second-by-second Difference (TAD) and Coefficient of Variation, were investigated to evaluate the variability in velocity. These parameters can reflect, to some extent, the “stop-and-go” pattern in traffic, where acceleration and deceleration play an important role [36]. In terms of environmental MOEs, Barth et al. used outputs from the Comprehensive Modal Emissions Model (CMEM) to compare the fuel consumption and CO_2 emissions of eco-driving vehicles versus non-eco-driving vehicles under a variety of conditions [37]. In this dissertation, we have analyzed a number of Safety, Mobility, and Environmental MOEs, and have developed a comprehensive list as described in Chapter 4.

1.2 Problem Statement

It is well recognized that Connected Vehicles (CVs) have great potential to improve road network safety, efficiency, and the environment; as such, CVs are expected to account for an increasing market share in the near future. Automobile and technology companies are quite active in developing CVs and testing CV-based applications to improve safety, mobility, and environmental sustainability (SME). However, very few studies evaluate these three performance measures holistically. There are important co-benefits and tradeoffs among SME when evaluating impacts CVs bring. I am one of the first who look at the safety, mobility, and environmental impacts of CV-based applications holistically rather than individually.

In this dissertation research, an integrated holistic analysis framework has been developed to evaluate CV-based applications from SME impacts both qualitatively and quantitatively. The co-benefit and tradeoff analysis framework for safety, mobility, and environmental impacts is shown in Figure 1-5. Many CV-based applications fall into different areas in this framework, representing tradeoffs and synergies (or co-benefits) these CV-based applications can bring.

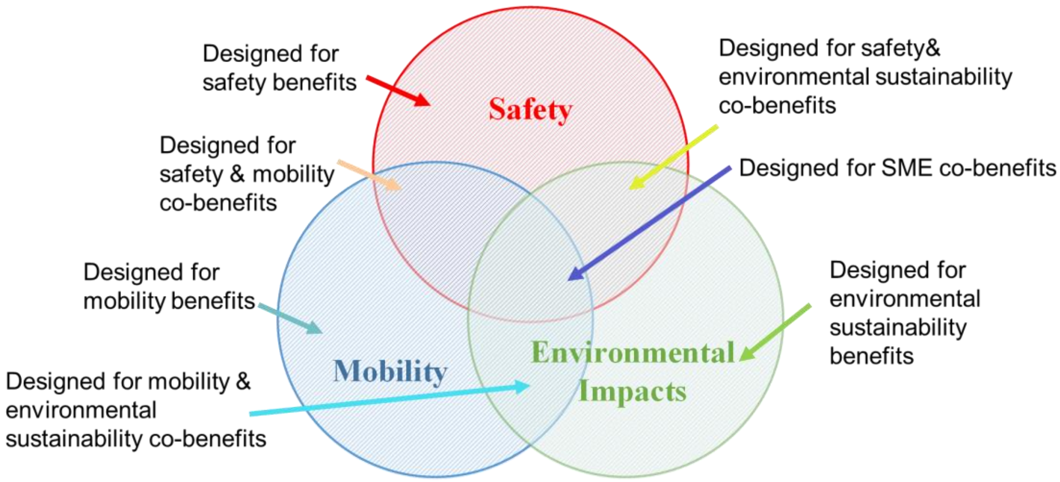

Figure 1-5. Co-Benefit and Tradeoff Analysis Framework from Safety, Mobility, and Environmental Impacts for CV-Based Applications

Under the developed qualitative analysis framework for SME, a series of innovative CV applications were proposed and developed, taking safety, mobility, and environmental impacts tradeoffs and co-benefits into consideration.

1.3 Contribution of the Dissertation

Safety, mobility and environmental sustainability are three major performance metrics when evaluating CV-based applications. These metrics can be quantified by various performance indicators, however, most of the existing CV research assesses the CV applications on only one (e.g., safety) or two (e.g., mobility and environment) aspects, without holistically evaluating the interactions among the three Measures of Effectiveness (MOEs). Rarely exists the co-benefit and tradeoff analysis. The primary objective of this dissertation is to develop a holistic evaluation environment for CV technology, analyzing the tradeoffs and synergies between safety, mobility, and environmental impacts both qualitatively and quantitatively. The dissertation has several major contributions as listed below:

- In this dissertation, an integrated holistic analysis framework of the safety, mobility, and environmental sustainability (SME) impacts of CV-based applications has been developed from both qualitative and quantitative aspects. A three-level classification of CV-based applications has been proposed first, i.e., vehicle-centric, infrastructure-centric, and traveler-centric applications. Based on both these three categories and the whole concept of SME tradeoffs and synergies in Figure 1-5, the qualitative analysis framework has been developed. Regarding the quantitative evaluation environment, three performance indicators representing the SME performance have been identified and used respectively, i.e., the conflict frequency, the average speed, and the fuel consumption. The tradeoffs and co-benefits (or synergies) among the SME impacts of CV-based applications have been analyzed under the developed holistic evaluation environment. In combination with co-benefit analysis of some typical CV-based applications, some key strategies have been identified to improve system performance and achieve SME co-benefits.
- In this dissertation, a unique innovative use of "entropy" has been developed and applied in the transportation field to help evaluate CVs holistically. To be specific, an innovative framework to evaluate the performance of CV-based applications has been proposed and developed from the perspective of Speed Variation-Based Entropy (SVE), which can accurately represent the speed variation of individual vehicles and the overall traffic. The developed SVE (and the SVE-based distribution) can be used as an MOE for CV applications in a more holistic way and at different scales. It has been concluded that the speed variation-based entropy has

a strong positive correlation with conventional MOEs (i.e., the conflict frequency and the fuel consumption), therefore, conventional MOEs can be well explained and/or estimated by the SVE as a unified measurement under a variety of scenarios.

- In this dissertation, taking into consideration the important tradeoffs and co-benefits of CV-based application, a series of innovative connected vehicle-based applications have been designed, developed, and evaluated, i.e., Lane Speed Monitoring (LSM), Optimal Lane Selection (OLS) application, and Cooperative Smart Lane Selection (CSLS) application. Specifically, the Lane Speed Monitoring application guides the vehicle driver to the fastest lane by utilizing short-range downstream vehicle information, helping the vehicle driver achieve mobility-benefits in terms of a faster travel speed. The Optimal Lane Selection adopts longer-range connectivity and guides the application-equipped vehicle driver to go through a micro-route (i.e., an optimal lane sequence) with the purpose of reducing the travel time and potential conflict risk of each individual application-equipped vehicle, obtaining mobility and safety co-benefits. The CSLS application can be regarded as an evolved version on top of the Lane Speed Monitoring (LSM) application, enabling multiple, application-equipped vehicles to cooperatively change lanes, with the goal of increasing mobility for the overall traffic system and the individual CV drivers. Finally, we aim to achieve corresponding dynamic application management under various traffic conditions.

1.4 Organization of the Dissertation

The dissertation is organized as follows: Chapter 2 describes vehicular connectivity technologies, including Dedicated Short Range Communication (DSRC) and cellular-based vehicle-to-everything technologies. Chapter 3 introduces conventional Measures of Effectiveness (MOEs) for CV-based applications performance evaluation, a variety of microscopic transportation simulation platforms and models which were used in the development and evaluation of CV applications. In Chapter 4, a broad classification of CV applications has been proposed, i.e., vehicle-centric, infrastructure-centric, and traveler-centric. Based on a comprehensive literature review, a number of typical CV-based applications have been examined in great detail, where a categorized analysis in terms of MOEs tradeoffs and co-benefits is performed. Chapter 5 uses the interdisciplinary concept and introduces the speed-variation-based entropy (SVE) and the SVE distribution, which can be regarded as a novel performance measure indicators to help evaluate CV-based applications holistically. Chapter 6 introduces the innovative connected vehicle application, Lane Speed Monitoring (LSM), and its SME tradeoff analysis under the developed integrated holistic SME analysis framework. Chapter 7 illustrates another innovative connected vehicle application, Optimal Lane Selection (OLS), which can guide the vehicle driver to go through an optimal lane sequence to reduce the travel time and conflict risk, using the spatial-temporal traffic state prediction model and the online path planning. In Chapter 8, an innovative lane selection algorithm has been designed, Cooperative Smart Lane Selection, to encourage cooperative lateral maneuvers (lane changes) and improve the network-wide mobility. We conclude the dissertation and describe potential future work in Chapter 9. In Figure 1-6, the red color represents novel parts developed in the dissertation, and black color represents technologies that have already been developed elsewhere.

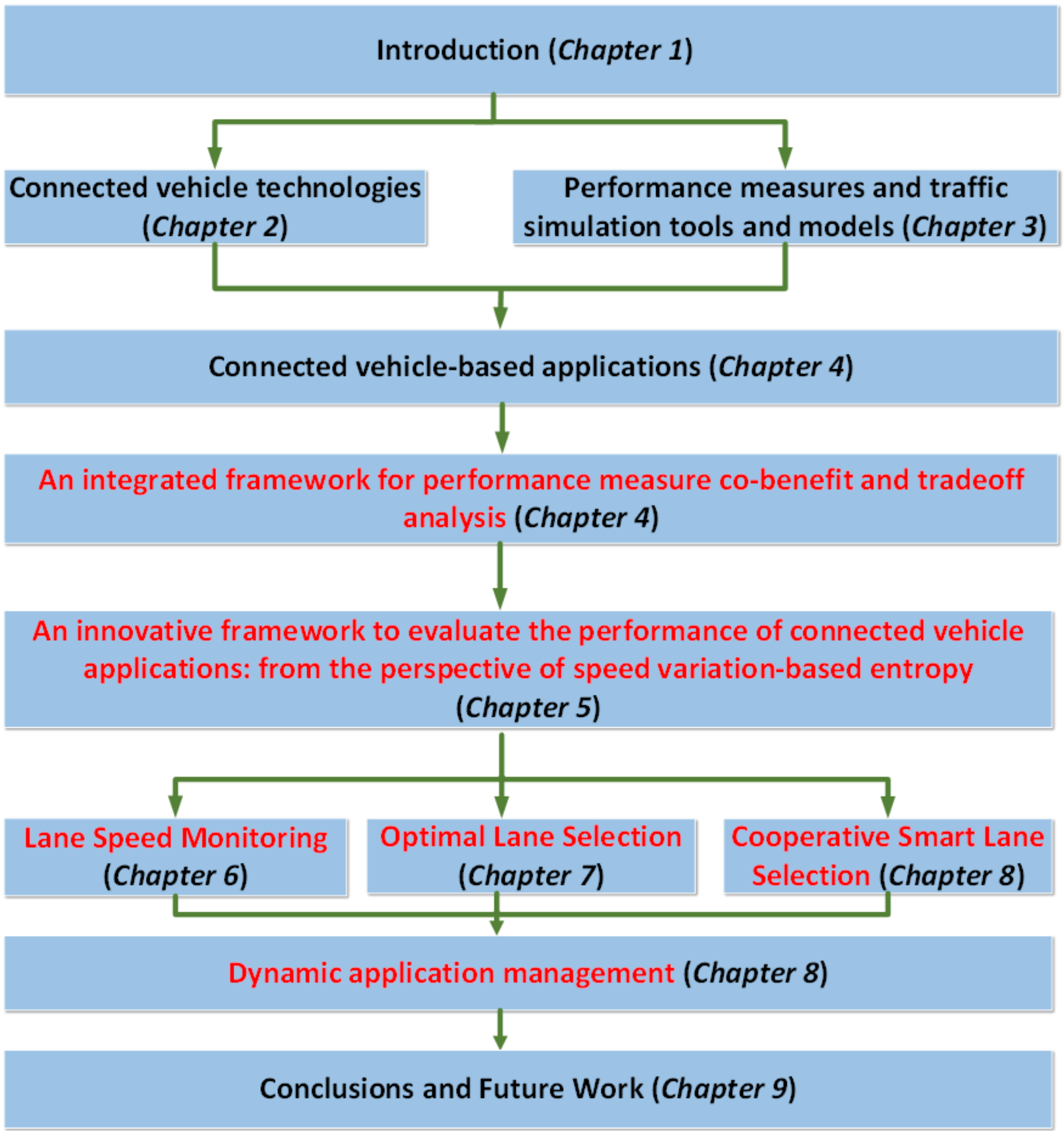

Figure 1-6. Organization of the Dissertation

2 RESEARCH BACKGROUND 1: CONNECTIVITY TECHNOLOGIES

The combination of information and communication technologies with the vehicular system significantly modernizes the transportation scenarios and patterns, enabling various Connected Vehicle (CV) based applications. Researchers around the world have been working on a variety of solutions to provide vehicle connectivity, with the goal of supporting Intelligent Transportation Systems (ITS) and CV deployments. Typical examples include Dedicated Short Range Communication (DSRC), Cellular based Vehicle-to-Everything (C-V2X) wireless communication technology, and non-standard "LTE-V", etc. Detailed descriptions of various connectivity technology models and standards are provided as follows.

2.1 Dedicated Short Range Communication (DSRC)

2.1.1 A Brief Introduction of DSRC

Dedicated short-range communications (DSRC) are one-way or two-way short-range wireless communication channels specifically designed for automotive use and a corresponding set of protocols and standards [14]. 75MHz of licensed spectrum is allocated to DSRC in the 5.9GHz bandwidth. The general name of the corresponding set of DSRC protocols and standards is Wireless Access Vehicular Environment (WAVE), which consists of IEEE 1609 standard family and IEEE 802.11p. Channel designation of DSRC is from 5.85GHz to 5.925GHz, which has been reserved for vehicular standard WAVE. In Figure 2-1, the division of time intervals include 50-millisecond Control Channel intervals (CCHI) and 50-millisecond Service Channel intervals (SCH), i.e., the total DSRC sync time interval is 100 milliseconds, which means the normal frequency for the DSRC data exchange is 10 Hz.

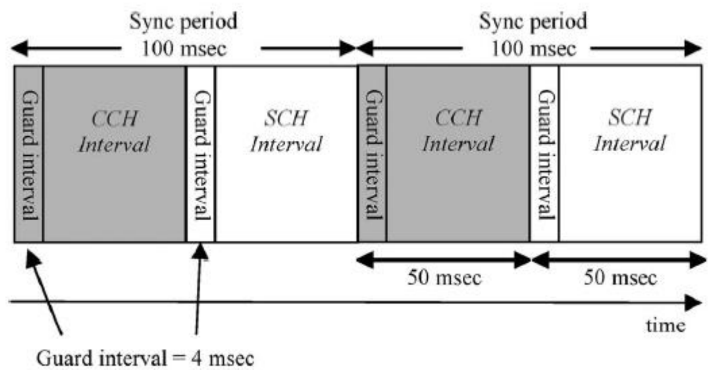

Figure 2-1. DSRC Sync Time Intervals (from [14])

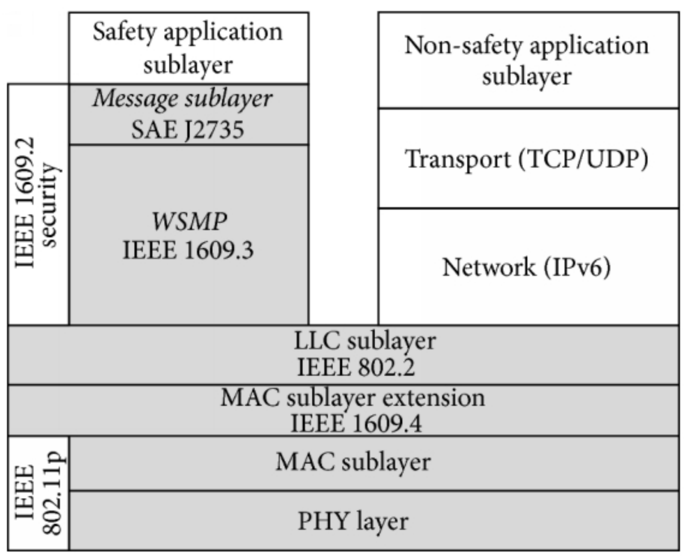

Figure 2-2. Layered Architecture for DSRC (from [14])

Figure 2-2 illustrates the layered architecture for DSRC. At the lower layer, DSRC utilizes IEEE 802.11p Wireless Access for Vehicular Environments (WAVE), which is a modified version of the IEEE 802.11 standard. The IEEE 1609.2 standard is related to the security topic in vehicular networks and responsible for security services of applications management messages. This standard defines mechanisms for authenticating and encrypting messages, especially authentication of vehicle safety messages, i.e., a Basic Safety Message (BSM) in a WAVE Short Message (WSM) (see Figure 2-3).

Data item name, Element/Frame, and length	**Description**
DSRC_MessageID element, 1 byte	The first element in every message, used by the parser to determine how to parse the rest of the message
MsgCount element, 1 byte	A sequence number, incremented with each successive transmission of a **BSM** by a given vehicle, used primarily to estimate packet error statistics.
TemporaryID element, 4 bytes	A value chosen randomly and held constant for a few minutes, it helps a receiver correlate a stream of **BSMs** from a given sender.
DSecond element, 2 bytes	The current time, modulo one minute, with resolution 1 millisecond.
Latitude, Longitude 2 elements, 4 bytes each	Geographic latitude and longitude, with resolution 1/10 microdegree.
Elevation element, 2 bytes	Position above or below sea level, resolution 0.1 meter.
PositionalAccuracy frame, 4 bytes	Conveys the one-standard-deviation position error along both semi-major and semi-minor axes, and the heading of the semi-major axis.
TransmisionAndSpeed frame, 2 bytes	3 bits encode vehicle transmission (gear) setting. 13 bits convey unsigned vehicle speed, resolution 1 cm/second.
Heading element, 2 bytes	Compass heading of vehicle's motion, resolution 1/80 degree.
SteeringWheelAngle element, 1 byte	Current position of the steering wheel, resolution 1.5 degree. Clockwise rotation is a positive angle.
AccelerationSet4Way frame, 7 bytes	Provides longitudinal acceleration, lateral acceleration, vertical acceleration, and yaw rate.
BrakeSystemStatus frame, 2 bytes	Conveys whether or not braking is active on each of four wheels, also conveys the status of the following control systems: Traction Control, Anti-Lock Brakes, Stability Control, Brake Boost, and Auxiliary Brakes.
VehicleSize frame, 3 bytes	Vehicle length and width, resolution 1 cm.

Figure 2-3. SAE J2735 DSRC Basic Safety Message Part I (from [14])

The BSM is perhaps the most important message in the J2735 standard, which conveys the core state information about the sending vehicle, namely its position, dynamics, system status, and size. It also has the flexibility to convey additional information as needed [14]. The topmost layer is about the applications. Connected vehicles-based communications serve for many applications, which imposes different requirements on Vehicular Ad hoc NETworks (VANETs). Based on the descriptions above, our major research work (CV application design and development) would be conducted based on such DSRC model, which enables DSRC-equipped vehicles to transmit and receive basic vehicle information within a short range (e.g., 300m to 500m) at 10 Hz.

2.1.2 DSRC Model in Simulation

Two types of vehicular communication technologies, i.e., dedicated short range communication (DSRC) and cellular based C-V2X wireless communication, were simulated/used in this dissertation, mimicking the current real-world V2X technology prototypes (with a few reasonable assumptions). Regarding the short range communication, the Dedicated Short-Range Communication (DSRC) was modeled in simulation based on the Packet Error Rate (PER) curves. Since Packet Error Rate (PER) for DSRC is a widely used performance indicator (PI) that is available in reports and papers, this communication model was built up in the traffic simulation tool based on such PI measured in the real world.

In the traffic simulation tool (e.g., VISSIM, note that, we introduce more details about the microscopic transportation simulation platforms in Chapter 3), the distance distribution curve was used as the tool to collect basic information (such as vehicular identity, position and kinematic information) of ego vehicle's surrounding vehicles' data. This function returns a collection of vehicle objects containing all vehicles within the range, and those vehicles were chosen stochastically based on the given distance distribution curve, which defines the possibility of a vehicle is not detected in the transmission range. Several other assumptions were made as follows:

1) As long as the Basic Safety Message (BSM) of a vehicle is correctly received within a certain time window (e.g., a simulation time step), the basic information of that vehicle can be detected.

2) The possibility $P(d)$ of a vehicle not detected in the transmission range is

$$P(d) = \left(1 - PDR(d)\right)^n \tag{2-1}$$

where *PDR(d)* is the packet deliver rate; *d* is the transmission range; *n* is number of packets sent in a certain time window.

At each simulation time step (e.g., 0.1 sec or 1 sec), if $n = 1$, then

$$P(d) = 1 - PDR(d) = PER(d) \tag{2-2}$$

Therefore, we assume that the possibility $P(d)$ of a vehicle not detected at certain transmission range is the *PER(d)* at that certain distance.

PER can be affected by various factors, such as network conditions, the packet size, the transmission rate, the transmission power, the transmission range, road conditions, the vehicular density and fading, etc. A random number generator mimics the packet error rate at certain distance in the microscopic transportation simulation software.

2.2 Cellular based Vehicle-to-Everything (C-V2X) Communication

In addition to the IEEE 802.11p based Dedicated Short-Range Communication (DSRC), the cellular-based communication, e.g., 5G based LTE-V2X, is attracting more and more worldwide attention as the essential technique that enables safe, reliable and efficient transportation service capacities, which can be deployed both near- and long-term and can meet the vehicular use case requirements of today and tomorrow [38].

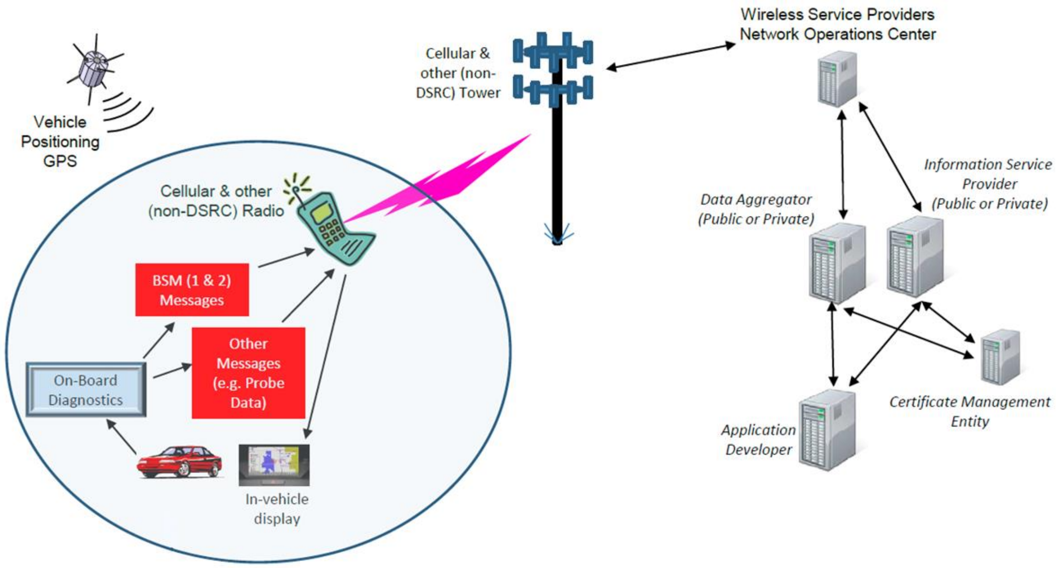

Figure 2-4. Combined (Both Long-Range and Short-Range Communication) Development Scenario for Private Vehicles (from [39]).

2.2.1 A Brief Introduction of C-V2X

Cellular based Vehicle-to-Everything (C-V2X) (developed in [16]-[17]) is a typical method for long range data transmission used in vehicular applications. To be specific, C-V2X reuses DSRC/Cooperative Intelligent Transport Systems' (C-ITS) established service and app layers. C-V2X develops abstraction layer to interface with 3GPP lower layers (in conjunction with 5GAA) and continuous enhancements to the radio/lower layers, which makes it well compatible with existing V2X technologies (see Figure 2-5).

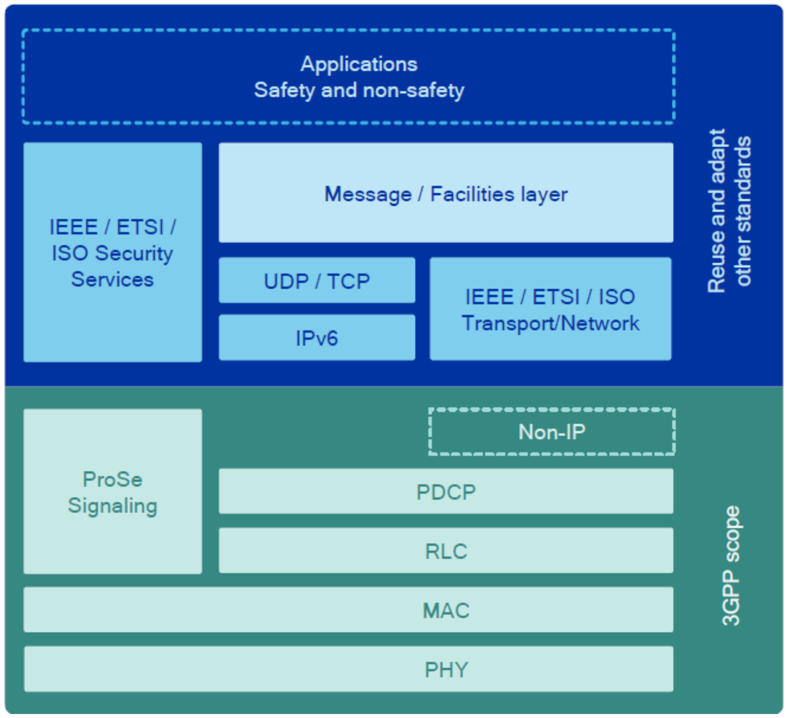

Figure 2-5. C-V2X Layers and Architecture (from [16])

For the C-V2X network communications, vehicles can send messages to the server via unicast communication, as shown in Figure 2-6. C-V2X uses LTE Broadcast to broadcast messages from the V2X server to the vehicles.

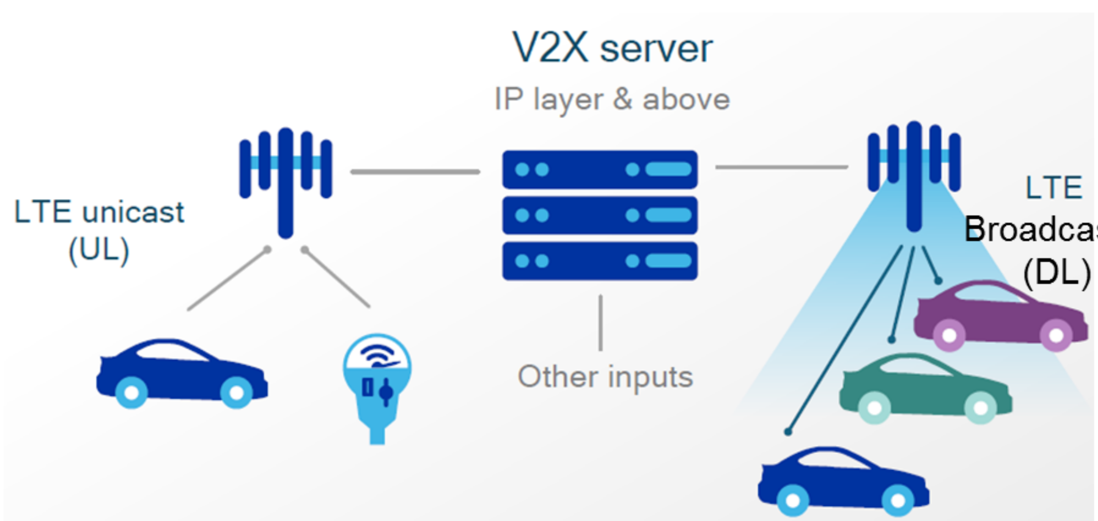

Figure 2-6. V2X Communications via the Network (from [17])

2.2.2 C-V2X Model in Simulation

Cellular based Vehicle-to-Everything (C-V2X) was selected as the real-world prototype for the cellular based wireless communication model in simulation. As a promising fifth generation (5G) technology, device-to-device (D2D) communication through C-V2X technique allows physically similar devices to communicate directly through a licensed cellular band [40]-[41]. Compared to 802.11p based communications, cellular based communication can achieve higher data rates and longer transmission ranges. Based on the use cases tested in [16] and the preliminary performance of C-V2X (see Table 2-1), several assumptions were made when simulating cellular based V2X communication in simulation as follows:

1) ***No packet loss in terms of Vehicle-to-Network (V2N).*** As shown in Table 2-1, C-V2X can guarantee no packet loss, even at high densities. No packet loss is assumed in terms of V2N in simulation, mainly due to the unavailability of real-world data or related references.

TABLE 2-1. COMPARISON: USE CASES AND PERFORMANCE [16]

Use Cases	802.11p	C-V2X Rel-14/15	C-V2X Rel-16(expected design)
Target Use Cases	Day 1 safety only	Day 1 safety & enhanced safety use cases	Advanced use cases to assist in autonomous driving including, ranging assisted positioning, high throughput sensor sharing & local 3D HD map updates
Performance			
High density support	✓ Packet loss at high densities	✓ Can guarantee no packet loss at high densities	✓ Can guarantee no packet loss at high densities
High mobility support	✓ Up to relative speeds of 500 km/hr with advanced receiver implementation	✓ Up to relative speed of 500 km/hr as a minimum requirement.	✓ Up to relative speed of 500 km/hr as a minimum requirement
Transmission range @ 90% error, 280 km/hr relative speed	Up to ~225m	-Over 450m using direct mode -Very large via cellular infrastructure	-Over 450m using direct mode -Very large via cellular infrastructure
Typical transmission frequency for periodic traffic	Once every 100msec (50ms is also possible)	Once every 100ms (20ms is also possible)	Supports packet periodicities of a few ms.

2) ***Large coverage by evolved NodeBs (eNodeBs) and one app server***. The evolved NodeB is a complex base station that handles radio communications with multiple devices in the cell and carries out radio resource management and handover decisions. In the simulation, it was assumed that sufficient evolved NodeBs supported wide coverage of information collection, and those data were transmitted to one application server for post-processing. In other words, it was assumed that no blind area existed among eNodeBs coverage; therefore, performance deterioration and impacts due to lack of network coverage were not taken into consideration.

3) ***Delay***. Since cellular-based wireless communication has a large range and needs certain time for calculation and transmission, the delay for control plane and user plane needs to be considered. A certain amount of lag (for example, 100 ms) was assumed between the time the cellular tower disseminated the information and when the communication-capable vehicle received the recommendation or command.

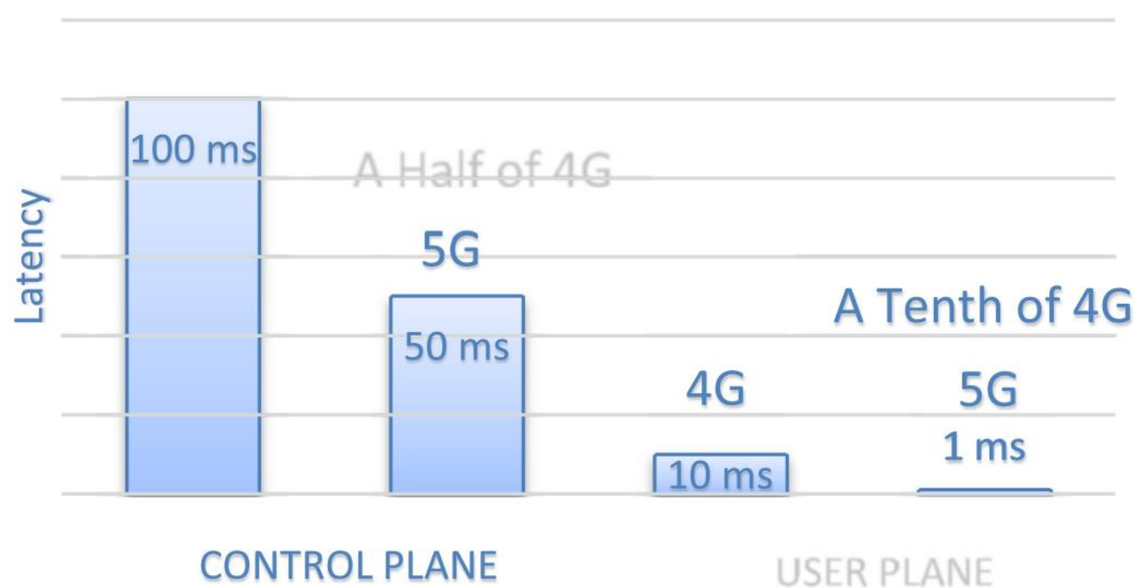

Figure 2-7. Demand to Delay in Control and User Planes for 4G/5G Networks (from [42])

2.3 Other Wireless Communication Technologies

Before 5G is fully expanded, a variety of “Towards-5G” techniques exist in the medium-term, such as the non-standard “LTE-V” that is already being explored by a number of the industry’s mega vendors in China [43]. LTE-V allows vehicle-vehicle, people-vehicle, and vehicle-network communications over the operators’ existing networks, which is the application of vehicular connectivity over existing operator mobile network infrastructure.

3 RESEARCH BACKGROUND 2: CONVENTIONAL MOEs AND MICROSCOPIC TRANSPORTATION SIMULATION TOOLS AND MODELS

3.1 Measures of Effectiveness (MOEs) for CV-Based Applications Performance Evaluation

Conventionally, SME (short for Safety, Mobility and Environmental sustainability) are three key areas where different types of Measures of Effectiveness (MOEs) have been defined when evaluating the performance of CV-based applications. Since we develop an integrated SME analysis for a series of CV applications, the corresponding SME performance measure indicators used for application performance evaluation in this dissertation are described in this chapter. (For more details about a variety of performance indicators of CV applications in the literature, please see Figure 3-1.)

3.1.1 Safety MOEs

Minimum time to collision (TTC) is regarded as a surrogate measure of the likelihood of a conflict occurring [44]. An occurrence when the minimum TTC drops below a predefined threshold may be recognized as a potential conflict. In this dissertation, safety performance is evaluated by the normalized conflict frequency defined below:

$$CF = \frac{\sum_{i=1}^{n} cn_i}{n} \tag{3-1}$$

where cn_i is the number of conflicts caused by vehicle i; n is the total number of vehicles. It is noted that each conflict is herein only associated with the second vehicle (i.e., the one occupying the conflict area at a later instant) which is assumed to be responsible for the potential conflict.

3.1.2 Mobility MOEs

Corridor efficiency or average speed, $\bar{v}$, is used to evaluate mobility performance:

$$\bar{v} = \frac{\sum_{t=1}^{T}\sum_{i=1}^{N_t} VMT_{i,t}}{\sum_{t=1}^{T}\sum_{i=1}^{N_t} VHT_{i,t}} \tag{3-2}$$

where $VMT_{i,t}$ and $VHT_{i,t}$ represent vehicle miles traveled and vehicle hours travelled, respectively, for vehicle i in time step t; N_t is the total vehicle number in a range of road network in time step t; T is the certain time duration of interest within the range of road network.

Moreover, travel time is another indicator used in this dissertation to measure the mobility relevant performance of specific CV applications.

3.1.3 Environmental MOEs

In this dissertation, the fuel consumption of an individual vehicle or fleet is used to measure the environmental performance, which is positively proportional to the generated greenhouse gas emissions (e.g., carbon dioxide equivalent). In addition, other environmental impacts can include pollutant emissions and number of stops, etc.

There exist some main performance measures when evaluating CVs as shown in Figure 3-1. Among them, safety, mobility, and environmental sustainability are the three cornerstones of the performance measures. A lot of work has been done to identify and define the indicators accordingly, shown in the corresponding boxes in Figure 3-1. Note that the performance measures which were focused in this dissertation research is written in red color.

In addition, there are also other key things regarding the social inclusion and land use. As a part of the potential future work, tradeoffs can be made across different measures of effectiveness, for example, an integrated analysis can be conducted for different performance measures in combination with the economic effects, by formulating optimization problems, to better plan the community distance and other social resources assignment.

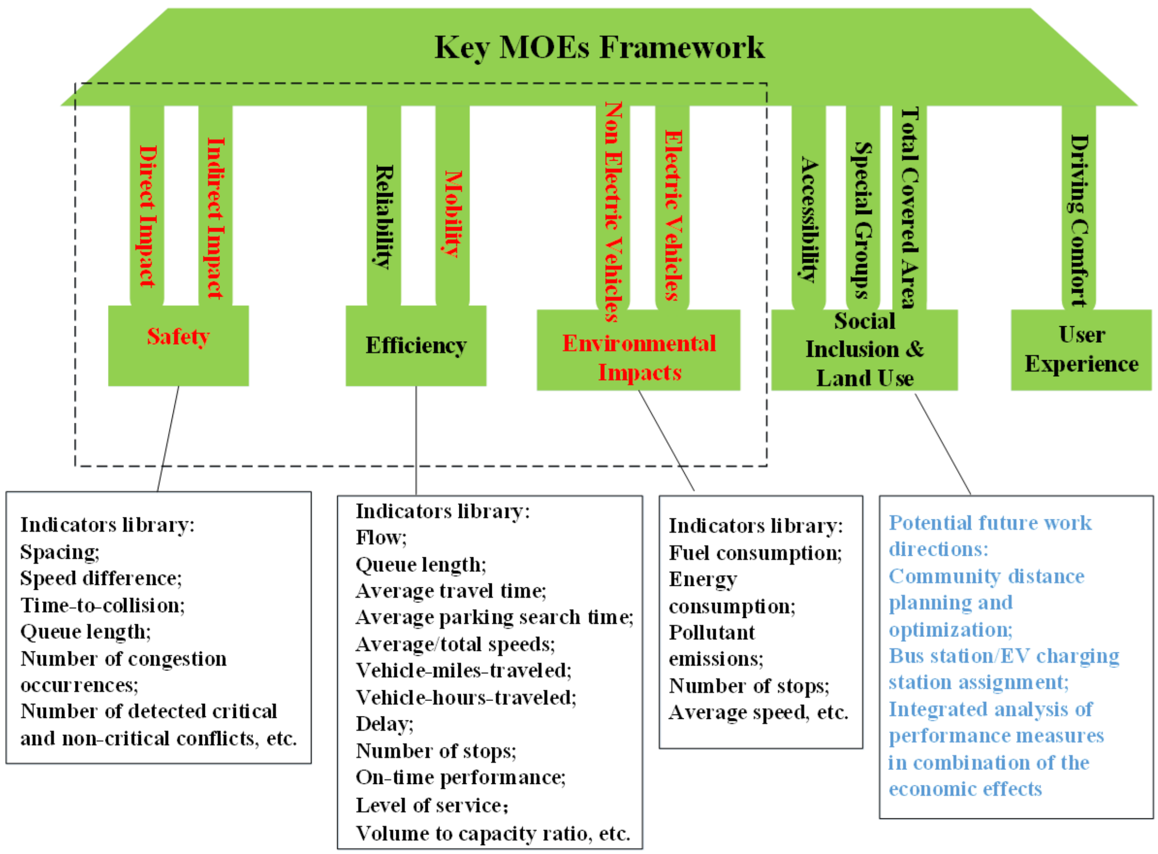

Figure 3-1. Overview of the Performance Measurement Framework (We focused MOEs in Red in This Dissertation) (from [45])

3.2 Microscopic Transportation Simulation Tools and Models

Characteristics of most existing traffic simulation tools are from microscopic, macroscopic, and sometimes mesoscopic perspective, able to model real-world networks, simulate vehicle or other objects movement in continuous space and discrete time, and generate network-wide, vehicle-based, and detector-based outputs. According to the work in [46] and [47], the main features of a few microscopic traffic simulation models are summarized and compared. Among them, two microscopic transportation simulation tools (i.e., PARAMICS and VISSIM) were investigated and utilized in this dissertation to establish various sophisticated traffic networks, simulate driver behaviors, and implement different traffic control strategies.

The PARAMICS is a high-resolution traffic simulation tool capable of modeling large-scale roadway networks and the movement of each individual vehicle [48]. The behavior of each vehicle such as car following, lane changing and route choice can be customized by users, via configuration of key parameters by Graphical User Interface (GUI) or development of Application Programming Interfaces (APIs) using the Programmer module. PTV VISSIM is based on a traffic flow model which considers driver-vehicle-units as single entities and contains a Wiedemann-based car following model for longitudinal vehicle movement and a rule-based algorithm for lateral movements [46], [49], [50], and [51]. VISSIM provides add-on modules programming interfaces, to enable the override of default behavior and development of various new functions or applications. Both PARAMICS and PTV VISSIM can generate various trajectory files (one type at one time) for further data analysis and post processing.

The Surrogate Safety Assessment Model (SSAM) is a post-processing model designed for the safety analysis of traffic facilities, roadway designs, and operational strategies [33]. SSAM can output the number of potential conflicts as aforementioned in Section 3.1.1. Specifically, the outputs of SSAM include the vehicle IDs associated with each conflict, severity and locations of simulated conflicts based on the predetermined threshold values of the maximum TTC, the maximum PET, the rear end angle, and the crossing angle [52], [53].

EPA MOVES is a state-of-the-art modeling tool developed by the U.S. Environmental Protection Agency (USEPA) for estimating the energy consumption and emissions from mobile sources at different scales [54]. MOVES categorizes all vehicles into over twenty source types and evaluates the emission rates of the vehicles in one source type under specific operation mode [55]. Compared to the MOVES model that belongs to data-driven models and generates the emission output of an individual vehicle by using the average behavior of all vehicles in same source type, CMEM takes specific parameters of the individual vehicle and is expected to be able to calculate the emissions and fuel consumption with higher accuracy [56].

In this dissertation, fuel consumption/emissions of a large number of vehicles on system level were evaluated, for example, aggregated data of application equipped vehicles, unequipped vehicles, and overall vehicles, rather than one specific individual vehicle. Thus EPA MOVES was herein used as the models for environmental evaluation. For details of the interaction among different modeling tools and the corresponding MOEs outputs, please see Figure 3-2.

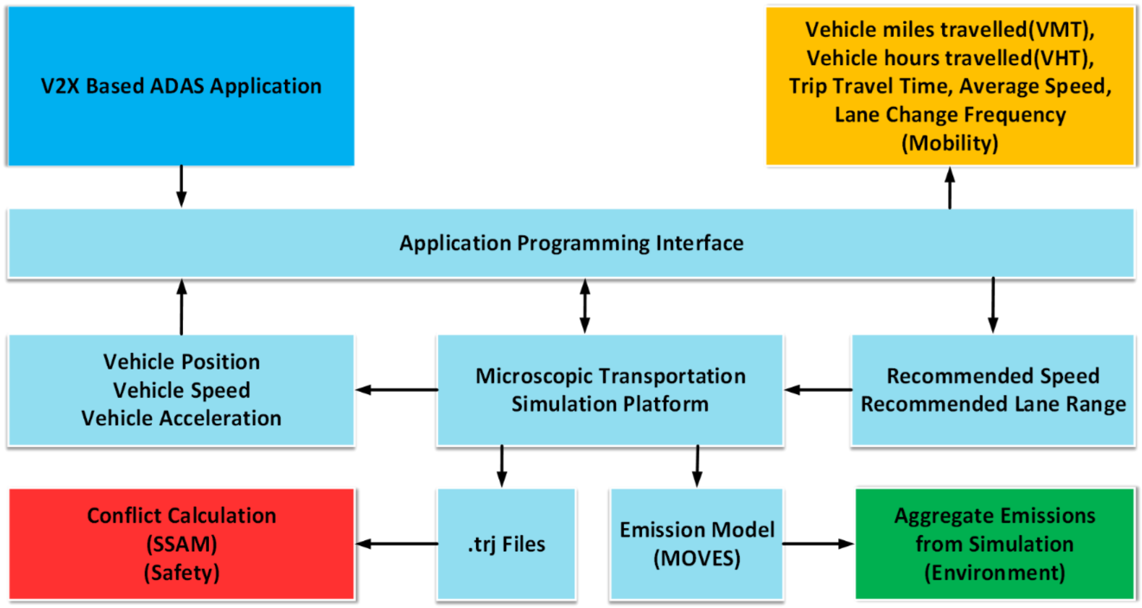

Figure 3-2. Interaction among Different Modeling Tools, and the Corresponding MOEs Outputs

4 FRAMEWORK OF PERFORMANCE MEASUREMENT AND MOEs CO-BENEFITS AND TRADEOFFS FOR CONNECTED VEHICLES BASED APPLICATIONS

To better understand the different CV-based applications in a systematic way, we have conducted an extensive survey of the literature, and have developed a framework to classify them. In a broad sense, the CV-based applications may be classified into three categories, depending on the type of objects targeted by the applications.

a) *Vehicle-centric*: Vehicle-centric applications are primarily driven by on-board sensors and communication technologies, aimed at the ego-vehicle and/or the surrounding traffic. This type of CV applications is mainly designed to adjust the ego vehicle's operations (e.g., longitudinal control), or to respond to its surroundings. Examples of vehicle-centric applications include adaptive cruise control and lane departure warning.

b) *Infrastructure-centric*: Infrastructure-centric applications enhance roadway performance by means of centralized surveillance, control, and analysis of roadway infrastructure via inductive loop detectors, communication-capable roadside units, and Traffic Management Centers (TMC). Examples of infrastructure-centric applications are ramp metering and variable speed limit systems.

c) *Traveler-centric*: Other than vehicles, travelers can also supply and receive information through connectivity to protect themselves from collisions and accidents or receive valuable information, such as route guidance. These travelers include drivers, transit riders, pedestrians, bicyclists, and even wheelchair users. Traveler-centric applications connect a variety of travelers with information regarding other objects in the traffic network, e.g., vehicles and infrastructure. Examples include advanced traveler information system and pedestrian collision warning.

There are numerous research activities all over the world focusing on CV-based application development and a large number of studies on impact assessment and cost-benefit analysis of CV-based applications have been conducted, especially in Europe. However, there have been very few research effort looking into all possible benefits of these applications simultaneously. In this chapter, we first present a benefit evaluation framework for CV-based applications and a performance-oriented taxonomy based on key performance metrics in Section 4.1. A category summary is then discussed in Section 4.2, followed by the detailed analysis of potential co-benefits of some CV-based applications in Section 4.3. Section 4.4 provides a summary of the research findings.

4.1 Performance-Oriented Taxonomy of CV-Based Applications

By incorporating advanced sensors, communication technologies and autonomous control into today's vehicles, CV-based applications are able to greatly benefit the transportation systems and significantly enhance safety, improve mobility, and reduce environmental impacts. Inspired by some existing performance measure analysis [57] and surveys [58]-[59], we developed a comprehensive performance measure evaluation framework, by including additional performance indicators used in other papers, of which the overview has been shown in Figure 3-1. A brief description of the three major performance metrics, i.e., safety, mobility and environmental impacts is provided below. Examples of CV-based applications that target one or more of the three performance metrics are given in Figure 4-1. Several of these applications are from the recent literature in 2015 and 2016. Some of these applications are also examined in detail in Section 4.3 of the paper.

A) ***Safety***

Safety is the primary goal of many ITS and CV-based applications. Safety-oriented CV-based applications enable vehicles to mitigate movement conflicts on roadways. Notifications or warnings for collision avoidance are issues through infrastructure-based and/or vehicle-based cooperative safety systems [60]. Examples include forward collision warning and lane keeping assistance.

B) ***Mobility***

Mobility-oriented CV-based applications employ methods and strategies aiming at increasing the operational efficiency of transportation systems and thus improving the mobility of individual travelers. Transportation system efficiency is referred to as the good use of transportation resources such as roadway capacity and travel time, with the objective of producing an acceptable level of transportation outputs such as roadway throughput and travel distance. Examples of mobility-oriented CV-based applications are platooning and traffic signal coordination.

C) ***Environmental Impacts***

The transportation sector has been a major contributor to air pollution and greenhouse gas emissions. It has now been widely accepted that ITS and CV-based technologies can help significantly reduce transportation-related emissions. Over the last several years, a number of CV-based applications have been developed that are focused on reducing energy and emissions associated with transportation activities. Examples include eco-routing navigation and eco-driving assistance.

4.2 Category Summary

According to Figure 4-1, most of the current CV-based applications are not designed to be capable of achieving the three aims at the same time and most of the applications listed are safety-oriented. While these applications are focused primarily on avoiding crashes and accidents [61] or even detecting and predicting on-road irregular driving behavior [62] resulting in direct safety benefits, many of them also provide indirect or co-benefits (e.g., mobility improvement and/or pollutant emissions reduction). On the other hand, some safety-oriented applications may result in negative indirect impacts on mobility and environment, which can be viewed as tradeoffs among the different metrics. These arguments also apply to the mobility-oriented and environment-oriented CV-based applications as well.

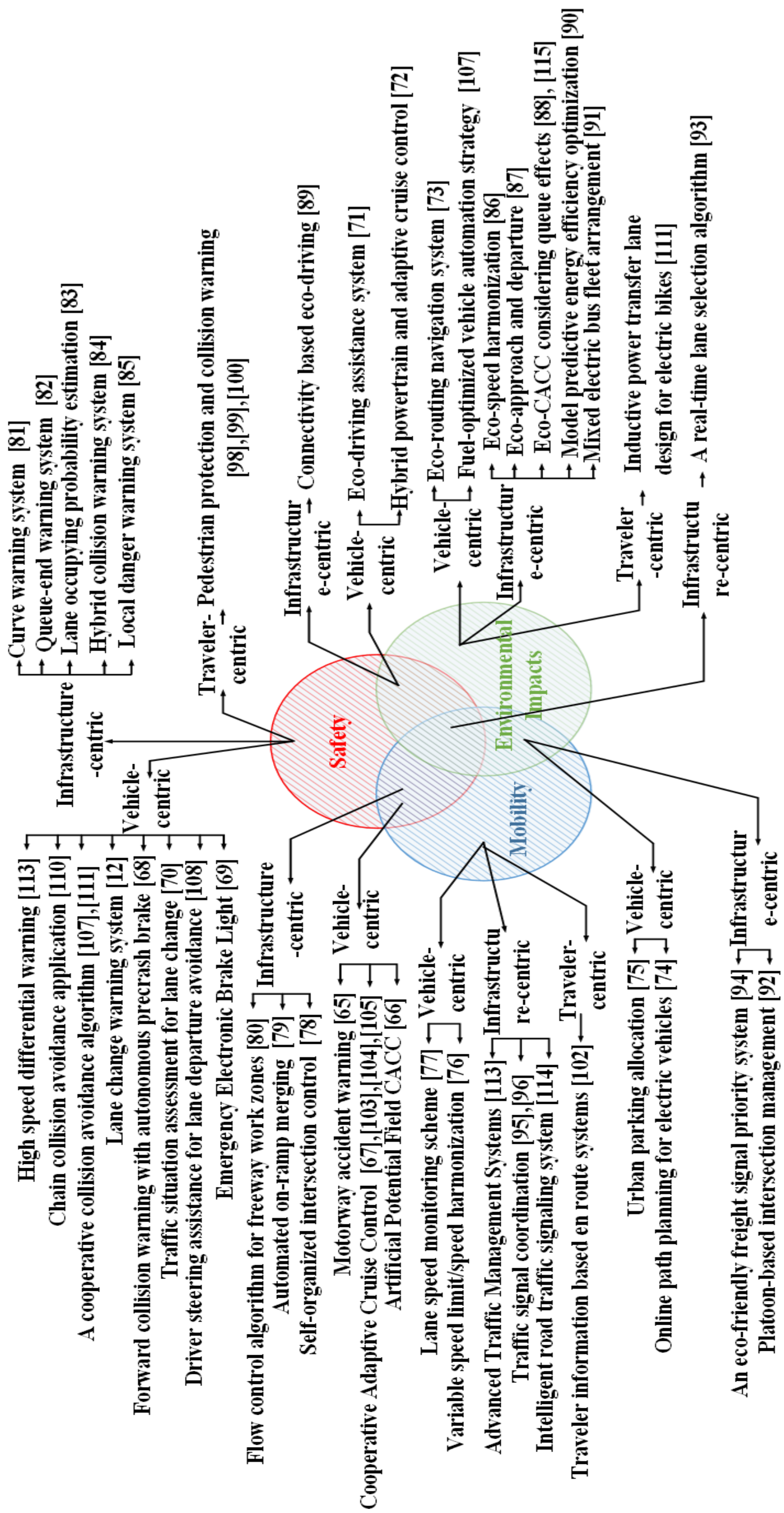

Figure 4-1. Taxonomy of CV-Based Applications (from [45])

Table 4-1 summarizes these co-benefits and tradeoffs. It can be seen that safety is the most common target among all the CV-based applications reviewed in this study. Please note that the criteria of whether the aims are achieved also depends on what the baseline is. The performance is usually compared under the same traffic situation with and without such CV-based application. For instance, a queue-end warning application may improve "safety" in highway work zones due to the potential reduction in rear-end collision, even though the collision risk in work zones may still be higher than in other areas.

TABLE 4-1. CATEGORY SUMMARY OF CV-BASED APPLICATIONS IN TERMS OF DIFFERENT MOEs

Safety focused (25)	S M E ↑ ? ?	S M E ↑ ↑ ?	S M E ↑ ? ↑	S M E ↑ ↑ ↑
	15 out of 25 (60%)	6 out of 25 (24%)	3 out of 25 (12%)	1 out of 25 (4%)
Mobility focused (18)	S M E ? ↑ ?	S M E ↑ ↑ ?	S M E ? ↑ ↑	S M E ↑ ↑ ↑
	7 out of 18 (39%)	6 out of 18 (33%)	4 out of 18 (22%)	1 out of 18 (6%)
Environmental impacts focused (15)	S M E ? ? ↑	S M E ↑ ? ↑	S M E ? ↑ ↑	S M E ↑ ↑ ↑
	7 out of 15 (47%)	3 out of 15 (20%)	4 out of 15 (27%)	1 out of 15 (7%)

S: Safety; **M**: Mobility; **E**: Environmental impacts; ↑: Improvement;**?**: Unknown, Neutral or Deteriorate

There are very few studies that evaluate all three MOEs, and the co-benefits and tradeoffs among the three MOEs of CV-based applications are rarely analyzed. Although a portion of CV-based applications are designed to improve more than one MOE (usually two), very few of them improve all the three MOEs. Several CV-based applications can be combined to achieve a comprehensive performance. For instance, vehicle platooning (increasing throughput) and collision avoidance functions (enhancing safety) can be incorporated into the intelligent energy management function in hybrid electric vehicle or plug-in hybrid electric vehicle platform (reducing fuel consumption). In terms of multiple

MOEs, this combined CV-based application will likely outperform the case where only individual applications are applied. In general, multiple CV-based applications tend to be combined to achieve improvements of transportation systems in a more holistic way.

4.3 Co-benefit Analysis of Typical V2X-Based CV Applications

All on-road communication-capable objects could share their information via wireless connectivity technologies, such as the Dedicated Short-Range Communication (DSRC) devices mounted on on-road units [14], and/or mobile devices enabled by cellular technologies (e.g., smart phones with built-in sensors) [15], [63]. The exchange of information between two terminals could supply users' basic motion dynamics to the CV-based applications and help increase the users' environmental awareness to benefit the transportation system, achieving the preset objectives in terms of transportation performance improvement.

Some typical examples of various CV-based applications in the latest literature are addressed herein. At the same time, co-benefits/tradeoffs among the three major MOEs are analyzed, under the categories introduced at the beginning of this chapter. Table 4-3 lists the vehicle-centric applications, and the symbols used in Table 4-3, Table 4-4 and Table 4-5 are listed in Table 4-2.

TABLE 4-2. SYMBOLS FOR MOEs CO-BENEFITS AND TRADEOFFS IN THE LITERATURE REVIEW TABLES

	Performance Validated		Performance Non-validated		
	Improvement	Deterioration	Improvement	Deterioration	Unknown
Targeted	●↑	●↓	◑↑	◑↓	○
Non-targeted	◐↑	◐↓	○↑	○↓	

4.3.1 Vehicle-Centric CV-Based Applications

4.3.1.1 Safety & Mobility Co-Benefits

Aimed at enhancing traffic safety, there are plenty of valuable research activities on CV-based applications that have been carried out, focusing on road environment awareness. Based on modern communications technologies, a lane closure alert has been proposed by Fullerton et al., allowing drivers to be notified sooner to emergency situations, e.g., a sudden lane drop or motorway vehicle breakdowns [64]. Based on the simulation results of this warning system, the authors concluded that a gradual slow-down ought to be enough to reduce the potential risk of follow-on rear-end collisions. For this safety-focused driver advice system, the relief of bottlenecks congestion has great potential to increase the capacity of lane closure areas to some extent, leading to mobility co-benefit. Another typical example of CV-based applications which aims to improve both traffic flow and safety is the Cooperative Adaptive Cruise Control (CACC) system [65]. Dey et al. presented an overall review of CACC system-related performance evaluation. Besides the front radar used to prevent potential conflicts, it was concluded that the CACC application also has the capability of enhancing mobility by increasing the traffic capacity (improving traffic flow) under certain penetration rates, and by harmonizing the speeds of platoons in a safe manner [66].

4.3.1.2 Safety Benefits

The Forward Collision Warning application is a relatively mature application, which is commonly used to improve situation awareness and enhance safety performance. The effectiveness among several pre-collision system algorithms was examined using

Time-to-Collision (TTC) as a surrogate collision risk evaluation in [67], where Kusano & Gabler proved that performance of the conventional forward collision warning was significantly improved by integrating a pre-crash brake assistance as well as an autonomous pre-crash braking scheme. Likewise, Szczurek et al. presented an Emergency Electronic Brake Light application-related algorithm, and showed safety benefits represented by the lower average number of collisions [68]. However, besides potential safety benefits, potential mobility and environmental impacts gains/costs still remain to be shown in both [69] and [68], where safety benefits are probably achieved at the expense of larger greenhouse gas (GHG) emissions due to increased stop-and-go behavior. This might happen in other similar safety-oriented collision avoidance applications, e.g., intersection collision warnings, curve speed warnings and pedestrian warning systems, where stop-and-go activity will likely increase.

As the safety of the lane change operation is one of the most concern issues in the transportation system, lane change warning systems and lane change assistance systems have been attracting more and more attention. Schubert et al. fused on-board cameras and a decision-making approach to execute automatic lane-change maneuvers, and tested the algorithm on a concept vehicle Carai [69]. However, detailed quantitative effectiveness evaluation regarding traffic safety was not evaluated in [69]. In addition, Dang et al. take into account the drivers' reaction delay and brake time and proposed a real-time minimum safe distance model [12]. The simulation results obtained from Simulink show that this system generate lane change warning with the assist of TTC analysis, however, no other MOEs evaluation was mentioned other than potential safety improvements.

4.3.1.3 Environmental Impacts & Safety Co-Benefits

As aforementioned, safety and environment protection are always the first two of the most concerned issues concerning CV-based applications preset objectives. Some co-benefits in terms of safety aspects can be well achieved by environmental impacts-oriented CV-based applications. In this direction, an Android system based eco-Driving application was developed by Orfila et al., comprising the integration of upcoming road features recognition and crash relevant events identification modules, estimating the recommended speed with the purpose of supplying drivers an eco-friendly speed [70]. Even though one of the objectives was to improve the safety performance, potential safety effectiveness was not evaluated other than fuel savings results. Furthermore, the speeds with the proposed system are slower probably due to the safe eco-driving system that contributes to the steady-speed, smooth-deceleration behavior, therefore resulting in reduced mobility with longer travel times. Another approach was proposed by Li et al. with the aim of achieving environment impacts improvement as well as safety improvement. A hybrid powertrain was incorporated with the conventional Adaptive Cruise Control (ACC) in [71], aiming to enhance traffic safety and to reduce the driver's effort. By comparing velocity profiles of vehicles without and with the proposed system, Li et al. show that vehicles' velocity profiles of the proposed system are smoother with lower overshoot. Moreover, since the study takes advantage of the high fuel efficiency scheme of hybrid electric systems, the engine torque and fuel improvement were investigated in [71] as well.

TABLE 4-3. VEHICLE-CENTRIC CV-BASED APPLICATIONS

Categories	Platform	Project/Application name & Ref	MOE focus			Contributions
			S	M	E	
Vehicle-centric	Non-EV	EU 7th Seventh Framework Programme research project SOCIONICAL [64]	◑↑	●↑	○	An emergency situation alert system leading to reduced and harmonized speed in the vicinity of motorway bottlenecks in order to ensure a smoother and safer traffic flow
		FP7 European project ecoDriver [70]	◑↑	◐↓	●↑	An Android based application taking into account upcoming events/evaluation and analysis of driver behavior to advise drivers the best actions for lower energy consumption
		MINECO/FEDER Project [108]	●↑	○	○	A stochastic model regarding the surrogate measurement for accidents evaluation of cooperative chain collision warning applications
		Cooperative Adaptive Cruise Control [65]	◑↑	◑↑	○	An analysis on gap closing and collision avoidance functionality of the Cooperative Adaptive Cruise Control system
		Cooperative Adaptive Cruise Control [66]	◑↑	◑↑	○	A review of Cooperative Adaptive Cruise Control systems which have the potential to improve traffic throughput by increasing the roadway capacity and to harmonize the speeds of moving vehicles in the platoon in a safe manner
		Advanced Forward Collision Warning [67]	●↑	○↓	○↓	A pre-collision system integrating forward collision warning, pre-crash brake assist and autonomous pre-crash brake to reduce severe highway crashes
		Emergency Electronic Brake Light [68]	● ↑	○↓	○↓	A machine learning approach-based emergency brake warnings relevance-decision estimation for safety applications
		Automatic Lane-Change [69]	◑↑	○	○	A situation awareness-based automatic lane-change scheme based on image processing, Kalman filtering and Bayesian networks approaches
		Lane Change Warning [12]	◑↑	○	○	A V2V-based lane change warning system, analyzing safe distance between the ego vehicle and its surrounding vehicles in both the original lane and the target lane
		Eco-routing navigation system [72]	○	◐↓	●↑	An eco-routing navigation system accommodating origin-destination inputs through user interfaces to assist the driver to find the most eco-friendly route
		Urban parking management [74]	○	◑↑	◑↑	Online localized cooperative resource allocation models for urban parking management to decrease available parking spots search time
		Connected Vehicles Harmonizer [75]	○↑	●↑	○↑	A connected vehicle-based shockwave propagation control system using an optimization program to reduce travel time in the freeway work zone bottleneck
		Lane Speed Monitoring [76]	◐↓	●↑	◐↓	A lane speed monitoring system using basic safety message exchange between communication-capable vehicles to advise the driver faster lane to change to
	EV	Adaptive Cruise Control [71]	◑↑	○	●↑	An intelligent hybrid electric vehicle (i-HEV) platform incorporating a hybrid powertrain scheme with the adaptive cruise control application to achieve comprehensive performance
		Online Path Planning [73]	○	◐↑	●↑	A real-time micro path planning algorithm tested on the robotic electric vehicle research platform ROboMObil together with the velocity profile generation to make the energy saving capabilities achievable

S: safety; M: mobility; E: environmental impacts

4.3.1.4 Environmental Impacts Benefits

As for the environmental impacts-focused CV-based applications, Eco-routing system scheme turns out to be a very valuable algorithm that is beneficial to the environment. Boriboonsomsin et al. proposed an eco-routing navigation system, fusing multiple sources traveler information, incorporating the optimal route calculation engine and the human-machine-interface to reduce fuel consumption and pollutant emissions [72]. The trade-off between mobility and environmental impacts of the proposed system was described in [72]. The authors concluded that significant fuel savings can be well achieved from eco-routes rather than the fastest route, leading to travel time increase, and the trade-off between travel time and fuel consumption can be comparable, especially for long trips.

4.3.1.5 Environmental Impacts & Mobility Co-Benefits

Some mobility improvement-oriented CV-based applications are developed from the angle of path planning. For example, Winter et al. presented an online micro geometric path planning methodology using curvature minimization algorithm to decrease travel time. Simultaneously the maneuverable robotic electric vehicle research platform ROboMObil was used to achieve the energy saving [73]. On the other hand, resource allocation is another approach to improve both mobility and environmental impacts. Zargayouna et al. proposed the resource allocation model to achieve the management of parking spots in an urban area taking into consideration both the location and the resources availability moment [74]. The urban parking management is expected to reduce fuel consumption by decreasing parking spots search time.

4.3.1.6 Mobility Benefits

There are very few CV applications purely focusing on mobility improvement to date. A freeway work zone harmonizer was proposed, which was mainly designed to control shockwave propagation to reduce travel time delay [75]. The congestion duration and travel time delay were evaluated and it turned out that a minimum penetration rate of equipped vehicles must exist to guarantee the satisfactory efficiency of the proposed system. Another application called Lane Speed Monitoring (LSM) system has been studied in [76], which was proposed to estimate lane-level traffic state and to advise the driver to change to a faster lane, targeting to improve travel time. The average speed of equipped vehicles and unequipped vehicles were compared, and the fuel consumption and potential conflict number were also investigated in [76]. Higher velocity is achieved for equipped vehicles, whereas the fuel consumption and potential conflict of equipped vehicles are higher as well due to the encouragement of more aggressive driving behaviors (e.g., frequent lane changes and higher speed).

4.3.2 Infrastructure-Centric CV-Based Applications

Infrastructure-centric CV application is another one of the key components regarding the traffic performance improvement and is well studied in the literature. Those infrastructure-centric applications can be further divided into two groups based on the control strategy implemented: decentralized (controlled by a localized infrastructure) and centralized (controlled by a traffic management center).

4.3.2.1 Safety & Mobility Co-Benefits

The fundamental task of localized infrastructure in the decentralized infrastructure-centric CV applications is to collect and relay the vehicles information within a certain range. A number of studies have explored the decentralized control strategies. Yang and Monterola proposed a self-organized approach where each individual vehicle approaching the intersection governs its own motion dynamics by using the equipped intersection cruise control device together with the beacon as the information relay of approaching vehicles in the intersections of urban area [77]. Since fully stopping right before crossing the intersection reduces the capacity of the intersection, the proposed decentralized traffic control system smoothens the individual vehicle dynamics and actively helps eliminate human driver errors to guarantee the overall safety when vehicles pass through the intersections. Fundamental traffic flow diagrams were plotted and compared in [77], and Yang and Monterola show the proposed control scheme's positive effects to the intersection capacity. Direct tests on safety, environmental impacts and other mobility-related indicators were not investigated. However, based on our analysis, it is expected that the fuel consumption likely decreases since there are smoother traffic flows in the intersections and more efficient braking operations. Considering the lane merging control schemes in the decentralized manner, Milanés et al. proposed an on-ramp merging system, which consists of a reference distance decision algorithm and a fuzzy controller to operate the vehicle's longitudinal control, based on information acquired from the localized infrastructure [78]. The study investigated the performance of the proposed system through real-world experiments, and Milanés et al. showed how three vehicles coordinate in order to alleviate the congestion and improve traffic flow in a merging situation by presenting the trajectories, speed profiles and relative distances results. In the same direction, Pei and

Dai presented an intelligent lane merge control system for freeway work zones [79]. Pei and Dai used a traffic information collection system to comprehensively identify traffic states (e.g., traffic volume, velocity and occupancy) and implemented a variable lane merge strategy in VISSIM simulation software to produce mobility-related performance indices, such as capacity, delay and queue length. Moreover, performance in terms of the observed collisions number was compared among several merge control strategies.

4.3.2.2 Safety Benefits

As aforementioned, most reported infrastructure-centric applications are also focused on safety benefits in terms of collision mitigation. A safety-oriented application based on vehicle-infrastructure-driver interaction, an advanced curve warning system, was proposed in [80] as speed limitation/harmonization scheme on sharp roadways. The proposed system was tested in Matlab/Simulink, integrating the upcoming road geometry feature and a safe speed implementation module. Similar to [64], a queue-end warning system was presented in [81] where numerous sensors and an artificial neural network model-based algorithm were used to predict queue-end location. The information was displayed on portable variable message signs to avoid rear-end collisions in highway work zones. VISSIM was utilized to test the queue formation and dissemination in highway work zones. Another example of safety-focused applications has been presented in [82], where a safety-critical situation awareness warning system based on lane occupying probability estimation algorithm via vehicle-to-infrastructure communication was proposed with the purpose of improving road users' safety at intersections.

TABLE 4-4. INFRASTRUCTURE-CENTRIC CV-BASED APPLICATIONS

Categories		Project/Application name & Ref	MOE focus			Contributions
			S	M	E	
Infrastructure-centric	Decentralized	A*STAR SERC "Complex Systems" [77]	◑↑	●↑	○↑	A self-organized intersection control algorithm with safe and efficient operations on individual vehicle dynamics control to smoothen intersection traffic flow and to increase the intersection capacity in urban area
		The 11th Five National Science and Technology Research Item [79]	●↑	●↑	○↑	An intelligent lane merge control system using traffic information collection, state estimation and variable merge strategy to improve safety and traffic flow in freeway work zones
		REM 2030 [89]	○	○	●↑	A model predictive energy efficiency minimization system implemented on the electric vehicle
		SAFESPOT [82]	◑↑	○	○	An intersection safety-critical situation awareness application based on lane occupying estimation via vehicle-to-infrastructure communication
		AERIS [85]	○↑	○	●↑	An eco-speed harmonization scheme using V2I and I2V to smooth the individual vehicle's speed profile and to reduce the overall energy consumption
		AERIS [86]	○↑	○↑	●↑	An eco-approach departure application which utilizes SPaT and preceding vehicles information to guide drivers to pass through intersections smoothly
		AUTOPIA [78]	◑↑	◑↑	○↑	An automated on-ramp merging system which consists of the distance reference system and a fuzzy control on vehicle's longitudinal control to improve traffic flow and congestion in a merging situation
		Queue-end warning [81]	◑↑	○	○	A queue-end location prediction algorithm using artificial neural network together with sensors and on-road message signs to reduce rear-end collisions in highway work zones
		Eco-CACC-Q [87]	○↑	○↑	●↑	An eco-cruise control system using shockwave prediction by SPaT messages and V2I information to refer the driver a fuel-optimal trajectory at the signalized intersections
		Connected eco-driving [88]	◑↑	○	●↑	A vehicle's longitudinal control system considering the inner driving operation and outer on-road factors to increase energy efficiency in a safe manner
		Curve warning system [80]	◑↑	○	○	A speed limitation algorithm integrating the upcoming road geometry and a safe speed decision scheme to achieve safe driving in sharp-curve roads
		Platoon-based MAS-IMA [91]	○↑	●↑	●↓	A multi-agent intersection management system based on the formation of platoons to increase mobility performance
		Optimal lane selection [92]	◑↑	●↑	●↑	An optimal lane change selection algorithm using on-road information and desired speed of individual vehicles to regulate traffic flow and reduce negative impacts induced by uncoordinated lane changes
		MA based Freight Signal Priority [93]	○↑	●↑	●↑	A regulation scheme of the signal timing for the priority of freight vehicles to decrease travel time and reduce fuel consumption
	Centralized	ADIS/ATMC Applications [114]	○	●↑	○	A dynamic traffic assignment model, seeking optimal assignment of vehicles to the network and supplying proper route guidance
		Hybrid collision warning system [83]	●↑	○↓	○↓	A hybrid collision warning system with integration of NGSIM loop detectors data, vehicle-to-vehicle information and the cloud center to offer the driver potential collision warnings in order to decrease collision risks
		Local Danger Warning System [84]	◑↑	○	○	A central information service and smartphone-based on-road dangerous situation awareness system to alleviate further dangers caused by congestion, full braking and tight bend

S: safety; M: mobility; E: environmental impacts

As underlined in many studies, a management center tactic is inevitable in the centralized control strategy. As reported in [83], a hybrid collision warning system, integrating macroscopic data acquired from loop detectors and microscopic inter-vehicle information data obtained from on-board smartphones, was proposed to describe potential collision risks in divided road segments using a deceleration-based surrogate safety measurement. Benefited from the cloud center tactic, the system efficiency can be increased by loading computation tasks on individual smartphones. The collision risks, herein defined as a ratio between the required deceleration and the representative maximum braking performance, were compared among several collision warning systems. Tak et al. concludedthat the proposed system outperforms other collision warning systems because of higher accuracy due to data fusion from multiple sources [83]. Other than driving behavior data (e.g., space headway difference, velocity difference and acceleration difference between the subject vehicle and the lead vehicle), mobility and environment impacts performance were not measured in [83]. Another typical example of safety-focused CV application is the danger notification/dissemination application. Haupt et al. presented a local danger warning system, which used a central information service and equipped smartphones with built-in sensors to collect local abnormal situations (e.g., collective full braking behaviors, congestion and tight bend) to disseminate warnings to app-enabled vehicles in the vicinity of hazards [84]. It was concluded that the potential congestion and collision risks caused by the dangerous situations should be avoidable and reduced, whereas no direct results were investigated in [84].

4.3.2.3 Environmental Impacts Benefits

To achieve pollution emissions reduction of transportation systems, Wu et al. proposed an eco-speed harmonization scheme to reduce the overall fuel consumption on freeways using mutual vehicle-to-infrastructure communication [85]. In the proposed method, individual vehicles communicate with infrastructure on the associated road segment and calculate a safe eco-friendly speed based on a speed determination scheme. It is interesting to note that even the proposed strategy was proposed with a focus on environment protection, the rear collisions might be mitigated as well due to the harmonized speeds. In the same direction, an environmental impacts-focused application, namely the eco-approach departure system, was proposed in [86], where the signal phase and timing information from the traffic signal controller together with preceding vehicles information was utilized to supply speed and acceleration guidance to the driver in an eco-friendly way. The fuel savings generated by the Comprehensive Modal Emissions Model (CMEM) were compared, and results show that there are higher fuel savings as the penetration rate of equipped vehicles increases. The mobility and safety performance were not estimated specifically in [86], whereas the individual vehicle’s speed is smoothened when passing through the intersection, possibly leading to a decrease of potential rear-end collisions.

Yang et al. proposed an eco-CACC system to obtain fuel savings at signalized intersections [87]. The proposed system used a queue length prediction algorithm and formulated a fuel efficiency optimization problem, recommending the vehicle trajectory and advising the driver when to approach the intersection stop bar (right after the last queued vehicle is discharged) and how to stop (e.g. supplying speed and acceleration advice). A minimum penetration rate value is required for the overall fuel efficiency improvement for the multi-lane intersection scenario. Besides trajectory and fuel savings, safety-related and mobility-related results were not mentioned, however, potential conflicts and congestion are supposed to be mitigated due to a decrease of the queue length. Another eco-driving approach has been proposed in [88], where a longitudinal control approach based on energy consumption-minimized was used, taking into account both the inner vehicle's operations and the outer traffic and roadway conditions to evaluate the fuel savings. At the same time, a safe headway principle was embedded into this proposed system as well to achieve safety benefits.

Saving fuel by taking advantages of (hybrid) electric vehicle is an emerging and attractive research topic as well. A variety of research activities on electric vehicles and electric buses have been carried out, with the purpose of increasing energy efficiency and reducing emissions. Guan and Frey presented a model predictive energy efficiency optimization system using a power-train model and traffic lights sequences information to increase energy efficiency of the electric vehicles [89], [90].

4.3.2.4 Environmental Impacts & Mobility Co-Benefits

Multi-agent systems (MAS) approach turns out to be another frequently used method to regulate traffic flow and to save fuel consumption [91]-[93]. A platoon-based intersection management system was proposed in [91], aiming to improve mobility and environmental sustainability by the formation of vehicle platoons using connected vehicles technologies. The intersection capacity is increased due to the vehicle platoons, therefore the travel time is reduced compared to traditional traffic light control and non-platoon intersection management schemes, and safety might be improved due to the formation of platoons as well, however, slightly higher fuel consumption is introduced (validated). MAS can be applied to not only longitudinal maneuvers but also lateral ones. Also, Jin et al. proposed a real-time optimal lane selection algorithm which also regulates the uncoordinated lane changes of vehicles on a localized road segment based on the lane occupied, speed, location and desired driving speeds of individual vehicles [92]. The overall conflict number was targeted to be zero in an optimization problem and it has been validated that the average travel time and fuel consumption are reduced at the same time. Making use of the freight signal priority on the basis of a connectivity-based signal control algorithm, Kari et al. addressed the issue of high NOx emissions from freight vehicles at intersections. Compared to fixed signal timing cases, both the fuel consumption and the travel time have been saved due to better traffic regulation, which benefits not only freight vehicles but also other vehicles [93]. Besides the freight vehicle priority algorithm, there are also some studies conducted, leading to a safe and smooth traffic society by using signal preemption systems for emergency vehicles [94], [95]. Table 4-4 lists some of the infrastructure-centric CV-based applications from the angle of co-benefits and trade-offs among different MOEs.

4.3.3 Traveler-Centric CV-Based Applications

4.3.3.1 Safety Benefits

Pedestrian protection is one of the urgent issues needed to be addressed, in order to enhance pedestrian safety. An interesting survey in this direction was carried out by Gandhi and Trivedi, which mainly focuses on pedestrian detection using sensors in vehicles and infrastructure, and collision avoidance based on collision prediction with pedestrian dynamics and behavior analysis [96]. Other than those computer vision based pedestrian detection techniques, there are also a few studies on pedestrian protection through V2X communications [97]-[100]. An approach to avoiding accidents by making use of sensors and communication technologies was discussed in [97]. The contributions focus on safety enhancement of active vulnerable road users (pedestrians, cyclists or powered two-wheelers) in a cooperative way. The proposed WATCH-OVER system can be triggered when there is a certain risk level measured by collision trajectories and send an alert to both the equipped vehicle and the active on-road traveler(s) to prevent any road accident. Similar projects V2ProVu and WiFiHonk were investigated in [98], [99], using a communication device NexCom (installed with the IEEE 802.11g and a conventional GPS chip) and a smartphone-based beacon stuffed with a Wi-Fi based Vehicle-to-Pedestrian (V2P) communication system, respectively. In [99], results are the probability of a collision, defined as the ratio of the required time to stop and the time available for stop. Results of systems with the proposed communication approach and with conventional Wi-Fi communication method were tested and compared.

4.3.3.2 Mobility Benefits

In addition to the presented safety application, multimodal traveler information based traffic situational awareness systems have been developed in order to detect user modes of travel and provide further proper suggestion for routing. Zhang et al. proposed an iPhone/Android-based Path2Go application which was designed to improve the mobility of equipped users, by fusing the GPS data from both transit vehicles and smart phones/detecting mobile users' activity/differentiating the user's travel modes/supplying proper routing advice (including mode choices) to users [101]. The performance test of the proposed application was carried out on CalTrain and several local bus routes, and the correction detection rate is as high as 92%. Table 4-5 lists some of the traveler-centric applications from the different MOEs benefits perspective.

TABLE 4-5. TRAVELER-BASED CV-BASED APPLICATIONS

Categories	Project/Application name & Ref	MOE focus			Contributions
		S	M	E	
Traveler-based	WATCH-OVER [97]	◑↑	○	○	A cooperative system framework integrating sensors and V2X communications to prevent road accidents that involve vulnerable active road users
	V2ProVu [98]	◑↑	○	○	A pedestrian protection application using Wi-Fi based NexCom devices for V2P communication for vehicle presence informing and/or hazard alarming
	Path2Go [101]	○	◑↑	○	A context-awareness routing service based on real-time Multi-Model traveler information to match proper travel modes and to provide users further route information
	WiFiHonk [99]	●↑	○	○	A collision estimation algorithm between providing issue warnings using the beacon stuffed Wi-Fi communication
	[110]	○	○	◑↑	A dynamic inductive power transfer lane designed for electric bikes

S: safety; M: mobility; E: environmental impact

4.4 Summary

This chapter provides an in-depth literature review on CV-based applications related research, and analyses the potential tradeoffs and co-benefits of three key MOEs among various CV-based applications in detail. A broad three-level classification of CV-based applications has been proposed, i.e., vehicle-centric, infrastructure-centric, and traveler-centric applications. It is concluded that a trend exists that a portion of those CV-based applications are being designed to improve more than one MOEs (usually two), however, very few CV applications improve all the three major MOEs (i.e., safety, mobility and environmental impacts) simultaneously. Based on the literature reviewed, we identify some influential factors on system performance. In combination with co-benefits analysis of some typical CV-based applications, we can conclude and identify some key strategies to improve system performance. Moreover, some CV applications may have co-benefits by combining several different-MOE-focused applications, to improve a combination of safety, mobility and environmental sustainability.

Furthermore, other than the application itself, many network-wide factors could affect the performance of a specific application. For instance, penetration rate of application-equipped vehicles is one important dimension that should be taken into account when the performance is measured, especially when there is a growing trend toward mixed traffic within the next decade. Other parameters we might also need consider include but not limit to traffic demand, truck percentage and even communication transmission range, etc.

5 AN INNOVATIVE FRAMEWORK TO EVALUATE THE PERFORMANCE OF CONNECTED VEHICLE APPLICATIONS: FROM THE PERSPECTIVE OF SPEED VARIATION-BASED ENTROPY

5.1 Introduction

To evaluate the performance of CV applications, a variety of conventional Measures of Effectiveness (MOEs) have been proposed over the years, mainly covering safety, mobility, and environmental sustainability. However, few studies have focused on *holistically* evaluating CV applications in terms of safety, mobility, and environment [111]. Even fewer studies have attempted to examine the speed variation-based MOE and explore its connection with conventional MOEs. In this chapter, Speed Variation-based Entropy (SVE) is recommended as a way to evaluate the effectiveness of different CV applications on application-equipped vehicles and unequipped vehicles in terms of the system's degree of order. Three CV applications, i.e., HSDW, ESH, and EAD, were selected and evaluated in the framework of SVE.

The rest of this chapter is organized as follows: Section 5.2 presents three selected CV applications, followed by the description of a developed framework for SVE-based evaluation in Section 5.3. Section 5.4 briefly introduces the simulation model and scenarios. In Section 5.5, simulation studies are conducted to evaluate the effectiveness of target applications from the perspective of SVE as well as safety, mobility, and environmental impacts. Section 5.6 concludes this chapter with a summary of the research findings.

5.2 Representative CV Applications

Three selected CV applications have been developed elsewhere and selected for analysis, representing safety-and environment-focused applications, respectively. These applications include High Speed Differential (HSDW), Eco-Speed Harmonization (ESH), and Eco-Approach and Departure (EAD).

5.2.1 High Speed Differential Warning (HSDW) Application

A vehicle-to-vehicle (V2V) communication-based CV application, named *High Speed Differential Warning* (*HSDW*), was recently developed [112]. Information (such as instantaneous speed and location) can be obtained via V2V communication in the form of Basic Safety Messages (BSM) [14]. By exchanging such information within the communication range, this application can identify different scenarios (see Figure 5-1) where high-speed differentials exist between the host vehicle and remote vehicles on the current lane or adjacent lanes. Then the application will provide the driver with guidance on deceleration or lane-changing operation, aiming to reduce the risk of collision [112].

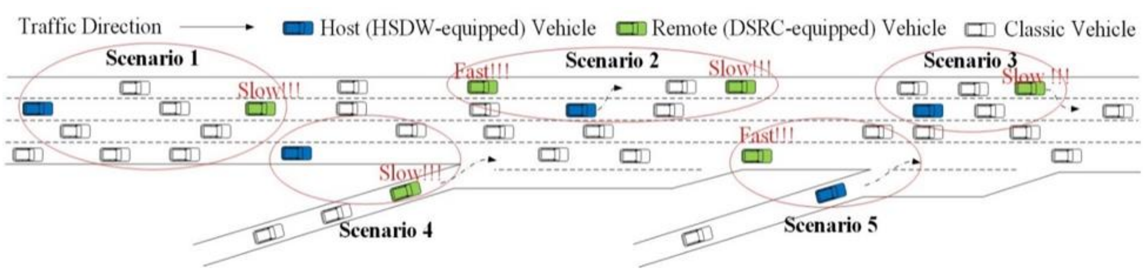

Figure 5-1. Possible HSDW Scenarios (from [112])

5.2.2 Eco-Speed Harmonization (ESH) Application

In addition to HSDW, another CV application developed by Wu et al. is Eco-Speed Harmonization (ESH), which is able to advise the driver with the appropriate speed needed to reduce unnecessary stop-and-go maneuvers, and thus, regulate traffic flow based on downstream traffic conditions, especially when approaching bottleneck/congestion areas [22]. Connected vehicles and DSRC-equipped roadside equipment exchange information with each other, and the average speed of road segments can be monitored and transmitted to the associated connected vehicles to encourage smooth driving at energy-efficient speeds for entire traffic flows [85].

5.2.3 Eco-Approach and Departure (EAD) Application

In addition to the two CV applications mentioned above, the Eco-Approach Departure (EAD) application [27] is designed to reduce energy consumption for the vehicle traveling along signalized corridors, by communicating with the signal phase and timing (SPaT) information of the upcoming traffic signals. More specifically, the application-equipped vehicle uses this traffic signal data, provides advisory speed profile to the driver and allows the driver to adapt the vehicle's speed to pass the next traffic signal in the most eco-friendly manner.

5.3 Framework of Speed Variation-based Entropy (SVE)

5.3.1 Entropy

Entropy has been widely used in many branches of science, ranging from classical thermodynamics to statistical mechanics and information theory [114]-[117]. In thermodynamics, entropy has been loosely associated with the amount of order or chaos. It can be understood as a measurement of molecular disorder within a macroscopic system and the maximum entropy will be achieved as an isolated system spontaneously evolves toward thermodynamic equilibrium. In his seminal paper, Shannon put forward the

Shannon entropy and used it as a measure of the amount of information that is missing before reception [118]. More specifically, the Shannon entropy of a discrete variable X with a probability mass function (PMF) $\mathrm{p}(x) = Pr\{X = x\}, x \in X,$ is defined as

$$H(X) = -\sum_{x} p(x) \, log_2 p(x) \quad (5\text{-}1)$$

Further, Prigogine and Lewis et al. defined entropy as a measure of ignorance [119], regarding the gain in entropy as loss of information [120]. In transportation-related research, Baslamisli et al. proposed an approach to identify the surface type of road by calculating the entropies of the sprung mass vertical acceleration of a vehicle running over roads with different qualities [121]. Tan et al. used the entropy of driver steering angle to measure discontinuity and to evaluate the effectiveness of drivers' steering controls to distinguish driving skill levels [122].

5.3.2 Speed Variation-based Entropy (SVE)

Fluctuations in vehicle speed have a significant impact on traffic operation. As mentioned previously, a variety of MOEs have been developed to address the variability in velocity. However, most of them rely on conventional statistics, such as mean and standard deviation, which may not be able to capture enough spectrum of the speed distribution. Inspired by the Shannon entropy (as described in Section 5.3.1), the Speed Variation-based Entropy (SVE) has been proposed and developed in this study to evaluate the performance of CV applications in terms of smoother maneuvering of equipped vehicles and entire traffic when additional information is introduced via connectivity. A three-step procedure to calculate the SVE from each individual vehicle's trajectory is show in Figure 5-2.

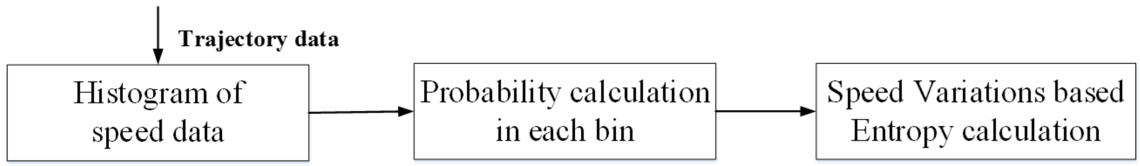

Figure 5-2. Three-Step Procedure for SVE Calculation

Based on second-by-second trajectory data, a histogram of the speed data classifies speed data into a certain number of bins, representing the distribution of sample frequency over the speed range. The probability value in each bin can be calculated by dividing the frequency per bin by the total size of the speed data. Equation (5-1) is applied to calculate the entropy of speed variations. The entropy in this study is in units of bits, since base-2 logarithms are used.

By calculating the SVE-based MOE on speed trajectories, the speed variations information can be grouped from a trip-by-trip perspective. For an individual vehicle, the time-speed diagram is employed to describe its speed characteristics changing with time. The 2-D time-speed information could then be reduced into one single entropy value, which is the SVE defined above. Therefore, for each vehicle trip, there is an associated SVE value to represent speed variations during the whole trip. Then, the SVE distribution based on the SVE values of all trips can be obtained. It is expected that the trip-based SVE distributions can well represent the effects of CV applications on traffic streams and the degree of traffic smoothness/chaos.

As one example, Figure 5-3 illustrates the speed distribution of two trips of an individual vehicle. The entropy of the high concentration distribution (red dash line) is smaller than that of the more spread-out distribution (black solid line). This result is consistent with the customized entropy “definition”: the less concentrated the speed value is, the larger customized entropy would be, leading to more uncertainties for complete knowledge of the event or process, e.g., stop-and-go behaviors and relevant traffic condition. Based on the definition of entropy as aforementioned, the corresponding trip-by-trip-based SVE values are calculated.

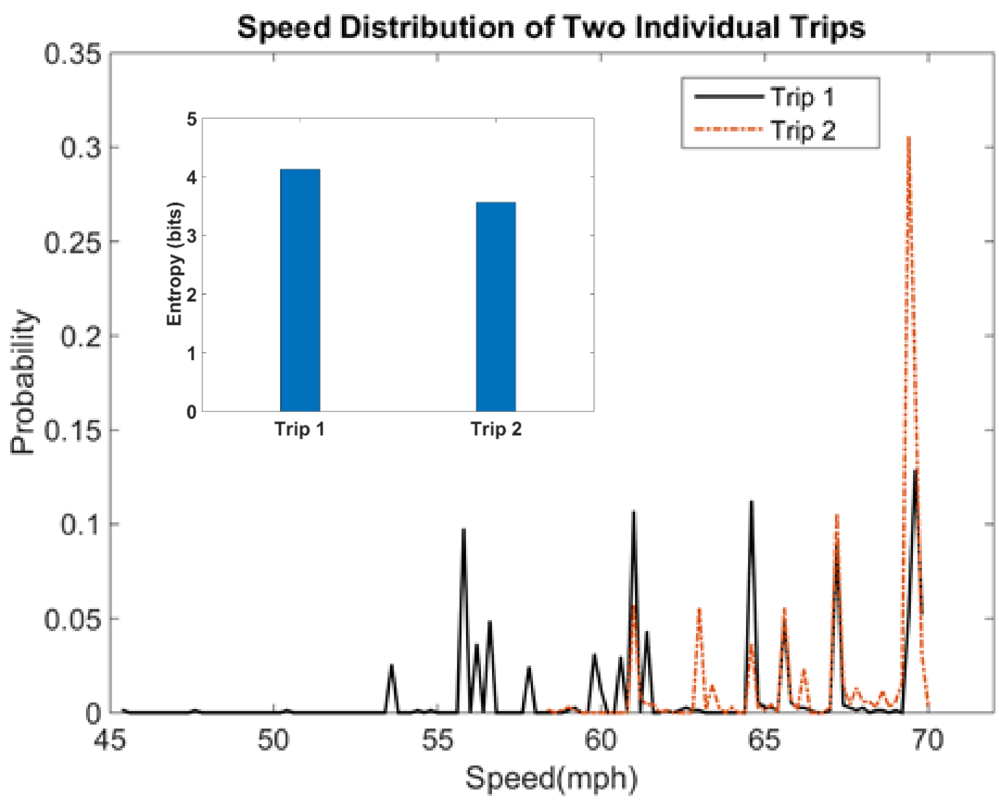

Figure 5-3. Time-Speed Diagram for Two Individual Trips

Moreover, based on the Fundamental Diagram (FD) [123] such as the Greenshield's one, as the traffic becomes denser, cars driven under constant time headway have lower equilibrium speed. In the meanwhile, the smallest speed variations and the stop-and-go behaviors can be amplified further by human drivers, causing traffic jam. It is expected that relevant performance (e.g., potential conflict risk, average speed and fuel consumption) in such traffic condition would deteriorate due to the increased stop-and-go behaviors. More insights relevant to the traffic jam propagation and the effects of driver behavior can be found in [124]. In addition, the Connected Cruise Control algorithms have been designed to control the longitudinal behavior of connected automated vehicles, in order to reduce speed variations, mitigate traffic waves and improve energy efficiency, which has been verified in field experiments [125]. Driving behavior control features such as the Cooperative Adaptive Cruise Control (CACC) may regulate the traffic flows by implementing the platooning of autonomous vehicles [126] and taking into consideration the stability of the vehicle string [127], to increase the road throughput. The CACC longitudinal control algorithm is robust against speed variations, therefore, the average speed might not reduce as the SVE increases in this case. It is noted that the SVE measures speed variations but not the average speed (i.e., high average speed and low average velocity cases could have the same SVE value), which might lead to a complicated relationship between SVE and the mobility performance. For example, driving behavior control features such as cooperative adaptive cruise control (CACC) may regulate the traffic flows, and then push traffic speed towards the peak of the fundamental diagram. In this case, the average speed might not reduce as SVE increases. The relation between the SVE and mobility performance (e.g., average speed) is relatively complicated.

5.3.3 Curve Fitting of Discrete SVE Distributions

When examining the empirical SVE distributions (i.e., using histograms), the Weibull distribution was selected in this study for histogram fitting to gain further insight. The Weibull distribution is widely used for weather forecasting [128], reliability engineering, and failure analysis of systems.

The probability density function (PDF) of a Weibull random variable is:

$$f(x; A, B) = \begin{cases} \frac{B}{A}\left(\frac{x}{A}\right)^{B-1} e^{-(x/A)^B} & x \geq 0 \\ 0 & x < 0 \end{cases} \quad (5\text{-}2)$$

where $B > 0$ is the shape parameter, and $A > 0$ is the scale parameter of the distribution.

In a Weibull distribution, $B > 1$ exists for an "aging" system, which by this hypothesis, means as time passes, the traffic system tends to be chaotic due to microscopic (e.g., stop-and-go maneuvers and lane changes) and macroscopic (e.g., demand fluctuations, vehicle mix, and roadway geometry) disturbances. Moreover, the mode and inter-quartile range (IQR) of the fitted Weibull distribution can be regarded as potential surrogate measures that indicate the traffic system degree of chaos. The smaller the mode of SVE distribution is, the smoother the traffic system is, since the majority of vehicles in roadway transportation have small speed variations. The larger the IQR of SVE distribution is, the more unpredictable and chaotic the traffic condition is, due to the larger diversity of SVE values.

For multi-modal distributions, the Weibull mixture [129] probability distribution function is used to better fit the discrete SVE distribution, which is defined as

$$f(x) = \sum_i p f_i(x) \quad (5\text{-}3)$$

where $f_i(x)$ is i-th component, which also follows a Weibull probability distribution; p is the mixture parameter or weight.

5.4 Simulation Setup

5.4.1 Simulation Model

In this work, a segment of California SR-91E has been used for a simulation study, which consists of a 15-mile corridor between the Orange County Line and Tyler Street in Riverside, California (see Figure 5-4). The number of lanes ranges from four to six, and there are nine pairs of on-/off-ramps. The traffic conditions usually fall into levels of service (LOS) C to E [130] during peak hours. Traffic demands, origin-destination (O-D) patterns, and driving behaviors have been calibrated to match that of a typical weekday morning in the summer [131]. The segment of California SR-91E is used to test HSDW, ESH. In addition, EAD is designed for vehicles when they pass through signalized intersections, therefore, the EAD application has been tested in a three-intersection signalized corridor in Palo Alto, CA, with three lanes in each direction, where the traffic patterns and signal control have been calibrated with field data.

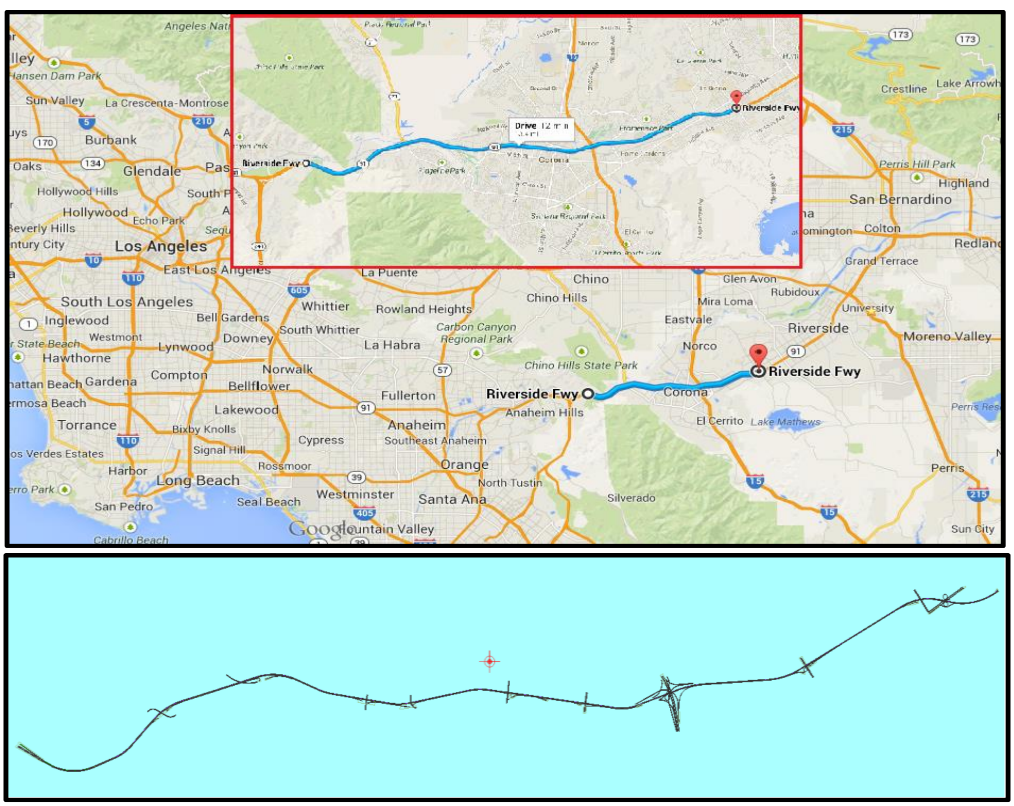

Figure 5-4. Road Network of the California SR-91E in Real-World and PARAMICS

5.4.2 Simulation Scenarios

To better understand the effectiveness of applications, comprehensive simulation tests have been conducted over the following system parameters:

1) *Penetration rate of DSRC-equipped vehicles*. In this study, a full range (8 total levels) of penetration rates are examined for conventional MOEs, including 0% (baseline), 10%, 20%, 30%, 40%, 50%, 80% and 100%, under the calibrated traffic demand pattern (LOS D). The application-equipped rate is set the same as the DSRC-equipped rate in this study.
2) *Congestion level*. For the highway scenarios, during a three-hour simulation period, two levels of traffic volume are to be evaluated: 25,000 vehicles (calibrated), and 32,000 vehicles per simulation run. Further analysis on the average speed indicates that these two cases represent the traffic conditions of LOS D (transitional flows) and LOS E (unstable flows), respectively, according to the *Highway Capacity Manual* (HCM) 2010 [130]. For the signalized intersection scenarios, there are two levels of traffic volume: 5000 vehicles/run (v/c = 0.38, referred to as moderate traffic), and 10000 vehicles/run (v/c = 0.76, referred to as relatively heavy traffic).

5.5 Simulation Results

5.5.1 SVE-based MOE Evaluation for CV Applications

5.5.1.1 CV Applications' Effects on Traffic

The SVE-based MOEs of all three selected applications (HSDW, ESH, and EAD) are first analyzed. All the four applications were first tested under the 20% penetration rate for application-equipped vehicles. For the highway scenarios and signalized intersections, total traffic volume levels are 25,000 vehicles per run and 5000 vehicles per run, respectively (both cases are moderate traffic condition). Figure 5-5 shows the SVE distributions of application-unequipped vehicles (before) and application-equipped vehicles (after) of corresponding applications, with the following key observations:

a) It can be observed that minor changes occurred in the SVE distributions between the HSDW-equipped and HSDW-unequipped vehicles, and they have very similar modes and IQRs. A potential explanation is that the HSDW application is not triggered frequently enough in this moderate and relatively stable traffic condition (25,000 vehicles/run).

b) In the ESH scenario, a significant left shift is observed in the SVE distribution of ESH-equipped vehicles compared with that of the ESH-unequipped vehicles. The mode of ESH-equipped vehicles and ESH-unequipped vehicles are 4.4 bits and 4.9 bits, respectively. Smaller modes and IQRs of ESH-equipped vehicles means they do have smaller speed variations as well as travel in a more predictable way than ESH-unequipped vehicles. In this case, ESH-equipped vehicles obtain smoother velocity and then smaller SVE via additional information brought by roadside infrastructure.

c) The SVE distributions in the EAD scenario are multi-mode. The reason could be that there are interruptions from external factors (such as traffic signals). Note that these disturbances affect the speed variations rather than the SVE distribution’s performance. In fact, the multiple modes in the SVE distributions show that there exist disturbances in the speed variations (such as many stop-and-wait behaviors caused by signalized intersections and/or highly congested traffic conditions).

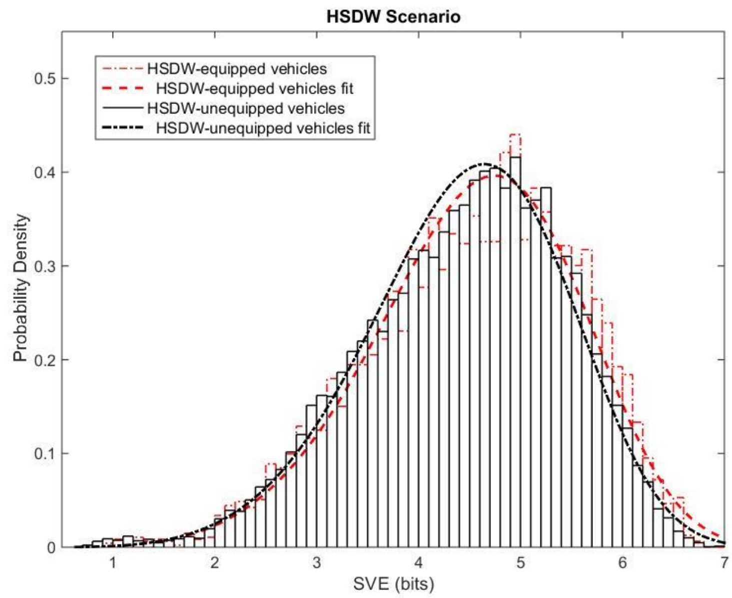

(a) HSDW Application

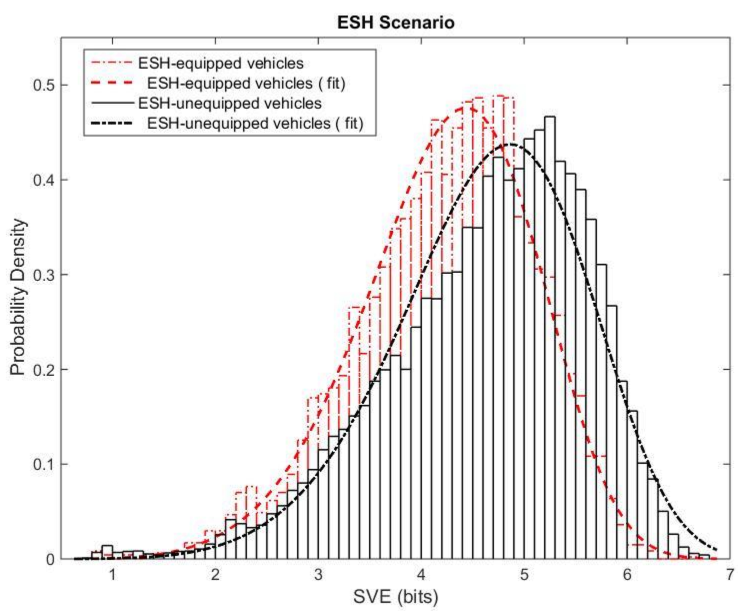

(b) ESH Application

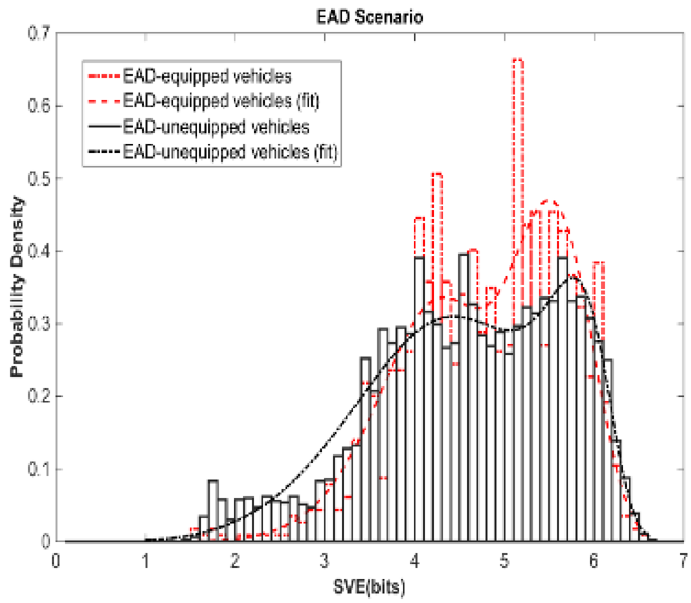

(c) EAD Application

Figure 5-5. Time SVE Distributions of Three Different CV Applications (25,000 Vehicles/Run, 20% Penetration Rate)

5.5.1.2 Sensitivity Analysis

a) Penetration rate:

The ESH and the EAD applications are taken as examples for penetration rate sensitivity analysis in moderate traffic (25,000 veh/run for ESH and 5000 veh/run for EAD), and three levels of penetration rate of application-equipped vehicles are selected: 10%, 50% and 80%. We can observe from Figure 5-6 that both the ESH and the EAD are robust to the variation of penetration rate compared to the other applications: the safety capability, mobility performance and fuel consumption have not changed much across different penetration rate levels (see Table 5-1). Therefore we used these applications as examples to verify that the entropy-based MOE (i.e., SVE) can be an indicator, showing how the other MOEs change (or even hardly change), in order to demonstrate the consistency in SVE with other MOEs. The cases showing how SVE varies with other MOEs as the number of application-equipped vehicles increases are presented in the following traffic volume sensitivity analysis (i.e., for the EAD application).

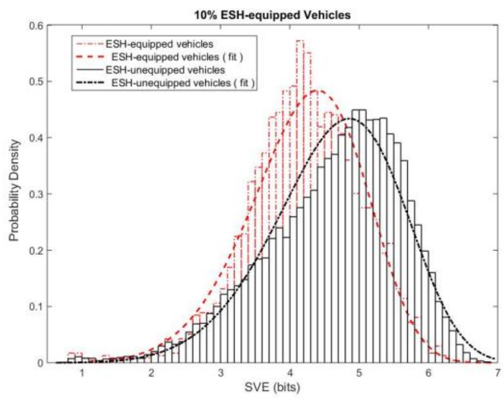

(a) 10% ESH

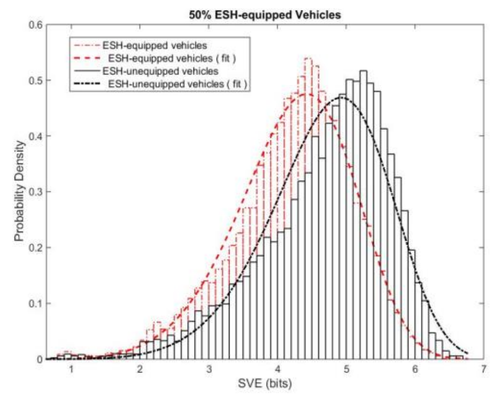

(b) 50% ESH

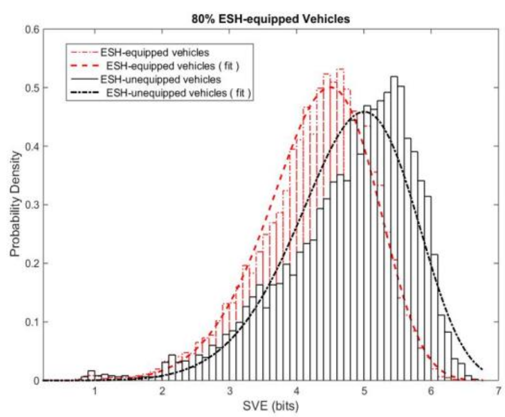

(c) 80% ESH

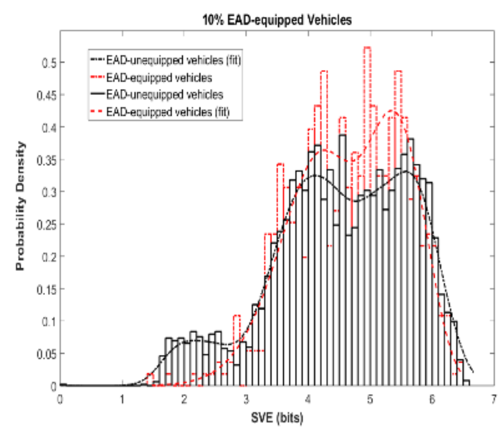

(d) 10% EAD

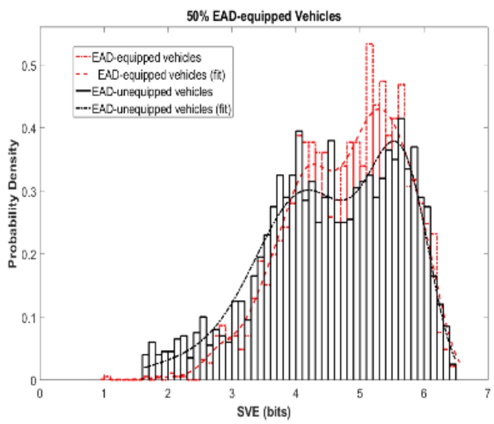

(e) 50% EAD

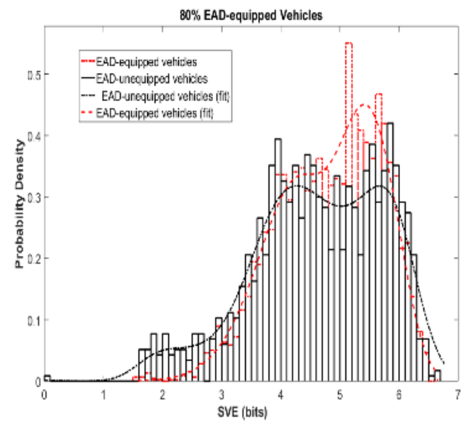

(f) 80% EAD

Figure 5-6. SVE Distributions of Different Penetration Rates in ESH and EAD Scenarios (25,000 Vehicles/Run)

TABLE 5-1. CONVENTIONAL MOES OF PENETRATION RATE SENSITIVITY ANALYSIS

Penetration Rate Sensitivity Analysis							
ESH (25,000 veh/run)					**EAD (moderate traffic)**		
Penetration rate		S[a]	M[b]	E[c]	S[a]	M[b]	E[c]
10%	Equipped	0.1504	58.3	4158.9	0.0973	22.1	4043.3
	Unequipped	0.1861	59.9	4295.3	0.0973	22.2	4332.5
50%	Equipped	0.1646	58.6	4168.4	0.0767	21.7	4139.0
	Unequipped	0.1812	59.3	4276.0	0.0801	22.3	4273.5
80%	Equipped	0.1711	59.0	4195.2	0.0616	21.7	4178.0
	Unequipped	0.2129	59.5	4291.5	0.1028	22.2	4317.4

[a] Safety MOE: Conflict frequency. [b] Mobility MOE: Average speed (mph). [c] Environmental impacts MOE: Fuel consumption (KJ/mile).

b) Traffic volume:

First, Figure 5-7 presents a comparison between two baselines (where there is a 0% penetration rate of application-equipped vehicles) of different congestion levels. It shows that a shift to the right of SVE distribution under the heavy traffic baseline case is observed with respect to that of the moderate traffic baseline case, because higher traffic demand may cause higher speed fluctuations/chaos on the road (See Figure 5-7(a)).

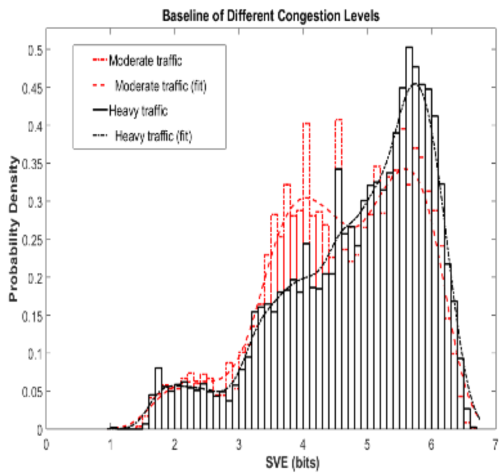

(a) 0% EAD

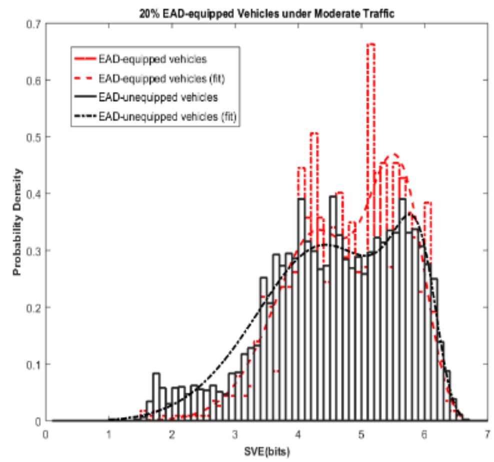

(b) Moderate Traffic for EAD

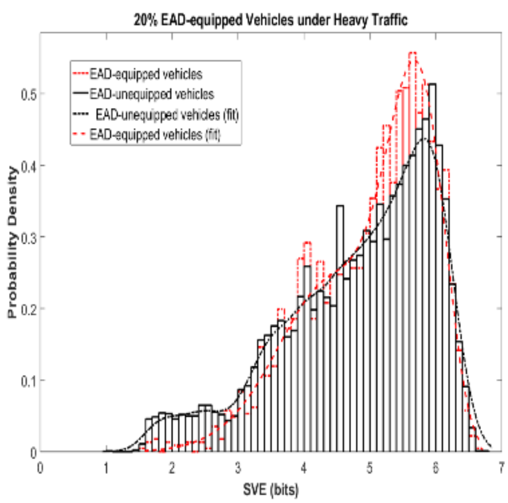

(c) Heavy Traffic for EAD

Figure 5-7. SVE Distributions of Different Traffic Volumes in EAD Scenario (Baseline Cases and 20% Penetration Rate)

Second, as for the congestion level sensitivity analysis, the penetration rate of application-equipped vehicles is fixed at 20%, and the EAD application are selected as the sensitivity analysis scenarios. It can be observed that there already exist multiple modes in the baselines of the SVE distributions under the signalized intersections scenarios, since the traffic light signals cause many stop-and-wait behaviors, leading to the fluctuations in speed variations and the multi-mode SVE distributions. In addition, by comparing the baselines in Figure 5-7, it can be concluded that the more congested traffic condition causes the right-shift of the SVE distribution' mode. The SVE values of the majority of vehicles will become larger in the relatively heavy traffic condition.

TABLE 5-2. CONVENTIONAL MOES OF TRAFFIC VOLUME SENSITIVITY ANALYSIS

Traffic Volume Sensitivity Analysis				
EAD (20% penetration rate)				
Traffic volume		S[a]	M[b]	E[c]
Moderate traffic	Equipped	0.0497	21.6	4120.3
	Unequipped	0.1006	22.3	4338.6
Heavy traffic	Equipped	0.1742	20.9	4203.9
	Unequipped	0.2144	21.6	4305.3

[a] Safety MOE: Conflict frequency. [b] Mobility MOE: Average speed (mph). [c] Environmental impacts MOE: Fuel consumption (KJ/mile).

5.5.2 Correlations between SVE and Conventional MOEs

5.5.2.1 Baseline SVE versus Conventional MOEs

Figure 5-8 shows the relationship between SVE and the other three conventional MOEs in the case of baseline settings (i.e., 0% application-equipped vehicles, and 25,000 veh/run in the highway scenario):

a) Safety. The number of conflicts is minor when SVE is small. When higher SVE is observed, vehicles are exposed to a higher conflict number;

b) Mobility. There is no strong correlation between SVE and the average speed. For example, overall traffic that moves slowly but smoothly may have similar SVE as fast, free-flow traffic;

c) Environment. When SVE is higher, the fuel consumption increases, floating within a certain bandwidth range, e.g., 300 KJ/mile (this testing scenario focuses on the region with dense data samples).

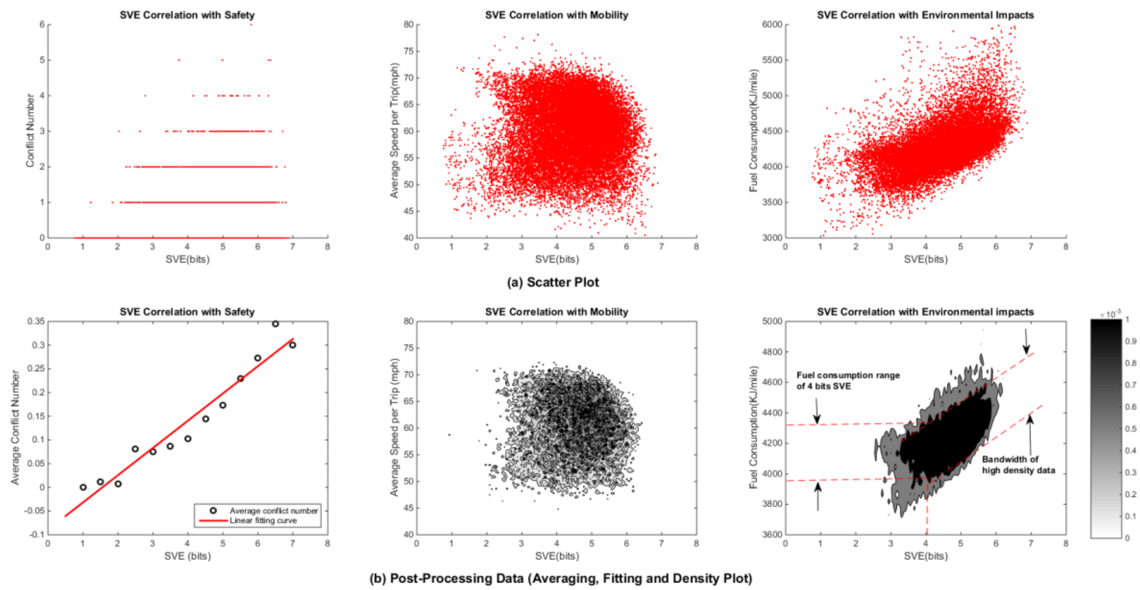

Figure 5-8. Baseline SVE Correlations with Three Conventional MOEs (0% Penetration Rate, 25,000 Veh/Run)

5.5.2.2 SVE versus Conventional MOEs for Three Selected CV Applications

It can be expected that the conventional MOEs of different CV applications can be roughly obtained through the corresponding SVE. Table 5-1 and Table 5-2 list the three conventional MOEs of sensitivity analysis cases in some CV application scenarios (corresponding to the SVE MOE sensitivity analysis in Section 5.5.2.1) to explore the correlations between SVE and conventional MOEs.

a) Penetration rate: Based on the general correlations between SVE and conventional MOEs in Figure 5-8, the corresponding estimated conflict frequencies of ESH-equipped and unequipped vehicles are 0.1638 and 0.1925, with estimated fuel consumption ranges from 4000-4,300 KJ/mile and 4,200-4,500 KJ/mile, which are consistent with the numerical results in Table 5-1. The conflict frequency difference between estimation and actual results is less than 0.02.

Moreover, the correlation between SVE and average speed, fuel consumption, and conflict frequency are plotted and calculated, respectively (see Figure 5-9 and Table 5-3). To be clear, in this case there are seven penetration rate levels for seven SVE samples, i.e., 10%, 20%, 30%, 40%, 50%, 80%, and 100%. Every entropy value is available for each penetration rate level under the moderate traffic (25,000 vehicles/run for the highway scenario and 5000 vehicles/run for the downtown scenario), where each entropy value is calculated based on the overall vehicle speed data in the entire network during the full simulation time. The corresponding conventional MOEs are average values of overall vehicles under the same scenarios.

In Figure 5-9, it can be concluded that SVE has a strong negative correlation with average speed, and an obvious positive correlation with fuel consumption and conflict frequency in the HSDW scenarios. This result meets the expectation that high entropy values reflect more chaotic traffic in terms of high conflict frequency, low average speed, and high fuel consumption. However, the ESH scenario is a special case where SVE versus safety and SVE versus mobility do not show such a trend in correlation coefficients. Several potential reasons are: a) for the safety aspect, since the traffic system is subject to less fluctuation across different penetration rates in the ESH scenario (as mentioned in penetration rate sensitivity analysis in terms of SVE MOE in Section 5.5.1.2), the fluctuation in conventional MOEs (e.g., conflict frequency) is very small (note that to be observed distinctly, the y-axis limit for safety in the ESH scenario is relatively small in

Figure 5-9) across different penetration rates, which leads to the 0.3916 correlation coefficient (see Table 5-3); and b) on the other hand, for the mobility aspect, it can be concluded that the ESH system sacrifices the mobility to some extent in order to smooth overall traffic flow and keep the speed within a certain range for energy saving, as the penetration rate increases. The EAD application is designed to smooth the longitudinal trajectories of the application-equipped vehicles and reduce the fuel consumption. However, the impacts of such application on other unequipped vehicles/the overall traffic could be amplified due to the signalized intersections. In Figure 5-9, we observe that the overall SVE increases as the penetration rate of the EAD application increases, while the EAD is robust against the surrounding variations (the three MOEs in the EAD scenario are relatively stable). Please note that to be observed distinctly, the y-axis limits for the three MOEs in the EAD scenario are relatively small. In this case, SVE versus conflict risk/fuel consumption is not positively correlated any more (see Table 5-3). By combining the conventional MOEs and the SVEs, we can understand how the application affects the overall traffic (smoothing or causing chaos in speed variations) and whether the application is robust against surrounding variations.

TABLE 5-3. CORRELATION COEFFICIENTS BETWEEN SVE AND CONVENTIONAL MOES (25,000 VEHICLES/RUN)

Application	HSDW			ESH			EAD		
MOE	SVE vs S[a]	SVE vs M[b]	SVE vs E[c]	SVE vs S	SVE vs M	SVE vs E	SVE vs S	SVE vs M	SVE vs E
Correlation coefficient	0.9811	-0.8950	0.9490	0.3916	0.9681	0.9941	-0.9499	-0.6765	-0.9131

a Safety MOE: Conflict frequency. b Mobility MOE: Average speed (mph). c Environmental impacts MOE: Fuel consumption (KJ/mi).

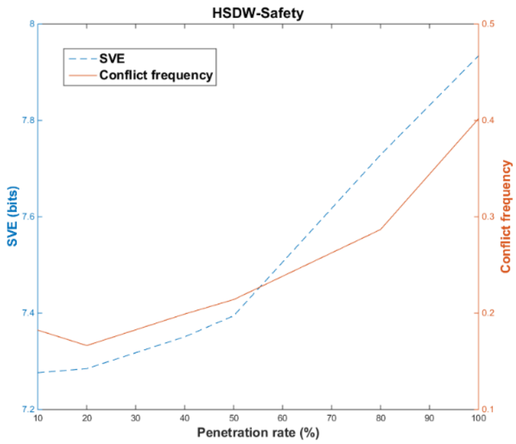

(a) HSDW-Safety Impacts

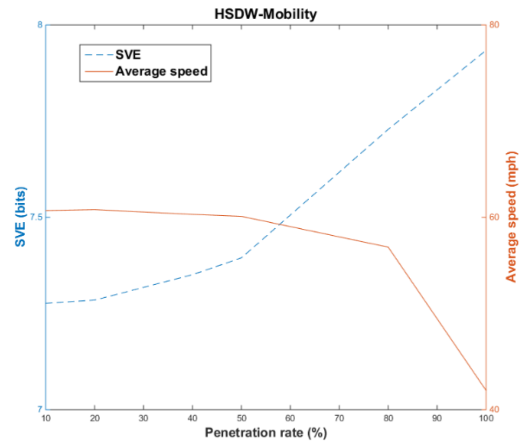

(b) HSDW-Mobility Impacts

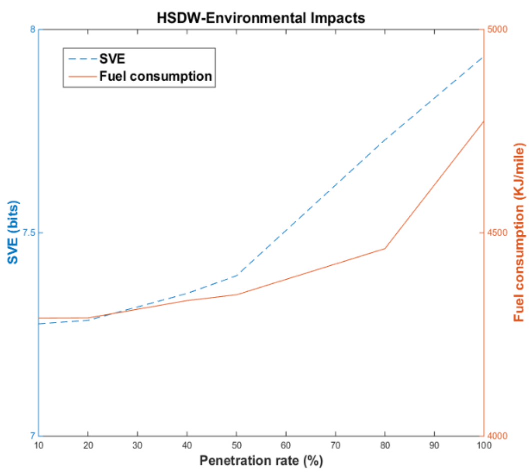

(c) HSDW-Environmental Impacts

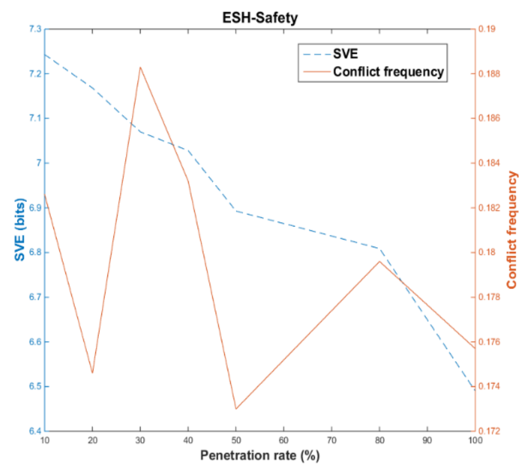

(d) ESH-Safety Impacts

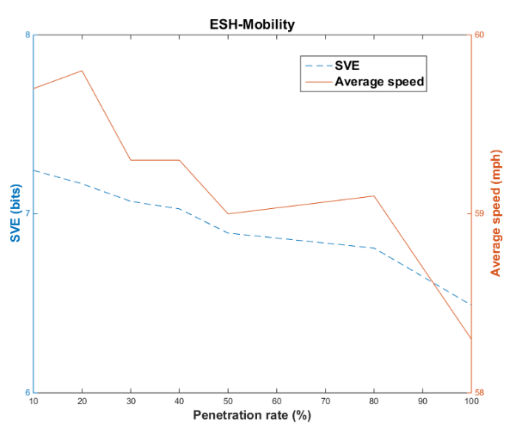

(e) ESH-Mobility Impacts

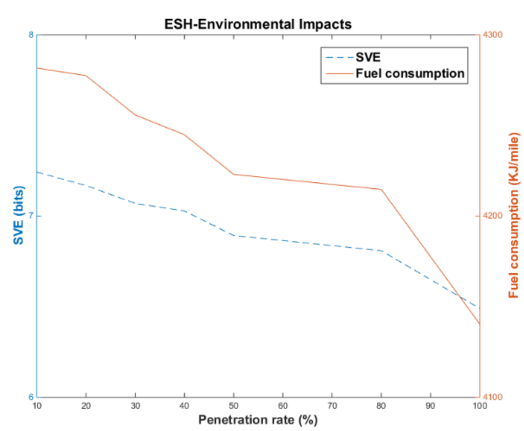

(f) ESH-Environmental Impacts

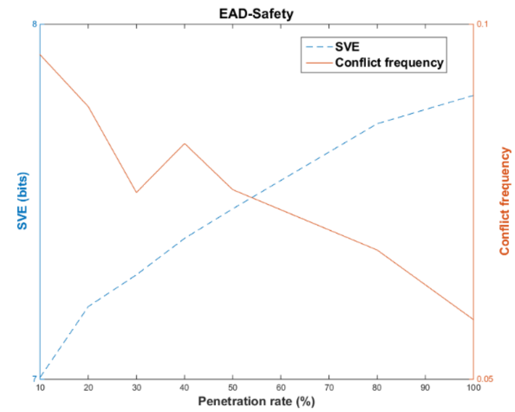

(g) EAD-Safety Impacts

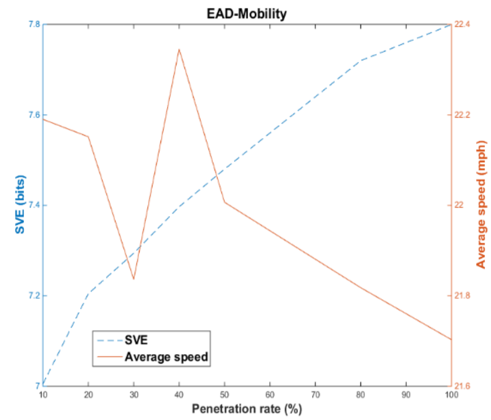

(h) EAD-Mobility Impacts

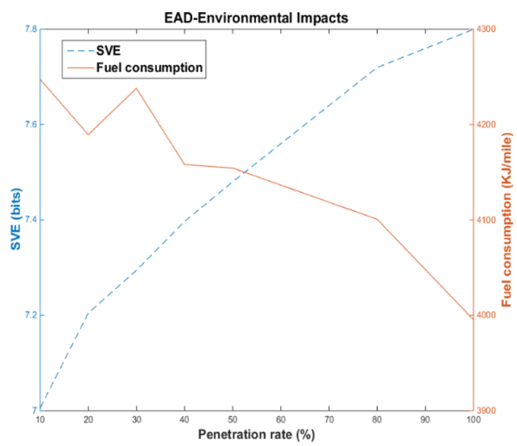

(i) EAD-Environmental Impacts

Figure 5-9. SVE versus Three Conventional MOEs across Different Penetration Rate Levels for Three Different CV Applications (Moderate Traffic)

b) Traffic volume: Regarding the EAD, the SVE value increases as the traffic volume increases, and the safety, mobility, and sustainability impacts performance deteriorate due to the higher speed variations in the heavy traffic condition (see Table 5-2 and Figure 5-10 (i), (j), (k), and (l)).

Lastly, the correlation between SVE and the three conventional MOEs of the three selected CV applications across two congestion levels is shown in Figure 5-10. Each entropy value is calculated based on the overall vehicle speed data on the entire network during the full simulation time. A 20% penetration rate of application-equipped vehicles is fixed herein. The results show that higher SVE is associated with higher conflict frequency, lower average speed, and higher energy consumption for both HSDW and ESH. Again, as mentioned in Section 5.3.2, as the traffic becomes denser, human drivers can amplify the smallest speed variations into a full-on stop-and-go jam. This could well explain the negative correlation results between the SVE and traffic mobility performance for HSDW, ESH, and EAD in Figure 5-10.

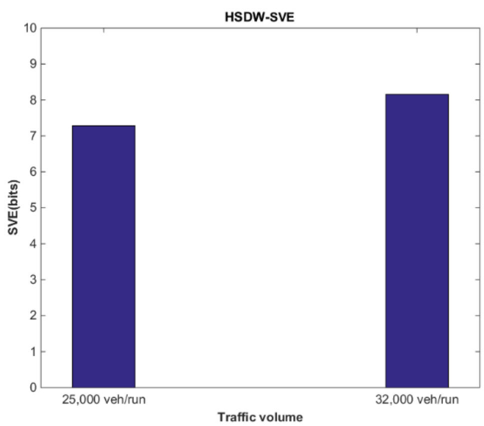

(a) HSDW-SVE

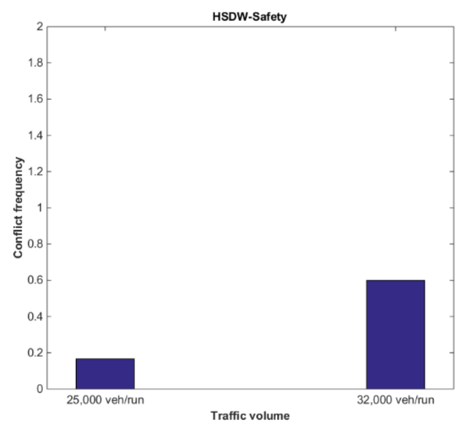

(b) HSDW-Safety Impacts

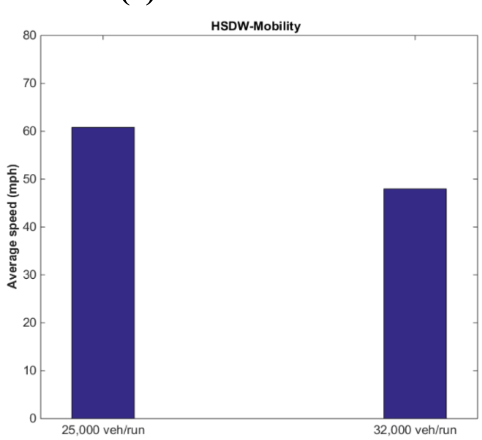

(c) HSDW-Mobility Impacts

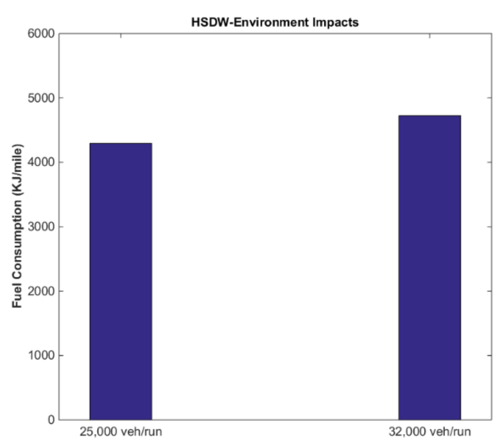

(d) HSDW-Environmental Impacts

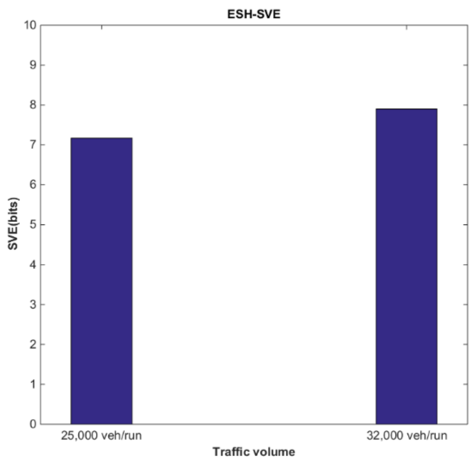

(e) ESH-SVE

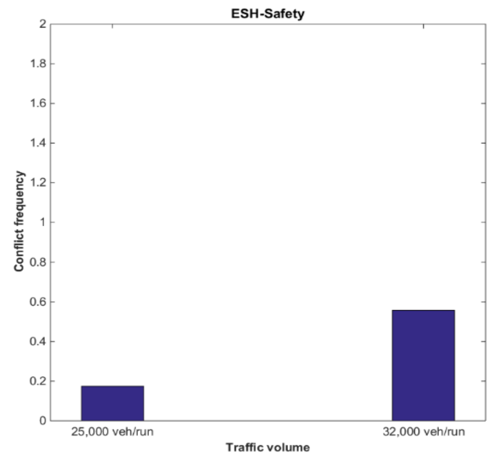

(f) ESH-Safety Impacts

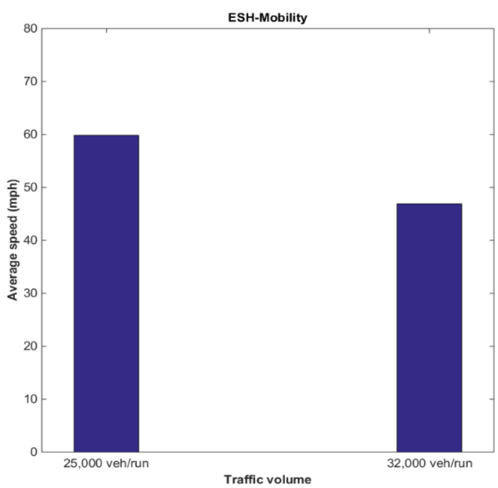

(g) ESH-Mobility Impacts

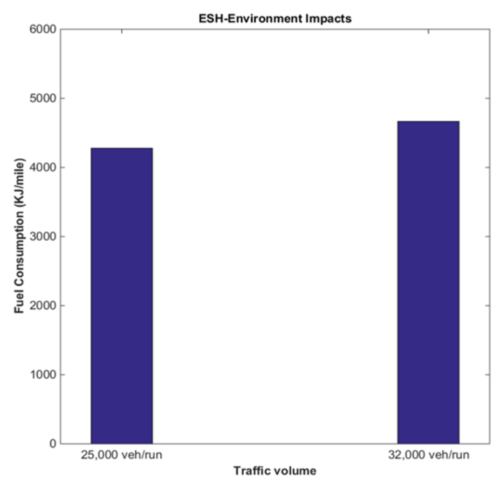

(h) ESH-Environmental Impacts

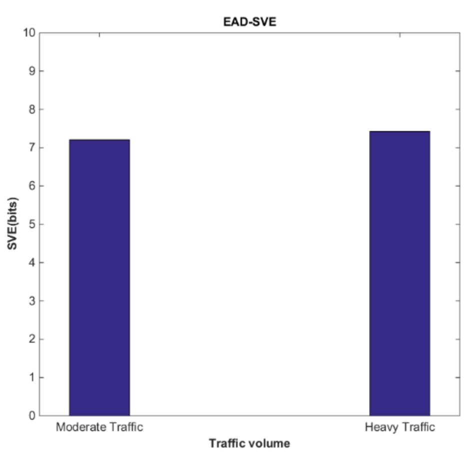

(i) EAD-SVE

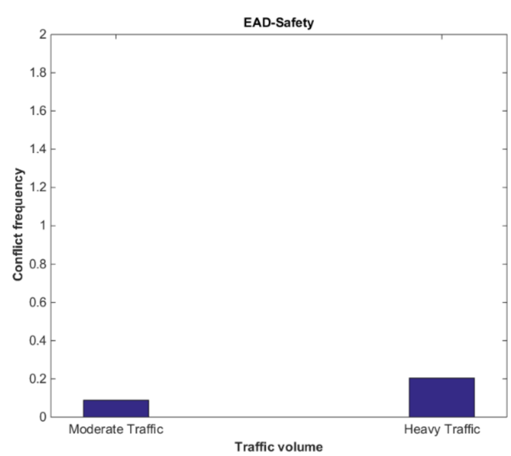

(j) EAD-Safety Impacts

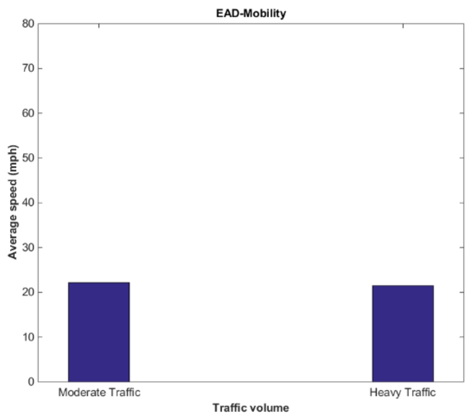

(k) EAD-Mobility Impacts

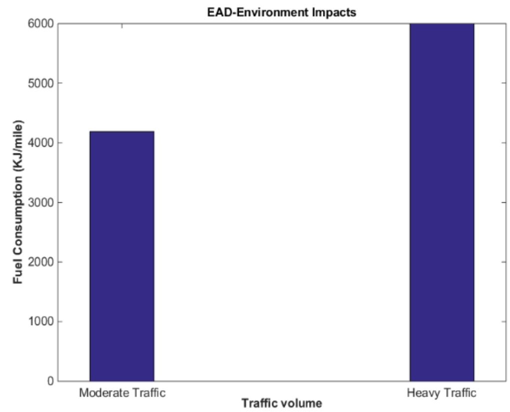

(l) EAD-Environmental Impacts

Figure 5-10. SVE versus Three Conventional MOEs across Two Different Congestion Levels for Three Different CV Applications (20% Penetration Rate of Application-Equipped Vehicles)

5.5.2.3 Discussions

To draw a more general conclusion on the correlation between SVE and vehicle performance, the conflict frequency, average speed and fuel consumption have been estimated for each individual vehicle (application-equipped) during its whole trip. The correlation coefficients between SVE values of individual vehicles and their safety, mobility and environmental sustainability performance measures for all the four CV applications are shown in Table 5-4. Comparing Table 5-3 with Table 5-4, the correlation coefficients between the SVE and the conflict frequency/fuel consumption are still positive. But the correlation of the SVE and the vehicle's performance measures from the individual vehicle perspective is not as strong as the correlation of the SVE distribution or the entropy of overall vehicles and the overall performance measures (e.g., average conflict number and average fuel consumption) (please also refer to Figure 5-8, as compared to all the individual samples, the SVE shows stronger positive correlation with the average conflict frequency).

Table 5-4 Correlation coefficients between SVE and conventional MOEs (Heavy Traffic, 20% Penetration Rate)

Application	HSDW			ESH			EAD		
MOE	SVE vs S[a]	SVE vs M[b]	SVE vs E[c]	SVE vs S	SVE vs M	SVE vs E	SVE vs S	SVE vs M	SVE vs E
Correlation coefficient	0.1040	-0.4092	0.1989	0.0812	-0.4362	0.1881	0.1589	0.0346	0.1435

a Safety MOE: Conflict frequency. b Mobility MOE: Average speed (mph). c Environmental impacts MOE: Fuel consumption (KJ/mi).

5.6 Summary

This chapter proposed and developed a Speed Variation-based Entropy (SVE) as a new measure of effectiveness (MOE) for CV applications, at both on the individual vehicle and the traffic levels. The SVE distribution (based on each individual trip) can be used as an alternative MOE for traffic systems. Three representative applications were selected, and the SVE distributions were analyzed in comparison to MOEs related to safety, mobility, and environmental impacts.

The SVE has a strong correlation with conventional MOEs for CV applications especially under freeway scenarios. For example, results from this study show that the average conflict frequency and the average fuel consumption have a strong positive correlation with the SVE especially under freeway scenarios. In addition, the SVE and its distribution can be used as an alternative MOE for CV applications evaluation in a more holistic way from the perspective of the entire traffic system status observation, which otherwise needs to be jointly reflected and evaluated by several (usually more than one) conventional MOEs. We can observe the entire traffic status through the SVE distributions (mode and IQR): A system with a larger mode and a broader inter-quartile range (IQR) of the SVE distribution is more chaotic and less predictable (usually with deteriorated conventional MOEs simultaneously).

However, the relation between the SVE and the average speed itself is relatively complicated (either positive or negative correlation), depending on the design of CV applications. Therefore the SVE might be not a proper indicator to evaluate the mobility performance (e.g., average speed) for the type of applications with string stability (e.g., cooperative adaptive cruise control). Please note that even the SVE is not closely associated with the speed values, but the noise in speed measurement could still affect the performance of the SVE measure since the inaccurate speed measurement could cause errored calculation of speed variations.

6 DEVELOPMENT AND EVALUATION OF A V2V-BASED LANE SPEED MONITORING APPLICATION

Acquiring the real-time traffic information is fundamental for many traffic research problems and intelligent transportation system applications. Conventionally, such information is collected from either fixed-location sensors (such as loop detectors [132], wireless sensor network [133], and cameras) or mobile sensors (e.g., Global Positioning System (GPS) enabled probe vehicles [134]-[135], radar, LiDAR [136]). However, these conventional sensing technologies may suffer from: 1) constrained detection range in space and time; 2) loss of information fidelity due to the inclement weather; or 3) high cost in data storage and processing. As an emerging technology, connected vehicles (CV) have shown great potential to significantly enhance roadway users' safety, mobility, and environmental sustainability.

In this chapter, a novel vehicle-to-vehicle (V2V) based application, Lane Speed Monitoring (LSM), has been developed as a CV-based driver assistance system example, to assist the vehicle driver in selecting the lane with the best traffic flow conditions. This guidance relies on the estimate of downstream lane-level vehicle states (lane-level recognition is a research problem in itself, some researchers proposed lane-level positioning based on carrier offset [137] and computer vision [138]), i.e., instantaneous speeds, obtained from Dedicated Short Range Communication (DSRC). The remainder of this chapter is organized as follows: Section 6.1 and Section 6.2 describe in detail the system architecture and the lane-level travel speed estimation of the developed LSM application, followed by a description of a simulation setup (including the tools, parameters, and test scenarios) for evaluating its performance in Section 6.3.

Comprehensive analyses of simulation results are presented in Section 6.4, in terms of Safety, Mobility and Environmental impacts (SME). Section 6.5 presents the SME tradeoff analysis of the LSM application. Section 6.6 presented the test results for LSM under the developed SVE performance measure framework. Section 6.7 concludes this chapter with potential future work in this area.

6.1 System Architecture

Figure 6-1 presents the system architecture for the developed LSM application, which includes three basic layers:

- *Input layer:* The position and speed information of downstream DSRC-equipped vehicles can be obtained via V2V communication, e.g., in the form of Basic Safety Messages (BSM);
- *Estimation layer:* The downstream traffic states (e.g., minimum speed and average speed) are estimated at the lane level. A more detailed description of traffic state estimation is presented further in Section 6.2;
- *Output layer:* By comparing the estimated traffic states between different lanes, the application will provide the recommendation on which lane the driver should choose. Such advisory (e.g., via in-vehicle display) provides the driver with sufficient information for real-world implementation, i.e., the driver can decide whether or not any lane-change maneuver should be performed.

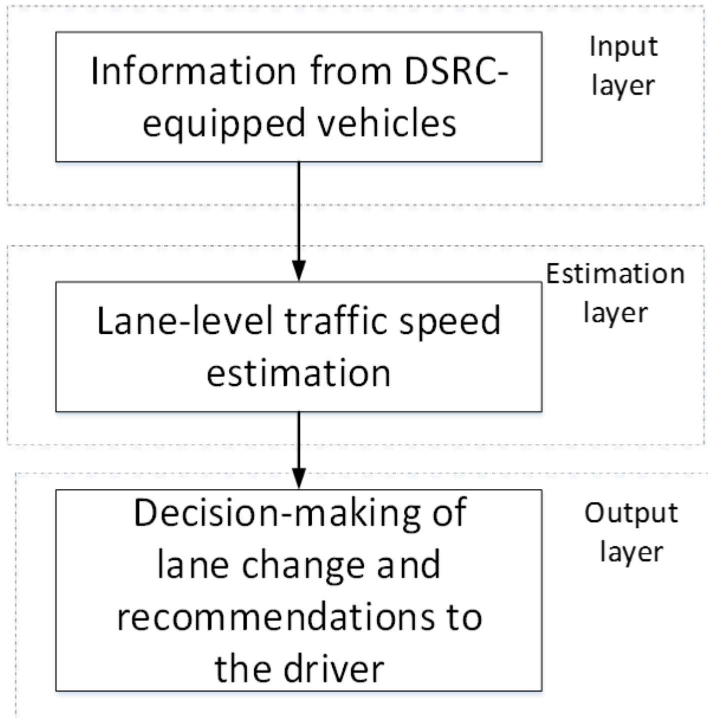

Figure 6-1. System Architecture for Lane Speed Monitoring

6.2 Lane-Level Traffic Speed Estimation

DSRC-equipped vehicles are defined as communication-capable vehicles with a DSRC device. These vehicles can transmit/receive the speed/location information within a specified transmission range. LSM-equipped vehicles are defined as vehicles with the in-vehicle lane-speed-monitoring application. Based on the real-time information transmitted from the downstream DSRC-equipped vehicles, lane-level traffic speed that may affect the lane selection decision can be evaluated using two key metrics: 1) minimum speed; and 2) average speed.

In the minimum speed based evaluation method, the system will continuously monitor the slowest instantaneous speed of the equipped vehicles (if any) along each downstream lane. Then, the system will compare the metric of other lanes with that of the current lane (i.e., where the host vehicle is traveling), and determine whether or not a lane-change suggestion should be disseminated. More specifically, we define the Measurement of Estimation (MOE) of traffic conditions for the minimum-speed based LSM as follows:

$$MOE1 = v_{i,m}^{min}(t) \tag{6-1}$$

where $v_{i,m}(t)$ is the instantaneous speed of the *m*-th downstream DSRC-equipped vehicle at time *t* in lane *i*. By comparing the detected minimum speed (i.e., *MOE1*) of all lanes, the system will recommend the lane with maximum value of *MOE1* to the driver.

However, the minimum speed based method may not be robust enough in real-world deployment, due to the variation in driving behavior (e.g., random abrupt decelerations). Some slow vehicles (or vehicles stopping suddenly) are considered as outliers on roads, which may not reflect the traffic condition in a comprehensive way. When a slow vehicle exists downstream, drivers usually overtake the slow vehicle and then still stay in the faster lane. Therefore, with the aim of showing drivers the general traffic stream information further downstream, we propose to use the lane average speed, $\bar{v}$, in the estimation layer instead, i.e.,

$$MOE2 = \bar{v} = \frac{\sum_{t_0}^{t_0+\Delta t} VMT(t)}{\sum_{t_0}^{t_0+\Delta t} VHT(t)} \tag{6-2}$$

where Δt is the time window for information collection; *VMT* and *VHT* represent the downstream (DSRC-equipped) vehicle-mile-traveled and vehicle-hour-traveled, respectively. As shown in Figure 6-2, during the time period from $t_1$to t_2,where $t_2 = t_1 + \Delta t$, instantaneous speeds of downstream DSRC-equipped vehicles are continuously monitored and the lane average speed is calculated for each lane. Then, the system will suggest the lane with maximum *MOE2*, i.e., the lane average speed.

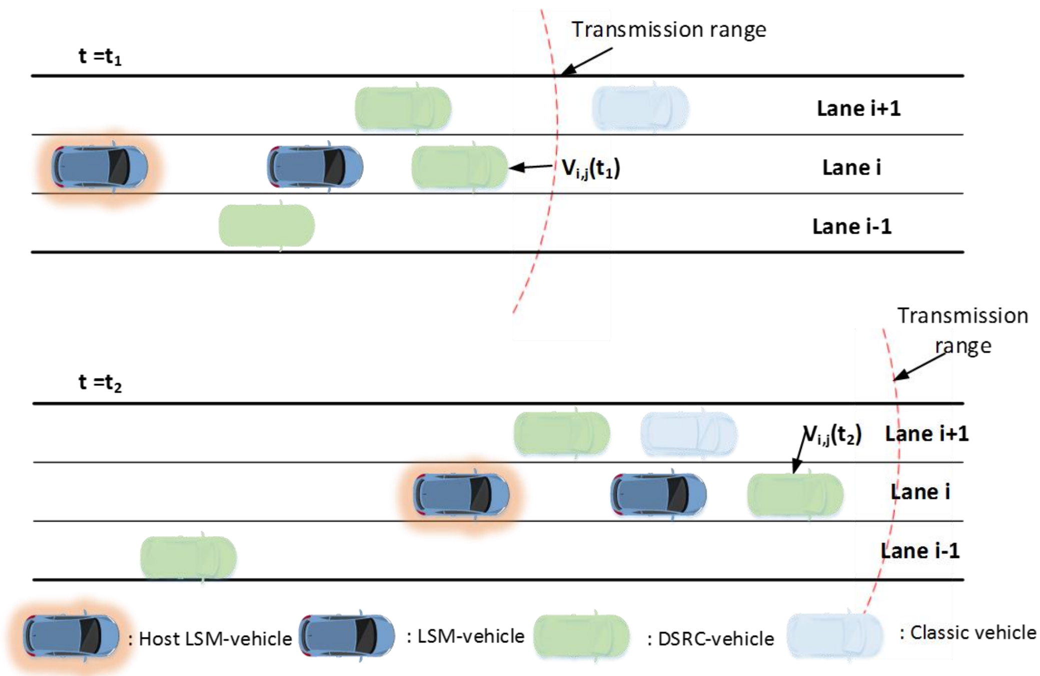

Figure 6-2. Example of Speed Monitoring for Average-Speed-Based Algorithm

6.3 Simulation Setup

6.3.1 Simulation Tools

In this study, we use PARAMICS (PARAllel MICroscopic Simulator), a microscopic traffic simulation tool, to model the movement and behavior of individual vehicles on road networks [48]. The PARAMICS model is used by a number of California projects [139]. An Application Programming Interface (API) has been developed to implement the LSM algorithm, collect vehicles' data, and evaluate the corresponding measures of effectiveness.

For safety performance evaluation, the Surrogate Safety Assessment Model (SSAM) is used to perform statistical analysis of vehicle trajectory data (.trj files) output from PARAMICS [33]. In this study, we analyze the number and type of conflicts. A 1.5s time-to-collision threshold was chosen to consider a conflict in the analysis.

To assess environmental impacts, we use the MOtor Vehicle Emission Simulator (MOVES), developed by the U.S. Environmental Protection Agency (EPA), and have coded the corresponding API for energy/emissions estimation [54]. The Vehicle Specific Power (VSP) based approach used in this study is to link traffic model through link-specific vehicle Operating Mode distribution, which is calculated based on the second-by-second vehicle speed and acceleration, second-by-second VSP and second-by-second OpMode. The second-by-second energy consumption can be obtained based on the energy consumption rate look-up table for the associated vehicle type and OpMode [140].

6.3.2 Simulation Network Model

We use the California SR-91E simulation model, which consists of a 15-mile corridor between the Orange County Line and Tyler Street in Riverside, California (see Figure 6-3). The number of lanes ranges from 4 to 6 and there are 9 pairs of on-/off-ramps. The speed limit is 65 miles per hour, and traffic conditions usually fall into level of service C to E [130] during the peak hours. Traffic demands, origin-destination (O-D) patterns, and driving behavior have been calibrated to match that of a typical weekday morning in the summer of 2006. For more detailed information about the model, please refer to [131].

6.3.3 Simulation Scenarios

To better understand the effectiveness of the LSM application, we have conducted a number of comprehensive simulation tests over the following system parameters:

1) Congestion level. During the 3-hour simulation period, there are three traffic volumes that were evaluated: 16,000 vehicles, 25,000 vehicles (calibrated), and 32,000 vehicles. Further analysis on the average speed indicates that these three cases represent the level of service (LOS) C (stable flow), D (transitional flow) and E (unstable flow), respectively, according to the Highway Capacity Manual 2010 [130].

2) Market penetration rate of DSRC-equipped vehicles. In this study, we have investigated a full range (a total of 8 levels) of penetration rate of communication-capable vehicles, including 0% (baseline), 1%, 5%, 10%, 20%, 50%, 80% and 100%, under the calibrated traffic demand pattern (i.e., LOS D). The LSM application equipped rate is set as 9% (out of all DSRC-equipped vehicles) in this study, which for example, is consistent with the US automobile market share of Honda vehicles in Year 2015 [141].

In addition to the aforementioned parameters, a 300 meters DSRC range is assumed. Further, to better model the real-world driver behavior in response to the LSM application, we have conducted a customer survey (including 1453 drivers as respondents) on: 1) the preferred information update frequency; and 2) the maneuver (i.e., lane change or not) that drivers will take. The survey results are shown in Figure 6-4 and Figure 6-5, respectively. As can be observed in Figure 6-4, the majority of subjects prefer receiving the information updates frequently. Therefore, we implemented a recommendation update period of 2 seconds in the LSM algorithm. Results from Figure 6-5 indicates that most of the drivers will change to other lanes when facing congestion, which supports us to develop the driver reaction model as following the lane change recommendations most of the time (if possible) in simulation. It is worth noting that we use the default lane change function in PARAMICS for LSM, which would operate lane changes in a certain compliance rate when safe and possible.

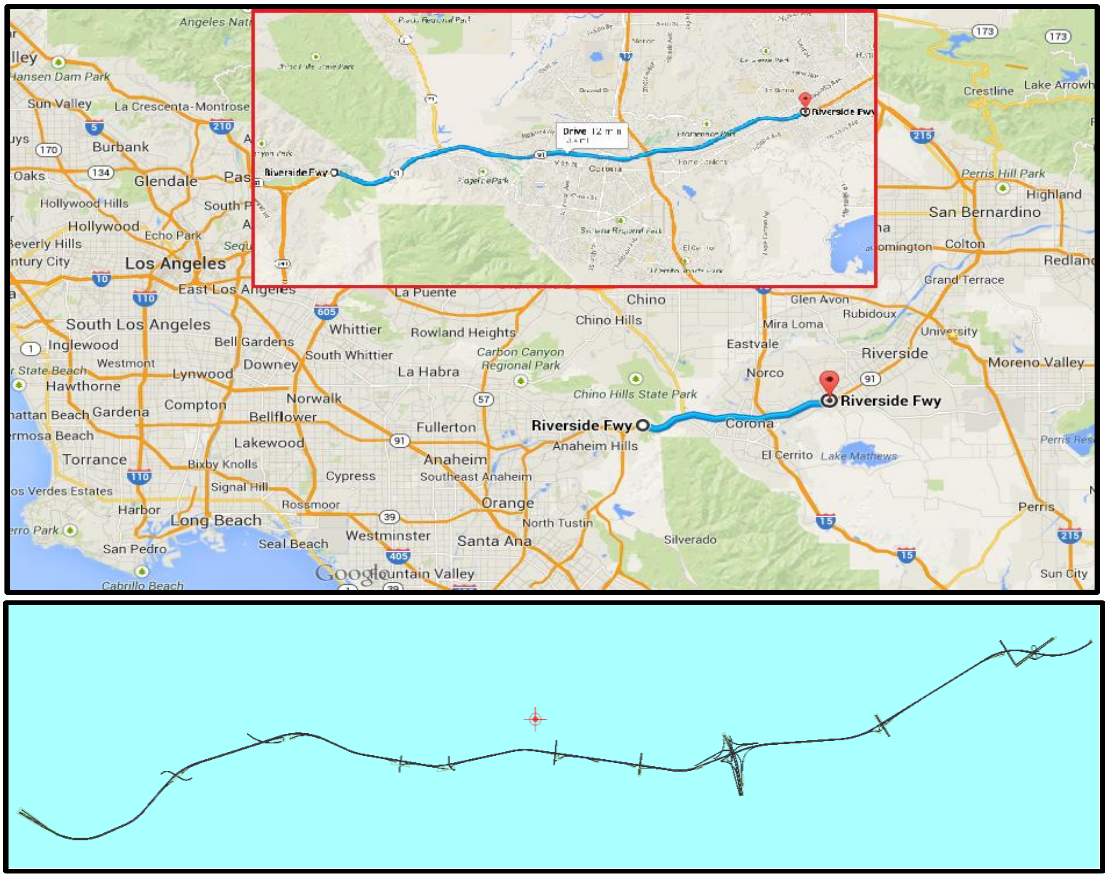

Figure 6-3. Road Network of California SR-91E in Real-World and Paramics

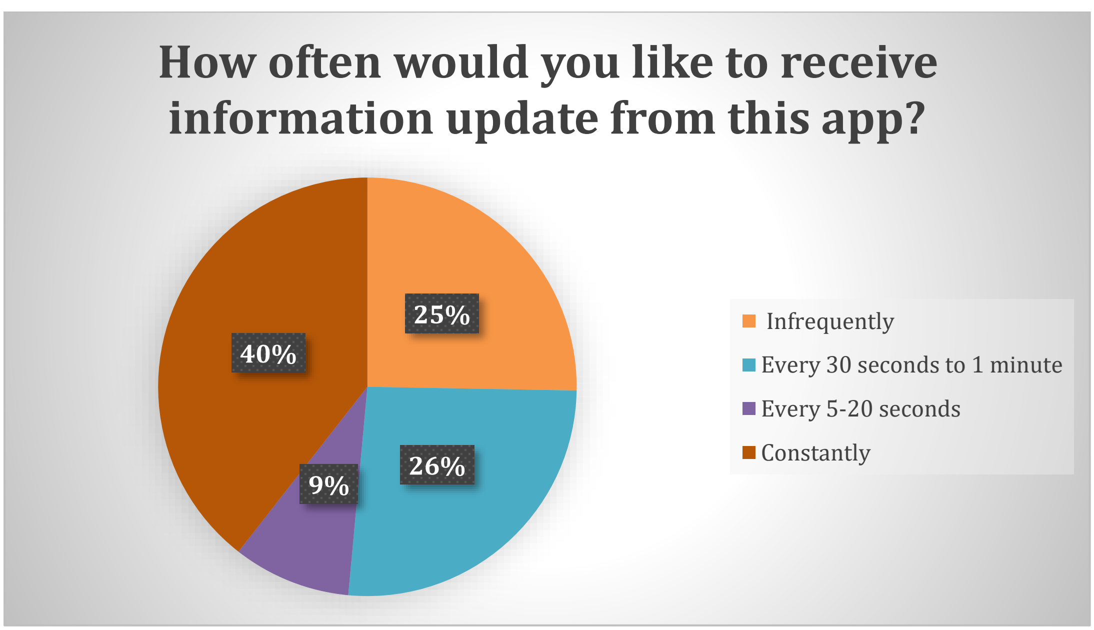

Figure 6-4. Survey Results Corresponding to Parameters Selection in Algorithm

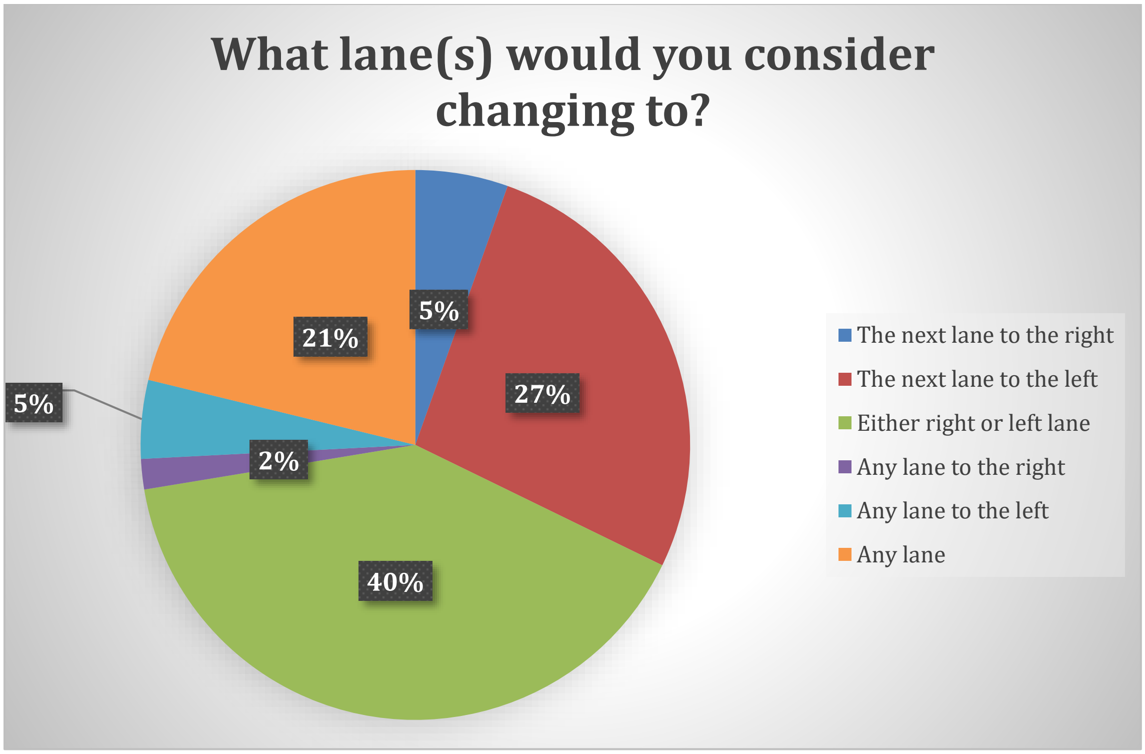

Figure 6-5. Survey Results Corresponding to Driver Behavior in Algorithm

6.3.4 Simulation Runs

Due to the stochastic nature of the micro-simulation, multiple runs were made using different seed numbers which are the starting numbers for the random number generator (RNG) used by PARAMICS.

Equation (6-3) provides a guidance on the recommended number of runs that may quantify the allowable error.

$$N = \left(t_{\alpha/2} \cdot \frac{\delta}{\mu\varepsilon}\right)^2 \qquad (6\text{-}3)$$

where μ and δ are the mean and standard deviation of the estimated metrics (e.g., average speed) based on the completed runs; ε is the allowable error specified as a fraction of the mean μ; and $t_{\alpha/2}$ is the critical value of the t distribution at the significance level of α. In our simulation, the significance level was set to 0.05. The allowable error was set at 5%. If the number of conducted runs is larger than the recommended number of runs, the simulation for that scenario is finished. Otherwise, one more run is made and the recommended number of runs is updated accordingly. Typically, 3-5 runs are needed for the 20% or higher penetration rate cases.

The detailed flowchart of the developed Lane Speed Monitoring is shown in Figure 6-6.

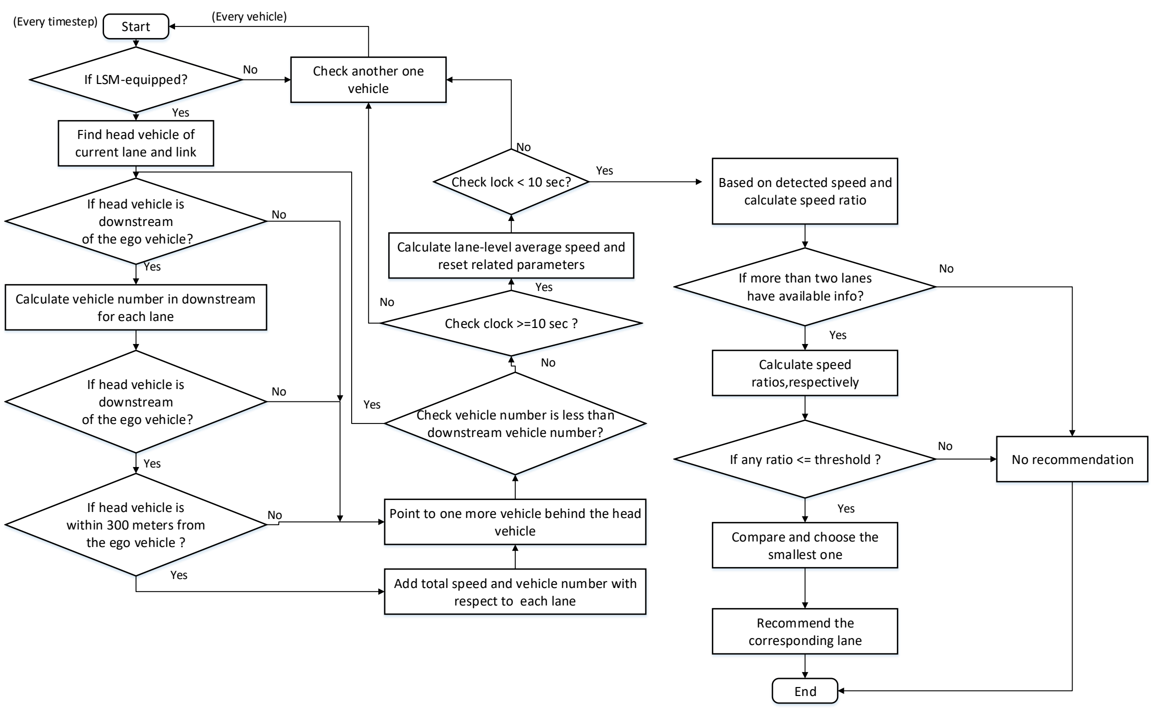

Figure 6-6. Detailed Flowchart of the Developed Lane Speed Monitoring Application

6.4 Simulation Results and Analysis

6.4.1 Mobility

To evaluate the mobility benefits, we defined the average speed improvement of equipped vehicles versus unequipped vehicles as:

$$\frac{v_e - v_n}{v_n} \cdot 100\% \tag{6-4}$$

where v_e is the average speed of LSM-equipped vehicles; v_n is the average speed of unequipped vehicles. Other average speed improvement between two different types of vehicles are defined similarly, where positive values in figures represent a reduction of the latter compared with the former and negative values represent an increase of the latter compared with the former. To be clear, all equipped vehicles defined in this study are LSM-equipped vehicles and unequipped vehicles mean LSM-unequipped vehicles.

6.4.1.1 Sensitivity Analysis on Penetration Rate

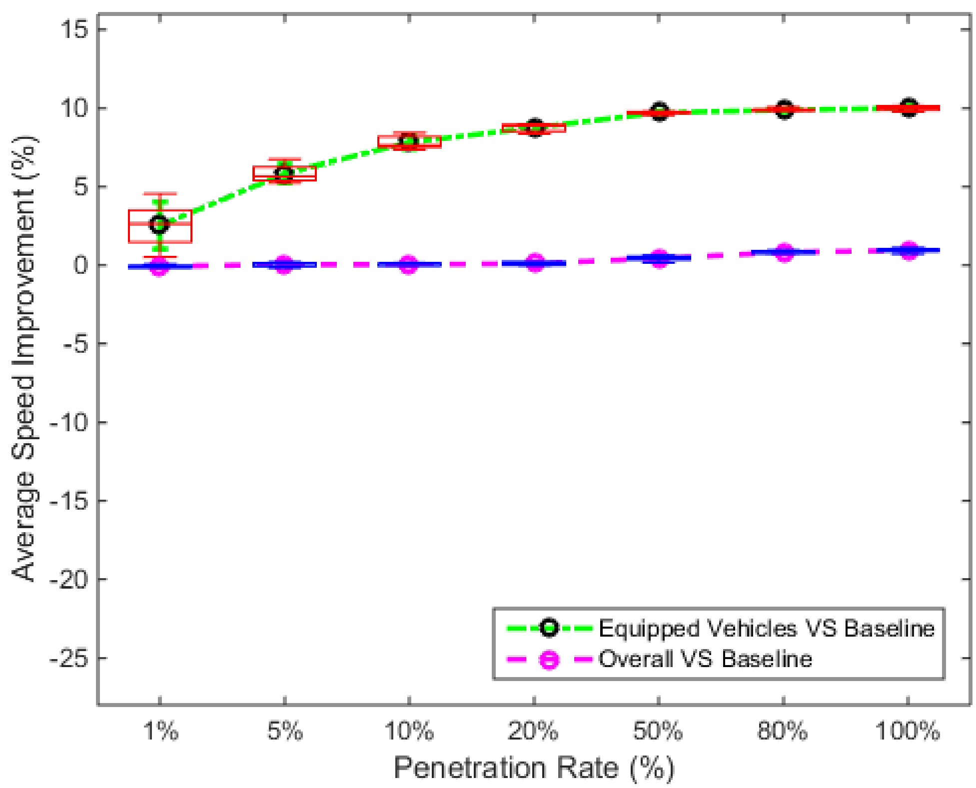

Figure 6-7. Average Speed Improvement Comparison at LOS D

According to Figure 6-7, as the penetration rate increases, higher average speed improvements (up to 11% on average) for equipped vehicles can be witnessed under the traffic condition with LOS D. When the penetration rate is high enough (i.e., greater than

10%), the improvement tends to be stable with much less variation. We can also see that overall traffic does not show any significant speed improvement beyond the baseline.

6.4.1.2 Sensitivity Analysis on Traffic Volume

Figure 6-8 shows that for all levels of service, equipped vehicles have positive speed improvement compared to unequipped vehicles. This means that from a user's perspective, around 10% benefits in average speed will be gained from the developed application. However, the performance of unequipped vehicles will be slightly negatively impacted especially under the unstable traffic flow (LOS E or 32,000 vehicles). A potential reason is that the LSM-induced lane change maneuvers may further delay the other unequipped equipped in the congested traffic condition. Such behavior does not show for LOS C and D.

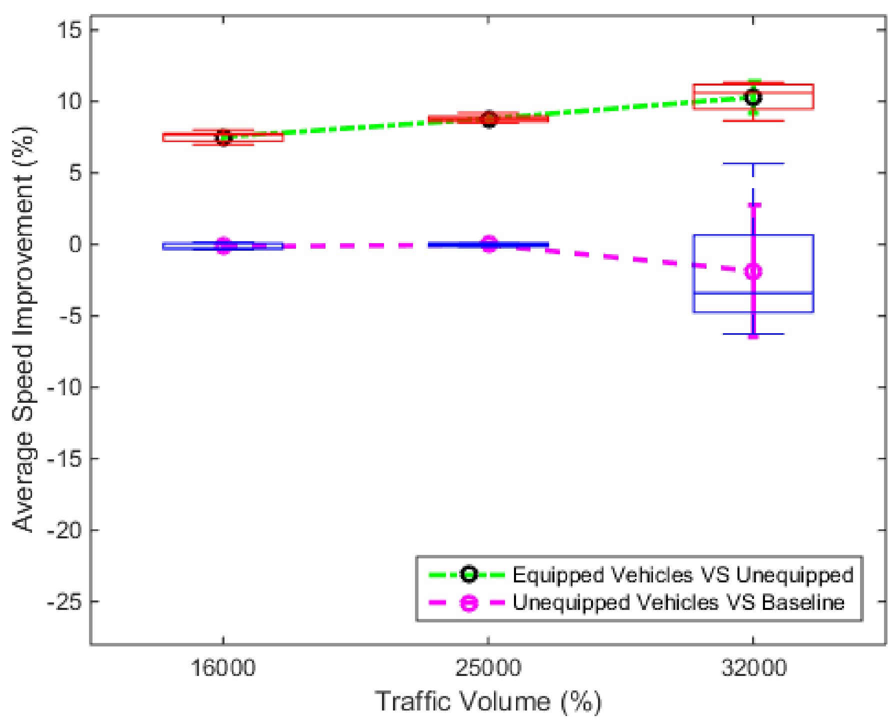

Figure 6-8. Average Speed Improvement Comparison at 20% Penetration Rate

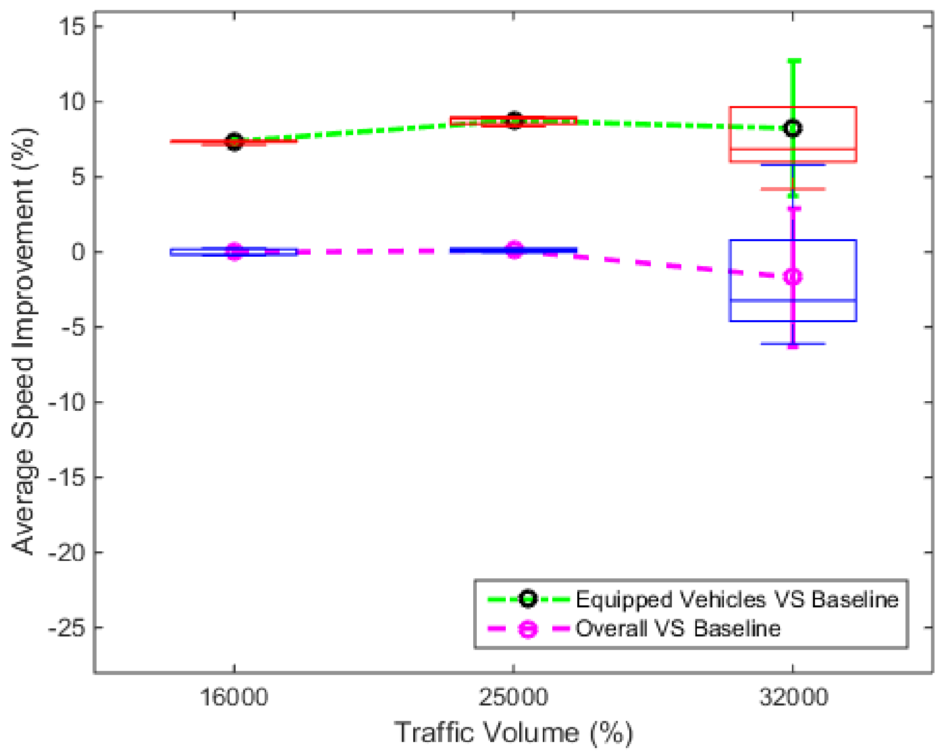

Figure 6-9. Average Speed Improvement Comparison at 20% Penetration Rate

From the perspective of an operator (see Figure 6-9), the introduction of this developed application will not affect the overall traffic performance significantly when the traffic volume is below 25,000 vehicles (LOS D). However, if the traffic gets congested (e.g., LOS E), the overall traffic performance will be degraded (20% of vehicles are equipped with DSRC in this case). This is consistent with the observation in Figure 6-8, as the unequipped vehicles dominate the entire traffic flow.

6.4.2 Safety

6.4.2.1 Sensitivity Analysis on Penetration Rate

The vast majority of conflict type are rear-end collision close calls, based on the SSAM results. The number of conflicts per LSM-equipped vehicle and that of overall case are compared with the baseline, respectively, as can be seen in Figure 6-10. It is observed that equipped vehicles have more conflicts than the baseline. A hypothesis is that as the penetration rate increases, the number of lane change per LSM-equipped vehicle increases and thus leads to an increase of the potential conflict frequency. Overall vehicles have more or less the same conflict frequency at lower penetration rate. The conflict frequency of overall vehicles increases a little bit as penetration rate increases. A hypothesis is that as the penetration rate increases, unequipped vehicle is impacted by the disturbance caused by the more frequent lane change maneuvers of LSM-equipped vehicles. The absolute conflict number per vehicle for the baseline case is about 0.18.

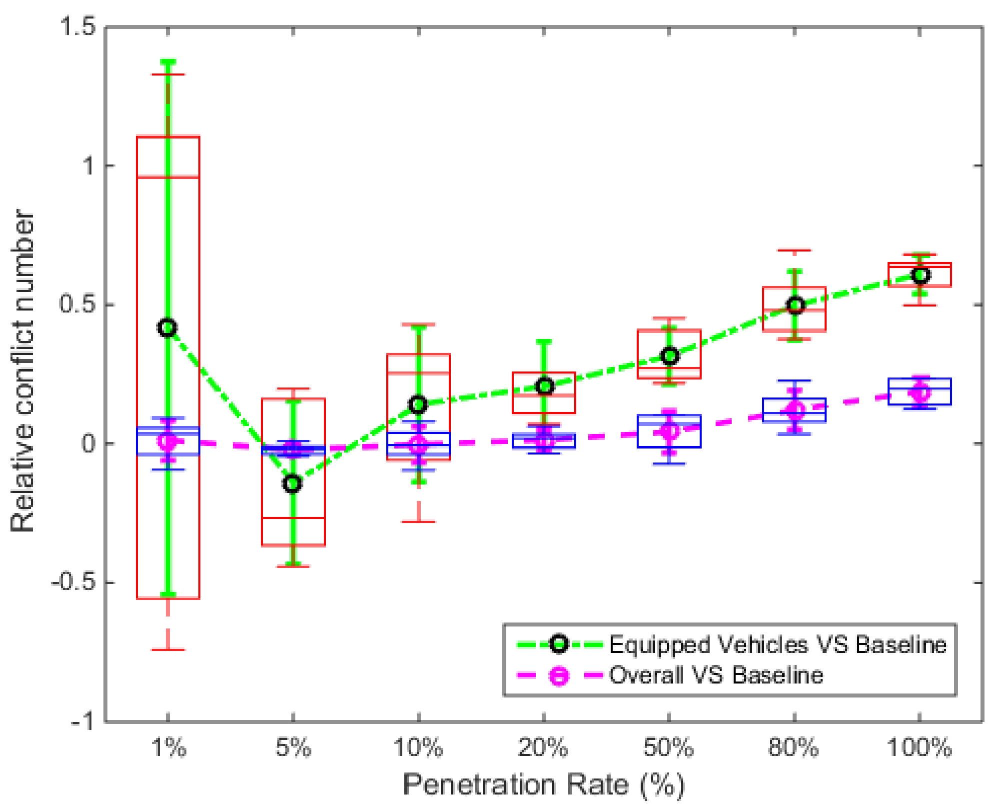

Figure 6-10. Relative Conflict Frequency under Different Penetration Rates at LOS D

6.4.2.2 Sensitivity Analysis on Traffic Volume

As shown in Figure 6-11, across all different LOS, the number of conflicts per equipped vehicle is relatively higher, while the number of conflicts for overall traffic is almost the same as that of the baseline (0% penetration rate) scenario.

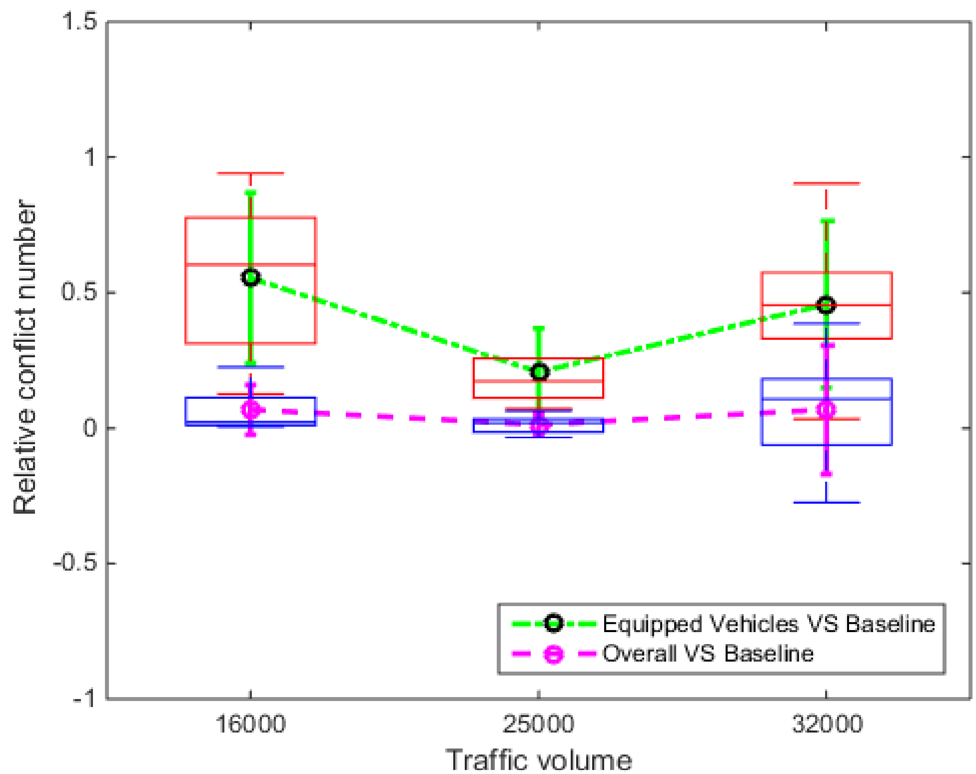

Figure 6-11. Relative Conflict Frequency for Overall at 20 % Penetration Rate and Baseline Case

There is a turning point at LOS D (25,000 veh/hr) in Figure 6-11, e.g., the case of equipped-vehicles versus baseline. The absolute conflict number per equipped vehicles/baseline at LOS C (1,6000 veh/hr) is about 0.1209/0.0784, And the absolute conflict number per equipped vehicles/baseline at LOS D (25,000 veh/hr) is about 0.2071/0.1714. This may result in the lower relative conflict number at LOS D even for higher absolute conflict numbers.

6.4.3 Environmental Sustainability

This section discusses environmental aspects of the LSM application. A penetration rate and traffic volume analyses are provided in the following. Similar analysis were also conducted in [142].

6.4.3.1 Sensitivity Analysis on Penetration Rate

It is interesting to observe from Figure 6-12 that the average fuel consumption of equipped vehicles at higher penetration rate is slightly higher (i.e., up to 3%) than that of the baseline. The overall vehicles, on the other hand, have little change in fuel consumption compared to the baseline scenario. A hypothesis is that the under the LOS D traffic condition, the application induced speed improvement and lane change maneuvers (thus variations in vehicle activities) may result in additional fuel consumption for the equipped vehicles.

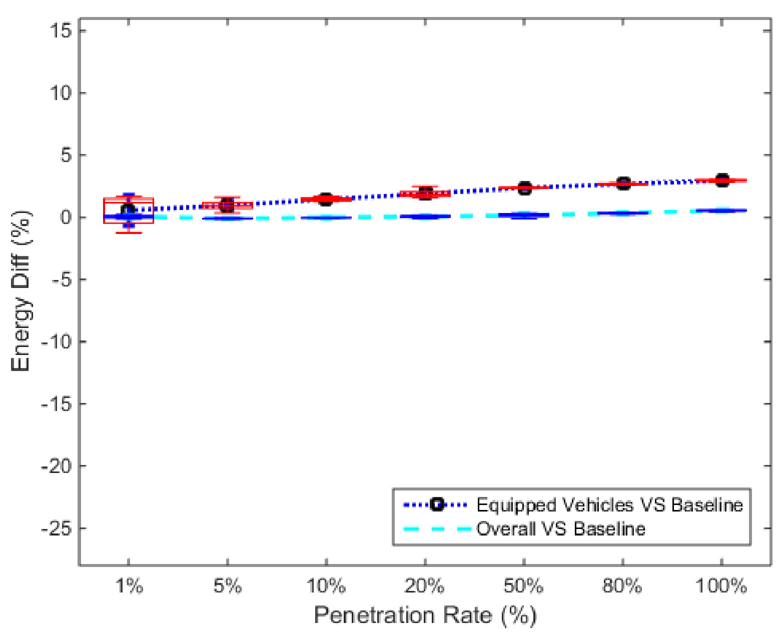

Figure 6-12. Average Energy Difference vs Penetration Rates at LOS D

6.4.3.2 Sensitivity Analysis on Traffic Volume

As can be observed from Figure 6-13, when the traffic volume increases, the fuel consumption of equipped vehicles is getting closer to that of unequipped vehicles and the fuel consumption of unequipped vehicles is getting higher than the baseline. This may mainly result from the degradation in the mobility of unequipped vehicles. A similar explanation can be applied to the findings in Figure 6-14 (in connection with the results from Figure 6-9). Future research may investigate optimizing the application's lane change suggestions taking into consideration the environmental aspects.

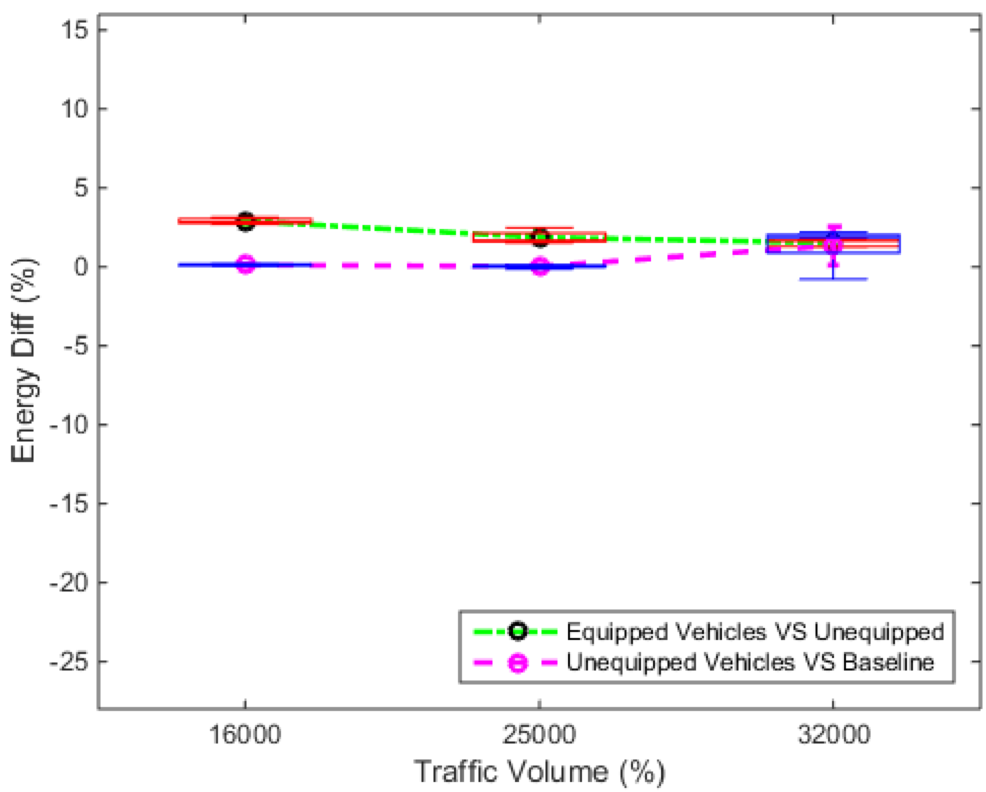

Figure 6-13. Average Energy Difference vs LOS at 20% Penetration Rate

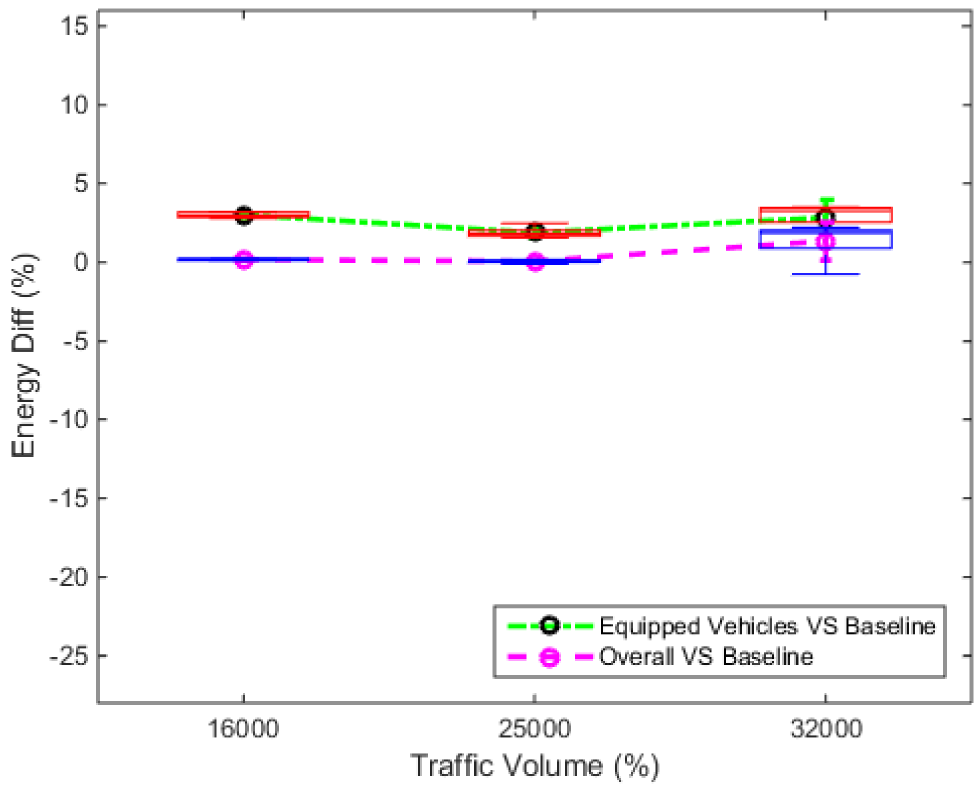

Figure 6-14. Average Energy Difference vs LOS at 20% Penetration Rate

6.5 SME Tradeoff Analysis of the LSM Application

The penetration rate of equipped vehicles is another dimension when evaluating the traffic flow impacts and overall performance measure. Four penetration rate cases were herein selected: 10%, 20%, 50% and 80% to generally observe the tradeoffs among three MOEs, i.e., safety, mobility, and environmental sustainability. The numerical results are listed in Table 6-1. Figure 6-15 shows radar plots, where the quantitative trade-offs among different MOEs can be observed and compared, and each performance measurement in radar plots is normalized for comparison purpose. To be specific, the normalized values in Figure 6-15 are obtained by choosing the baseline data in Table 6-1 as one and the others are calculated in accordance with the relative proportions. Moreover, the average speed indicator is replaced by the average trip travel time, and the bigger value in each radar plot in Figure 6-15 represents the worse quality in terms of each MOE. The baseline case is 0% penetration rate of application-equipped vehicles. Besides the baseline, the performance measure results of the other scenarios in Table 6-1 are for application-equipped vehicles.

TABLE 6-1. NUMERICAL RESULTS OF THE LSM CASE STUDY

	Baseline	**LSM**			
Penetration rate	0%	10%	20%	50%	80%
Average conflict number per vehicle	0.1673	0.2841	0.3922	1.1029	2.8443
Average speed (mph /vehicle)	60.6	65.5	65.5	59.6	34.8
Average fuel consumption (KJ/mile/vehicle)	4275.3	4398.1	4502.1	5062.6	5917.2

Figure 6-15 illustrates the trade-off among travel time decreases, conflict number increases and fuel consumption increases and shows:

a) 10% penetration rate: the mobility-focused LSM application provides lower travel time due to faster-lane change behavior, but is exposed to higher potential conflicts and fuel consumption because of the lane change operations and higher traveling speed. With regard to the trade-off, LSM application would provide 8% travel time decrease while costing 3% more fuel and introducing higher potential conflict risks;

b) 20% penetration rate: As the penetration rate of LSM-equipped vehicles increases to 20%, the trade-off is similar to the case where the penetration rate is 10%;

c) 50% penetration rate: Both the fuel consumption and average conflict number of the LSM-equipped vehicles group continue increasing compared to the baseline, while the travel time barely decreases when the penetration rate increases to 50% because of highly mixed traffic;

d) 80% penetration rate: As the penetration rate increases to 80%, where the majority of the on-road users are LSM-application-equipped vehicles, all the performance of the LSM-equipped vehicles deteriorates compared to the baseline since most vehicles in roadway transportation were trying to operate lane changes, which leads to more traffic chaos. Since the traffic system is disturbed by extra lane changes, the LSM application does not benefit equipped vehicles any longer in this high-penetration-rate scenario.

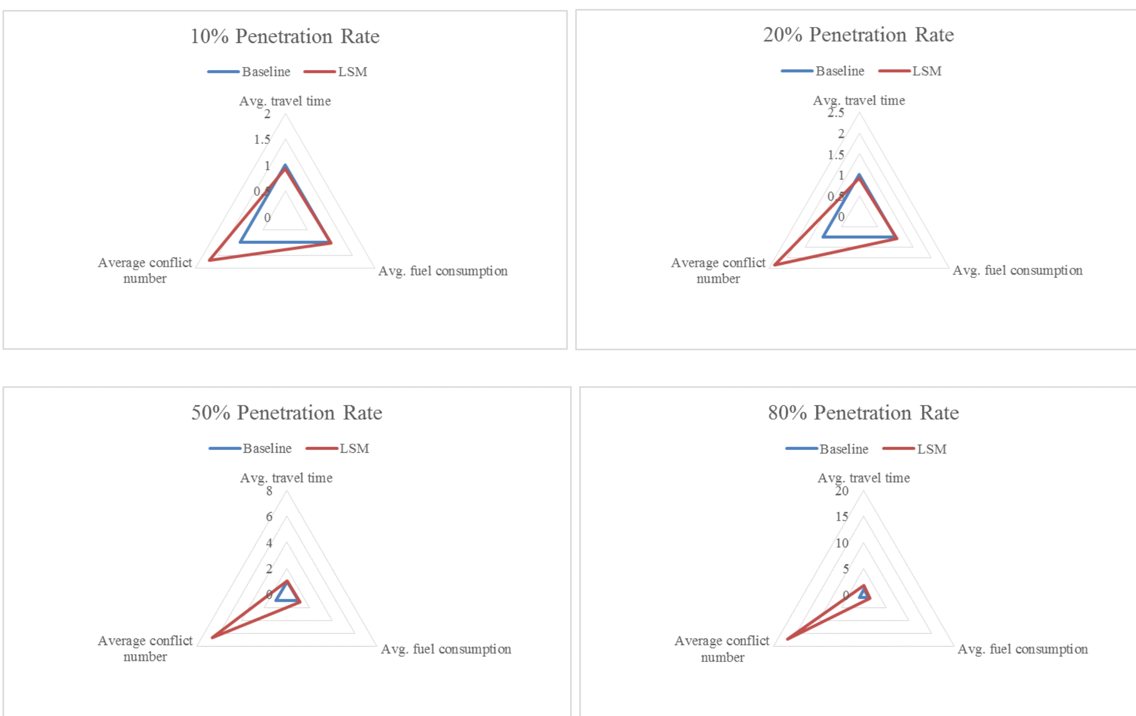

Figure 6-15. Radar Plots of Three Normalized MOEs for LSM

6.6 Speed-Variation Based Entropy Analysis for LSM

The LSM has been evaluated under the developed SVE framework (see Chapter 5) as well. The segment of California SR-91E is used to test LSM across different penetration rate levels and congestion levels. Figure 6-16 shows the SVE distributions of LSM application-unequipped vehicles (before) and LSM application-equipped vehicles (after). It can be observed that the SVE distribution of LSM-equipped vehicles shifts to the right, compared with that of LSM-unequipped vehicles. A hypothesis is that LSM-equipped vehicles always switch to faster lanes, and those extra lateral disturbances cause higher velocity fluctuations.

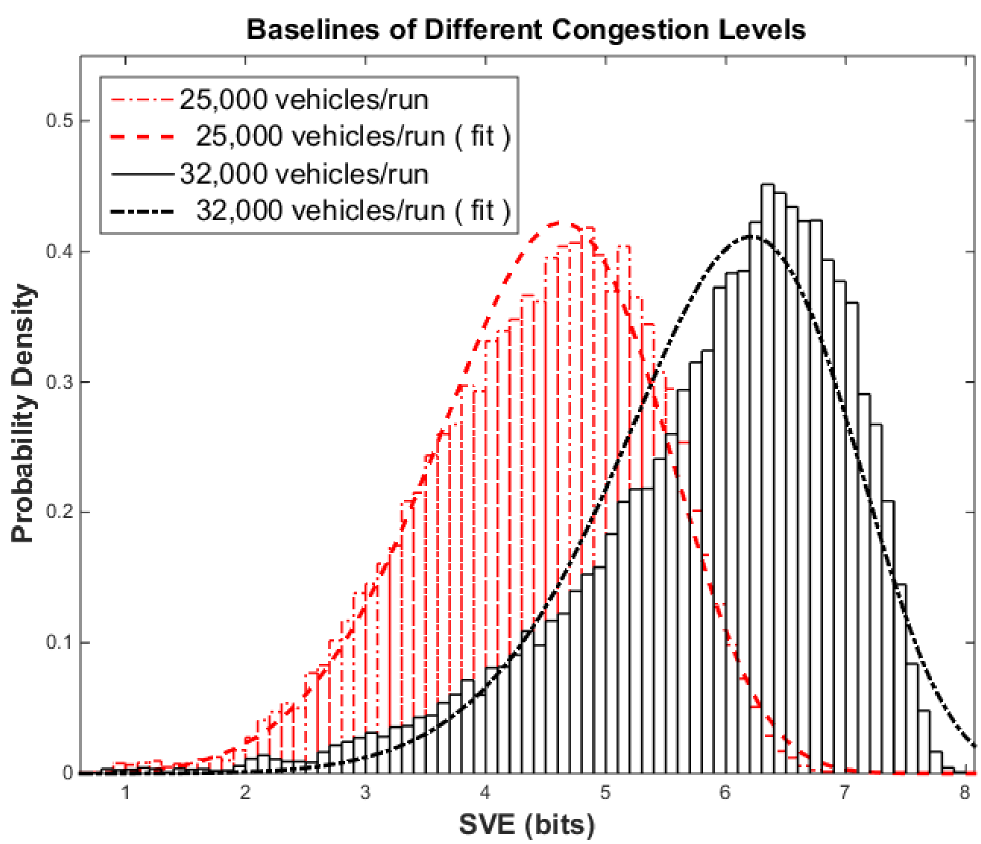

(a) no LSM-equipped vehicles

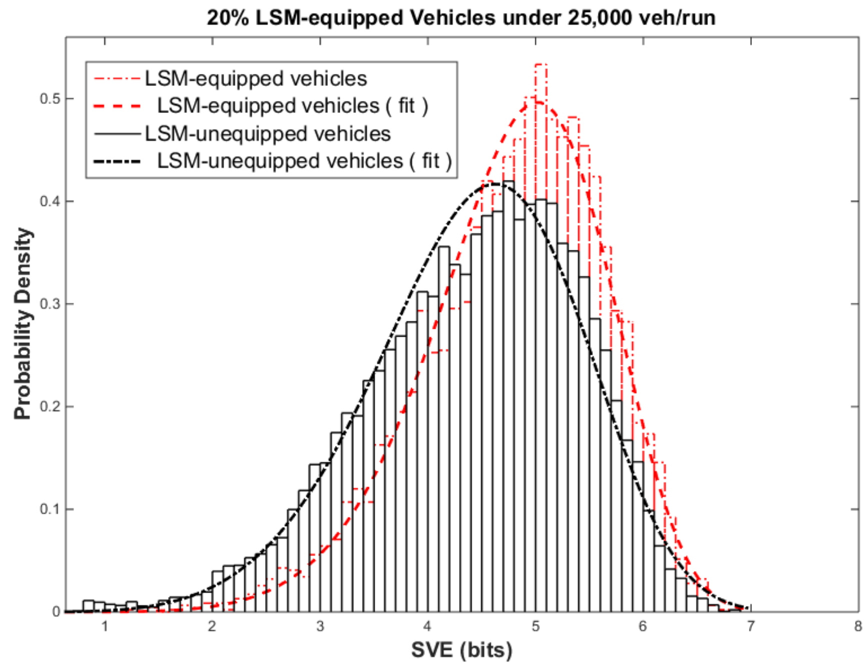

(b) 25,000 veh/run for LSM

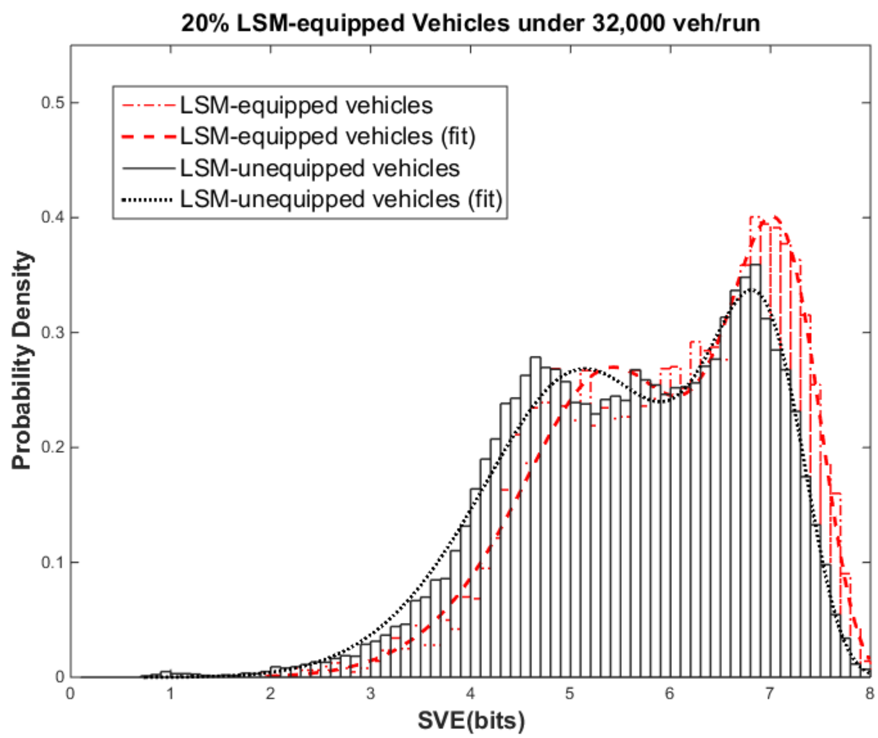

(c) 32,000 veh/run for LSM

Figure 6-16. SVE Distributions of Different Traffic Volumes in LSM scenario (Baseline Cases and 20% Penetration Rate)

In comparison of Figure 6-16(b) and Figure 6-16(c), significant changes in SVE distributions in the LSM scenario can be observed. The SVE distribution tends to be dual-modal, instead of unimodal, under heavier traffic conditions. Figure 6-16(c) shows that besides the vehicles that are subject to higher speed variations (the high mode), a certain number of vehicles have smaller speed variations (the low mode). An explanation for the dual-mode phenomena in Figure 6-16(c) is that the whole traffic flow slows down as vehicle numbers keep increasing on the network in such a congested traffic condition, and additional lane change behaviors induced by the LSM applications as extra disturbances to the traffic lead to much slower speeds with smaller speed variations.

TABLE 6-2 CONVENTIONAL MOES OF TRAFFIC VOLUME SENSITIVITY ANALYSIS

Traffic Volume Sensitivity Analysis				
LSM (20% penetration rate)				
Traffic volume		S[a]	M[b]	E[c]
Moderate traffic	Equipped	0.3922	65.5	4502.1
	Unequipped	0.2189	61.1	4315.6
Heavy traffic	Equipped	2.1334	21.3	6005.0
	Unequipped	1.4382	21.4	5733.0

[a] Safety MOE: Conflict frequency. [b] Mobility MOE: Average speed (mph). [c] Environmental impacts MOE: Fuel consumption (KJ/mile).

Based on Figure 6-17, it can be concluded that SVE has a strong negative correlation with average speed, and an obvious positive correlation with fuel consumption and conflict frequency in the LSM scenarios. This result meets the expectation that high entropy values reflect more chaotic traffic in terms of high conflict frequency, low average speed, and high fuel consumption.

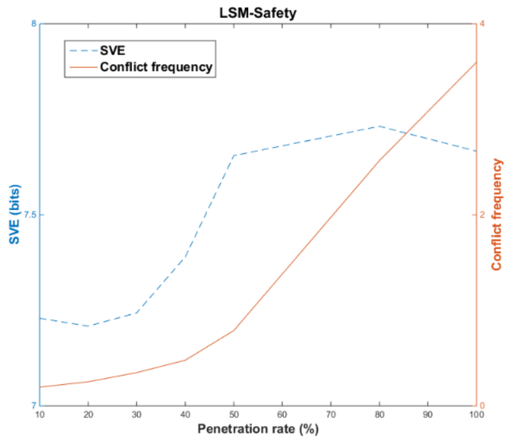

(a) LSM-Safety Impacts

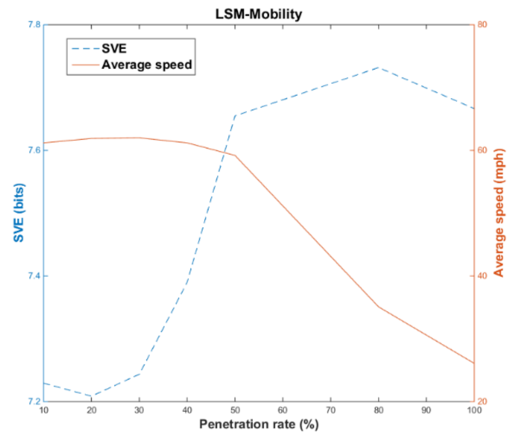

(b) LSM-Mobility Impacts

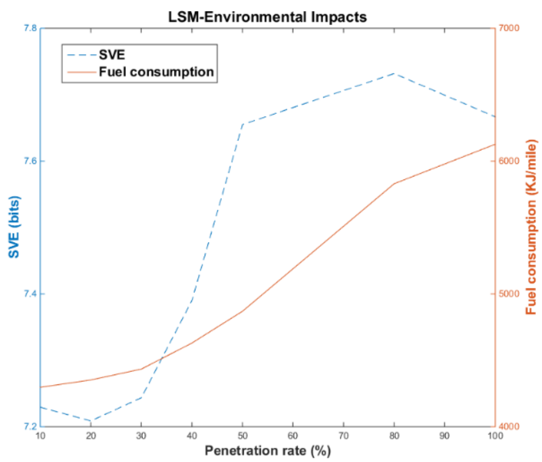

(c) LSM-Environmental Impacts

Figure 6-17. SVE versus Three Conventional MOEs across Different Penetration Rate Levels for LSM (moderate traffic)

In combination with Figure 6-16(c), it can be concluded that average traffic speeds drop dramatically from 47 mph (baseline) to 21 mph, and significant increases of fuel consumption and conflict frequency are witnessed in the congested LSM scenario (see Table 6-2). In addition, since the relation between the SVE and the average speed itself is relatively complicated (see analysis in Chapter 5), the SVE is smaller in denser traffic and the SVE distributions are used at the same time to evaluate the LSM scenario. The SVE distributions of the LSM scenario are associated with a more unpredictable and chaotic traffic condition (the chaos can be determined from the dual-mode SVE distributions with large variance) (see Figure 6-16(c)), indicating higher conflict risk, lower traffic speed, and high fuel consumption (see Figure 6-18).

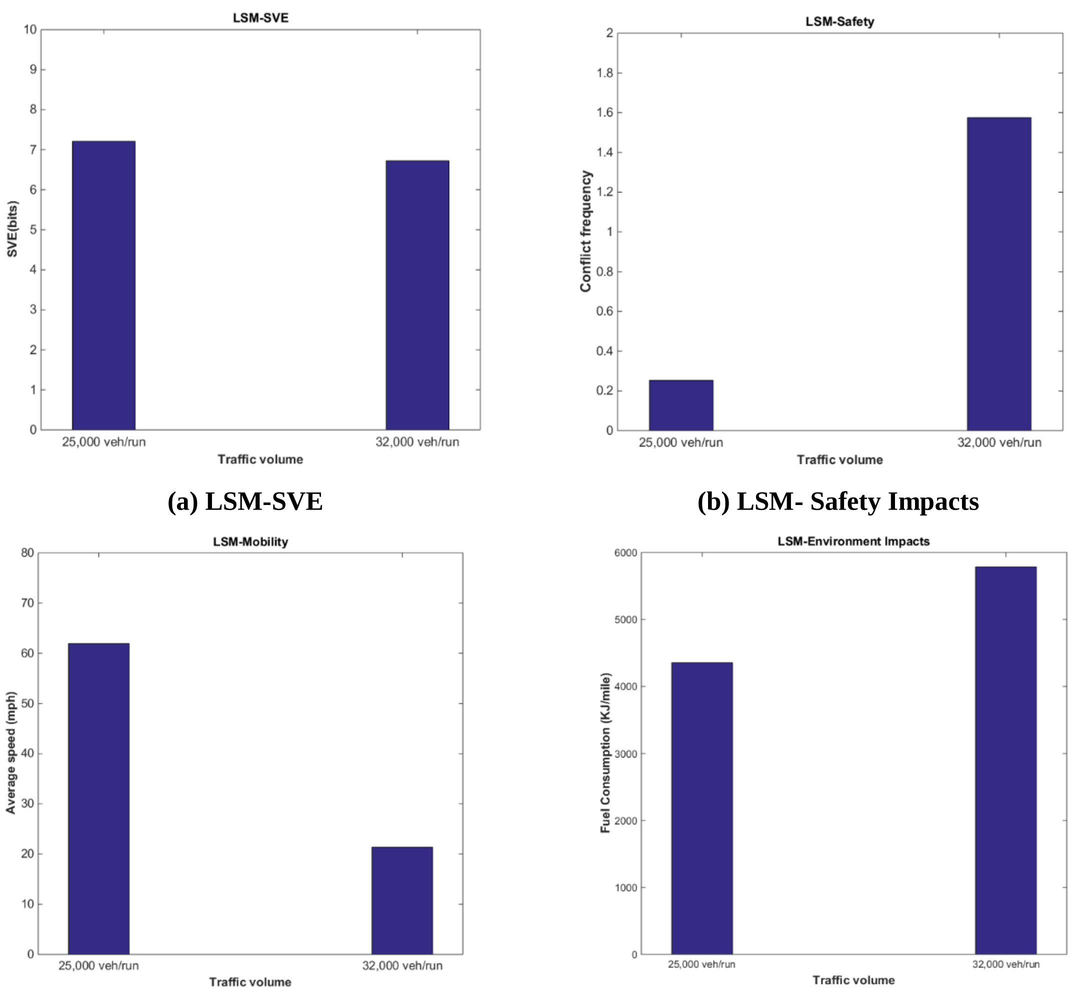

(a) LSM-SVE **(b) LSM- Safety Impacts**

(c) LSM-Mobility Impacts **(d) LSM-Environmental Impacts**

Figure 6-18. SVE versus Three Conventional MOEs across Two Different Congestion Levels for LSM (20% Penetration Rate of Application-Equipped Vehicles)

6.7 Summary

In this chapter, we have developed and analyzed a novel connected vehicle application, i.e., *Lane Speed Monitoring*, based on V2V communication. The application collects all the available real-time information from downstream DSRC-equipped vehicles and provides lane change guidance to the driver. Results from our comprehensive simulation study show that the LSM-equipped vehicles can gain significant mobility benefits (i.e., up to 11% improvement in average speed) under various scenarios (including different penetration rate and congestion levels). A slight increase of potential conflict frequency and fuel consumption was observed from simulation analyses which may be explained by increased speed and lane changes. An attractive feature of the developed application is that noticeable benefits in mobility can be achieved even under relatively low penetration rate of DSRC-equipped vehicles (e.g., 20%) and much lower penetration rate of LSM-equipped vehicles (i.e., 9% of DSRC-equipped vehicles).

After analysis on the LSM application's MOE trade-offs, more related future research direction can be inspired by the drawbacks of the current application. In general, some applications can be combined together to overcome the disadvantage of one single application, leading to some co-benefits. However, note that not all the applications can take advantages from every MOE perspective, which is why we also need to choose the most-focused-aspect application and make some trade-offs.

7 CONNECTED VEHICLE-BASED LANE SELECTION ASSISTANCE

7.1 Introduction

Although a large number of CV applications have been proposed and developed for driving assistance, only a small number of them are focused on lateral control assistance. Examples include lane assignment [143]-[144] and optimal lane selection [145]. Dao et al. presented a decentralized lane assignment approach for a group of single vehicles [143] or vehicle platoons [144] within the vicinity of on/off ramps (entries and exits) via inter-vehicle communication. Another research effort on lane selection was proposed to regulate freeway uncoordinated lane changes via two-way Vehicle-to-Infrastructure (V2I) communication, by minimizing potential vehicle conflicts [145]. The results in [145] showed that, due to the regulated lane-changing behaviors, the mean average travel time is reduced (by 0.57% to 3.79%) as compared to the non-lane selection scenario. These studies all hold a strong assumption that all the vehicles on the freeway are application-equipped vehicles (under control), which makes it challenging to implement these lane assignment approaches in practice within the next ten years or more. Even so, mobility-focused lateral control assistance applications still has not been very well studied yet so far.

On the other hand, traffic state prediction has been well studied for years using statistical models, such as Kalman filtering, nonparametric regression models, or neural networks [146]-[150]. Kwon et al. predicted travel times on freeway using a linear regression model based on measurements from loop detectors [146]. Rice et al. proposed a simple robust time-series model for travel time prediction for a section of a freeway [147]. At the same time, many model-driven and data-driven algorithms have been proposed for short-term traffic state prediction, such as Hidden Markov Models [151]-[152], K-nearest neighbors approach for traffic state prediction [153], Particle Filter algorithm [154]-[155], Kalman Filter [156], and deep neural networks [157].

A few Markov chain based traffic forecasting methods has been developed [152] [158]. The Markov chain (discrete) model was mainly used to decide the traffic state of the next interval based on the traffic model. For example, nearest neighbor classification in combination with variable-length Markov chains was used to predict the traffic pattern [152]. After the traffic state of each new time step is classified into a cluster, the specific speed value is estimated using the appropriate locally weighted regression model which is trained with data only from the relevant cluster. In addition, a combined forecasting method based on Markov chain theory and Grey Verhulst model was proposed for high prediction accuracy of short-term traffic flow forecasting method [158]. In order to improve the accuracy of forecasting, the volatility of data is dealt with by Markov chain theory on the basis of Grey Verhulst model. The results show that the relative error (between real-world data and prediction data) of traffic flow of one road segment across 16 time steps (5 min per time step) ranges from 0% to 13%.

At the same time, a short-term traffic prediction method based on spatial-temporal correlations was also proposed. In [159], Pan et al. brought up that the traffic state of a specific site is highly affected by its upstream and downstream traffic conditions; and free-flow speeds are spatially correlated (cell-to-cell, lane-to-lane correlated). An extended stochastic cell transmission model (SCTM) was used to support short-term traffic state prediction, taking into account the spatial-temporal correlation of traffic flow. In [159], a section of I210-W was divided into four cells, with about 0.5 mile per cell. The overall mean absolute percentage error (MAPE) was calculated for effectiveness validation, which was around 10.8%-14% [159]. In [160], a traffic state estimation approach was proposed, which utilizes road network correlation and sparse traffic sampling to estimate the traffic conditions of different road segments. This method derives Multiple Linear Regression (MLR) based mathematical model to represent traffic relations and applies both the MLR model and the compressive sensing technique to achieve a city-scale traffic estimation via tracking a small number of probe vehicles. The traffic estimation model was validated by extensive trace-driven experiments with real-world traffic data (within a large network with 1826 road segments in Shanghai city). Results show that the absolute speed differences between the estimated results and the pseudo ground truths over different traffic scenarios are 5.2 km/h to 11.0 km/h (around 3.23 mph to 6.84 mph).

Another approach to traffic state estimation and prediction is to use an improved Ensemble Kalman Filter to estimate and predict realistic large-scale freeway network, whose computation time can be decreased due to smaller matrix inversions [156]. In [157], a machine learning deep neural network was adopted to model the evolution of the traffic state in a freeway. However, all these approaches mentioned are focused on link level traffic state prediction instead of lane level. At the same time, studies of lane-based methods have attracted more and more attention recently, including but not limit to vehicle trajectory predictions, queue warning effectiveness analysis and lateral motion prediction of autonomous vehicles [161]-[163]. In order to support the implementation of lane-level applications in reality, there is also lane-level vehicle guidance technology, e.g., using enhanced GPS/multi-layer map model for ego-lane estimation and lane-level navigation service [164]-[167]. Also, advanced sensing devices have been developed as the key enabler for accurate position tracking, such as the Radio Frequency IDentification (RFID) technology [168]-[169], which will support numerous applications in transportation in the future [170]. Inspired by the work mentioned above, we developed a regression model for lane-level traffic state prediction by utilizing traffic state correlations between adjacent road segments along the same lane (intra-lane information) and across the adjacent lanes (inter-lane information).

In this chapter, we proposed and developed a lane selection assistance application to help the driver find an optimal lane-level "micro" route in terms of minimizing the travel time. The decision making process is based on the prediction of traffic states at the lane level via connected vehicle technology (e.g., cellular network). The rest of this chapter is organized as follows: Section 7.2 presents the problem formulation, followed by the detailed description of the lane selection algorithm, system architecture and the developed spatial-temporal traffic state prediction model in Section 7.3. Simulation model and scenarios are introduced in Section 7.4. In Section 7.5, simulation studies are conducted to evaluate the performance of the developed application by varying different parameters, such as traffic congestion level, penetration rate of communication-capable vehicles and information update cycle. Section 7.6 concludes this chapter.

7.2 Problem Formulation

In the real world, drivers usually perform lane changes based on their observations within sight distance, many of which are not well planned. For example, consider a target vehicle (the individual vehicle of interest) driving on a 5-lane freeway under heavy traffic conditions (see Figure 7-1). Since the traffic downstream of the target vehicle (in lane 2) is congested within the range of the driver's vision, the target vehicle driver needs to make a decision on which lane to change to (i.e., space 1 in lane 1 or space 2 in lane 3). Because of the limited sight distance, it is hard for the driver to know exactly which lane has lighter traffic. Assume that the driver changes to space 2 in lane 3 and he/she will face two alternatives again, changing to space 3 in lane 4 or staying in lane 3. The driver would probably change to space 3 in lane 4 rather than staying in lane 3 since there is more room in space 3. However, a congestion shockwave could be propagating from the downstream to the upstream in lane 4 (beyond the range of the driver's vision) at the same time. In this circumstance, staying in space 2 in lane 3 might be a better choice. Therefore, in order to obtain mobility benefits, predicted information of downstream traffic at the lane-level is essential for drivers to make smarter choices on lane selection.

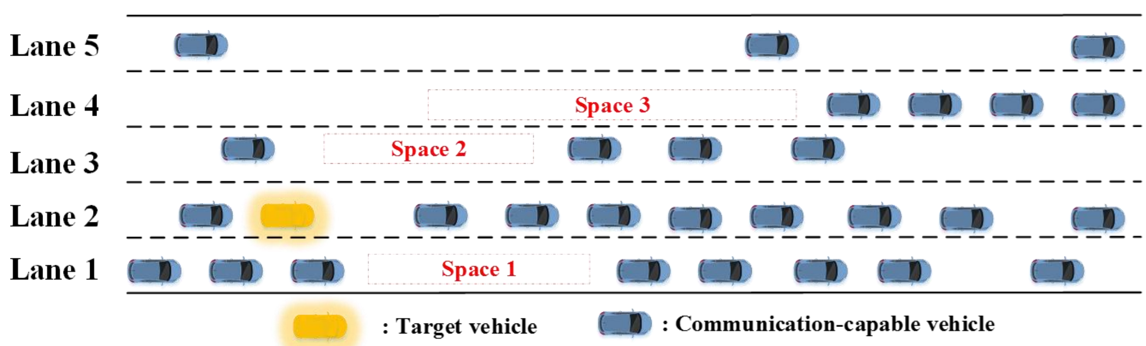

Figure 7-1. An Example of the Problem Description

We define vehicles which could share their basic information (e.g., velocity and position) as communication-capable vehicles, and define vehicles equipped with the developed application as application-equipped vehicles. We assume cellular-based connectivity for data collection is available (see Figure 7-2). We assume that sending messages over the cellular network in an end-to-end manner is technically feasible. An application-equipped vehicle is always communication-capable, but a communication-capable vehicle is not necessarily application-equipped. Communication-capable vehicles can send their activity information to a centralized center via on-board smartphones with built-in sensors for traffic/vehicle states prediction. Based on the data collected from on-road communication-capable vehicles, the traffic state (e.g., average speed) can be estimated and even predicted with certain models by an application server (or the traffic management center, or the cloud center). The application server stores and broadcasts the prediction results to the application-equipped vehicles so that the developed application can support the decision-making process of lane changing. We also assume that vehicles have complete knowledge of which lane it is in (this is a research problem in itself).

Note that the traffic state changes with time, therefore dynamic models are needed to forecast the traffic state. The lane-level traffic state prediction can be conducted using regression models. Aimed at searching for the best lane-level path for an application-equipped vehicle, an optimization problem is formulated to determine which space (e.g., a lane-level segment) the vehicle should occupy at certain time.

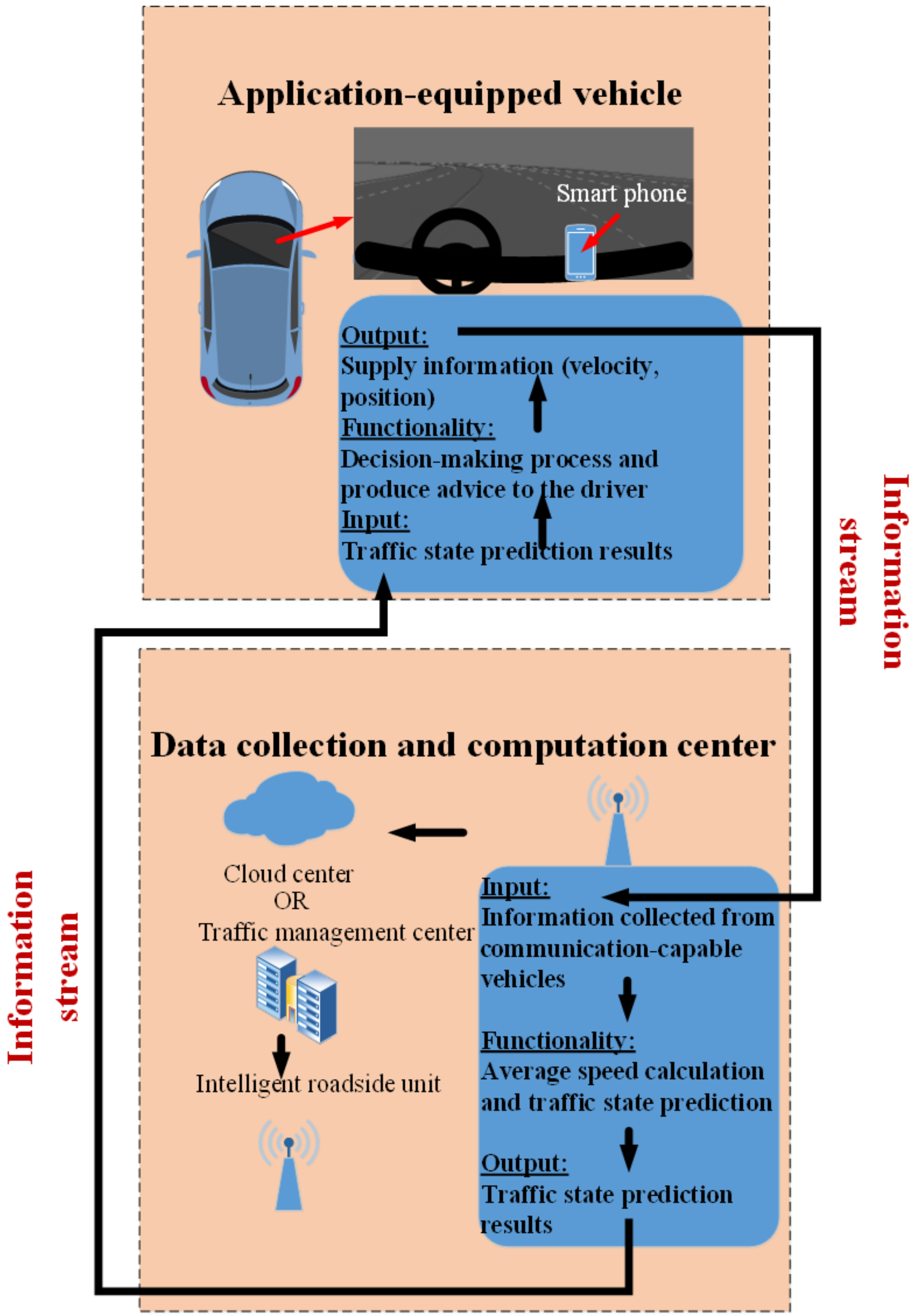

Figure 7-2. Information Flow of the Lane Selection Assistance Application

7.3 Lane Selection Assistance Application

To solve this problem, a detailed three-step approach has been developed: 1) spatial-temporal discretization of roadway network; 2) data-driven traffic state prediction at the lane level; 3) optimal lane sequence identification based on dynamic programming (DP).

7.3.1 Spatial-Temporal Discretization

As shown in Figure 7-3, the road network can be divided into K road segments and $K \times I$ cells, where I is the total number of lanes of interest. To make this approach more feasible and reduce the complexity for implementation, we did not include those "discontinuous lanes of the mainline" as the lanes of our interest in this study. These discontinuous lanes of the mainline include where mandatory lane changes have to be performed, such as auxiliary lane(s) before lane-drop areas (e.g., lane m and lane n in Figure 7-3). Another major assumption is that there exists speed difference across different lanes especially in heavy traffic. Usually fluctuations of traffic may be caused by the mainline vehicles which make mandatory lane changes to leave the freeway from the off-ramp exit, or the influx of traffic from the on-ramp. These factors cause large speed difference among lanes, especially in heavy traffic.

The spatial discretization method is more applicable to freeways where road segments of same traffic direction are correlated with each other. It might be more challenging for urban areas and intersections. Some details about the spatial segment discretization are as follows:

- The length of each segment does not have to be the same.

- A segment should have consistent geometric characteristics throughout.
- Optimal segment length, varying with traffic speed, balances between capturing the variability in traffic state versus limiting the size of optimization problem.

The road stretch used in this paper is California SR91-E, a 15-mile corridor with 4 to 6 lanes and ten pairs of on/off-ramps (see Section 7.4.1 for more details). The spatial discretization in this paper was done offline, splitting this freeway into 15 road segments, almost each of which is about one mile long. The approach can be extended to different freeways as a generalized method, however it could be slightly different for various road ways, depending on the traffic direction and specific road geography.

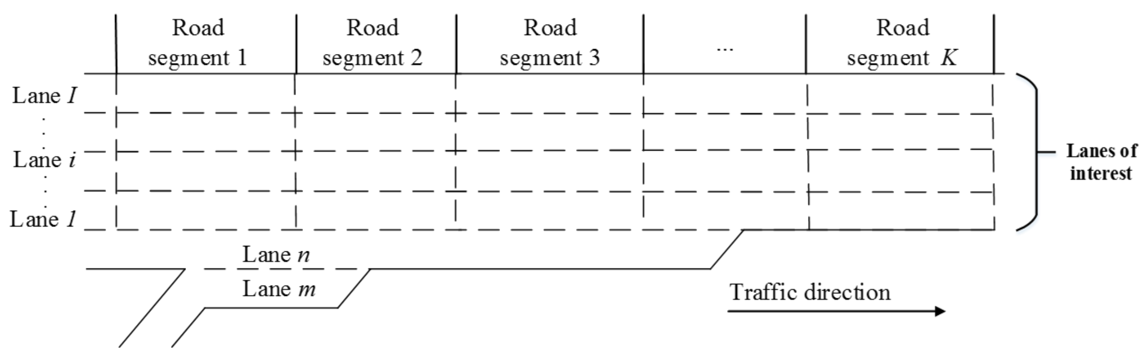

Figure 7-3. Sketch Map of Spatial Discretization on Freeways

7.3.2 Lane-Level Traffic State Prediction

For each cell in Figure 7-3, we can further define the associated traffic state that can be used to guide the lane change. We do not estimate the traffic state of the discontinuous lanes ("non-of-interest" lane) of the mainline, such as auxiliary lane(s) before lane-drop areas (e.g., lane *m* and lane *n* in Figure 7-3). We assume that the communication-capable vehicles can transmit their state information such as instantaneous speed and location (both longitudinal and lateral with lane-level accuracy) over the entire roadway network in real-time. Then the lane-level average speed of each road segment at each time step can be estimated and used as the critical traffic state. More specifically,

$$x_{i,k}(n) = \frac{VMT_{i,k}(n)}{VHT_{i,k}(n)} \tag{7-1}$$

$$\forall\, i \in I, k \in K$$

where $x_{i,k}(n)$ is the average speed on lane *i* of road segment *k* within the *n*-th time interval, $n \cdot \Delta T$. *VMT* and *VHT* represent the vehicle miles traveled and vehicle hours traveled, respectively. Assuming the time interval ΔT at each step is uniform, the average speed can be also estimated by the ratio of the sum of all sampled speeds to the total number of speed samples for all vehicles of interest. In addition, we use a fixed average speed value (65 mph in this study) to represent the traffic state $x_{i,k}(n)$, when no communication-capable vehicle is available in the specific cell.

It has been brought up that the traffic state of a specific site is highly affected by its upstream and downstream traffic conditions, and free-flow speeds are spatially correlated (cell-to-cell, lane-to-lane correlated) [159]. Inspired by the aforementioned research, we propose a linear regression model (referred to as Spatial-Temporal model or ST-model in this paper) for traffic state (i.e., average speed) prediction at the lane level by utilizing traffic state association between adjacent road segments along the same lane (intra-lane information) and across the adjacent lanes of both sides (inter-lane information) during consecutive time steps, in order to serve as the basis of the lane selection algorithm developed in Section 7.3.3.

Considering the lane-based impacts on traffic state prediction, we herein utilize both intra-lane and inter-lane traffic state information for traffic state prediction. Therefore, the linear regression model of one single lane is defined as

$$\vec{X}_i(n) = A_i \vec{X}_{mi}(n-1) + \vec{u}_i \qquad \forall\, i \in I \tag{7-2}$$

which can be extended as Equation (7-3).

$$\begin{bmatrix} x_{i,1}(n) \\ x_{i,2}(n) \\ x_{i,3}(n) \\ \vdots \\ x_{i,k}(n) \\ \vdots \\ x_{i,K}(n) \end{bmatrix} =$$

$$\begin{bmatrix} a_{i-1,1} & a_{i-1,2} & \cdots & a_{i,1} & a_{i,2} & \cdots & a_{i+1,1} & a_{i+1,2} & \cdots & & & & & \\ a_{i-1,1} & a_{i-1,2} & a_{i-1,3} & \cdots & a_{i,1} & a_{i,2} & a_{i,3} & \cdots & a_{i+1,1} & a_{i+1,2} & a_{i+1,3} & \cdots & & \\ & a_{i-1,2} & a_{i-1,3} & a_{i-1,4} & \cdots & a_{i,2} & a_{i,3} & a_{i,4} & \cdots & a_{i+1,2} & a_{i+1,3} & a_{i+1,4} & \cdots & \\ & & & & & \ddots & & & & & & & & \\ & & a_{i-1,k-1} & a_{i-1,k} & a_{i-1,k+1} & \cdots & a_{i,k-1} & a_{i,k} & a_{i,k+1} & \cdots & a_{i+1,k-1} & a_{i+1,k} & a_{i+1,k+1} & \cdots \\ & & & & & & \ddots & & & & & & & \\ & & & & & & a_{i-1,K-1} & a_{i-1,K} & \cdots & a_{i,K-1} & a_{i,K} & \cdots & a_{i+1,K-1} & a_{i+1,K} \end{bmatrix}$$

$$\times \begin{bmatrix} x_{i-1,1}(n-1) \\ \vdots \\ x_{i-1,k}(n-1) \\ \vdots \\ x_{i-1,K}(n-1) \\ x_{i,1}(n-1) \\ \vdots \\ x_{i,k}(n-1) \\ \vdots \\ x_{i,K}(n-1) \\ x_{i+1,1}(n-1) \\ \vdots \\ x_{i+1,k}(n-1) \\ \vdots \\ x_{i+1,K}(n-1) \end{bmatrix} + \vec{u}_i \tag{7-3}$$

In Equation (7-3) the output variable matrix is $\vec{X}_i(n) \epsilon R^{K\times 1}$; input variables matrix is multiple lanes' traffic state $\vec{X}_{mi}(n-1) \epsilon R^{3K\times 1}$; coefficient matrix is $A_i \epsilon R^{K\times 3K}$ (considering the impacts from immediate downstream and upstream segments of the original lane and adjacent lanes); and intercept matrix is $\vec{u}_i\ \epsilon R^{K\times 1}$. The coefficient and intercept matrices of the above linear regression model can be trained by historical data. In this study, we assume that the *i*-th lane traffic state on road segment *k* during the *n*-th time interval, $x_{i,k}(n)$, can be represented by a linear function of the lane-level traffic states on road segments *k*-1 (immediate upstream), *k* and *k*+1 (immediate downstream) of the original lane and adjacent lanes of both sides, during the (n-1)-th time interval, i.e., $x_{i-1,k-1}(n-1)$, $x_{i-1,k}(n-1)$, $x_{i-1,k+1}(n-1)$, $x_{i,k-1}(n-1)$, $x_{i,k}(n-1)$, $x_{i,k+1}(n-1)$, $x_{i+1,k-1}(n-1)$, $x_{i+1,k}(n-1)$ and $x_{i+1,k+1}(n-1)$. Please note that the Equation (7-3) is the general form, only one-side adjacent lane was considered for the left-most lane (or the right-most lane).

The full linear regression model of the entire network with K segments and I lanes of interest can be formulated as follows:

$$\begin{bmatrix} \vec{X}_1(n) \\ \vec{X}_2(n) \\ \vdots \\ \vec{X}_I(n) \end{bmatrix} = \begin{bmatrix} A_1 & & & \\ & A_2 & & \\ & & \ddots & \\ & & & A_I \end{bmatrix} \begin{bmatrix} \vec{X}_{m1}(n-1) \\ \vec{X}_{m2}(n-1) \\ \vdots \\ \vec{X}_{mI}(n-1) \end{bmatrix} + \begin{bmatrix} \vec{u}_1 \\ \vec{u}_2 \\ \vdots \\ \vec{u}_I \end{bmatrix} \tag{7-4}$$

For comparison purpose, we also evaluated another simple traffic state prediction model (as a baseline), which used the traffic state in the last time step as the predicted state in the current time step without considering the spatial interaction (similar estimation model was also proposed in [76]), i.e.,

$$x_{i,k}(n) = x_{i,k}(n-1) \tag{7-5}$$

Therefore, for lane i, the baseline can be simply written as

$$\vec{X}_i(n) = \vec{X}_i(n-1) \tag{7-6}$$

and for the entire network,

$$\begin{bmatrix} \vec{X}_1(n) \\ \vec{X}_2(n) \\ \vdots \\ \vec{X}_I(n) \end{bmatrix} = \begin{bmatrix} \vec{X}_1(n-1) \\ \vec{X}_2(n-1) \\ \vdots \\ \vec{X}_I(n-1) \end{bmatrix} \tag{7-7}$$

More details on the comparison results between the ST-model and the basic estimation model in terms of traffic state prediction will be presented in Section 7.5.2.2.

7.3.3 Optimal Lane Selection Algorithm

As previously mentioned, the objective of the proposed lane selection assistance application is to improve the mobility performance of application-equipped vehicles. With the spatial-temporal discretization of the entire roadway network, we formulate the problem as dynamically searching a lane-level path that maximizes the sum of average speed of each lane segment that the vehicle traverses. The variables of optimal solutions are the binary variables $\omega_{i,k}(n)$ given the system equations of lane-level traffic states $x_{i,k}(n)$. The optimization problem is solved only for the next *N*-min (an information update cycle). Assume that the ego application-equipped vehicle is on lane *p* of segment *q*. To obtain the optimal lane index solution for time step *n*, the objective function and constraints of the ego application-equipped vehicle are shown as follows:

$$\max_{\Omega(n)} \sum_{i=1}^{I} \sum_{k=q}^{K} \omega_{i,k}(n) x_{i,k}(n) \tag{7-8}$$

s.t.

$$\begin{bmatrix} \vec{X}_1(n) \\ \vec{X}_2(n) \\ \vdots \\ \vec{X}_I(n) \end{bmatrix} = \begin{bmatrix} A_1 & & & \\ & A_2 & & \\ & & \ddots & \\ & & & A_I \end{bmatrix} \begin{bmatrix} \vec{X}_{m1}(n-1) \\ \vec{X}_{m2}(n-1) \\ \vdots \\ \vec{X}_{mI}(n-1) \end{bmatrix} + \begin{bmatrix} \vec{u}_1 \\ \vec{u}_2 \\ \vdots \\ \vec{u}_I \end{bmatrix} \tag{7-9}$$

$$\omega_{i,k}(n) \epsilon \{0,1\} \qquad \forall i \epsilon [1, I], \forall k \epsilon [1, K] \tag{7-10}$$

$$\sum_{i=1}^{I} \omega_{i,k}(n) = 1, \qquad k \epsilon [q, K] \tag{7-11}$$

$$\text{If } \omega_{i,k}(n) = 1 \text{, then } \omega_{j,k+1}(n) = 1,$$

$$\forall i \epsilon [1, I], j = i-1, or\ i, or\ i+1, k \epsilon [q, K-1] \tag{7-12}$$

where *I* is number of lanes of interest, *K* is number of road segments, and *n* is the next *N*-min time step (length of the prediction window). The aforementioned lane-level traffic state prediction model is used as a constraint to drive the evolution of traffic states (see

(7-9)). As mentioned above, $\omega_{i,k}(n)$ is a 0-1 binary variable indicating if the target vehicle is present ($\omega_{i,k}(n) = 1$) or not ($\omega_{i,k}(n) = 0$) on lane i of road segment k during time interval *n* (see (7-10)). Equation (7-11) guarantees that at any time step, the target vehicle would be only present in one cell for each road segment *k*. The last if-then constraint (i.e., (7-12)) denotes that the solution $\Omega(n)$ only allows adjacent lane changes within one *N*-min time step. The solution $\Omega(n)$ (i.e., optimal lane-level micro-routing from the current road segment *q* to road segment *K*, within the next *N*-min) is obtained by Dynamic Programming (DP) [171], based on traffic status of time step *n-1*.

The proposed lane selection assistance application is implemented through the application programming interface (API) in PARAMICS microscopic traffic simulation tool [48]. Figure 7-4 presents an illustrative example of optimal lane-level path (as time elapses) calculated by the proposed lane selection assistance algorithm (with spatial discretization of roadway network). The average speeds of each road segment in different lanes are grouped into different levels: very low, low, medium and high, which are represented by different colors in Figure 7-4. Since the lane-level speed is time-varying, we don’t assign fixed speed partition range for each level. The purpose of defining different levels in Figure 7-4 is to show the spatial discretization and the lane-level traffic state more intuitively. Note that the speed levels of lanes in each road segment are updated every *N*-min information collection cycle. Compared to the unguided path (baseline), the target vehicle (application-equipped) follows the optimal lane sequence during the whole trip based on the time-varying lane-level traffic state prediction results, aiming to minimize the travel time over the same length of distance traveled. It is possible but not necessary that the application-equipped vehicles change lanes only at cell boundaries (Figure 7-4 is a schematic diagram). After changing to the target lane, the target vehicle is restricted to the corresponding target lane without performing any extra lane changes. The proposed lane selection assistance algorithm is shown in Table 7-1.

TABLE 7-1. LANE SELECTION ASSISTANCE ALGORITHM

Algorithm	Lane Selection Assistance Algorithm
Input:	1. Traffic state at (n-1)-th N-min
Output:	2. **Identify** the Level of Service of current traffic state
	3. **Apply** corresponding regression model
	4. **Predict** the n-th N-min traffic state
	5. **Update** the optimal lane sequence
	6. **Follow** current optimal lane-level route
	7. **Accumulate** travel time t
	8. **if** in the middle of trip **do**
	if t > update period **do**
	Update N-min step index $n = n+1$
	Do *step* 1
	else Do *step* 6
	end if
	end if

In summary, with discretization of roadway network (in time and lane-level space), the lane selection assistance application can be implemented as depicted in Table 7-1:

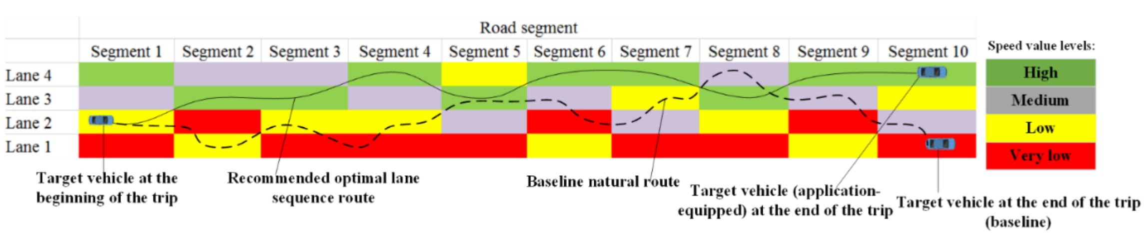

Figure 7-4. An Illustrative Example of the Optimal Lane-Level Path in a Discretized Roadway Network

1) *Model training for lane-level traffic state prediction*. The linear regression model (i.e., matrix A and vector $\vec{u}$) for state prediction can be trained (even offline) by

real-world traffic data and can be differentiated by various traffic conditions or Level of Service (LOS) defined in Highway Capacity Manual [130]. In the following simulation study, we trained different models for LOS C (free flow), LOS D (transitional flows) and LOS E (unstable flows), respectively, to cover three representative levels of congestion.

2) *Online guidance of optimal lane for the next time steps.* With the most updated prediction of lane-level traffic state downstream, the optimization problem is solved to determine the best lane for the target vehicle (following the steps described in (7-8) through (7-12)). A table of the lane index sequence for every road segment is generated/updated online for the application-equipped vehicles. For online implementation, a rolling horizon technique [172] is applied where the optimization problem is solved within every N-min information update cycle, based on the updated prediction of downstream traffic states (at the lane level).

7.4 Simulation Setup

To validate the proposed application, we conducted a comprehensive simulation study as described below.

7.4.1 Simulation Network Model

The simulation network is California's SR-91(eastbound), consisting of a 15-mile corridor located between the Orange County Line and Tyler Street in Riverside (see Figure 7-5). The number of lanes varies from 4 to 6, and there are ten on/off-ramp pairs. The traffic demand (25,000 vehicles released in the network, stable traffic flow) and driving behavior have been well calibrated against a typical weekday morning in the summer of Year 2006 based on historical traffic data from California Freeway Performance System (PeMS) to represent the network's real-world conditions [132]. In this study, we use PARAMICS (PARAllel MICroscopic Simulator), a microscopic traffic simulation tool that is capable of modeling the movement and behavior of each individual vehicle on road networks, to generate detailed traffic data (i.e., to simulate as in a connected environment) for system performance evaluation.

7.4.2 Implementation Details

Traffic state prediction model's inputs were generated from the simulation network. Those raw data were post processed by aggregating and averaging for different road segments and lanes at different time horizons which were afterwards trained using the regression model ("fitlm" function) with ordinary least squares in MATLAB.

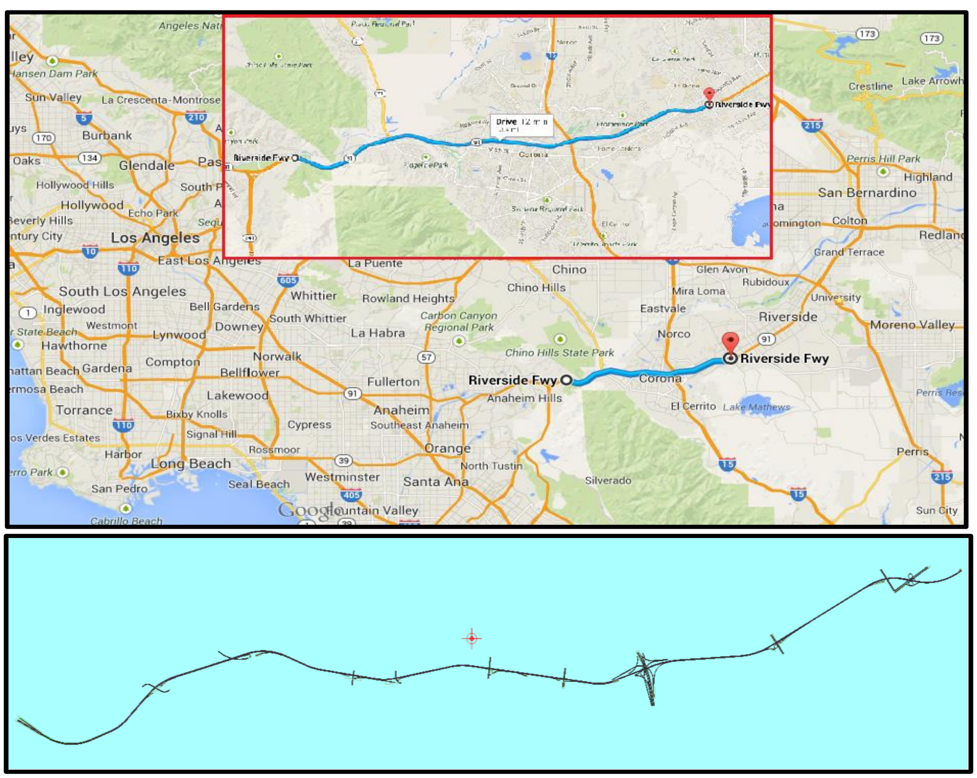

Figure 7-5. Road Network of the California SR-91E in Real-World and PARAMICS

The optimization process is implemented online through the application programming interface (API) in PARAMICS microscopic traffic simulation tool using C++ language. In the PARAMICS API, the obtained prediction model coefficients are applied to real-time collected data to acquire traffic state prediction results. After the prediction was made, recursion method of dynamic programming algorithm is used to obtain the optimal solution (i.e., the lane index sequence for the current road segment the vehicle was traveling on and every road segment downstream). Within the N-min duration, the target lane index is assigned to the application-equipped vehicle based on its optimal lane index sequence.

7.4.3 Simulation Scenarios

To test the lane selection assistance application, we divided the road stretch into about fifteen 1-mile road segments and chose a specified traffic information update cycle. The simulation period is from 6:00 AM to 9:00 AM with a 15-minute warm-up period. From 6:16 AM to 7:51 AM (to guarantee the last target vehicle can complete its trip by the end of simulation) with 5- minute intervals (called a case), there are 20 cases corresponding to 20 departure time intervals for each simulation run. At the start of each case (the first ten seconds), a few application-equipped vehicles (usually 4-6, i.e., a case) with the same Origin-Destination (OD) are randomly selected into the network for further effectiveness evaluation purpose. All the selected vehicles are released from the left end of the mainline and traveled to the right end of the mainline. In addition, since the number of lanes along the mainline ranges from 4 to 6, the lanes of interest herein only consist of the four left-most lanes (as conceptually illustrated in Figure 7-3).

As mentioned above, 4-6 application-equipped vehicles in each case are released into the network at certain frequency (i.e., every 5 minutes) to evaluate the effectiveness of the proposed lane selection assistance application. Moreover, comprehensive sensitivity tests are conducted over the following system parameters:

- *Congestion level*. With a major focus on the traffic pattern, three networked traffic volumes that represent free flow, medium and heavy traffic are evaluated: 16,000 vehicles/simulation run, 25,000 vehicles/simulation run and 32,000 vehicles/simulation run. An analysis on average traffic speed indicates that these three levels of traffic demand correspond to LOS C (free flow), LOS D (transition flows) and LOS E (unstable flows), respectively, according to the Highway Capacity Manual (HCM) 2010 [130]. For LOS C, LOS D (calibrated) and LOS E cases, results of 100% penetration rate of communication-capable vehicles are investigated for the sensitivity analysis on congestion level.
- *Penetration rate of communication-capable vehicles*. Ten levels of penetration rate of communication-capable vehicles are studied in this paper, including 0.01%, 1%, 2%, 5%, 10%, 20%, 40%, 60%, 80% and 100% in the penetration rate sensitivity analysis.
- *Information update cycle*. As aforementioned, *N*-min is a specific traffic information update cycle for the target vehicles, during which time real-time information is collected. The traffic predict results are updated every *N*-min and the optimal lane sequence is overwritten at the same time. A set of {1 min, 2 min, 3 min, 4 min, 5 min} is selected for the information update cycle sensitivity test in

order to observe its impacts on travel time improvement. The information update cycle is also related to the penetration rate of communication-capable vehicles. The information update cycle may be shorter due to more sufficiently available data.

Under these simulation scenarios, a baseline case for each scenario is defined as the case where the vehicles make lane changes as normal without any assistance. We use PARAMICS default lane change model. The vehicles of the baseline would consider to change to another lane when it needs to overtake a slow vehicle in front, taking into consideration its accepted gap at the same time. For more detailed information, please refer to [173]. On the other hand, the application-equipped vehicles would follow the lane selection guidance and make lane changes to the target lane smoothly in the simulation environment. As soon as the target lane was assigned, the optimal lane selection application-equipped vehicles would follow the recommendation of the target lane number and make lane changes as quickly as it can to get into its lane range but in a safe manner.

We conduct simulations with ten random seed numbers, generating 800-1200 (i.e., 10 seeds*20 departure time* (4-6 vehicles/departure time)) vehicle samples for each scenario and the corresponding baseline respectively. For every scenario, we compare the application-equipped vehicles with the same amount of non-application-equipped vehicles under the same environment (i.e., similar departure time, same OD and same traffic status). Moreover, for the same seed, the traffic status for both application-equipped vehicles and the corresponding baseline vehicles at the same departure time should be the same. “Travel time baseline” is calculated by averaging those baseline vehicles with the same departure time across ten seeds, and the average travel time of the application-equipped vehicles of ten seed of each departure time was compared with the corresponding "Travel time baseline". The performance of ST-model based traffic state prediction is evaluated in the simulation as well.

7.5 Simulation Analysis

7.5.1 An Example of the Individual Vehicle

To give a general idea of how the proposed algorithm works, an example of the driving is analyzed in detail. Figure 7-6 displays the driving features of one application-equipped vehicle (green solid line on the left) and the corresponding baseline vehicle (blue dashed lines on the right), respectively. Both vehicles start from the same lane with similar speeds and departure time (the departure time difference is within 10 seconds), and are assumed to get encountered the same traffic state. The time at each black vertical dashed line (except those at the end of the trip) is the time when a lane-changing maneuver happens. The individual vehicles are traveling under the relatively heavy traffic scenario (32000 vehicles/simulation run).

In the example of Figure 7-6, the example vehicles are released at departure time 1 in the heavy traffic scenario. Figure 7-6 (a) shows that for the same distance, the vehicle equipped with the proposed application spends less travel time than the baseline vehicle whose driver changes lane without lane selection guidance. In Figure 7-6 (b), the overall velocity of the application-equipped vehicle is higher than that of the baseline vehicle. After the guidance starts, the application-equipped vehicle is assigned to target lane 6 (see Figure 7-6 (c)). Note that the target vehicle might cross several lanes at its current road segment to change to the target lane after the prediction results are updated.

In combination with Figure 7-6 (c), the lane changes of the baseline vehicle are more event-based operations, i.e., changing to an adjacent left lane to pursue a faster speed. On the other hand, we observe that, by taking full advantage of the long-range information, the proposed application would help the driver ahead of time make a better decision (in terms of lane index sequence) to obtain mobility benefits. Please note that non-adjacent lane changes might still happen at the beginning of the vehicle's trip or when the solution updates at each *N*-min, such as the lane changing behavior from lane 3 to the target lane 6 at the beginning of the vehicle's trip in Figure 7-6 (c).

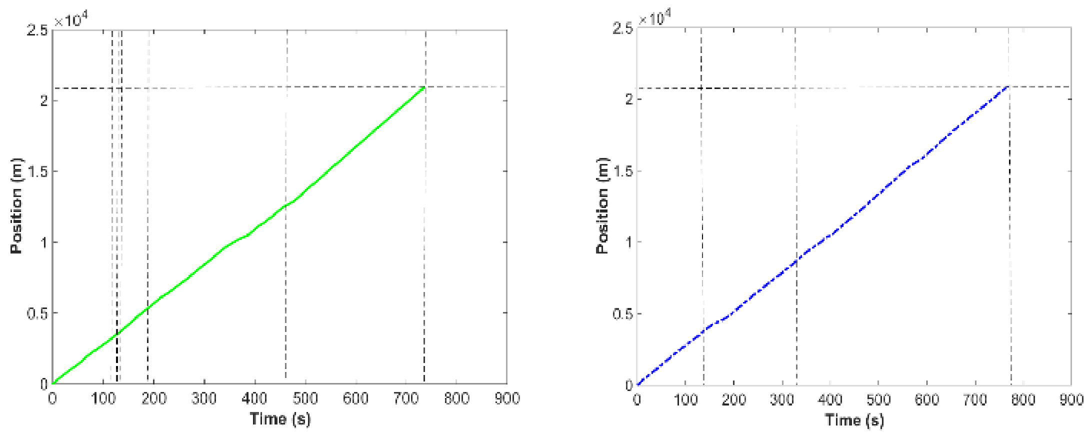

(a)

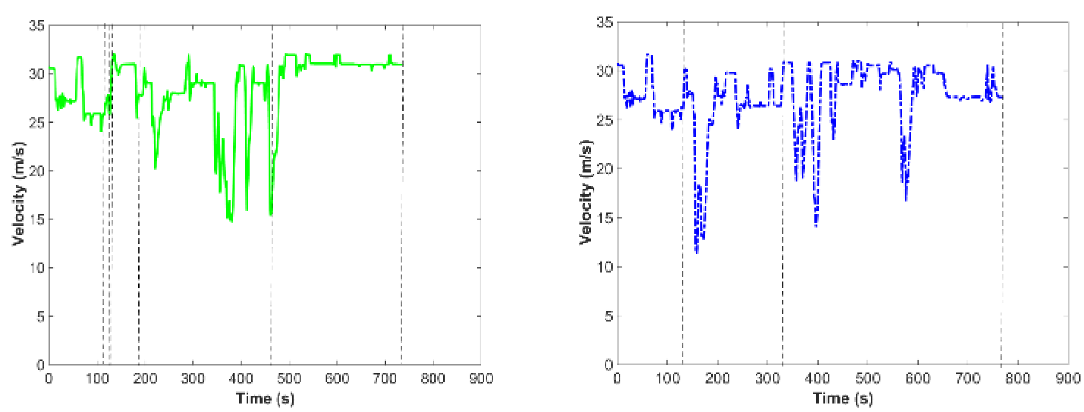

(b)

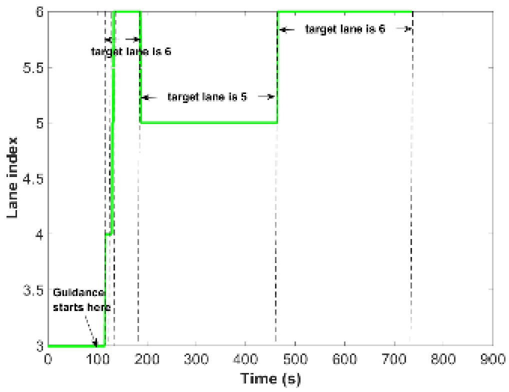

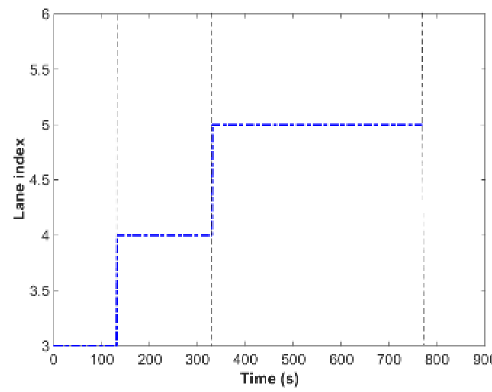

(c)

Figure 7-6. An Example of the Application-Equipped Vehicle (Left) and the Corresponding Baseline (Right). (a) Trajectory. (b) Velocity. (c) Lane Index

7.5.2 Statistical Analysis of the Application Performance

In order to comprehensively test the robustness of the proposed lane selection assistance application, simulation results were obtained statistically as well.

7.5.2.1 Measures of Effectiveness (MOEs)

To assess the mobility benefits of the lane selection assistance application, two types of performance measures were selected for statistical analysis as follows:

a) Forecast Accuracy

Mean Absolute Percentage Error (MAPE) was used to measure the forecast errors from each trip of target vehicle:

$$MAPE = \frac{1}{n}\sum_{t=1}^{n}\left|\frac{A_t - F_t}{A_t}\right| \times 100\% \qquad (7\text{-}13)$$

where A_t is the actual value, F_t is the prediction value, and n is the total number of all samples involved in the MAPE calculation. This MOE is used to evaluate the traffic average speed prediction accuracy for all the cases. In addition, due to the fact that these MOEs are less influenced by low average speed, we also use Mean Absolute Error (MAE) and Root Mean Squared Error (RMSE) to evaluate the ST-model forecast accuracy under specific scenarios (e.g., the heavy traffic scenarios).

$$MAE = \frac{1}{n}\sum_{t=1}^{n}|A_t - F_t| \tag{7-14}$$

$$RMSE = \sqrt{\frac{1}{n}\sum_{t=1}^{n}(A_t - F_t)^2} \tag{7-15}$$

b) Performance of Application-Equipped Vehicles

Relative Travel Time Difference (RTTD) is used to evaluate travel time difference between ST-model based scheme and baseline, i.e.,

$$RTTD_i = \frac{t_{ST}^i - t_B^i}{t_B^i} \times 100\% \tag{7-16}$$

where $RTTD_i$ is the relative travel time difference between ST-model based scheme and baseline at *i*-th departure time. t_{ST}^i is the mean travel time of 40-60 target vehicles at *i*-th departure time (as mentioned in Section 7.4.3), and t_B^i is the mean travel time of the corresponding baseline case at *i*-th departure time (same amount of vehicles with the application-equipped vehicles). This MOE shows mobility benefits in terms of individual travel time for the application-equipped vehicles portion (target vehicles) over the baseline (no-application). Again, to show the statistical significance, we ran simulation runs with ten random seeds, generating 800-1200 (i.e., 10 seeds*20 departure time* (4-6 vehicles/departure time)) vehicle samples for each scenario and the corresponding baseline, respectively.

In addition to RTTD, normalized conflict frequency is calculated for each individual vehicle based on the conflict occurrence results obtained from the Surrogate Safety Assessment Model (SSAM) [33], which is defined as potential conflict when the minimum time to collision drops below a predefined threshold (i.e., 3 seconds).

$$CF = \frac{\sum_{i=1}^{n} cn_i}{n} \tag{7-17}$$

where cn_i is the number of conflicts caused by vehicle i; n is the total number of vehicles. It is noted that in this study each conflict is only associated with the second vehicle (i.e., the one occupying the conflict area at a later instant) which is assumed to be responsible for the potential conflict.

7.5.2.2 Sensitivity Analysis

As aforementioned, sensitivity analysis is conducted on three parameters: congestion level, penetration rate of on-road communication-capable vehicles and *N*-min information update cycle. We use ten random number seeds for simulation. The test results are shown in boxplots, each of which contains 20 cases (i.e., 20 departure times) and there were 4-6 vehicles released for each case, thus one seed generating 80-120 vehicle samples for this scenario (ten seeds generating 800-1200 vehicle samples in total). The sample value of each departure time is the mean value calculated from 40-60 sample vehicles of the same case with similar departure time and the same origin/destination, so is the baseline case. Therefore, for one scenario, the results were collected and compared between 800-1200 application-equipped vehicles, and 800-1200 vehicles of the corresponding baseline.

a) Sensitivity Analysis on Congestion Level

Figure 7-7 illustrates the results for three different traffic demands when the penetration rate of communication-capable vehicles was 100% at 1-min information update cycle. Every 1-min prediction cycle for each application-equipped vehicle has one MAPE value. Each MAPE value is calculated based on a comparison between the forecast and actual traffic state value of each cell across the four lanes of interest and 15 road segments. The final MAPE value for one application-equipped vehicle is calculated out by averaging all the MAPE values from multiple prediction cycles during its whole trip. We then average the MAPE values of application-equipped vehicles of each departure time, and draw the MAPE boxplot using 20 departure times' MAPE samples (each sample is the mean value of 40-60 target vehicles). It's worthy to mention that only from departure 1 to departure 10 cases are shown in Figure 7-7 and Figure 7-8. Since there exists too much bump-to-bump status (traffic breakdowns) after departure 10 in the heavy traffic scenario, the proposed prediction method generates large MAPE, so in Figure 7-7 and Figure 7-8 we do not include those vehicles which are beyond departure 10.

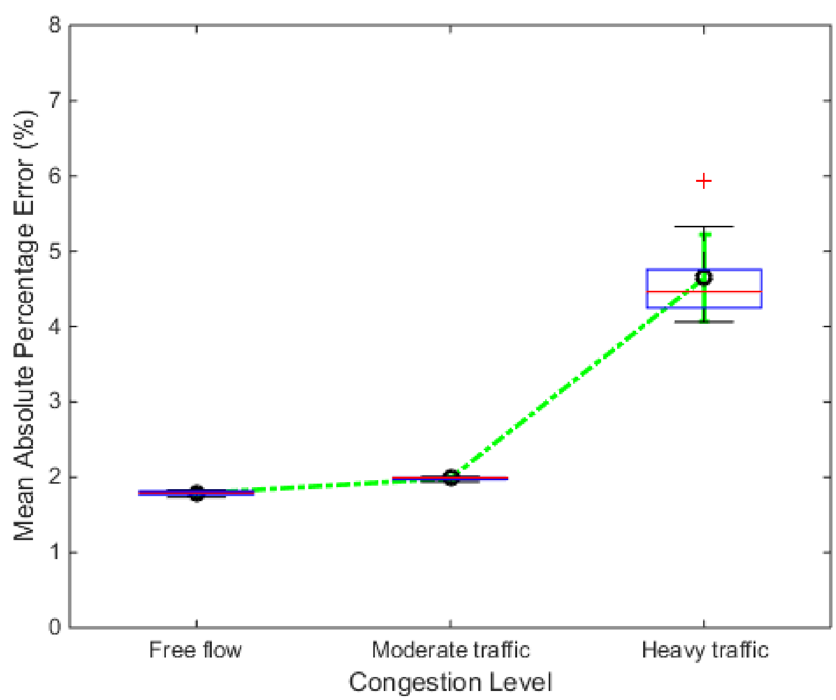

(a)

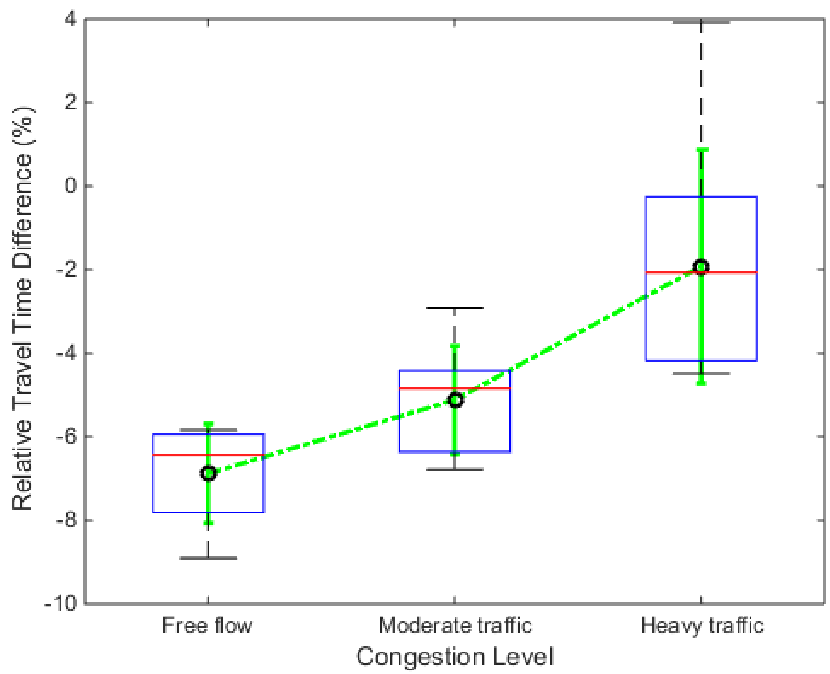

(b)

Figure 7-7. Measures of Effectiveness for Different Congestion Levels. (a) Mean Absolute Percentage Error (b) Relative Travel Time Difference

Figure 7-7 (a) displays the average speed prediction accuracy in terms of MAPE for three congestion levels (across 20 different departure time cases), which ranges from 1%-2% (for LOS C and LOS D). Assume the highest speed is 70 mph in the 25,000 veh/run case, the prediction error is less than 2 mph on average when traffic is stable and moderate, which could provide good prediction for the lane selection assistance application.

From Figure 7-7 (b), we observe the travel time improvement of the target vehicles is 5%-7% (median) compared with baseline under free flow and moderate traffic condition, whereas the travel time improvement is less (the median is around 2%) in the heavy traffic scenario.

In order to mimic the real-world lane change behavior, a three-second lock between two consecutive lane-changing operations for the application-equipped vehicles was set up to prevent too frequent/abrupt lane change. Moreover, we observe that the actual lane change number is less than the lane change recommendation number (see Table 7-2) due to the limited time and space for performing lane changes, which could be the major reason for the less mobility improvement under the heavy traffic scenario.

We also tested the relative travel time difference of the proposed application without the three-second lane change lock (see Figure 7-8), and results show that the relative travel time difference is significantly reduced in the heavy traffic scenario. The proposed lane selection assistance application is able to take advantages of the traffic state prediction scheme and be capable of dynamically guiding the driver for lane selection and thus can help squeeze the individual travel time, even under such unstable flows condition.

TABLE 7-2. THE RECOMMENDED NUMBER AND THE ACTUAL LANE CHANGING NUMBER OF APPLICATION-EQUIPPED VEHICLES (1200 APPLICATION-EQUIPPED VEHICLE SAMPLES, 1-MIN INFO UPDATE CYCLE, 100% PENETRATION RATE OF COMMUNICATION-CAPABLE VEHICLES, 32,000 VEHICLES PER RUN)

Scenario	***Baseline***	***1-min info cycle***
Recommendation number		34.55
Actual lane change	3.60	5.53

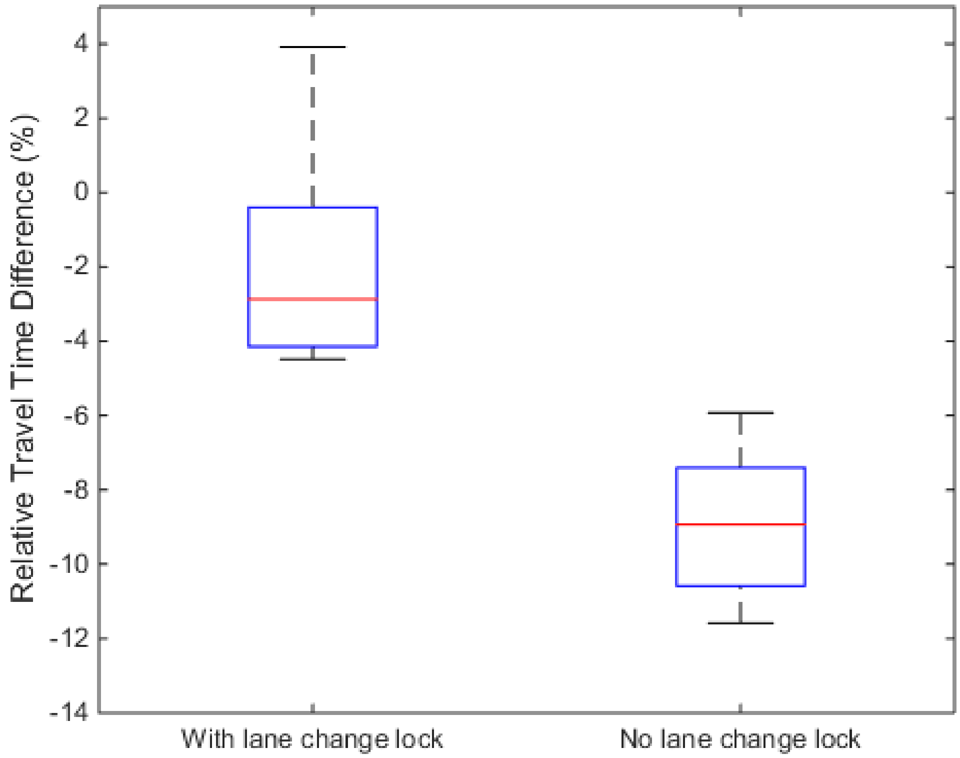

Figure 7-8. Relative Travel Time Difference with and without the Lane Change Lock

In addition, the forecast accuracy (MAPE, MAE and RMSE) of departures 11-20 in the heavy traffic status was evaluated as well (see Table 7-3), in order to provide a more comprehensive assessment of the ST-model. Since the ST-model becomes less effective when there are too many traffic breakdowns, the prediction accuracy is lower, very likely leading to no benefits in the travel time improvement any more.

TABLE 7-3. THE AVERAGE VALUES FOR MAPE, MAE, AND RMSE IN THE HEAVY TRAFFIC SCENARIOS (100% PENETRATION RATE OF COMMUNICATION-CAPABLE VEHICLES, 32000 VEHICLES/RUN)

	Departures 1-10	*Departures 11-20*
MAPE	4.64%	20.60%
MAE	2.49	4.36
RMSE	3.57	6.67

b) Sensitivity Analysis on Penetration Rate of Communication-capable Vehicles

It is worthy to mention that, when the penetration rate is low, there may be not sufficient communication-capable vehicles inside a cell. As aforementioned in Section 7.3.2, we set up a fixed average speed value for the cell with no communication-capable vehicles. In this study, the value used in simulation is 65 mph, which is the speed limit on most California highways. In the algorithm, once there exists one cell with no communication-capable vehicles, no target lane would be assigned to the target vehicles for that road segment. Moreover, we aim to show effects of a specific application at the stage of early deployment of connected vehicles based applications, and only a minority of vehicles were application-equipped in this paper. Specifically, there are about 4-6 application-equipped vehicles for each case (each departure time) for one run, appearing within the vicinity of each other, where we thus assume these application-equipped vehicles do not significantly affect each other.

In order to test the application reliability under various penetration rates, the application performance under different penetration rate levels of communication-capable vehicles was tested in the 25,000 veh/run case.

Figure 7-9 (a) summarizes the MAPE statistics results for ten levels of penetration rates (each containing 20 different departure time cases). The MAPE (median) concentrates on below 3% (starting from 20% penetration rate), which means that the performance of the ST-model is robust to the variation of high penetration rate of communication-capable vehicles which shows the application reliability to certain extent.

In Figure 7-9 (b), it can be observed that the travel time (median) decrease is quite stable as the penetration rate increases (starting from 10%), which can be still more than 5% even when only 10% vehicles on road could supply their information for the traffic state prediction. Using the one-way analysis of variance (ANOVA) as the statistical analysis method, we conduct statistical analysis for the last seven group data (i.e., 5%, 10%, 20%, 40%, 60%, 80%, and 100%) of different levels of penetration rate. The result of a rather big p-value 0.81 (which is >0.05) indicates that the means between the seven groups are not statistically significantly different from each other. The p-value turns out to be small (0.02) when the 2% penetration rate case is added into the analysis. Therefore, we conclude that there is no significant difference in travel time improvement, when penetration rate of communication-capable is higher than 5%, due to relatively sufficient information.

TABLE 7-4. THE AVERAGE VALUES OF MAPE, MAE, AND RMSE OF THE ST-MODEL AND THE BASIC ESTIMATION MODEL UNDER MODERATE TRAFFIC (100% PENETRATION RATE OF COMMUNICATION-CAPABLE VEHICLES, 25,000 VEHICLES PER RUN)

	ST-model	*Estimation model*
MAPE	2.06%	2.62%
MAE	1.28	1.64
RMSE	1.76	2.25

Moreover, to better assess the benefits of the ST-model, the forecast accuracy (MAPE, MAE and RMSE) of both the ST-model and basic estimation model (see Equation (7-5)-(7-7)) are compared (see Table 7-4). It can be seen that the accuracy of the proposed ST-model outperforms the basic estimation model in every aspect.

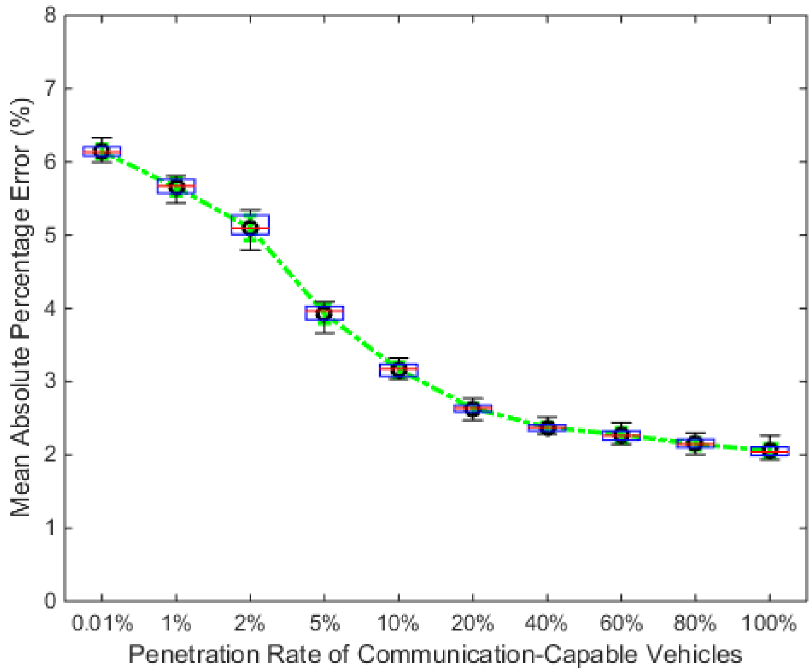

(a)

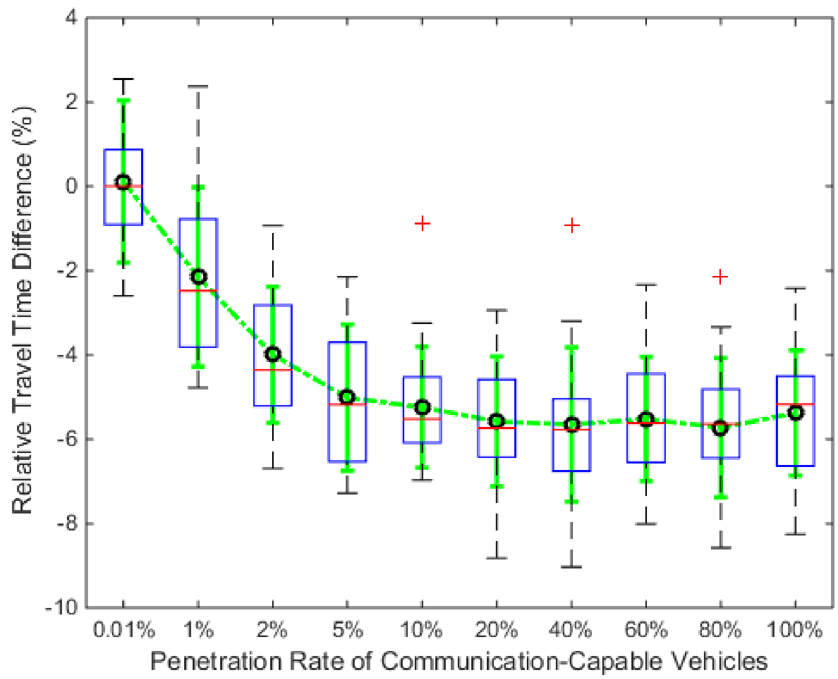

(b)

Figure 7-9. Measures of Effectiveness for Different Penetration Rates of Communication-Capable Vehicles. (a) Mean Absolute Percentage Error. (b) Relative Travel Time Difference

c) Sensitivity Analysis on Information Update Cycle

Besides traffic demand and penetration rate, the *N*-min information update cycle may also have impacts on the proposed application performance. Whereas, what is different with the other two factors (traffic demand and penetration rate, whose impacts on the traffic time decrease are relatively pure) is the information update cycle has more combined impacts.

As displayed in Figure 7-10 (a), the longer information collection duration/information update cycle (i.e., the lower information update frequency) leads to higher prediction accuracy. To be specific, the 5-min case has better MAPE than 1-min case as it aggregates the results of five 1-min error, i.e., $\left|\sum_{i=i}^{N} x_i\right|/N \leq \sum_{i=i}^{N}|x_i|/N$, which could clearly explain the MAPE results in Figure 7-10 (a).

From Figure 7-10 (b), we observe less relative travel time decrease (median) is achieved as the information update cycle gets longer, even though the corresponding MAPE gets smaller. Due to the longer information collection process, the lane change recommendation generated from the proposed application is less frequent. Simultaneously, due to the lagged real-time lane change guidance, it can be expected that the corresponding lane-changing operation number induced by the proposed application drops as well, leading to weakened application performance in terms of travel time decrease.

In addition, the traffic status of lane-level speed change even at every one minute. 1-min cycle can provide the target vehicle the more up-to-date information used for updating the micro-routing compared to the 5-min cycle: the chances of application-equipped vehicles staying at the correct target lane is increased.

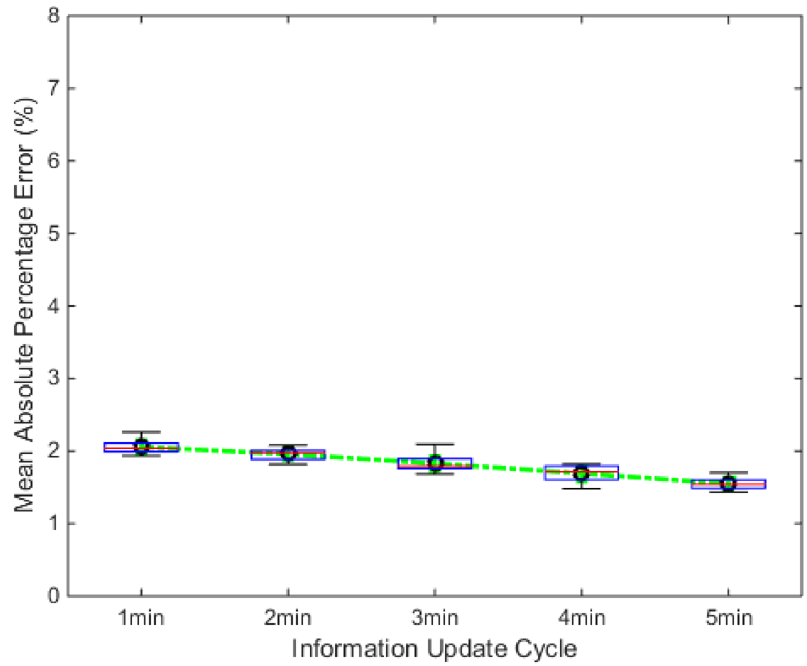

(a)

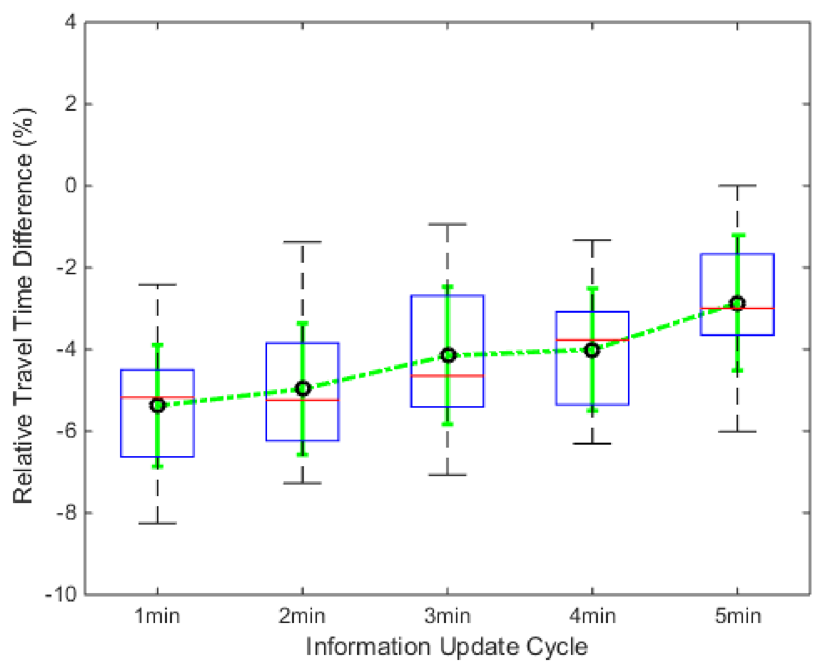

(b)

Figure 7-10. Measures of Effectiveness Analysis for Different Information Update Cycle (a) Mean Absolute Percentage Error (b) Relative Travel Time Difference

7.5.2.3 Safety Performance Analysis

Moreover, to evaluate the safety performance of the proposed application, we analyzed the risk index in terms of the potential conflict frequency (mentioned in Section 7.5.2.1) using SSAM software [33]. The potential conflict frequency results (there are ten simulation runs for each result) are summarized in Table 7-5.

There are slightly higher lane changes induced by the proposed application, however, the potential conflict frequency is lower than the baseline. There are several reasons: 1) The restriction strategy on extra lane changes within one lane/road segment prevents the application-equipped vehicles from performing too frequent lane changes; and 2) only adjacent lane changes are allowed in the proposed application within *N*-min, which helps reduce conflict risk as well.

TABLE 7-5. THE MEAN ACTUAL LANE CHANGE NUMBER AND POTENTIAL CONFLICT FREQUENCY FOR THE PROPOSED APPLICATION (100% PENETRATION RATE OF COMMUNICATION-CAPABLE VEHICLES, 25,000 VEHICLES PER RUN) AND THE CORRESPONDING BASELINE

Scenario	*Baseline*	*5-min info cycle*	*1-min info cycle*
Mean actual lane change number	3.64	4.42	4.96
Potential conflict frequency	0.1446	0.0879	0.0800

7.6 Summary

Based on predicted lane-level traffic states enabled by CV technology, a CV application called Lane Selection Assistance Application was developed and evaluated in this chapter. This application can help drivers choose a relatively faster travel lane at any point in time. The results can be summarized as: 1) the ST-model outperforms the basic estimation model in terms of traffic state prediction accuracy; 2) for all the scenarios simulated in this study, the lane selection assistance application does help the application-equipped driver reduce travel time, compared with the baseline case (i.e., normal driving without any assistance); 3) results of traffic volume sensitivity analysis indicate that the developed application can provide travel time benefits under various congestion levels. Travel time improvements can be observed even under heavy traffic condition (i.e., LOS E (unstable flow), or 32,000 vehicles/run); 4) the developed application performs robustly and can be effective even in an early deployment of CV technology with relatively low penetration; 5) different information update cycles have combined impacts on the travel time improvements. Higher travel time improvements can be achieved if the real-time state information of on-road vehicles is updated more frequently; and 6) the potential conflict risk of application-equipped vehicles is reduced as well, due to the more strategic and informed lane changes suggested by the developed application.

Furthermore, it should be noted that more advanced models can be explored in the future to better predict the lane-level traffic states [174]. In addition, further tests on the impacts of key spatial-temporal related parameters remain as future research topics. Moreover, since this application can help vehicles in the traffic stream obtain mobility benefits in terms of travel time reduction, unintended issues (e.g., oscillations in lane changes) might happen if a significant number of vehicles use this application independently and simultaneously. This will lead to the necessity of considering a priority strategy, arbitration mechanism, or optimization methods of vehicle groups in the next steps. To test the effectiveness in a more comprehensive way, it is also necessary to consider a more realistic driver behavior (lane-changing) model [175].

8 COOPERATIVE SMART LANE SELECTION APPLICATION AND DYNAMIC MANAGEMENT AMONG CV APPLICATIONS

8.1 Introduction

The CSLS application is designed from the cooperative perspective for lane assignment, which can be regarded as an evolved version on top of LSM. Regarding the lane assignment strategies, more and more probe vehicle-based or CV-based lateral control schemes have been designed to enhance traffic system efficiency and stability, such as CV-based driver assistance systems and traffic control strategies in [143], [144], [176]-[179]. Specifically, a lane assignment approach for highway vehicles was proposed to increase traffic throughput and reduce travel time, while ensuring vehicles to exit successfully at their destinations, by forming a distributed control strategy for cars to select lanes using inter-vehicle communication [143]. In a study by Dao et al. [144], vehicles were organized into platoons, to enhance traffic safety and increase road capacities, and a distributed control strategy was used to select lanes in which the vehicle platoons would travel. Simulation results show the control strategy for platooning vehicles could achieve greater reduction in travel time than single vehicle lane assignments. Ramaswamy et al. [176], defined lane assignments as the scheduling strategy of the vehicle path when the vehicle entered an automated multi-lane corridor, which consisted of system-wide traffic flow monitoring and advanced traffic management. An optimization problem was formulated with the performance in terms of the combination of both total travel time for all vehicles on a segment of the corridor and maneuver costs. In addition, Hu et al. proposed a novel lane change maneuver called “politely change lane” (PCL), to achieve a compromise between traffic safety and efficiency [177]. The scheme was validated by extensive simulations, showing improvement in the safety and efficiency of the overall traffic, especially in heavy traffic. Other similar techniques include path assignment for vehicle tracking [178]-[179]. In "Lane assignment using a Genetic Algorithm in the automated highway systems" [179], the lane assignment problem was formulated as an optimal problem to find proper positions of partitions on an itinerary matrix, using the partitioned lane assignment strategies. The optimal problem was then solved with Genetic Algorithm (GA).

Most current driver-assistance lane assignment strategies do not take into account both network-wide parameters and drivers' speed preferences simultaneously. Moreover, with the emergence of more application-enabled vehicles, such as LSM (see Chapter 6), the application may not provide the same level of effectiveness to improve the system's performance as a whole. To address this issue, we have developed herein an innovative lane selection algorithm, enabling multiple, equipped vehicles to cooperatively change lanes, with the goal of increasing mobility for the overall traffic system and the individual CV drivers.

Flow equilibrium exists in a non-free-flow homogenous network [180], suggesting that traffic flow can be further smoothed and regulated. In other words, there is still room for network flow improvement between the unstable flow and the flow equilibrium. In this regard, a lane assignment strategy should be investigated that absorbs and incorporates vehicle heterogeneity (different vehicles' desired speeds), to push the unstable traffic toward network equilibrium and further improve network mobility. In "Validation of a macroscopic lane-changing model" [181], spontaneity in lane-changing traffic within the vicinity of on-ramp /lane drop areas is mentioned. This spontaneity indicates that on-ramp vehicles will be linearly distributed across all lanes at some point after they enter the network. This means that the on-ramp traffic flow might be able to spontaneously produce a reasonable per-lane flow distribution (where there may be oscillations depending on the vehicles' routes). This paper describes a lane assignment strategy, which does not significantly change the original per-lane flow distribution, in order to follow the spontaneity of per-lane flow distribution and avoid significant disparity in lane utilization. This strategy can streamline lane selection by efficiently facilitating lane changes based on vehicle drivers' speed preferences, to improve the network throughput thus the mobility performance. To determine the effects of the proposed strategy on the traffic network in different scenarios, microscopic simulations runs have been performed for both a hypothetical traffic network and a real-world traffic network with various traffic demands and penetration rates. The remainder of this chapter is organized as follows:

- Section 8.2 describes the system architecture of the proposed cooperative smart lane assignment application.
- Section 8.3 discusses the centralized lane assignment strategy in detail.
- Section 8.4 illustrates the simulation setup.
- Section 8.5 provides the results analysis on the algorithm performance by simulations with different penetration rate levels and traffic demands.
- Section 8.6 concludes this chapter.

8.2 System Architecture

The cooperative smart lane selection (CSLS) application is a centralized system, which aims to leverage connected vehicle (CV) technology (mainly based on a cellular network) and provide a cooperative protocol for the lateral maneuvers (lane changes) for a group of application-enabled vehicles. The overall traffic is expected to benefit from such lateral regulation due to improved network mobility performance. To achieve this, the equipped vehicles are first grouped according to their spatial vicinity (see Figure 8-1 (a)). Then, the downstream lane-level traffic states are estimated and used to determine the (centralized) cooperative lane assignment strategy, which can dynamically guide the application-equipped vehicles, via long-range cellular communication, to perform lane changes to their target lanes over certain time periods. The CSLS algorithm includes three key parts:

- Spatial discretization—The CSLS-equipped vehicles form a group near a certain area (see "Cooperative lane assignment group *n*" in Figure 8-1 (a)), in order to follow the (centralized) cooperative lane assignment, which requires spatial discretization of the traffic network.
- Lane-level estimation—Multiple factors could be selected to determine lane-level traffic states downstream, such as average speed, flow, and density. In this study, we use the downstream lane-level average speed of the road segment as the key factor.
- Cooperative lane assignment scheme—A centralized lane assignment strategy is conducted to dynamically guide the application-equipped vehicles to perform

cooperative lane changes to their target lanes, based on the desired speeds of CSLS users and lane-level downstream congestion. The goals of the lane assignment strategy include: 1) to even up the number of vehicles in all lanes (not deteriorating a single lane); and 2) to assist CSLS-equipped vehicles to drive at their desired speeds, with the lowest speed difference as possible from the vehicles in the current lane in the road segment downstream, resulting in the least number of disturbances to overall traffic flows.

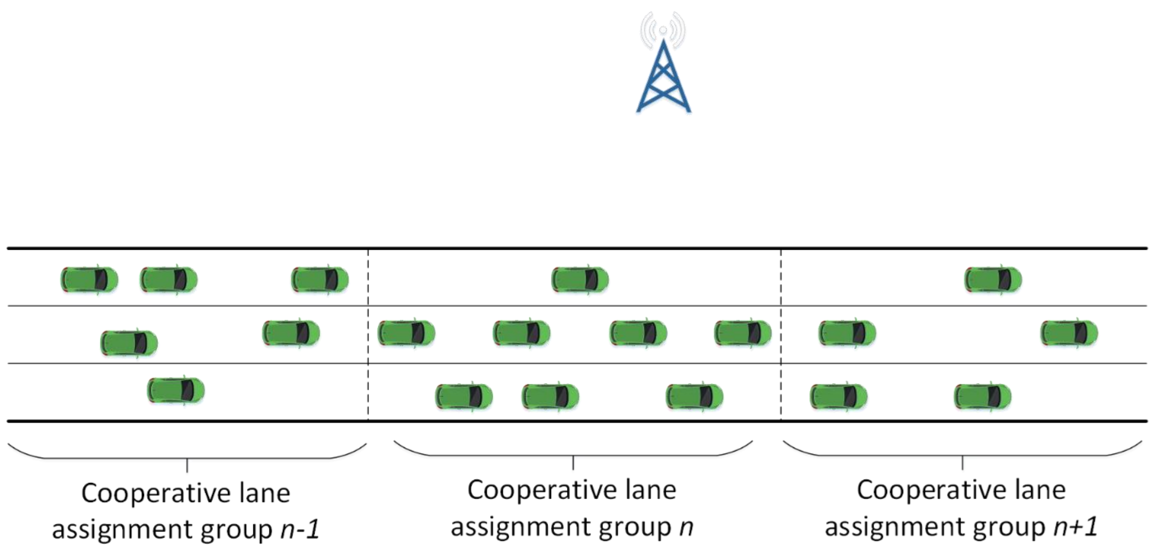

(a) Schematic Diagram of the CSLS Groups

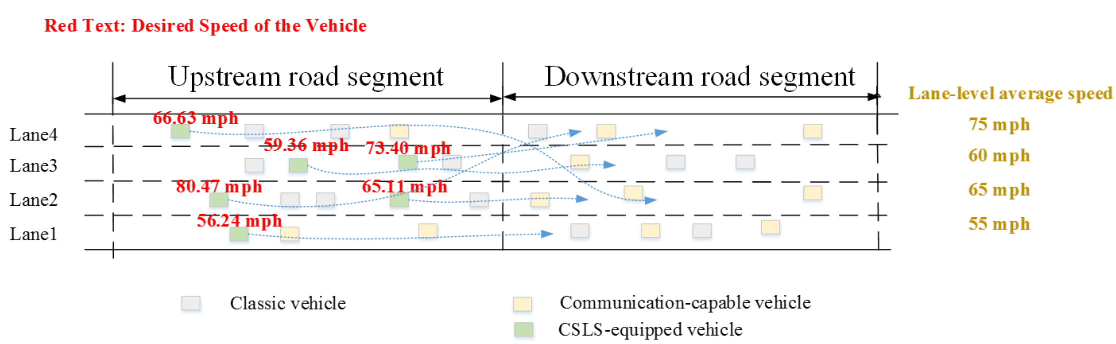

(b) An Illustrative Example of the CSLS Lane Assignment Strategy

Figure 8-1. Schematic Diagrams for the CSLS Application

Figure 8-1 (b) shows an illustrative example of the CSLS application lane assignment strategy. CSLS application-equipped vehicles' information within the upstream road segment is collected, including their desired speeds, and the lanes in which they are currently traveling. Every *N* seconds (e.g., 20 seconds), CSLS-equipped vehicles of this group (the ones in the upstream road segment) are reassigned to corresponding target lanes, depending on the downstream segment traffic status, obtained from the communication-capable vehicles within the downstream segment, and the lane assignment strategy. Figure 8-2 presents a high-level flowchart, showing the roles and functionalities of CSLS-equipped vehicles and other types of vehicles (for example, legacy vehicles and CVs without CSLS application).

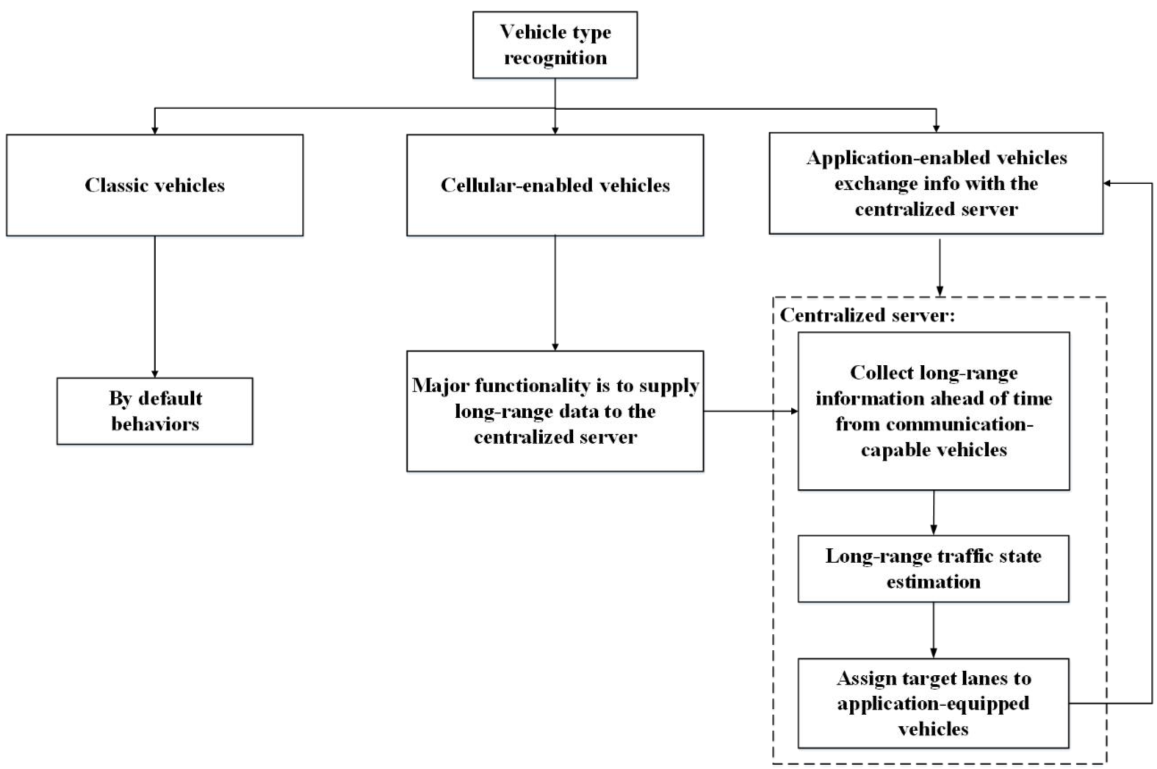

Figure 8-2. Flowchart of CSLS Application Algorithm

8.3 Lane Assignment Strategy

We developed a lane assignment strategy with the aim to improve the network output flow by efficient flow exchange on different lanes, so that the network mobility improvements are achieved.

The steps of the lane assignment strategy at each time step are:

- A group of CSLS-equipped vehicles near each other (e.g., inside the upstream road segment, see Figure 8-1 (b)) are classified as the cooperative lane assignment group *n* (see Figure 8-1 (a)). The number of CSLS-equipped vehicles in each lane n_l ($l \in [1, L]$) in this segment is logged, and L is the total number of lanes.
- All CSLS-equipped vehicles of the group *n* are sorted based on their desired speeds (for example, from high to low).
- All CSLS-equipped vehicles are clustered into L "similar-desired-speed" subgroups (again, L is the total number of lanes). The number of vehicles in each "similar-desired-speed" subgroup depends on n_l ($l \in [1, L]$).
- Each "similar-desired-speed" subgroup is distributed to the matching lane in the downstream road segment (it is assumed that each vehicle will try to drive at their desired speed in the downstream road segment as far as possible).

The process of the lane assignment strategy within one road segment at one time step t is described in detail as follows.

i. Initialization.

   a. $C^t = \{C_1^t, C_2^t, C_l^t, \ldots, C_L^t\}$ is a set of clusters at the t-th time step. L is the total number of the clusters (the total number of lanes). $\vec{x}_l^t$ is a $n_l \times 2$ matrix

($l\epsilon[1, L]$), where n_l is the number of observations on lane l within the upstream road segment at the t-th time step. Note that the observation is a CSLS-application equipped vehicle within the observed road segment. Each row of $\vec{x}_l^t$ represents an observation on lane l within the upstream road segment at the t-th time step, and each column represents one dimension in the feature space. The two feature dimensions in $\vec{x}_l^t$ include the current lane l in which the vehicle is traveling, and the vehicle's desired speed.

b. All the observations within the upstream road segment at the t-th time step are stored in set X^t, i.e.,

$$X^t = \left\{\vec{o}_j^t \middle| \vec{o}_j^t \epsilon R^{1\times 2}, j\epsilon[1, M]\right\} \tag{8-1}$$

where row vector $\vec{o}_j^t$ represents one observation; $M = \sum_{l=1}^{L} n_l$, which is the total number of observations within the upstream road segment.

ii. Assignment step.

a. Arrange the observations (row vectors) $\vec{o}_j^t$ ($j = 1,2, \dots, M$) according to their desired speeds from big to small, where $M = \sum_{l=1}^{L} n_l$ is the total number of observations within the upstream road segment, then we have matrix $S^t \epsilon R^{M\times 2}$. In S^t, we have:

$$S_{k,2}^t > S_{k+1,2}^t, \; k = 1,2, \dots, M-1 \tag{8-2}$$

where $S_{k,2}^t$ represents the second element of the k-th row in matrix S^t.

b. Sort n_l ($l = 1,2, \dots, L$) from big to small, then we have sequence ns_l as follows:

$$ns_j \geq ns_{j+1}, j = 1,2, \dots, L-1 \quad (8\text{-}3)$$

c. Classify the row vectors of matrix S^t into cluster C_l^t, i.e.,

$$C_l^t = \begin{cases} \{S_1^t, S_2^t, \dots, S_{ns_l}^t\}, & l = 1 \\ \{S_{ns_{l-1}+1}^t, \dots, S_{ns_l}^t\}, & l = 2, \dots, L \end{cases} \quad (8\text{-}4)$$

where S_m^t represents the m-th row vector in S^t.

d. Calculate the lane-level average speed $\bar{v}_l^t$ of the downstream road segment on lane l within timestep t, i.e.,

$$\bar{v}_l^t = \frac{\sum_{i=1}^{N} VMT_{l,i}^t}{\sum_{i=1}^{N} VHT_{l,i}^t} \quad (8\text{-}5)$$

where $VMT_{l,i}^t$ represents vehicle miles traveled for communication-capable vehicle i on lane l in the downstream road segment within time step t; and $VHT_{l,i}^t$ represents vehicle hours traveled for communication-capable vehicle i on lane l in the downstream road segment within time step t.

e. Obtain matrix $A^t \epsilon R^{L\times 2}$, where column 1 represents the lane index and column 2 represents the average speed $\bar{v}_l^t$ of that lane. In A^t,

$$A_{l,2}^t \geq A_{l+1,2}^t, \; l = 1, \dots, L-1 \quad (8\text{-}6)$$

where $A_{l,2}^t$ represents the second element of l-th row in A^t.

f. Reassign target lanes to all observations, i.e., the lane $A_{l,1}^t$ (the first element of l-th row in A^t) is assigned to the vehicles in cluster C_l^t $(l = 1, \dots, L)$ as their target lane.

iii. Update step:

a. Update X^t, n_l, and A^t with $t = t + 1$.

8.4 Simulation Setup

In simulation, networks with different geometries and input traffic demands can be provided to observe and verify the effects of the proposed CSLS application on various traffic networks, which is difficult to realize with real-world traffic data. The microscopic traffic simulation software VISSIM [182] is used to establish various sophisticated traffic networks, simulate driver behaviors, and implement different traffic control strategies.

8.4.1 Network

Most lane assignment methods formulate optimization problems to improve efficiency or reduce travel time (see Section 8.1), but very few differentiate the traffic state (for example, heterogeneous or homogenous network and equilibrium or non-equilibrium traffic) before applying these strategies. Results could be totally different when the same approach is implemented on different traffic states or networks, since the macroscopic characteristics (e.g., fundamental diagram shapes) are different for homogeneous and heterogeneous traffic networks [183]-[185]. A traffic network equilibrium is a network traffic state where the average traffic flow reaches and stays on the equilibrium point, if the network flow input does not change. The traffic network can reach the flow equilibrium if the network is free-flow, even if the network flows are heterogeneous; however, the network flow equilibrium exists for non-free-flow traffic only if the traffic network flows are homogeneous [180]. The homogeneity of a traffic network is an ideal situation; however, traffic flows are heterogeneously scattered most of the time.

Since the structure of traffic networks, the traffic demands, and control strategies are all factors that influence the network macroscopic characteristics, the tests in this study were conducted on both a hypothetical (homogeneous) network and a real-world (heterogeneous) network to see the application's effects on different types of networks, under various traffic demands (see Section 8.4.3 for details).

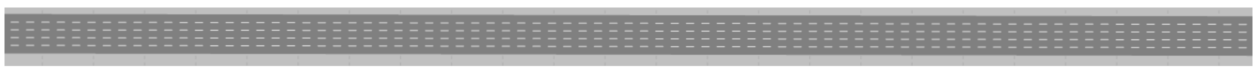

(a) Hypothetical Network

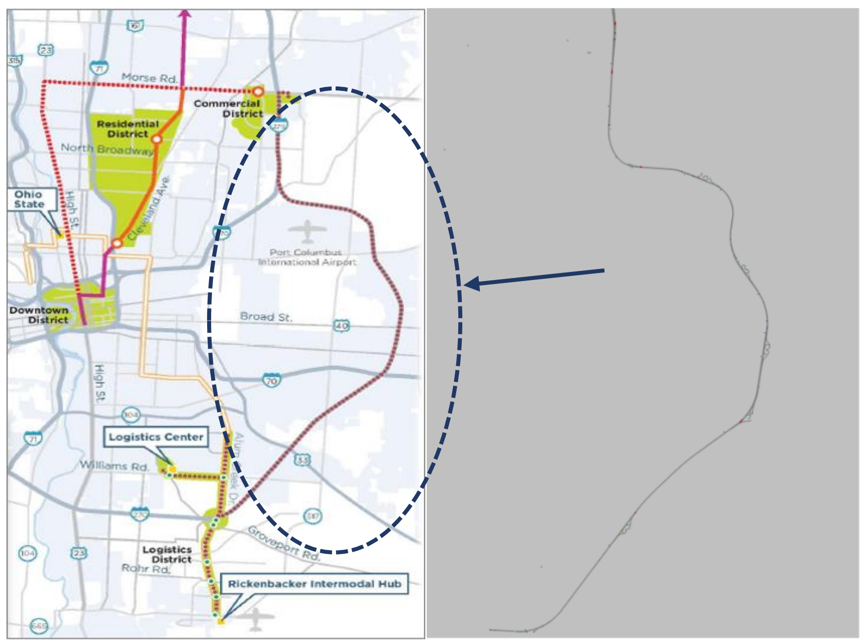

(b) Real-World Network, Ohio I-270 N (on Map and in VISSIM)

Figure 8-3.Traffic Networks under Study

The first test was conducted on a three-mile, five-lane hypothetical (homogeneous) network, which consisted of one link with one origin-destination pair and no extra road features (e.g., on-/off-ramps and lane drop areas) [180], to see how the proposed application would work without disturbances caused by complicated road features. A real-world network (i.e., Ohio I-270 N) is selected for further tests, which is a 15-mile stretch of road with three to six lanes and seven on-ramp/off-ramp pairs. The traffic demands have been well calibrated using real-world data in the City of Columbus. I-270 N is a heterogeneous network, since the traffic flows are not scattered evenly inside the network, and the traffic densities on some links are different than others [180].

8.4.2 General Parameters Settings of VISSIM

The simulation was performed in the VISSIM 9.0 (X64) environment. In VISSIM, the vehicles inside the network have different vehicle dynamics models. Examples include the desired speed curves applied to vehicles. VISSIM provides typical default values for desired speed distributions. Based on the desired speed distribution curve, each vehicle is assigned a fraction number and a desired speed. If not hindered by other vehicles or network objects, e.g. signal controls, a driver will travel at the desired speed. If the desired speed is higher than the current speed, the driver will check if he/she can overtake other vehicles without endangering anyone. Desired speed has an impact on link capacity and achievable travel time. In this study, a VISSIM default curve was selected to model the desired speed features of overall vehicles.

In addition, the detailed process to model latency in simulation was as follows:

In VISSIM, the time step(s) per simulation second can be set as a number between 1 and 20, which equates to the number of times the script will be executed per simulation second. In this work, the script was executed every 100 milliseconds, 10 time steps per simulation second. The purpose is to mimic the latency between the transmitters (app server) and the receivers (vehicles). More specifically, the information is collected and processed, then stored during a particular time step. Finally, it is used for assisting drivers at the next consecutive time step (e.g., 100 ms later) at which time the status of vehicles whose data were collected may have slightly changed due to vehicles' motion.

8.4.3 Scenario

The simulation test was performed in a homogeneous hypothetical network and a heterogeneous real-world network. Ten levels of penetration rate were simulated: 0%, 1%, 5%, 10%, 20%, 50%, 100% communication-capable vehicles (where CSLS-equipped vehicles are 9% of the above penetration rate levels), and 20%, 50%, 100% CSLS-equipped vehicles out of 100% communication-capable vehicles.

Mobility and safety performance were tested. The mobility performance indicator is defined as the average speed of a collection of vehicles, which can be obtained through the API in VISSIM. Safety performance information is obtained using conflict frequency outputs from the transportation safety evaluation software SSAM [33]. The outputs are produced in SSAM after it is fed by the specified trajectory files generated by VISSIM. Details of such effectiveness evaluation approaches can also be found in [76] and [111]. In addition to performance indicators, user and system benefits are also compared based on application-equipped vehicles, unequipped vehicles, overall vehicles, and baselines. To be specific, user benefits compare performance between application-equipped vehicles and unequipped vehicles within the same scenario, while system benefits measure the differences between overall vehicles inside a network with CSLS applications and the baselines where there are 0% application-equipped vehicles.

Both user and system benefits were evaluated in terms of mobility (average speed difference) and safety (conflict frequency difference) under three levels of traffic volumes (in the hypothetical network), stable flow traffic, approaching unstable flow traffic, and unstable flow traffic , calculated based on the network's macroscopic average travel speed and flow [130].

8.5 Simulation Results and Analysis

This section presents the effectiveness evaluation for CSLS from three aspects: 1) mobility and safety analysis of CSLS equipped, unequipped and overall vehicles in a homogenous, hypothetical network; 2) mobility comparison between CSLS and LSM in a homogenous, hypothetical network; and 3) mobility and safety analysis of CSLS equipped, unequipped and overall vehicles in a real-world network.

8.5.1 CSLS Mobility and Safety Analysis in Hypothetical Network

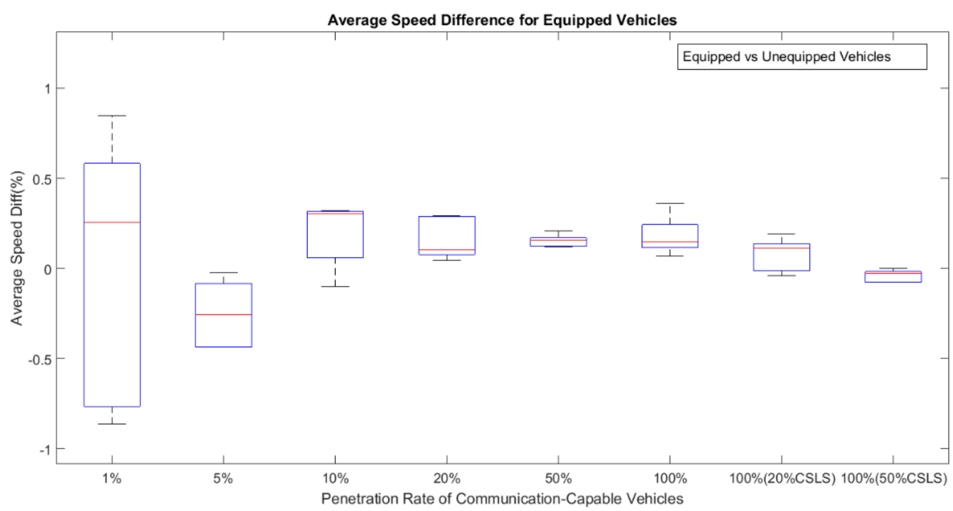

(a) Influence of CSLS Application on Mobility-User Benefits of Penetration Rate Sensitivity Analysis

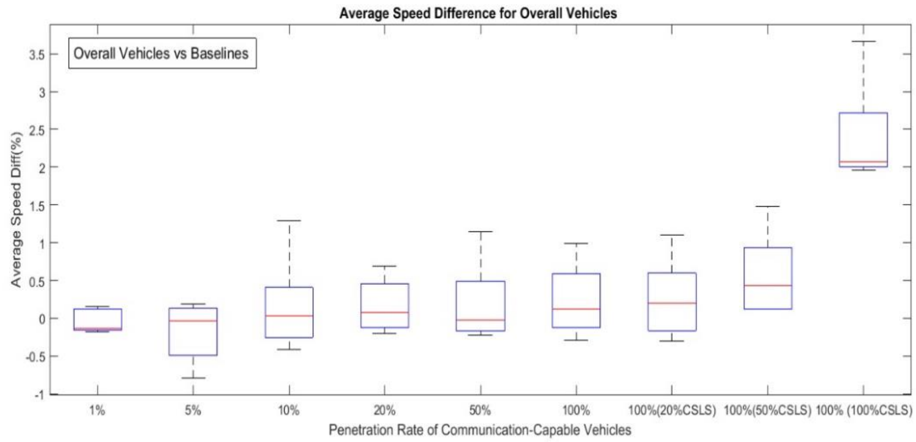

(b) Influence of CSLS Application on Mobility-System Benefits of Penetration Rate Sensitivity Analysis

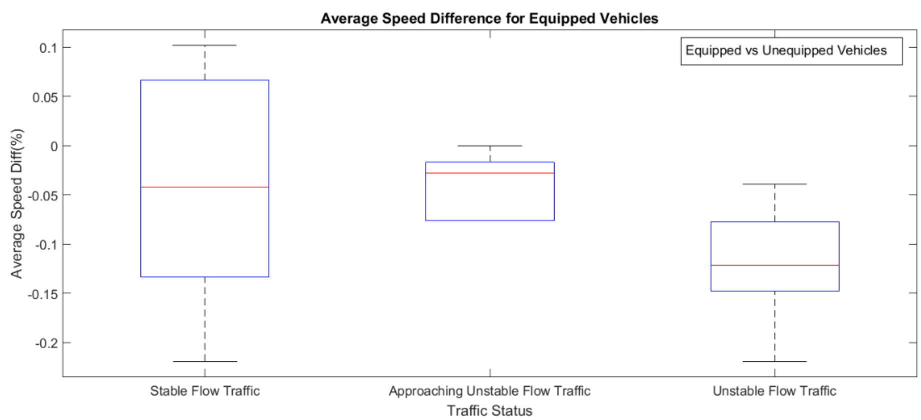

(c) Influence of CSLS Application on Mobility-User Benefits of Traffic Volume Sensitivity Analysis

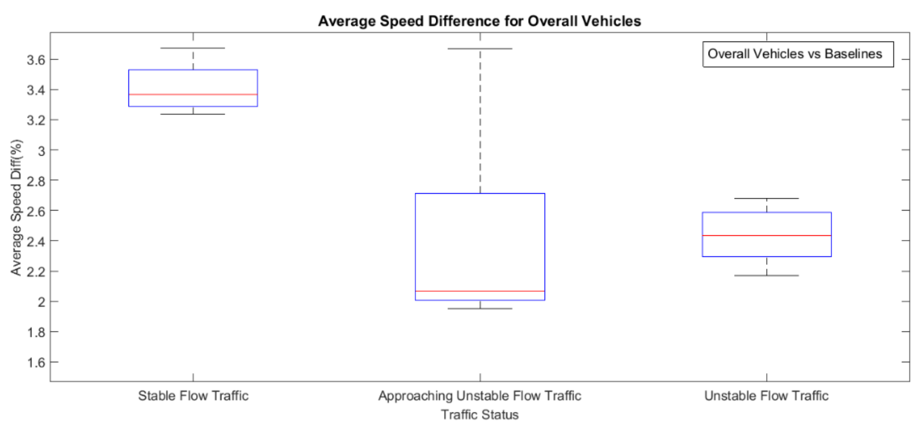

(d) Influence of CSLS Application on Mobility-System Benefits of Traffic Volume Sensitivity Analysis

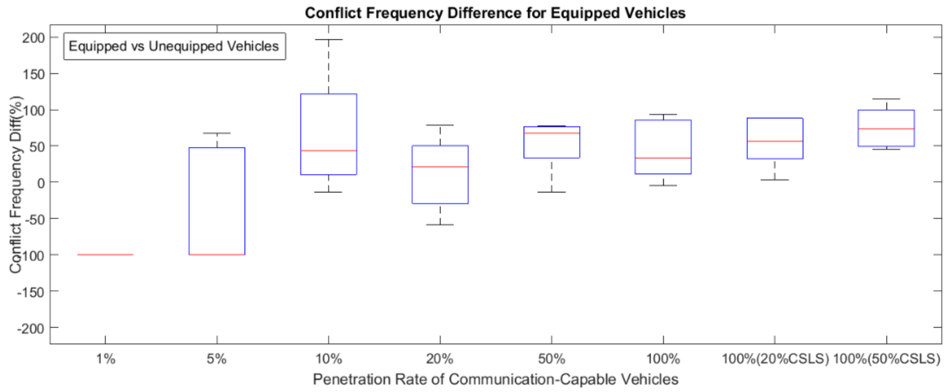

(e) Influence of CSLS Application on Safety-User Benefits of Penetration Rate Sensitivity Analysis

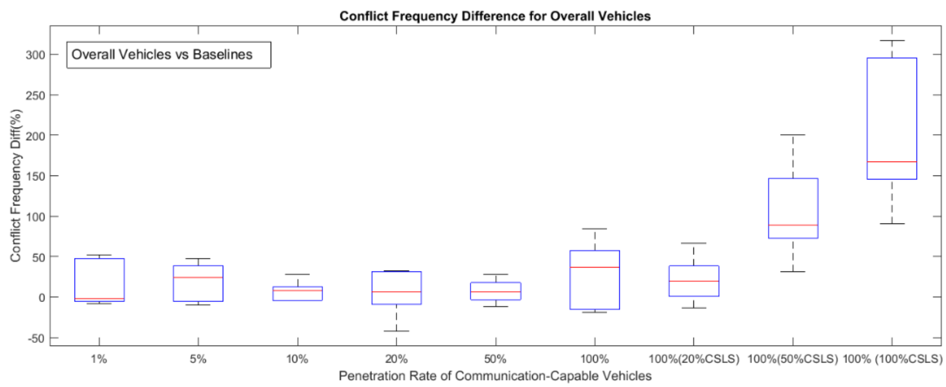

(f) Influence of CSLS Application on Safety-System Benefits of Penetration Rate Sensitivity Analysis

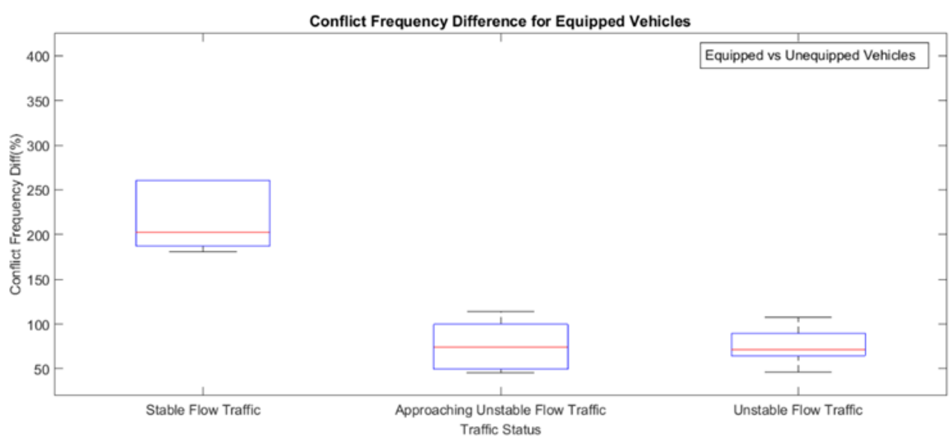

(g) Influence of CSLS Application on Safety-User Benefits of Traffic Volume Sensitivity Analysis

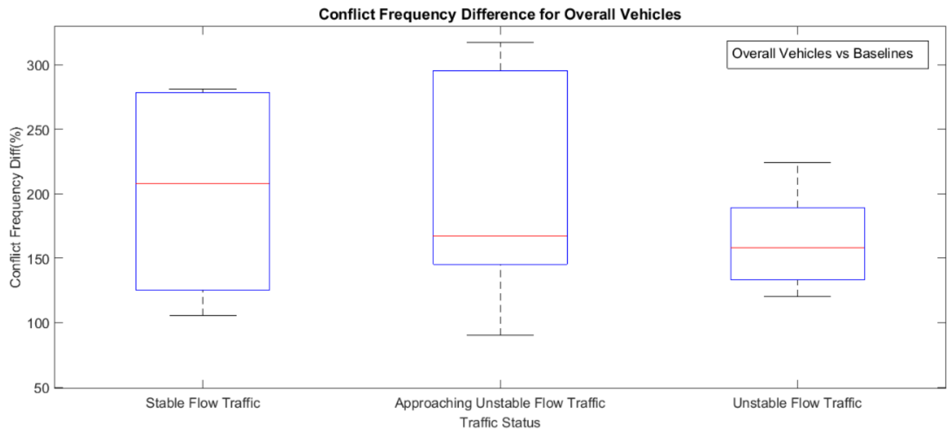

(h) Influence of CSLS Application on Safety-System Benefits of Traffic Volume Sensitivity Analysis

Figure 8-4. Influence of CSLS Application on Mobility and Safety

Figure 8-4 (a), (b), (c), and (d) shows the user and system benefits, respectively, in terms of mobility, under different penetration rate levels and traffic demands. The penetration rate sensitivity analysis was conducted under the "approaching unstable flow" traffic condition. In addition, the user benefit results of traffic volume sensitivity analysis in Figure 8-4 (a), (b), (c), and (d) are based on the scenario where all vehicles are communication-capable vehicles, and the penetration rate of CSLS-equipped vehicles is 50%, while system benefit results of traffic volume sensitivity analysis in Figure 8-4 (a), (b), (c), and (d) are based on the scenario where all vehicles are CSLS-equipped.

Based on the major findings of penetration rate sensitivity analysis (see Figure 8-4 (a) and (b)), regarding system benefits, average speed difference (median value of multiple simulation runs) is increased by +2.07% when all the vehicles are CSLS vehicles (the largest gain is +3.67% in one simulation run). As shown in Figure 8-4 (c) and (d), with the change in traffic volume, trivial benefits (or even negative results) in mobility can be witnessed from the perspective of user benefits. In terms of system benefits, the average speed difference (median) is increased by +2.07% to +3.36%.

According to the work in [180], the network flow equilibrium exists even under the non-free-flow traffic since the traffic flows are homogeneous in this hypothetical network. That is, CSLS application grasps this chance to push the traffic status toward the flow equilibrium, which theoretically exists, with the purpose of improving network mobility. The system benefits are achieved across all three non-free-flow traffic conditions in this study (see Figure 8-4 (d)), however, the results were obtained under the 100% penetration rate of CSLS-equipped vehicles. In the mixed traffic situations, the benefits may be diminished.

As shown in Figure 8-4 (e), (f), (g), and (h), for penetration rate sensitivity analysis, conflict frequency difference (in median) ranges from -100% to +73.78% from the perspective of user benefits. Regarding system benefits, the conflict frequency difference is increased by 1.67 times to 3.17 times (median). Also, with the change in traffic volume, the conflict frequency difference is increased by a factor of 0.73 to 2.02 (median value). In terms of system benefits, the conflict frequency is increased by 1.58 times to 2.08 times. The increase in the conflict risk may result from the periodic cooperative lane change behaviors introduced by the CSLS application.

8.5.2 Mobility Comparison between CSLS and LSM in Hypothetical Network

CSLS application can be regarded as an evolved version of the Lane Speed Monitoring (LSM) application (see Chapter 6), which is a distributed lane guidance strategy, mainly designed from the user benefit perspective. Simply put, the LSM application is a selfish lane selection, decision-making, ego application-equipped vehicle, collecting downstream vehicle information via inter-vehicle communication, always changing to the fastest lane to achieve a higher speed. For more details, please refer to Chapter 6.

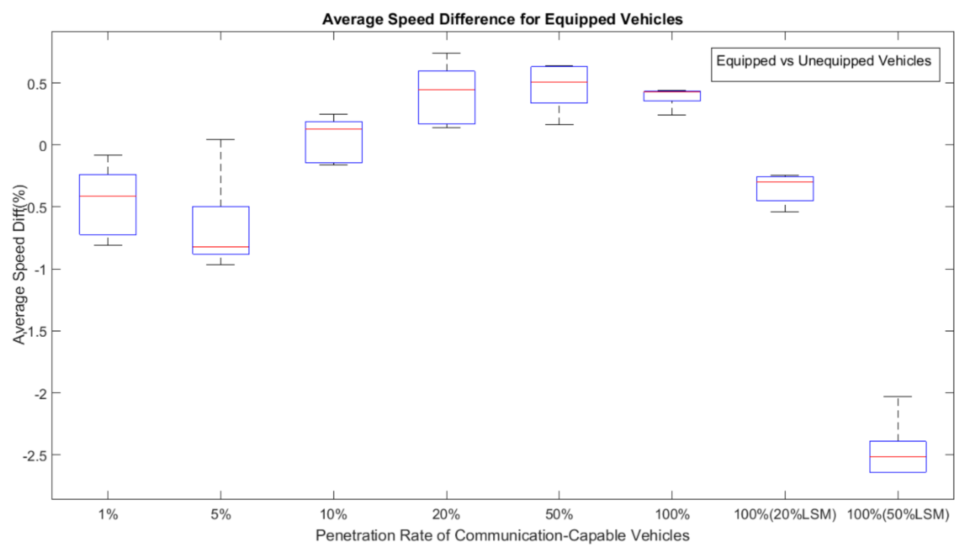

(a) Influence of LSM Application on Mobility-User Benefits of Penetration Rate Sensitivity Analysis

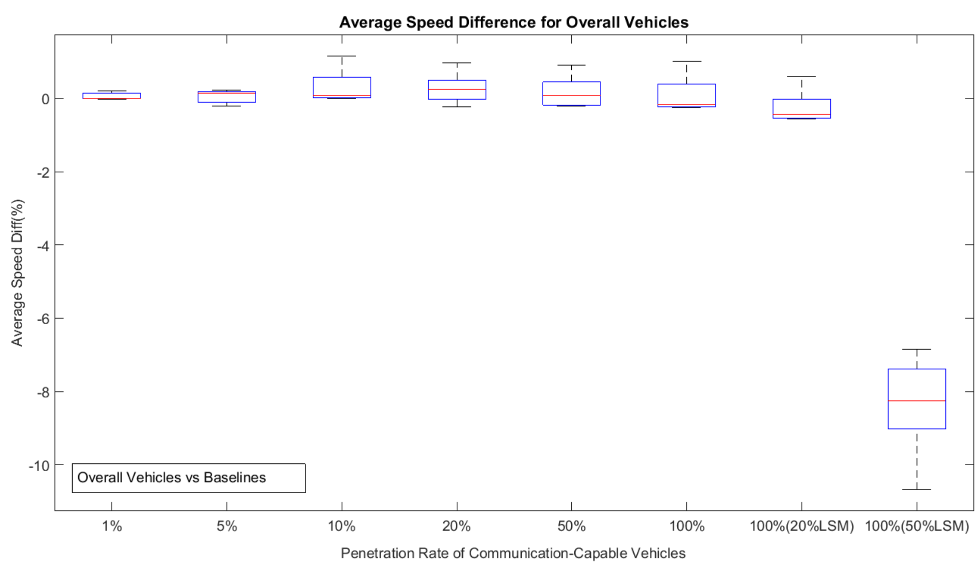

(b) Influence of LSM Application on Mobility-System Benefits of Penetration Rate Sensitivity Analysis

Figure 8-5. Influence of LSM Application on Mobility

To further investigate the difference between CSLS and LSM, the LSM application was tested in the hypothetical network under the same parameter settings and scenarios. LSM can bring user benefits in terms of average speed increase (when the penetration rate of LSM is small). For more LSM performance in terms of user benefits under low penetration rates, please refer to the work in [76]. In this study, very high penetration rate of LSM cases were tested as well, e.g., 20% LSM and 50% LSM. Comparing Figure 8-4 (a) and (b) with Figure 8-5, we see that LSM does not help achieve system benefits. In contrast to CSLS, the LSM network mobility deteriorates, i.e., the average speed of overall vehicles decreases by 8.2% when the LSM penetration rate is 50%, due to interference caused by non-cooperative lane changes at very high connected vehicle and LSM application penetration rates.

8.5.3 CSLS Mobility and Safety Analysis in Real-World Network

In addition to the hypothetical network, a heterogeneous real-world network Ohio I-270 N was tested. Please note that the spatial discretization of Ohio I-270 N followed a few rules: inconsistent lanes were ruled out to reduce the extra impacts of irregular geography. Since only the vehicles whose routes followed the mainline were selected, a relatively small penetration rate of application-enabled vehicles was tested in the real-world network, i.e., 9% of communication-capable vehicles were CSLS application-enabled vehicles. Moreover, two levels of traffic demands were selected for traffic volume sensitivity analysis: light traffic (free-flow and calibrated based on real-world data) and moderate traffic. The purpose was to see how the small portion of application-enabled vehicles affected the network mobility under free-flow traffic status, where the flow equilibrium is expected to exist in a heterogeneous network [180].

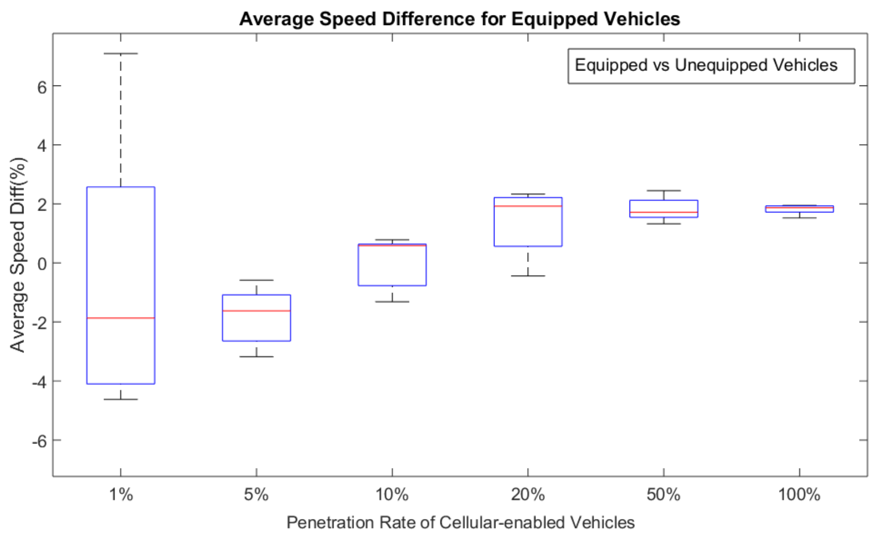

(a) Influence of CSLS Application on Mobility (Real-World Network)-User Benefits of Penetration Rate Sensitivity Analysis

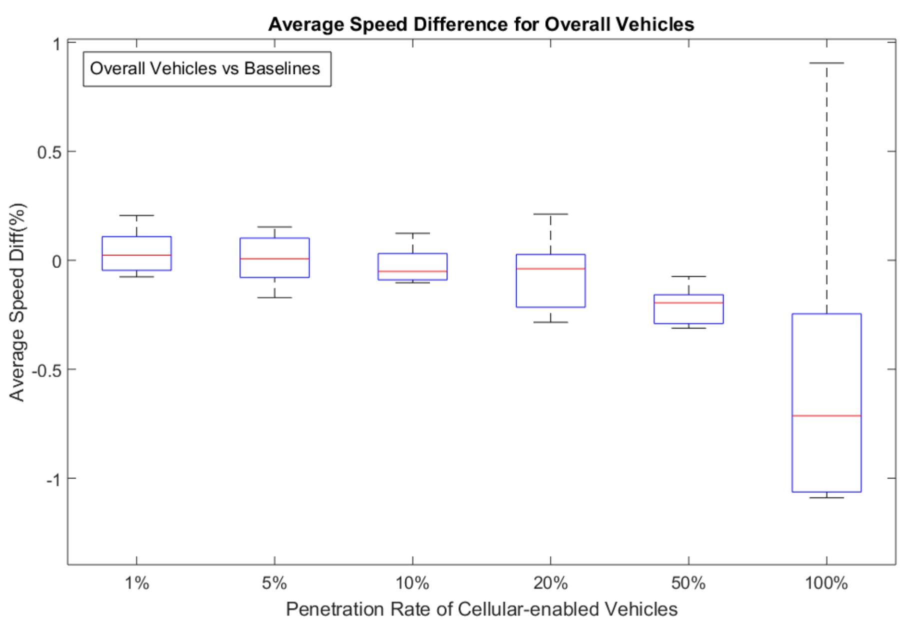

(b) Influence of CSLS Application on Mobility (Real-World Network)-System Benefits of Penetration Rate Sensitivity Analysis

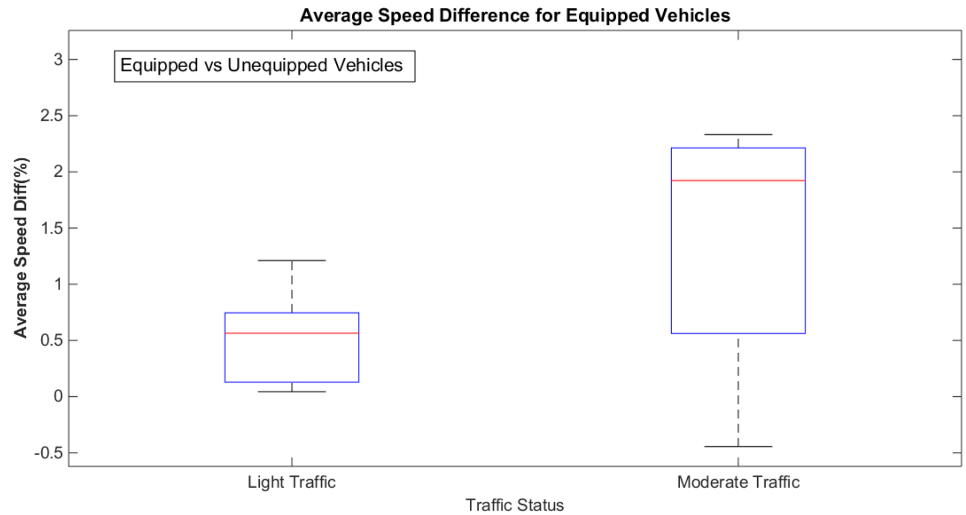

(c) Influence of CSLS Application on Mobility (Real-World Network)-User Benefits of Traffic Volume Sensitivity Analysis

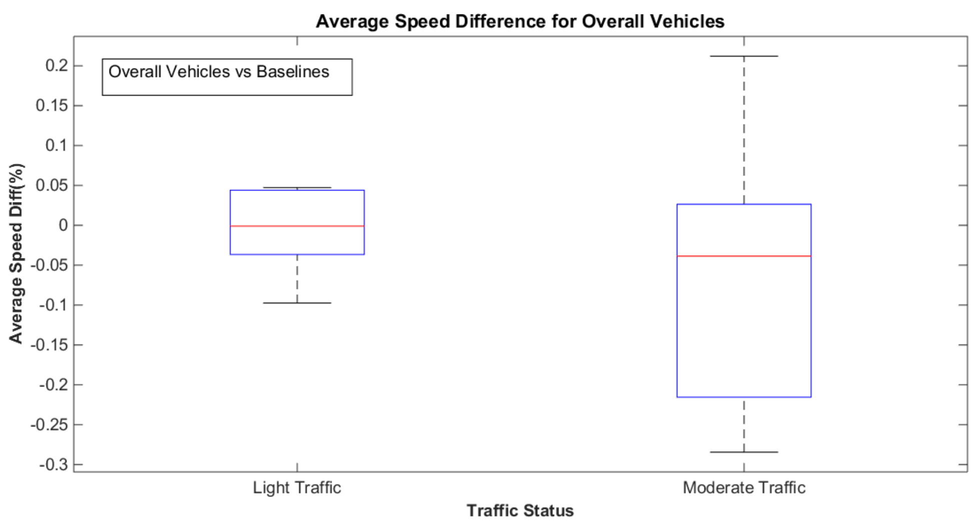

(d) Influence of CSLS Application on Mobility (Real-World Network)-System Benefits of Traffic Volume Sensitivity Analysis

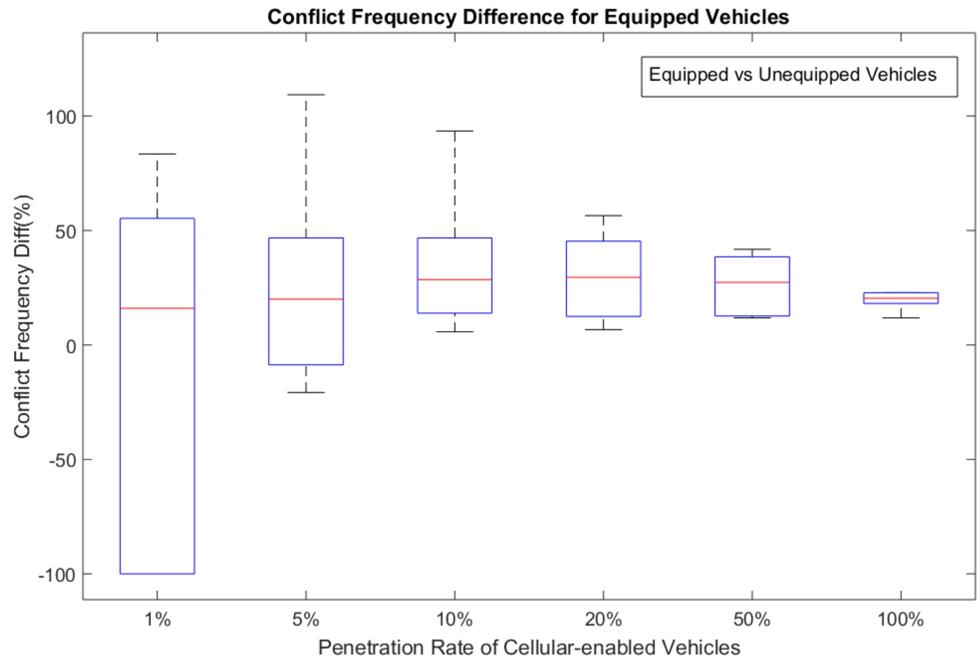

(e) Influence of CSLS Application on Safety (Real-World Network)-User Benefits of Penetration Rate Sensitivity Analysis

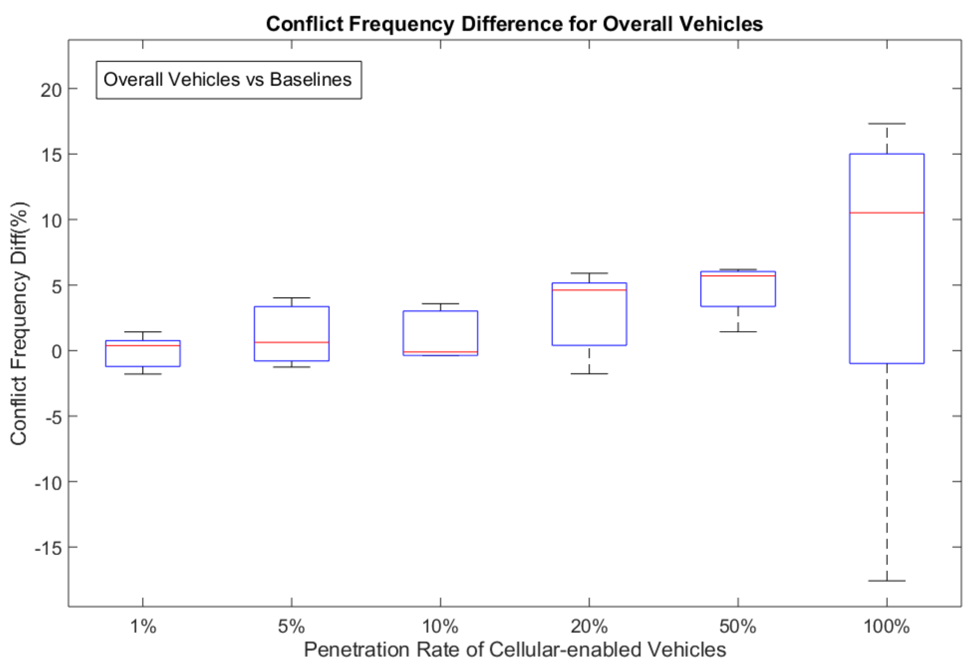

(f) Influence of CSLS Application on Safety (Real-World Network)-System Benefits of Penetration Rate Sensitivity Analysis

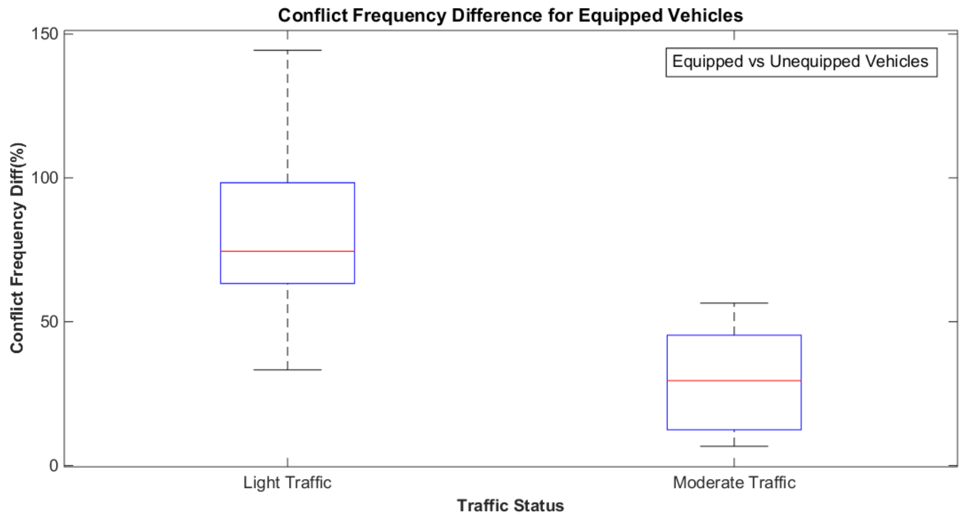

(g) Influence of CSLS Application on Safety (Real-World Network)-User Benefits of Traffic Volume Sensitivity Analysis

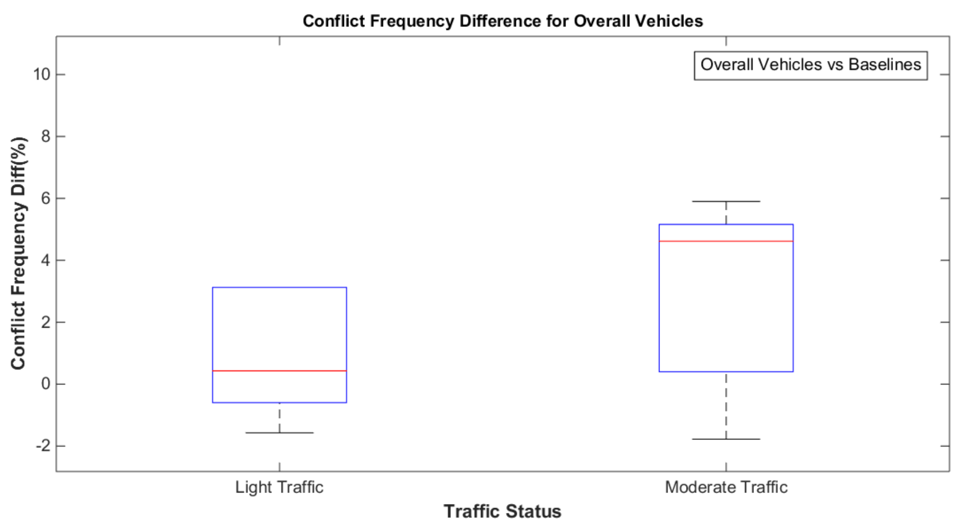

(h) Influence of CSLS Application on Safety (Real-World Network)-System Benefits of Traffic Volume Sensitivity Analysis

Figure 8-6. Influence of CSLS Application on Mobility and Safety (Real-World Network)

In Figure 8-6 (a), the mobility performance of CSLS application users is improved under a different penetration rate, i.e., there is +0.64% to +1.87% average speed difference between CSLS users and ordinary vehicles (when penetration rate of communication-capable vehicles is 10% or higher). Regarding the traffic volume sensitivity analysis, the penetration rate of communication-capable vehicles was selected as 20% (close to reality short-term market share of connected vehicles [9]), and the average speed difference is +0.56% to +1.92% under different traffic volume levels. However, the system benefits are negligible (there are -0.04% to -0.001% average speed differences between the CSLS network with baselines). Reasons could be that: 1) the number of on-road CSLS vehicles is not sufficient for the application to regulate the overall traffic; 2) the geographies of the real-world features are complicated compared to a hypothetical network, leading to difficulties in reaching flow equilibrium under such conditions. On the other hand, conflict risk is increased due to the periodic lane change behaviors induced by the application (see Figure 8-6 (e), (f), (g), and (h)).

8.6 Summary

In this chapter, a Connected Vehicle (CV)-based application, Cooperative Smart Lane Selection (CSLS), was designed and comprehensively evaluated. To examine the effects of CSLS on overall traffic, microscopic traffic simulations have been made for different traffic networks with various penetration rates and traffic demands. A similar mobility-oriented CV application, Lane Speed Monitoring (LSM), was tested for comparison purposes. The simulation results show that a system with 100% CSLS-equipped vehicles achieves network mobility benefits (in a homogenous, hypothetical network) in terms of average speed improvement of overall vehicles, as compared to the corresponding baselines; whereas, mobility of the traffic network system with high penetration rates for LSM deteriorates due to the lane changes without cooperation. The impacts on a real-world traffic network (i.e., Ohio I-270 N) were assessed, and it was observed that when the penetration rate of CSLS vehicles is low, CSLS vehicles may cause disturbances resulting from periodic lane changes; whereas, the average speed of CSLS application users is increased.

Future work includes integration of vehicles' routes in the real-world network with the CSLS application, as well as improvements on the application design to enable its functionality on a complicated real-world network at a high penetration rate.

In addition, we can achieve dynamic management of CV-based applications under diversified development environment of connected vehicle applications by tuning parameters of CV applications (see Figure 8-7).

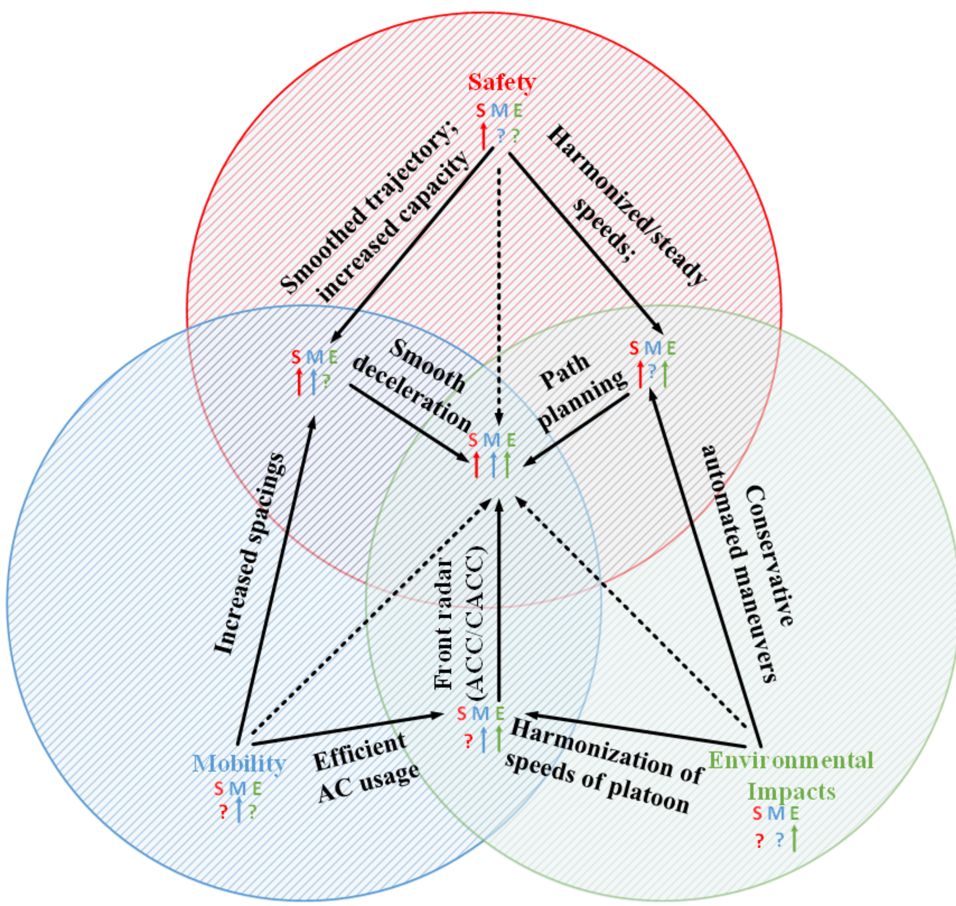

Figure 8-7. Parameters Tuning Strategy

Moreover, examples of dynamic application conversion include the proposed innovative mobility-oriented connected vehicle-based applications: Lane Speed Monitoring (LSM, see Chapter 6) and Optimal Lane Selection (OLS, see Chapter 7), and Cooperative Smart Lane Selection (CSLS). Application switching pairs can include LSM vs OLS (DSRC communication vs cellular communication); and OLS vs CSLS (minority connected vehicles vs majority connected vehicles), depending on different traffic conditions.

9 CONCLUSIONS AND FUTURE WORK

In this dissertation, an integrated holistic analysis framework has been developed to evaluate CV applications from three types of performance measures both qualitatively and quantitatively. Under the developed qualitative analysis framework for safety, mobility, and environmental sustainability, a series of innovative CV-based applications have been developed, taking the tradeoffs and co-benefits into consideration. These developed CV applications have been comprehensively evaluated, using microscopic traffic simulation tools and effectiveness evaluation models. This chapter provides a brief summary of the dissertation, as well as the possible future work.

9.1 Conclusions

A number of Connected Vehicle (CV)-based applications have recently been designed to improve the performance of the transportation system. Safety, Mobility and Environmental sustainability (SME) are three key performance metrics when evaluating CV-based applications. Chapter 4 first presents a broad classification of CV-based applications, i.e., vehicle-centric applications, infrastructure-centric applications, and traveler-centric applications. Based on a comprehensive literature review, a number of typical CV-based applications have been examined in great detail then, where a categorized analysis in terms of the SME relevant co-benefits and tradeoffs has been performed. Some key strategies to improve system performance have been identified, for example, better trajectory planning, increased spacing, capacity increase, speeds/deceleration smoothing, regenerative braking, vehicle's dynamics and exogenous signal phase and timing adjustment, etc.

To better understand the influence of different CV applications on traffic in a unified manner, a novel Measure of Effectiveness (MOE) called Speed Variation-based Entropy (SVE) has been investigated in Chapter 5. An analytical study was carried out on different types of CV applications by relating SVE with other conventional MOEs on safety, mobility, and environmental sustainability. Three applications—the High Speed Differential Warning (HSDW), the Eco-Speed Harmonization (ESH), and Eco−Approach Departure (EAD)—were selected for detailed evaluation. Results from the sensitivity analysis on the technology penetration rate and the congestion level reveal that SVE can well represent the speed variation of individual vehicles and the overall traffic. The proposed SVE has a strong positive correlation with conventional MOEs (i.e., conflict frequency and fuel consumption). Therefore, conventional MOEs can be well explained and even estimated and by SVE under a variety of scenarios.

In Chapter 6, a Lane Speed Monitoring (LSM) application based on vehicle-to-vehicle (V2V) communication has been proposed and developed. This application takes advantage of the Basic Safety Messages (BSM) transmitted from equipped vehicles via dedicated short range communication (DSRC), to estimate the real-time traffic states at the lane level. It then provides the vehicle driver with a recommendation on the fastest lane to travel in. A comprehensive simulation study has been conducted to evaluate the performance of the LSM application, including safety, mobility, and environmental impacts, under various scenarios. Results indicate that the LSM application is beneficial to the individual user even under a low market penetration rate. Vehicles equipped with the application demonstrate up to 11% average speed improvement. Using the Lane Speed

Monitoring application as one specific example, the in-depth relationship between different types of Measures of Effectiveness (MOEs) under various scenarios (e.g., different penetration rates of the LSM technology) has been explored, to investigate the association between the application focus and tradeoffs to be made among different performance measures.

Chapter 7 presents another CV-based application for online path planning, which assists with lane selection, i.e., finding the best travel lane sequence in terms of travel time based on predicted lane-level traffic states. The Spatial-Temporal model (ST-model) has been developed, which utilizes spatial and temporal information of road cells to predict future traffic states at the lane level. This information was used by the proposed lane selection assistance application to select an optimal lane sequence for the individual application-equipped vehicles, using the dynamic programming method. A comprehensive simulation-based evaluation has been conducted under various scenarios then, e.g. with different traffic volumes, penetration rates of communication-capable vehicles, and information update cycles. We observe that the proposed ST-model outperforms the basic estimation model in terms of traffic state prediction accuracy, and travel times of application-equipped vehicles can be reduced by up to 8% with the use of the proposed lane selection assistance application when compared with the baseline with 0% penetration rate for the proposed application, under various traffic scenarios. It can be concluded that the application can be effective in the early deployment stage of CV technology, where the penetration rate of communication-capable vehicles is still low. This application can help obtain mobility and safety co-benefits: both the travel time and the potential conflict risk of application-equipped vehicles are reduced. The safety benefits are achieved due to the more strategic and informed lane changes suggested by the proposed application.

In Chapter 8, a CV-enabled application, Cooperative Smart Lane Selection (CSLS), has been developed to encourage cooperative lateral maneuvers (lane changes) and improve the network-wide mobility. This application includes both the vehicle drivers' desired speeds and the network's mesoscopic (link-level and lane-level) travel speeds in its decision-making process. To examine CSLS effects on traffic, microscopic simulations have been made for different road networks with various CV market penetration rates and traffic levels. The performance of the proposed CSLS application has been compared with another CV application, Lane Speed Monitoring (LSM), which was proposed, developed, and evaluated in Chapter 6. The simulation results on a hypothetical network show that a system with 100% CSLS-equipped vehicles achieves traffic network mobility benefits, i.e., the average speed of overall vehicles increases by 3.4% as compared to the baseline with 0% penetration rate for CSLS. In contrast, mobility of the traffic network with high penetration rates for LSM deteriorates, i.e., the average speed of overall vehicles decreases by 8.2% within the same scenario, due to its non-cooperative lane selection strategy. Furthermore, impacts of CSLS on a real-world traffic network were assessed, and it was observed that when the penetration rate of CSLS vehicles is low, the average travel speed of CSLS users is increased. Finally, the dynamic application management among different CV-based applications (e.g., LSM, OLS, and CSLS) can be achieved under various traffic situations, for example, depending on the short- or long-range communication availability, and users' needs.

Overall, there are a couple of key contributions from the PhD work. First, an integrated holistic analysis among the three cornerstones of the performance measures has been designed and developed when evaluating CV based applications. The innovative structures and frameworks to evaluate the impacts of CV applications from safety, mobility, and environmental impacts both qualitatively and quantitatively. Second, an interdisciplinary concept "Speed Variation-based Entropy" is used in the transportation field, to help evaluate the degree of traffic system chaos and the impacts that the CV application brings in a more holistic way. Third, based on the similar thought process between the wireless communication systems and the transportation systems, I proposed and developed the Spatial-Temporal model for traffic state prediction and implemented real-time online path planning for connected vehicles, by using correlations between upstream and downstream lanes. Lastly, a couple of CV based applications have been proposed and developed, taking the SME tradeoffs and co-benefits into consideration. Dynamic management can be conducted under the developed integrated analysis framework, depending on traffic conditions, availability of different wireless communication technologies, and users' needs.

9.2 Selected Publications Resulting from This Research

[1] Danyang Tian, Guoyuan Wu, Kanok Boriboonsomsin, and Matthew J. Barth, “Performance measurement evaluation framework and co-benefit/: tradeoff analysis for Connected and Automated Vehicles (CAV) applications: a survey,” *IEEE Intelligent Transportation Systems Magazine,* vol. 10, no. 3, pp. 110-122, 2017.

[2] Danyang Tian, Weixia Li, Guoyuan Wu, Kanok Boriboonsomsin, Matthew Barth, Samer Rajab, and Sue Bai, "Evaluating the effectiveness of V2V-based lane speed monitoring application: a simulation study," *in Proc. 19th IEEE Intelligent Transportation Systems*, Rio, Brazil, 2016, pp: 1592-1597.

[3] Danyang Tian, Guoyuan Wu, Kanok Boriboonsomsin, and Matthew J. Barth, "A co-benefit and tradeoff evaluation analysis framework for connected vehicle applications," *in Proc. 25th IEEE Intelligent Vehicles Symposium*, Redondo Beach, CA, USA, 2017, pp: 953-958.

[4] Danyang Tian, Guoyuan Wu, Peng Hao, Kanok Boriboonsomsin, and Matthew J. Barth, "A connectivity based lane selection assistance application," *IEEE Transactions on Intelligent Transportation Systems*, 2018. (Accepted and online early access)

[5] Danyang Tian, Guoyuan Wu, Kanok Boriboonsomsin, Matthew J. Barth, Samer Rajab, and Sue Bai, "Connected vehicle-enabled cooperative smart lane selection," *Transportation Research Board (TRB) 98th Annual Meeting*, Washington, DC, USA, Jan. 2019. (Accepted)

[6] Danyang Tian, Guoyuan Wu, Chao Wang, Kanok Boriboonsomsin, Matthew J. Barth, Samer Rajab, and Sue Bai, "An innovative framework to evaluate the performance of connected vehicle applications: from the perspective of speed variation-based entropy," *IEEE Intelligent Transportation Systems Magazine*, 2017. (Under review)

9.3 Future Work

In combination with co-benefit analysis of some typical CV-based applications, we can conclude and identify some key strategies to improve system performance. It is valuable to further investigate parameter-level tuning strategy to tune a CV-based application, with the goal of achieving different functionalities depending on different traffic situations. Moreover, several different types of CV-based applications may be combined in the sense that they can improve different performance measures simultaneously and obtain co-benefits.

In addition, this dissertation has explored various CV-based applications to achieve benefits, based on traffic status estimation/prediction via short- and/or long-range wireless communication technologies. However, fusion of other data sources such as on-board sensors (e.g., radar and camera) may provide more accurate and reliable estimate of real-time downstream traffic conditions, which will help improve the effectiveness of the developed CV-based applications.

To test the effectiveness of the developed CV-based application in a more comprehensive way, it is also necessary to consider a more realistic driver behavior model, e.g., based on real-world human drivers' experience about lane-changing behaviors. In addition, the CV applications should be evaluated with field test. As a step toward the potential real-world test, one way is the "hardware-in-the-loop" where one or two real vehicles represent the model in the simulation and interact with other vehicles in the microscopic simulation.

In addition to the Speed Variation-based Entropy (SVE), entropy calculation from different perspectives (e.g., space-based and time-based SVE calculation) and its relationship with other fundamental traffic system parameters (e.g., capacity, density, and flow) remain as work for the future.

BIBLIOGRAPHY

[1] Texas A&M Transp. Inst. and INRIX. *2015 Urban Mobility Scorecard*. Accessed: Jan. 15, 2018. [Online]. Available:http://d2dtl5nnlpfr0r.cloudfront.net/tti.tamu.edu/documents/mobility-scorecard-2015.pdf

[2] Federal Highway Administration (FHWA). *2016 Urban Congestion Trends*. Accessed: Jan. 15, 2018. [Online]. Available: https://ops.fhwa.dot.gov/publications/fhwahop17010/fhwahop17010.pdf

[3] National Highway Traffic Safety Administration (NHTSA). *Traffic Safety Facts 2016*. Accessed: Jan. 21, 2018. [Online]. Available: https://crashstats.nhtsa.dot.gov/Api/Public/ViewPublication/812491

[4] World Health Organization. *Global status report on road safety 2015*. Accessed: Feb. 3, 2018. [Online]. Available: http://www.who.int/violence_injury_prevention/road_safety_status/2015/en/

[5] Environmental Protection Agency (EPA). *Annual Report and Accounts 2016*. Accessed: Feb. 5, 2018. [Online]. Available: http://www.epa.ie/pubs/reports/other/corporate/EPA_AnnualReport_2016_English_Final_Web.pdf

[6] Environmental Protection Agency (EPA). *Ireland's provisional greenhouse gas emissions in 2015*. Accessed: Feb. 5, 2018. [Online]. Available: http://www.epa.ie/pubs/reports/air/airemissions/ghgemissions/GHG%201990-2015%20Provisional%20November%202016.pdf

[7] N. Kumar Singh, L. Vanajakashi, A. K. Tangirala, "Segmentation of vehicle signatures from Inductive Loop Detector (ILD) data for real-time traffic monitoring," in *Proc. 10th*

Int. Conf. on Communication Systems & Networks (COMSNETS), Bengaluru, India, Jan. 2018, pp. 601-606.

[8] S. Shinde and S. Jagtap, “Intelligent traffic management systems: a review,” *Int. Journal for Innovative Research in Science & Technology*, vol. 2, no. 9, pp. 293-298, Feb. 2016.

[9] Catapult Transport Systems. *Market Forecast for Connected and Autonomous Vehicles*. Accessed: Mar. 5, 2018. [Online]. Available: https://assets.publishing.service.gov.uk/government/uploads/system/uploads/attachment_data/file/642813/15780_TSC_Market_Forecast_for_CV_Report_FINAL.pdf

[10] S. Zeadally, R. Hunt, Y.-S. Chen, A. Irwin, and A. Hassan, “Vehicular ad hoc network: status, results, and challenges,” *Telecom. Syst.*, vol. 50, no. 4, pp. 217-241, Aug. 2012.

[11] K.-C. Su, H.-M. Wu, W.-L. Chang, and Y.-H. Chou, “Vehicle-to-vehicle communication system through Wi-Fi network using android smartphone,” in *Proc. 1st Int. Conf. on Connected Vehicles and Expo*, Beijing, China, Dec. 2012, pp.191-196.

[12] R. Dang, J. Ding, B. Su, Q. Yao, Y. Tian, and K. Li, “A lane change warning system based on V2V communication,” in *Proc. 14th IEEE Conf. on Intell. Transp. Syst.*, Qingdao, China, Nov. 2014, pp.1923- 1928.

[13] W. Guan, J. He, L. Bai, and Z. Tang, “Adaptive congestion control of DSRC vehicle networks for collaborative road safety applications,” in *Proc. 36th IEEE Int. Workshop on Wireless Local Networks*, Bonn, Germany, Oct. 2011, pp.913-917.

[14] J. B. Kenney, “Dedicated Short-Range Communications (DSRC) standards in the United States,” in *Proc. of the IEEE Journal*, vol. 99, no. 7, pp. 1162–1182, Jul. 2011.

[15] R. Murugesh, U. Ramanadhan, N. Vasudevan, A. Devassy, D. Krishnaswamy, and A. Ramachandran, “Smartphone based Driver Assistance System for coordinated lane change,”

in *Proc. 4th Int. Conf. on Connected Vehicles and Expo*, Shenzhen, China, Oct. 2015, pp.385-386.

[16] Qualcomm. *Accelerating C-V2X commercialization*. Accessed: Mar. 7, 2018. [Online]. Available: https://www.qualcomm.com/documents/path-5g-cellular-vehicle-everything-c-v2x

[17] Qualcomm. *Leading the world to 5G: Cellular Vehicle-to-Everything (C-V2X) technologies*. Accessed: Mar. 7, 2018. [Online]. Available: https://www.qualcomm.com/media/documents/files/cellular-vehicle-to-everything-c-v2x-technologies.pdf

[18] G. Wu, K. Boriboonsomsin, and M. J. Barth, "Supplementary benefits from partial vehicle automation in an Eco-Approach/Departure application at signalized intersections," *Transp. Res. Rec., J. Transp. Res. Board*, vol. 2424, no. 2, pp. 66-75, Sep. 2014.

[19] U. S. Department of Transportation (USDOT). *Smart City Challenge*. Accessed: Jan. 20, 2017. [Online]. Available: https://www.transportation.gov/smartcity

[20] E. Uhlemann, "Connected-vehicles applications are emerging," *IEEE Vehicular Technol. Mag.*, vol. 11, no. 1, pp. 25-28, Mar. 2016.

[21] Bourns College of Engineering Center for Environmental Research and Technology (CE-CERT). *V2X Connected Vehicle Applications*. Accessed: Sep. 01, 2016. [Online]. Available: https://www.cert.ucr.edu/research/tsr/v2x.html

[22] Iteris. *Connected Vehicle Reference Implementation Architecture*. Accessed: Sep. 01, 2016. [Online]. Available: http://www.iteris.com/cvria/html/applications/applications.html

[23] European Commission. *FP7-COOPERATION-EUROPA Research Transport*. Accessed: Sep. 22, 2017. [Online]. Available: http://cordis.europa.eu/fp7/transport/home_en.html

[24] Futurism. *Tokyo 2020: The Olympics Of The Future*. Accessed: Sep. 22, 2017. [Online]. Available: https://futurism.com/images/tokyo-2020-olympics-future/

[25] U.S. Department of Transportation (USDOT). *Connected Vehicle Safety Pilot*. Accessed: Oct. 19, 2015. [Online]. Available: http://www.its.dot.gov/safety_pilot/index.htm

[26] U.S. Department of Transportation (USDOT). *Dynamic Mobility Applications (DMA)*. Accessed: Oct. 19, 2015. [Online]. Available: http://www.its.dot.gov/dma/index.htm

[27] U.S. Department of Transportation (USDOT). *Applications for the Environment: Real-time Information Synthesis (AERIS)*. Accessed: Oct. 25, 2015. [Online]. Available: http://www.its.dot.gov/aeris/index.htm

[28] U.S. Department of Transportation (USDOT). *Road Weather Connected Vehicle Applications*. Accessed: Oct. 28, 2015. [Online]. Available: http://www.its.dot.gov/road_weather/index.htm

[29] European Research and Technological Development 7th Framework Programme. *DRIVing implementation and evaluation of C2X communication technology in Europe (DRIVEC2X)*. Accessed: Oct. 28, 2015. [Online].Available:http://www.transport-research.info/project/drive-c2x-driving-implementation-and-evaluation-c2x-communication-technology-europe

[30] European Research and Technological Development 6th Framework Programme. *Cooperative vehicle-infrastructure systems (CVIS)*. Accessed: Oct. 25, 2015. [Online]. Available: http://www.transport-rese

[31] X. Jiang, W. Wang, and K. Bengler, "Intercultural analyses of time-to-collision in vehicle-pedestrian conflict on an urban midblock crosswalk," *IEEE Trans. Intell. Transp. Syst.*, vol. 16, no. 2, pp. 1048–1053, Apr. 2015.

[32] R. Fan, H. Yu, P. Liu, and W. Wang, " Using VISSIM simulation model and Surrogate Safety Assessment Model for estimating field measured traffic conflicts at freeway merge areas," *IET Intell. Transp. Syst.*, vol. 7, no.1, pp. 68-77, May 2013.

[33] Federal Highway Administration (FHWA). *Surrogate Safety Assessment Model (SSAM)*. Accessed: Oct. 18, 2015. [Online]. Available: http://www.fhwa.dot.gov/publications/research/safety/08049/

[34] J. M. Ernst, J. V. Krogmeier, and D. M. Bullock, "Kullback-Leibler comparison framework for the evaluation of travel time distribution estimates," in *Proc. 15th Int. IEEE Conf. on Intell. Transp. Syst.*, Alaska, USA, Sep. 2012, pp. 564-569.

[35] C. Chen, Z. Jia, and P. Varaiya, "Causes and cures of highway congestion," *IEEE Control Systems*, vol.21, no.6, pp. 26-32, Dec. 2001.

[36] Bourns College of Engineering Center for Environmental Research and Technology (CE-CERT), "Analysis of GPS-based data for light duty vehicles," California Air Resources Board, Sacramento, CA, USA, Final Rep., Aug. 2006. [Online]. Available: https://www.arb.ca.gov/research/apr/past/04-327.pdf

[37] M. J. Barth and K. Boriboonsomsin, "Energy and emissions impacts of a freeway-based dynamic eco-driving system," *Transp. Res. D, Transport and environment*, vol.14, no.6, pp. 400-410, Aug. 2009.

[38] IEEE 5G Tech Focus. *Cellular V2X as the essential enabler of superior global connected transportation services*. Accessed: Jul. 18, 2018. [Online]. Available: https://futurenetworks.ieee.org/tech-focus/june-2017/cellular-v2x

[39] U.S. Department of Transportation (USDOT). *Vehicle based data and availability*. Accessed: Jul. 8, 2017. [Online]. Available: https://www.its.dot.gov/itspac/october2012/PDF/data_availability.pdf

[40] A. Asadi, Q. Wang, and V. Mancuso, “A survey on device-to-device communication in cellular networks,” *IEEE Commun. Surveys Tuts.*, vol. 16, no. 4, pp. 1801-1819, 4th Quart. 2014.

[41] F. Abbas and P. Fan, “A hybrid low-latency D2D resource allocation scheme based on cellular V2X networks,” in *Proc. IEEE Int. Conf. on Communications Workshops (ICC Workshops)*, Kansas City, MO, USA, May 2018, pp. 1-6.

[42] A. Gupta and R. K. Jha, “A survey of 5G network: architecture and emerging technologies,” *IEEE Access*, vol. 3, pp. 1206-1232, Aug. 2015.

[43] Y. Gao and T. Luo, “A load balancing scheme for supporting safety applications in heterogeneous software defined LTE-V networks,” in *Proc. IEEE 28th Annual Int. Symposium on Personal, Indoor, and Mobile Radio Communications (PIMRC)*, Montreal, QC, Canada, Oct. 2017, pp. 1-5.

[44] S.-B. Choi and J. K. Hedrick, “Vehicle longitudinal control using an adaptive observer for automated highway systems,” in *Proc. IEEE Amer. Control Conf.*, Seattle, Washington, USA, Jun. 1995, pp. 3106–3110.

[45] Danyang Tian, Guoyuan Wu, Kanok Boriboonsomsin, and Matthew J. Barth, “Performance measurement evaluation framework and co-benefit/: tradeoff analysis for Connected and Automated Vehicles (CAVCV) applications: a survey,” *IEEE Intelligent Transportation Systems Magazine*, vol. 10, no. 3, pp. 110-122, 2017.

[46] N. T. Ratrout and S. M. Rahman, “A comparative analysis of currently used microscopic and macroscopic traffic simulation software,” *The Arabian Journal for Science and Engineering*, vol. 34, no. 1B, pp. 121–133, Apr. 2009.

[47] D. Krajzewicz, G. Hertkorn, C. Feld, and P. Wagner, "SUMO (Simulation of Urban MObility): An open-source traffic simulation," in *Proc. 4th Middle East Symposium on Simulation and Modeling*, Sharjah, United Arab Emirates, Jan. 2002, pp. 183–187.

[48] Quadstone PARAMICS. *Quadstone Parallel Microscopic Simulator (PARAMICS)*. Accessed: Oct. 19, 2016. [Online]. Available: http://www.paramics-online.com/

[49] R. Wiedemann, "Modeling of RTI-elements on multi-lane roads," in *Advanced Telematics in Road Transport: Proc. of the Drive Conf.*, Brussels, Belgium, Feb. 1991, pp. 1001–1019.

[50] Choa, F., Milam, R. T. and Stanek, D, "CORSIM, PARAMICS, and VISSIM: What the manuals never told you," in *Proc. 9th TRB Conference on the Application of Transportation Planning Methods*, Baton Rouge, LA, USA, Apr. 2003, pp. 392–402.

[51] CLR Analytics. *Paramics vs Vissim on Network Coding and Simulation Speed*. Accessed: Feb. 13, 2018. [Online]. Available: http://www.clranalytics.com/resources/microsimulation-comparisons/paramics-vs-vissim

[52] R. Fan, H. Yu, P. Liu, and W. Wang, "Using VISSIM simulation model and Surrogate Safety Assessment Model for estimating field measured traffic conflicts at freeway merge areas," *IET Intelligent Transport Systems*, vol. 7, no. 1, pp. 68–77, May 2013.

[53] Siemens Energy & Automation, Inc., "Surrogate safety assessment model and validation," Federal Highway Administration (FHWA), McLean, VA, USA, Final Rep., Jun. 2008. [Online]. Available: https://www.fhwa.dot.gov/publications/research/safety/08051/08051.pdf

[54] U.S. Environmental Protection Agency. *Motor Vehicle Emission Simulator (MOVES)*. Accessed: Jun. 10, 2016. [Online]. Available: http://www.epa.gov/otaq/models/moves/

[55] Y. Zhang and P. A. Ioannou, "Environmental impact of combined variable speed limit and lane change control: a comparison of MOVES and CMEM model," *IFAC-PapersOnLine*, vol. 49, no. 3, pp. 323–328, 2016.

[56] Bourns College of Engineering Center for Environmental Research and Technology (CE-CERT). *Comprehensive Modal Emissions Model (CMEM), version 3.01, User's Guide*. Accessed: Jun. 12, 2016. [Online]. Available: https://www.cert.ucr.edu/cmem/docs/CMEM_User_Guide_v3.01d.pdf

[57] Imperial College London. *Key performance indicators for traffic management and intelligent transport systems*. Accessed: Oct. 04, 2016. [Online]. Available: https://pdfs.semanticscholar.org/5453/8f8cf18c169d139390d09309adf4fdf8b4f7.pdf

[58] C. Bila, F. Sivrikaya, M. A. Khan, and S. Albayrak, "Vehicles of the future: A survey of research on safety issues," *IEEE Trans. Intell. Transp. Syst.*, vol. 18, no. 5, pp. 1046–1065, Sep. 2016.

[59] B. Chen and H. H. Cheng, "A review of the applications of agent technology in traffic and transportation systems," *IEEE Trans. Intell. Transp. Syst.*, vol. 11, no. 2, pp. 485–497, Jun. 2010.

[60] Booz Allen Hamilton, "USDOT's intelligent transportation systems (ITS) ITS strategic plan 2015-2019," U.S. Department of Transportation (USDOT), Washington, DC, USA, Final Rep., Dec. 2014. [Online]. Available: https://www.its.dot.gov/strategicplan.pdf

[61] Y. Li, Y. Zheng, J. Wang, L. Wang, K. Kodaka, and K. Li, "Evaluation of forward collision avoidance system using driver's hazard perception," in *Proc. 19th IEEE Intell. Transp. Syst.*, Rio, Brazil, Nov. 2016, pp. 2273–2278.

[62] R. Sun, W. Y. Ochieng, and S. Feng, "An integrated solution for lane level irregular driving detection on highways," *Transp. Res. C, Emerging Technol.*, vol. 56, pp. 61–79, Jul. 2015.

[63] N. Lyamin, Q. Deng, and A. Vinel, “Study of the Platooning Fuel Efficiency under ETSI ITS-G5 Communications,” in *Proc. 19th IEEE Intell. Transp. Syst.*, Rio, Brazil, Nov. 2016, pp. 551–556.

[64] M. Fullerton, A. Leonhardt, S. Assenmacher, M. Baur, F. Busch, C. Beltrán, JJ. Mínguez, and T. Paadín, “Simulation study on improving traffic safety and traffic flow in the vicinity of a motorway accident through vehicle-to-vehicle communication,” in *Proc. 18th IET Road Transp. Info. And Control Conf. and the ITS United Kingdom Members' Conf.*, London, UK, May 2010, pp. 1–6.

[65] E. Semsar-Kazerooni, J. Verhaegh, J. Ploeg, and M. Alirezaei, “Cooperative adaptive cruise control: An artificial potential field approach,” in *Proc. 27th IEEE Intell. Veh. Symp.*, Gothenburg, Sweden, Jun. 2016, pp. 361–367.

[66] K. C. Dey, L. Yan, X. Wang, Y. Wang, H. Shen, M. Chowdhury, L. Yu, C. Qiu, and V. Soundararaj, “A review of communication, driver characteristics, and controls aspects of cooperative adaptive cruise control (CACC),” *IEEE Trans. Intell. Transp. Syst.*, vol. 17, no. 2, pp. 491–509, Feb. 2016.

[67] K. D. Kusano and H. C. Gabler, “Safety benefits of forward collision warning, brake assist, and autonomous braking systems in rear-end collisions,” *IEEE Trans. Intell. Transp. Syst.*, vol. 13, no. 4, pp. 1546–1555, Dec. 2012.

[68] P. Szczurek, B. Xu, O. Wolfson, and J. Lin, “Estimating relevance for the emergency electronic brake light application,” *IEEE Trans. Intell. Transp. Syst.*, vol. 13, no. 4, pp. 1638–1656, Dec. 2012.

[69] R. Schubert, K. Schulze, and G. Wanielik, “Situation assessment for automatic lane-change maneuvers,” *IEEE Trans. Intell. Transp. Syst.*, vol. 11, no. 3, pp. 607–616, Sep. 2010.

[70] O. Orfila, G. S. Pierre, and M. Messias, “An android based ecodriving assistance system to improve safety and efficiency of internal combustion engine passenger cars,” *Transp. Res. C, Emerging Technol.*, vol. 58, Part D, pp. 772–782, Sep. 2015.

[71] K. Li, T. Chen, Y. Luo, and J. Wang, “Intelligent Environment-Friendly Vehicles: Concept and Case Studies,” *IEEE Trans. Intell. Transp. Syst.*, vol. 13, no. 1, pp. 318–328, Mar. 2012.

[72] K. Boriboonsomsin, M. J. Barth, W. Zhu, and A. Wu, “Eco-routing navigation system based on multisource historical and real-time traffic information,” *IEEE Trans. Intell. Transp. Syst.*, vol. 13, no. 4, pp. 1694–1704, Dec. 2012.

[73] C. Winter. P. Ritzer, and J. Brembeck, “Experimental investigation of online path planning for electric vehicles,” in *Proc. 19th IEEE Intell. Transp. Syst.*, Rio, Brazil, Nov. 2016, pp. 1403–1409.

[74] M. Zargayouna, F. Balbo, and K. Ndiaye, “Generic model for resource allocation in transportation Application to urban parking management,” *Transp. Res. C, Emerging Technol.*, vol. 71, pp. 538–554, Oct. 2016.

[75] H. Ramezani and R. F. Benekohal, “Optimized speed harmonization with connected vehicles for work zones,” in *Proc. 18th IEEE Intell. Transp. Syst.*, Canary Islands, Spain, Sep. 2015, pp. 1081–1086.

[76] D. Tian, W. Li, G. Wu, K. Boriboonsomsin, M. J. Barth, S. Rajab, and S. Bai, “Evaluating the effectiveness of V2V-based lane speed monitoring application: a simulation study,” in *Proc. 19th IEEE Intell. Transp. Syst.*, Rio, Brazil, Nov. 2016, pp. 1592–1597.

[77] B. Yang and C. Monterola, “Efficient intersection control for minimally guided vehicles: A self-organised and decentralised approach,” *Transp. Res. C, Emerging Technol.*, vol. 72, pp. 283–305, Nov. 2016.

[78] V. Milanés, J. Godoy, J. Villagrá, and J. Pérez, "Automated on-ramp merging system for congested traffic situations," *IEEE Trans. Intell. Transp. Syst.*, vol. 12, no. 2, pp. 500–508, Jun. 2011.

[79] Y. Pei and L. Dai, "Study on intelligent lane merge control system for freeway work zones," in *Proc. 10th IEEE Intell. Transp. Syst.*, Seattle, Washington, USA, Oct. 2007, pp. 586–591.

[80] S. Glaser, L. Nouveliere, and B. Lusetti, "Speed limitation based on an advanced curve warning system," in *Proc. 18th IEEE Intell. Veh. Symp.*, Istanbul, Turkey, Jun. 2007, pp. 686–691.

[81] A. M. Khan, "Intelligent infrastructure-based queue-end warning system for avoiding rear impacts," *IET Intell. Transp. Syst.*, vol. 1, no. 2, pp. 138–143, Feb. 2007.

[82] T. Schendzielorz, P. Mathias, and F. Busch, "Infrastructure-based vehicle maneuver estimation at urban intersections," in *Proc. 16th IEEE Intell. Transp. Syst.*, Hague, Netherlands, Oct. 2013, pp. 1442–1447.

[83] S. Tak, S. Woo, and H. Yeo, "Study on the framework of hybrid collision warning system using loop detectors and vehicle information," *Transp. Res. C, Emerging Technol.*, vol. 73, pp. 202–218, Dec. 2016.

[84] C. Haupt, J. Rohnstock, and S. Wappler, "smartLDW: A smartphone-based local danger warning system," in *Proc. 2th Intl. Conf. on Connected Veh. And Expo*, Las Vegas, USA, Dec. 2013, pp. 139–144.

[85] G. Wu, D. Kari, X. Qi, K. Boriboonsomsin, and M. J. Barth, "Developing and evaluating an eco-speed harmonization strategy for connected vehicles," in *Proc. 4th Intl. Conf. on Connected Veh. And Expo*, Shenzhen, China, Oct. 2015, pp. 373–378.

[86] H. Xia, K. Boriboonsomsin and M. J. Barth, "Dynamic eco-driving for signalized arterial corridors and its indirect network-wide energy/emissions benefits," *Journal of Intell. Transp. Syst.: Technol., Planning, and Operations*, vol. 17, no. 1, pp. 31–41, Sep. 2012.

[87] H. Yang, H. Rakha, and M. V. Ala, "Eco-cooperative adaptive cruise control at signalized intersections considering queue effects," *IEEE Trans. Intell. Transp. Syst.*, vol. 18, no. 6, pp. 1575–1585, 2016.

[88] Q. Jin, G. Wu, K. Boriboonsomsin, and M. J. Barth, "Power-based optimal longitudinal control for a connected eco-driving system," *IEEE Trans. Intell. Transp. Syst.*, vol. 17, no. 10, pp. 2900–2910, Oct. 2016.

[89] T. Guan and C. W. Frey, "Predictive energy efficiency optimization of an electric vehicle using information about traffic light sequences and other vehicles," in *Proc. 19th IEEE Intell. Transp. Syst.*, Rio, Brazil, Nov. 2016, pp. 919–926.

[90] D. Santos, Z. Kokkinogenis, J. F. de Sousa, D. Perrotta and R. J. F. Rossetti, "Towards the integration of electric buses in conventional bus fleets," in *Proc. 19th IEEE Intell. Transp. Syst.*, Rio, Brazil, Nov. 2016, pp. 90–95.

[91] Q. Jin, G. Wu, K. Boriboonsomsin, and M. J. Barth, "Platoon-based multi-agent intersection management for connected vehicle," in *Proc. 16th IEEE Intell. Transp. Syst.*, Hague, Netherlands, Oct. 2013, pp. 1462–1467.

[92] Q. Jin, G. Wu, K. Boriboonsomsin, and M. J. Barth, "Improving traffic operations using real-time optimal lane selection with connected vehicle technology," in *Proc. 25th IEEE Intell. Veh. Symp.*, Dearborn, USA, Jun. 2014, pp. 70–75.

[93] D. Kari, G. Wu, and M. J. Barth, "Eco-friendly freight signal priority using connected vehicle technology: A multi-agent systems approach," in *Proc. 25th IEEE Intell. Veh. Symp.*, Dearborn, USA, Jun. 2014, pp. 1187–1192.

[94] M. Miyawaki, Z. Yamashiro, and T. Yoshida, “Fast emergency preemption systems (FAST),” in *Proc. 2nd IEEE/IEEJ/JSAI Intl. Conf. on Intell. Transp. Syst.*, Tokyo, Japan, Oct. 1999, pp. 993–997.

[95] W. Kang, G. Xiong, Y. Lv, X. Dong, F. Zhu, and Q. Kong, “Traffic signal coordination for emergency vehicles,” in *Proc. 17th IEEE Intell. Transp. Syst.*, Qingdao, China, Oct. 2014, pp. 157–161.

[96] T. Gandhi and M. M. Trivedi, “Pedestrian protection systems: Issues, survey, and challenges,” *IEEE Trans. Intell. Transp. Syst.*, vol. 8, no. 3, pp. 413–430, Sep. 2007.

[97] L. Andreone, F. Visintainer and G. Wanielik, “Vulnerable road users thoroughly addressed in accident prevention: The WATCH-OVER European project,” in *Proc.14th World Congr. on Intell. Transp. Syst.*, Beijing, China, Jan. 2007, pp. 1–8.

[98] J. J. Anaya, P. Merdrignac, O. Shagdar, F. Nashashibi, and J. E. Naranjo, “Vehicle to pedestrian communications for protection of vulnerable road users,” in *Proc. 25th IEEE Intell. Veh. Symp.*, Dearborn, USA, Jun. 2014, pp. 1037–1042.

[99] K. Dhondge, S. Song, B.-Y. Choi, and H. Park, “WiFiHonk smartphone-based beacon stuffed WIFI car2x-communication system for vulnerable road user safety,” in *Proc. 79th IEEE Vehicular Technol. Conf.*, Seoul, Korea, May 2014, pp. 1–5.

[100] D. Greene, J. Liu, J. Reich, Y. Hirokawa, A. Shinagawa, H. Ito, and T. Mikami, “An efficient computational architecture for a collision early-warning system for vehicles, pedestrians, and bicyclists,” *IEEE Trans. Intell. Transp. Syst.*, vol. 12, no. 4, pp. 942–953, Dec. 2011.

[101] L. Zhang, S. D. Gupta, J.-Q. Li, K. Zhou, and W.-B. Zhang, “Path2Go: Context-aware services for mobile real-time multimodal traveler information,” in *Proc. 14th IEEE Intell. Transp. Syst.*, Washington, DC, USA, Oct. 2011, pp. 174–179.

[102] S. E. Li, Y. Zheng, K. Li, and J. Wang, “An overview of vehicular platoon control under the four-component framework,” in *Proc. 26th IEEE Intell. Veh. Symp.*, Seoul, Korea, Jun. 2015, pp. 286–291.

[103] Y. Zheng, S. E. Li, J. Wang, D. Cao, and K. Li, “Stability and scalability of homogeneous vehicular platoon: Study on the influence of information flow topologies,” *IEEE Trans. Intell. Transp. Syst.*, vol. 17, no. 1, pp. 14–26, Jan. 2016.

[104] Y. Zheng, S. E. Li, K. Li, F. Borrelli, and J. K. Hedrick, “Distributed model predictive control for heterogeneous vehicle platoons under unidirectional topologies,” *IEEE Trans. Ctrl. Syst. Tech.*, vol. 25, no. 3, pp. 899–910, May 2017.

[105] J. Wang, S. E. Li, Y. Zheng, and X. Lu, “Longitudinal collision mitigation via coordinated braking of multiple vehicles using model predictive control,” *Integrated Computer-Aided Engineering*, vol. 22, no. 2, pp. 171–185, Apr. 2015.

[106] S. E. Li, K. Deng, Y. Zheng, and H. Peng, “Effect of pulse-and-glide strategy on traffic flow for a platoon of mixed automated and manually driven vehicles,” *Computer-Aided Civil and Infrastructure Engineering*, vol. 30, no. 11, pp. 892–905, Aug. 2015.

[107] N. M. Enache, S. Mammar, M. Netto, and B. Lusetti, “Driver steering assistance for lane-departure avoidance based on hybrid automata and composite Lyapunov function,” *IEEE Trans. Intell. Transp. Syst.*, vol. 11, no. 1, pp. 28–39, Mar. 2010.

[108] C. García-Costa, E. Egea-López, and J. García-Haro, “A stochastic model for design and evaluation of chain collision avoidance applications,” *Transp. Res. C, Emerging Technol.*, vol. 30, pp. 126–142, May 2013.

[109] T. Liu, Y. Wang, W. E, D. Tian, G. Yu, and J. Wang, “Vehicle collision warning system and algorithm at intersection under internet-connected vehicles environment,” in *Proc. 12th COTA Intl. Conf. of Transp. Pro.*, Beijing, China, Dec. 2012, pp. 1177–1185.

[110] L. A. Lisboa Cardoso, M. Comesaña Martinez, A. A. Nogueiras Meléndez, and J. L. Afonso, “Dynamic inductive power transfer lane design for E-Bikes,” in *Proc. 19th IEEE Intell. Transp. Syst.*, Rio, Brazil, Nov. 2016, pp. 2307–2312.

[111] W. Li, G. Wu, M. J. Barth, and Y. Zhang, “Safety, mobility and environmental sustainability of Eco-Approach and Departure application at signalized intersections: a simulation study,” in *Proc. 27th IEEE Intell. Vehicles Symposium*, Gothenburg, Sweden, Jun. 2016, pp. 1109–1114.

[112] Center for Transportation Research at the University of Texas at Austin, “Development and testing of dynamic traffic assignment and simulation procedures for ATIS/ATMS applications,” U.S. Department of Transportation (USDOT), McLean, Virginia, USA, Final Rep., Jun. 1994. [Online]. Available: https://pdfs.semanticscholar.org/9b6f/c72e6ea237867207c38b40d332a4d142b7ea.pdf

[113] W. Li, G. Wu, K. Boriboonsomsin, M. J. Barth, S. Rajab, S. Bai, and Y. Zhang, “Development and evaluation of High Speed Differential Warning application using vehicle-to-vehicle communication,” *Transp. Res. Rec., J. Transp. Res. Board*, vol. 2621, pp. 1–17, 2017.

[114] C.G. Chakrabarti and I. Chakrabarty, “Shannon entropy: axiomatic characterization and application,” *International Journal of Mathematics and Mathematical Sciences*, vol. 2005, no. 17, pp. 2847–2854, Feb. 2005.

[115] E.T. Jaynes, “Information theory and statistical mechanics,” *The Physical Review*, vol. 106, no. 4, pp. 620–630, May 1957.

[116] K. A. Shahkooh, M. Fasanghari, and A. Sharifi, “Prioritization of SMEs strategies in IT fields of developing countries using entropy Shannon,” in *Proc. 3rd Int. Conf. on*

Convergence and Hybrid Information Technology, Busan, South Korea, Nov. 2008, pp. 261–266.

[117] M. Bhowmik, A. Sarkar, and R. Das, “Shannon entropy based fuzzy distance norm for pixel classification in remote sensing imagery,” in *Proc. 3rd Int. Conf. on Computer, Communication, Control and Information Technology*, Hooghly, India, Feb. 2015, pp.1–6.

[118] C. E. Shannon, “A mathematical theory of communication,” *The Bell System Technical Journal*, vol. 27, no. 4, pp. 623–656, 1948.

[119] I. Prigogine, “The End of Certainty,” New York: Simon & Schuster, Inc.

[120] A. Ben-Naim, “A Farewell to Entropy: Statistical Thermodynamics Based on Information,” Singapore: World Scientific Publishing Co. Pte. Ltd.

[121] S. C. Baslamisli and S. Onel, “Entropy based classification of road-profiles,” in *Proc. 10th Biennial Conf. on Engineering Syst. Design and Analysis*, Istanbul, Turkey, Jul. 2010, pp. 1–8.

[122] H.-S. Tan, F. Bu, J. Huang, and Y.-K. Chin, “Charactering driving skills based on entropy analysis of steering frequency response,” in *Proc. Amer. Society of Mechanical Engineers 2010 Dynamic Systems and Control Conf.*, Cambridge, Massachusetts, USA, Sep. 2010, pp. 887–894.

[123] University of Kentucky, “Traffic Flow Fundamentals,” [Online]. Available: https://web.engr.uky.edu/~rsouley/CE%20331/Part%20III%20F13/Traffic-4-TrafficFlowFundamentals.ppt

[124] G. Orosz, R. E. Wilson, and G. Stepan, “Traffic jams: dynamics and control,” *Philosophical Transactions of the Royal Society A*, vol. 368, no. 1928, pp. 4455–4479, Sep. 2010.

[125] J. I. Ge, S. S. Avedisov, C. R. He, W. B. Qin, M. Sadeghpour, and G. Orosz, "Experimental validation of connected automated vehicle design among human-driven vehicles," *Transportation Research Part C*, vol. 91, pp. 335–352, Jun. 2018.

[126] J. Ploeg, N. van de Wouw, and H. Nijmeijer, "*Lp* string stability of cascaded systems: application to vehicle platooning," *IEEE Transactions on Control Systems Technology*, vol. 22, no. 2, pp. 786–793, Mar. 2014.

[127] S. E. Li, X. Qin, Y. Zhang, J. Wang, K. Li, and H. Zhang, "Distributed platoon control under topologies with complex eigenvalues: stability analysis and controller synthesis," *IEEE Transactions on Control Systems Technology*, early access, pp. 1–15, 2018.

[128] R. Ihaddadene, N. Ihaddadene, and M. Mostefaoui, "Evaluation of three methods for estimating annual and seasonal wind speed distributions," in *Proc. 2nd International Renewable and Sustainable Energy Conf.*, Ouarzazate, Morocco, Oct. 2014, pp. 311–316.

[129] A. Maqsood and A. Mohammad, "A comparative study to estimate the parameters of mixed-Weibull distribution," *Pakistan Journal of Statistics and Operation research*, vol. 4, no. 1, pp. 1–8, Jan. 2008.

[130] Transportation Research Board. *Highway Capacity Manual 2010*. Accessed: Jan. 22, 2018. [Online]. Available: http://onlinepubs.trb.org/onlinepubs/trnews/trnews273HCM2010.pdf

[131] Bourns College of Engineering, "Modeling the effectiveness of high occupancy vehicle (HOV) lanes at improving air quality," California Dept. Transp., Sacramento, CA, USA, Final Rep., Dec. 2006. [Online]. Available: http://www.dot.ca.gov/newtech/researchreports/2002-2006/2006/modeling_effectiveness_hov_lanes_air_quality.pdf

[132] California Department of Transportation. *Performance Measurement System (PeMS)*. Accessed: Apr. 13, 2015. [Online]. Available: http://pems.dot.ca.gov/

[133] M. Shuai, K. Xie, X. Ma, and G. Song, "An on-road wireless sensor network approach for urban traffic state monitoring," in *Proc. 11th Int. IEEE Conf. on Intell. Transp. Syst.*, Beijing, China, Oct. 2008, pp. 1195–1200.

[134] Z. Shan, Y. Wang, and Q. Zhu, "Feasibility study of urban road traffic state estimation based on taxi GPS data," in *Proc. 17th Int. IEEE Conf. on Intell. Transp. Syst.*, Qingdao, China, Oct. 2014, pp. 2188–2193.

[135] University of Berkeley. *Mobile millennium*. Accessed: Apr. 16, 2016. [Online]. Available: http://traffic.berkeley.edu/

[136] W. Yao and U. Stilla, "Comparison of two methods for vehicle extraction from airborne LiDAR data toward motion analysis," *IEEE Geoscience and remote sensing letters*, vol. 8, no. 4, pp. 607–611, Jan. 2011.

[137] N. Alam, A. Tabatabaei Balaei, A. G. Dempster, "An instantaneous lane-level positioning using DSRC carrier frequency offset," *IEEE Trans. on Intell. Transp. Syst.*, vol. 13, no. 4, pp. 1566–1575, May 2012.

[138] Y. Gu, L. Hsu, and S. Kamijo, "Integration of 3D-MAP-GNSS and vision-based road marking detection for vehicle localization in urban traffic environment," in *Proc. 95th Annu. Meeting Transp. Res. Board*, Washington, DC, USA, Jan. 2016, pp. 1–14.

[139] Y. Gardes, A. D. May, J. Dahlgren, and A. Skabardonis, "Freeway calibration and application of the Paramics model," in *Proc. 81st Annu. Meeting Transp. Res. Board*, Washington, DC, USA, Jan. 2002, pp. 1–22.

[140] U.S. Environmental Protection Agency. *Evaporative emissions from on-road vehicles in MOVES 2014*. Accessed: Jan. 22, 2016. [Online]. Available: https://cfpub.epa.gov/si/si_public_file_download.cfm?p_download_id=527183&Lab=OTAQ

[141] Center for Automotive Research. *The Automotive Industry in North America-What lies Ahead?*. Accessed: Oct. 14, 2016. [Online]. Available: https://www.slideshare.net/NicoleScott1/auto-summit-2015-53201663

[142] W. Zeng, T. Miwa, T. Morikawa, "Prediction of vehicle CO2 emission and its application to eco-routing navigation," *Transportation Research Part C*, vol. 68, pp. 194–214, Jul. 2016.

[143] T.-S. Dao, C. M. Clark, and J. P. Huissoon, "Optimized lane assignment using inter-vehicle communication," in *Proc. 18th IEEE Intell. Vehicles Symposium*, Istanbul, Turkey, Jun. 2007, pp.1217–1222.

[144] T.-S. Dao, C. M. Clark, and J. P. Huissoon, "Distributed platoon assignment and lane selection for traffic flow optimization," in *Proc. 19th IEEE Intell. Vehicles Symposium*, Eindhoven, The Netherlands, Jun. 2008, pp.739–744.

[145] Q. Jin, G. Wu, K. Boriboonsomsin, and M. Barth, "Improving traffic operations using real-time optimal lane selection with connected vehicle technology," in *Proc. 25th IEEE Intell. Vehicles Symposium*, Dearborn, Michigan, Jun. 2014, pp.70–75.

[146] J. Kwon, B. Coifman, and P. Bickel, "Day-to-day travel time trends and travel time prediction from loop detector data," *Transp. Res. Rec., J. Transp. Res. Board*, vol. 1717, pp. 120–129, 2000.

[147] J. Rice and E. V. Zwet, "A simple and effective method for predicting travel times on freeways," *IEEE Trans. Intell. transp. syst.*, vol. 5, no. 3, pp. 200–207, Sep. 2004.

[148] J. Du, D. Deng, U. Demiryurek, C. Shahabi, and M. V. D. Schaar, "Mining the Situation: Spatiotemporal Traffic Prediction With Big Data," *IEEE Jounal of Selected Topics in Signal Processing*, vol. 9, no. 4, pp. 702–715, Jan. 2015.

[149] Z. Liang and Y. Wakahara, “City traffic prediction based on real-time traffic information for intelligent transportation systems,” in *Proc. 13th Int. Conf. on ITS Telecom.*, Tampere, Finland, Nov. 2013, pp. 378–383.

[150] C. Goves, R. North, R. Johnston, and G. Fletcher, “Short term traffic prediction on the UK motorway network using neural networks,” *Transp. Res. Procedia*, vol. 13, no. 2016, pp. 184–195, Sep. 2015.

[151] Y. Qi and S. Ishak, “A hidden Markov model for short term prediction of traffic conditions on freeways,” *Transp. Res. C, Emerging Technol.*, vol. 43, part 1, pp. 95–111, Jun. 2014.

[152] C. Antoniou, H. N. Koutsopoulos and G. Yannis, “Traffic state prediction using Markov chain models,” in *Proc. 17th European Control Conference 2007*, Kos, Greece, Jul. 2007, pp. 2428–2435.

[153] S. Oh, Y.-J. Byon, and H. Yeo, “Improvement of search strategy with k-nearest neighbors approach for traffic state prediction,” *IEEE Trans. Intell. transp. syst.*, vol. 17, no. 4, pp. 1146–1156, Dec. 2015.

[154] S. Ren, J. Bi, Y. F. Fung, X. I. Li, and T. K. Ho, “Freeway traffic estimation in Beijing based on particle filter,” in *Proc. 6th Int. Conf. on Natural Computation*, Yantai, China, Aug. 2010, pp.292–296.

[155] H. Chen, H. A. Rakha and S. Sadek, “Real-time freeway traffic state prediction: a particle filter,” in *Proc. 14th IEEE Intell. Transp. Syst.*, Washington, DC, USA, Oct. 2011, pp.626–631.

[156] Y. Yuan, F. Scholten, and Hans van Lint, “Efficient traffic state estimation and prediction based on the Ensemble Kalman Filter with a fast implementation and localized deterministic scheme,” in *Proc. 18th IEEE Intell. Transp. Syst.*, Las Palmas, Spain, Nov. 2015, pp.477–482.

[157] M. Elhenawy and H. Rakha, “Stretch-wide traffic state prediction using discriminatively pre-trained deep neural networks,” in *Proc. 19th IEEE Intell. Transp. Syst.*, Rio de Janeiro, Brazil, Nov. 2016, pp.1065–1070.

[158] D. Huang, Z. Deng, L. Zhao, and B. Mi, “A short-term traffic flow forecasting method based on Markov Chain and Grey Verhulst model,” in *Proc. 16th IEEE Data Driven Control and Learning Systems Conference*, Chongqing, China, May 2017, pp. 606–610.

[159] W. Min and L. Wynter, “Real-time road traffic prediction with spatiotemporal correlations,” *Transp. Res. C, Emerging Technol.*, vol. 19, no. 4, pp. 606–616, Aug. 2011.

[160] Z. Liu, Z. Li, M. Li, W. Xing, and D. Lu, “Mining road network correlation for traffic estimation via compressive sensing,” *IEEE Trans. Intell. Transp. syst.*, vol. 17, no. 7, pp. 1880–1893, Jul. 2016.

[161] J.-H. Kim and D.-S. Kum, “Threat prediction algorithm based on local path candidates and surrounding vehicle trajectory predictions for automated driving vehicles,” in *Proc. 26th IEEE Intell. Vehicles Symposium*, Seoul, Korea, Jun. 2015, pp. 1220–1225.

[162] A. Elfar, A. Talebpour, and H. S. Mahmassani, “Analyzing queue warning in connected environment: a micro simulation approach,” in *Proc. 95th Annu. Meet. Transp. Res. Board*, Washington, DC, USA, Jan. 2016, pp. 1–15.

[163] S. Yoon and D. Kum, “The multilayer perceptron approach to lateral motion prediction of surrounding vehicles for autonomous vehicles,” in *Proc. 27th IEEE Intell. Vehicles Symposium*, Gothenburg, Sweden, Jun. 2016, pp. 1307–1312.

[164] J. Rabe, M. Necker, and C. Stiller, “Ego-lane estimation for lane-level navigation in urban scenarios,” in *Proc. 27th IEEE Intell. Vehicles Symposium*, Gothenburg, Sweden, Jun. 2016, pp. 896–901.

[165] T. Song, N. Capurso, X. Cheng, J. Yu, B. Chen, and W. Zhao, "Enhancing GPS with lane-level navigation to facilitate highway driving," *IEEE Trans. vehicular tech.*, vol. 66, no. 6, pp. 4579–4591, Jun. 2017.

[166] C. Liu, K. Jiang, Z. Xiao, Z. Cao, and D. Yang, "Lane-level route planning based on a multi-layer map model," in *Proc. 20th IEEE Intell. Transp. Syst.*, Yokohama, Japan, Oct. 2017, pp. 1–7.

[167] J.-W. Lee, C.-R. Yoon, J. Kang, B.-J. Park, and K.-H. Kim, "Development of lane-level guidance service in vehicle augmented reality system," in *Proc. 17th Advanced Comm. Tech.*, PyeongChang, South Korea, Jul. 2015, pp. 263–266.

[168] S. F. Khan, "Health care monitoring system in Internet of Things (IoT) by using RFID," in *Proc. 6th Industrial Tech. and Management*, Cambridge, UK, Mar. 2017, pp. 198–204.

[169] O. Takizawa, M. Hosokawa, K. Takanashi, Y. Hada, A. Shibayama, and B. Jeong, "Pinpointing the place of origin of a cellular phone emergency call using active RFID tags," in *Proc. 22nd Int. Conf. Adv. Inf. Netw. Appl.*, Okinawa, Japan, 2008, pp. 1123–1128.

[170] V. Sharma, A. Vithalkar, M. Hashmi, "Lightweight security protocol for chipless RFID in Internet of Things (IoT) applications," in *Proc. 10th Comm. Syst. & Networks*, Bengaluru, India, Jan. 2018, pp. 468–471.

[171] University of Michigan. *Recursion and Dynamic Programming*. Accessed: Apr. 15, 2018. [Online]. Available: http://csg.sph.umich.edu/abecasis/class/2006/615.05.pdf

[172] K. D. Le and J. T. Day, "Rolling horizon method: a new optimization technique for generation expansion studies," *IEEE Trans. Apparatus and Syst.*, vol. PER-2, no. 9, pp. 3112–3116, Sep. 1982.

[173] Y. Z. Tan, R. L. Cheu, and D.H. Lee, "Comparison of Paramics and Getram/Aimsun for ITS simulations," *Journal of the Institution of Engineers*, vol. 45, no. 2, pp. 78–96, 2005.

[174] T. Schreiter, H. V. Lint, M. Treiber and S. Hoogendoorn, “Two fast implementations of the Adaptive Smoothing Method used in highway traffic state estimation,” in *Proc. 13th IEEE Conf. on Intell. Transp. Syst.*, Funchal, Portugal, Sep. 2010, pp.1202–1208.

[175] V. L. Knoop, M. Keyvan-Ekbatani, M. De Baat, H. Taale, S.P. Hoogendoorn, “Strategy-based driving behaviour on freeways: findings of test-drive and on-line survey study,” in *Proc. 96th Annu. Meet. Transp. Res. Board*, Washington, DC, USA, Jan. 2017, pp. 1–16.

[176] D. Ramaswamy, J. V. Medani´c, W. R. Perkins, and R. F. Benekohal, “Lane assignment on automated highway systems,” *IEEE Trans. Vehicular Technology*, vol. 46, no. 3, pp. 755–769, Aug. 1997.

[177] J. Hu, L. Kong, W. Shu, and M.-Y. Wu, “Scheduling of connected autonomous vehicles on highway lanes,” in *Proc. 24th IEEE Global Communications Conference (Globecom)*, Anaheim, CA, USA, Dec. 2012, pp. 5556–5561.

[178] R. Altendorfer and S. Wirkert, “Path assignment techniques for vehicle tracking,” in *Proc. 25th IEEE Intell. Vehicles Symposium*, Dearborn, Michigan, USA, Jun. 2014, pp. 1451–1456.

[179] K. Kim, D.-il Cho, and J. V. Medani´c, “Lane assignment using a Genetic Algorithm in the automated highway systems,” in *Proc. 8th IEEE Conf. on Intell. Transp. Syst.*, Vienna, Austria, Sep. 2005, pp. 332–337.

[180] Shu Lin, Qing-Jie Kong, and Qingming Huang, “A simulation analysis on the existence of network traffic flow equilibria,” *IEEE Trans. Intell. Transp. syst.*, vol.15, no.4, pp. 1706–1713, Aug. 2014.

[181] Qi-jian Gan and Wenlong Jin, “Estimation of the number of left lane changes in laterally unbalanced traffic using lane-based loop detector data,” in *Proc. 94th Annu. Meet. Transp. Res. Board*, Washington, DC, USA, Jan. 2015, pp. 1–13.

[182] PTV GROUP. *PTV VISSIM*. Accessed: Jan. 7, 2018. [Online]. Available: http://vision-traffic.ptvgroup.com/en-us/products/ptv-vissim/

[183] N. Geroliminis and C. Daganzo, “Existence of urban-scale macroscopic fundamental diagrams: Some experimental findings,” *Transp. Res. B, Methodol.*, vol. 42, no. 9, pp. 759–770, Nov. 2008.

[184] C. Buisson and C. Ladier, “Exploring the impact of homogeneity of traffic measurements on the existence of macroscopic fundamental diagrams,” *Transp. Res. Rec., J. Transp. Res. Board*, vol. 2124, no. 1, pp. 127–136, 2009.

[185] Y. Ji, W. Daamen, S. Hoogendoorn, S. Hoogendoorn-Lanser, and X. Qian, “Investigating the shape of the macroscopic fundamental diagram using simulation data,” *Transp. Res. Rec., J. Transp. Res. Board*, vol. 2161, no. 1, pp. 40–48, 2010.